UNIVERSITÀ
DEGLI STUDI
DI PADOVA

Sede Amministrativa: Università degli Studi di Padova
Dipartimento di Scienze Chimiche

SCUOLA DI DOTTORATO DI RICERCA IN SCIENZE MOLECOLARI
INDIRIZZO: SCIENZE CHIMICHE
CICLO XXII

NEW CATALYTIC SYSTEMS FOR THE SELECTIVE FUNCTIONALIZATION OF ORGANIC MOLECULES

Direttore della Scuola: Ch.mo Prof. Maurizio Casarin
Coordinatore d'Indirizzo: Ch.mo Prof. Maurizio Casarin
Supervisore: Ch.mo Prof. Gianfranco Scorrano

Dottorando: Serena Berardi

Abstract

Green chemistry revolution is providing a number of challenges to chemists, in order to develop new processes, products and services able to achieve the now required social, economic and environmental targets. The achievement of these goals needs new approaches, in order to reduce materials and energy consumption, through the discovery and the development of innovative synthetic pathways, using renewable feedstocks and more selective chemistry, but also identifying alternative reaction conditions and media, in order to design less toxic and safer chemical processes.

In this context, lots of efforts are aimed to the development of innovative catalytic methodologies for industrially relevant applications. In this Thesis, different strategies have been used to implement benchmark transformations, such as oxidations, C-C bond formation and dehalogenation reactions.

The choice of the catalyst package has been established within the class of molecular polyanionic metal oxides clusters, known as polyoxometalates (POMs) with general formula $[X_xM_mO_y]^{q-}$, where M is the main metallic component (Mo^{VI}, W^{VI}, V^{V}) and X is an heteroatom (such as P^{V} or Si^{IV}).

These complexes offer a unique opportunity because of their prevalent inorganic, robust nature and high versatility in terms of structure, chemical composition, electron density and polyanionic charge. Moreover, a rewarding approach has been recently devised for the catalyst up-grade, by decorating the POM scaffold with tailored organic domains, yielding hybrid organic-inorganic catalysts with superior performances. Heterometals (such as Ru, Fe, Pd, Al,…) can also be incorporated in POMs structures (yielding Transition Metal-substituted Polyoxometalates, *TMSPs*), introducing diversification and opening new catalytic possibilities. Besides, POMs display high thermal, hydrolytic and oxidative resistance, as well as tuneable solubility. Heterogeneous catalysis is also possible, by anchoring POMs on solid supports.

Both hybrid POMs and *TMSPs* have been successfully used in this Thesis to implement benchmark oxidative transformations, C-C bond formation and dehalogenation reactions.

The research approach has been based on some key issues, involving the use of: (i) bulk reactants with low environmental impact; (ii) sustainable reaction media (ionic liquids and water); (iii) non conventional activation techniques, such as microwave (MW) irradiation; (iv) alternative reactors, as microchannel reactors.

In the specific, Chapter 2 will summarize the results of the combined use of a hybrid polyoxometalate, ionic liquids and MW-irradiation as an innovative strategy for the immobilization, recycling and activation of an efficient catalytic phase for the epoxidation of olefins with hydrogen peroxide. Both internal and terminal olefins can be epoxidized with yields and selectivities up to 99%. In particular, under MW-irradiation, epoxidation of *cis*-cyclooctene occurs in minutes, with unprecedented turnover frequencies (TOF > 200 min^{-1}). Moreover, the proposed system is recyclable (quantitative production of cyclooctene epoxide in four consecutive runs) and its miniaturization is also possible, using microreactor technology coupled with continuous flow processing of the reaction mixture.

Chapter 3 will summarize the results of a collaboration with the University of Rome – Tor Vergata. The proposed catalytic system, combining the use of scandium triflate, ionic liquids and MW-irradiation, has resulted, at present, the most efficient protocol in Friedel-Crafts acylation of ferrocene.

Chapter 4 will focus onto different organic transformations, such as C-C bond formation and dehalogenation reactions. Our approach has regarded the synthesis of tailored hybrid multi-metallic catalysts, providing a synergistic interaction between the organic and inorganic frameworks and a fine tuning of the stereo-electronic properties of the resulting complexes, both instrumental to access multi-turnover catalysis. In particular, the covalently bound organic moieties have been accurately designed in order to afford a binding site for palladium. The resulting POM-based *N*-heterocyclic carbene (NHC) palladium complex has displayed an interesting catalytic activity toward MW-assisted Suzuki-Miyaura cross-coupling (also for less reactive aryl chlorides) and dehalogenation reaction.

Chapter 5 will describe a novel catalytic system for H_2O_2-based oxidations. A new aluminium-substituted POM has been synthesized and fully characterized, and it has displayed an interesting catalytic activity for oxidation of alcohols, olefins and sulfides in acetonitrile (yields and selectivities up to 99%). Changing the POM counteraction can yield water-soluble complexes, displaying high catalytic activity toward cyclohexanol oxidation in water (cyclohexanone yield up to 99%).

Riassunto

Con l’avvento della chimica sostenibile, i chimici si trovano a dover affrontare numerose sfide, soprattutto per quanto riguarda lo sviluppo di nuovi processi, prodotti e servizi che soddisfino i requisiti sociali, economici ed ambientali ora richiesti. Il raggiungimento di questi obiettivi richiede nuovi approcci, finalizzati principalmente alla riduzione delle materie prime e dell’energia utilizzate. Lo sviluppo di nuove metodologie sintetiche deve pertanto prevedere un maggiore impiego di materie prime rinnovabili e non tossiche, ma anche di condizioni e mezzi di reazione alternativi, col fine di ottenere processi più selettivi e sicuri.

Lo sviluppo di processi catalitici innovativi per applicazioni industrialmente rilevanti risulta perciò di primario interesse. In particolare, in questa Tesi sono state impiegate diverse strategie per implemetare processi chimici importanti, quali ossidazioni, reazioni di formazione di legame C-C e dealogenazioni.

I catalizzatori impiegati appartengono alla famiglia degli ossidi metallici polianionici noti come poliossometallati, di formula generale $[X_xM_mO_y]^{q-}$, dove M è il metallo costituente principale (Mo^{VI}, W^{VI}, V^{V}) e X un eventuale eteroatomo (P^{V} or Si^{IV}).

Questi complessi risultano dei catalizzatori vantaggiosi, grazie alla loro natura totalmente inorganica che li rende resistenti alla degradazione termica e ossidativa. Essi possiedono, inoltre, struttura, composizione chimica, densità elettronica e carica modulabili. Di particolare interesse è, poi, la possibilità di funzionalizzare i POMs con domini di natura organica, ottenendo così catalizzatori organici-inorganici di natura ibrida che possono permettere il miglioramento delle prestazioni catalitiche. Inoltre, diversi metalli (Ru, Fe, Pd, Al,…) possono essere incorporati nelle strutture dei POM con formazione di poliossometallati sostituiti, aprendo, quindi, nuove prospettive di catalisi. Queste specie possono, infine, essere facilmente ancorate su diversi supporti solidi per impieghi in catalisi eterogenea.

In particolare, in questa Tesi sono stati utilizzati sia POM ibridi che sostituiti con eterometalli per reazioni di ossidazione, formazione di legame C-C e dealogenazione.

La ricerca ha previsto l'uso di: (i) reagenti a basso impatto ambientale; (ii) mezzi di reazione sostenibili (liquidi ionici e acqua); (iii) tecniche di attivazione non convenzionali, quali l'irraggiamento con microonde (MW); (iv) reattori alternativi (microcanalari).

Nello specifico, nel Capitolo 2 verranno presentati i risultati di una strategia catalitica alternativa, basata sull'uso combinato di un poliossometallato ibrido, liquidi ionici e irraggiamento con microonde. Tale approccio ha permesso l'immobilizzazione, il riciclo e l'attivazione di una fase catalitica particolarmente efficiente per l’epossidazione di alcheni con

acqua ossigenata. L'epossidazione di olefine interne e terminali procede, infatti, con rese e selettività fino al 99%. In particolare, in condizioni di irraggiamento con microonde, l'ossidazione del *cis*-cicloottene procede quantitativamente in un minuto, con frequenze di turnover > 200 min^{-1}. Il sistema proposto si è dimostrato, inoltre, riciclabile, con rese quantitative di cicloottene epossido in almeno 4 cicli successivi. E' stato, infine, possibile miniaturizzare il sistema impiegando reattori microcanalari in processi a flusso continuo.

Nel Capitolo 3 verranno discussi i risultati di una collaborazione con l'Università di Roma – Tor Vergata. Il sistema catalitico studiato ha previsto l'uso di scandio triflato, liquidi ionici e irraggiamento con microonde per l'acilazione di Friedel-Crafts del ferrocene. Tale sistema risulta, ad oggi, il protocollo sintetico più efficiente per tale reazione.

Nel Capitolo 4 verrà, invece, descritto un nuovo sistema catalitico, efficiente sia per reazioni di formazione di legame C-C che per dealogenazioni. L'approccio proposto si basa sulla sintesi di POM ibridi opportunamente progettati in modo da fornire un'interazione sinergica tra le porzioni organica e inorganica, nonchè una modulazione delle proprietà stereoelettroniche. Entrambi questi aspetti risultano necessari per l'ottenimento di una catalisi efficiente e *multi-turnover*. In particolare, le porzioni organiche covalentemente legate al POM sono state studiate in modo da fornire un sito di legame specifico per il palladio. Il POM ibrido sintetizzato presenta, infatti, due carbeni *N*-eterociclici (NHC) leganti un atomo di palladio. Tale complesso si è dimostrato un efficiente catalizzatore sia per reazioni di Suzuki-Miyaura (anche per substrati meno reattivi, quali i cloruri arilici) che per dealogenazioni, entrambe promosse da microonde.

Infine, nel Capitolo 5 verrà descritto un nuovo sistema catalitico per l'ossidazione di diverse classi di substrati con acqua ossigenata. In particolare è stato sintetizzato e caratterizzato un nuovo POM sostituito con atomi di alluminio. Tale complesso è risultato particolarmente efficiente nell'ossidazione di alcoli, olefine e solfuri in acetonitrile (rese e selettività fino al 99%). Variando opportunamente il controcatione associato al POM, si possono ottenere, inoltre, complessi solubili in acqua. Questi ultimi hanno mostrato un'interessante attività catalitica per l'ossidazione del cicloesanolo in acqua (rese e selettività in cicloesanone fino a 99%).

Contents

1. General introduction

1.1 Green chemistry and sustainable catalysis

During the last years, one of the main concerns for chemists has been the search for environmentally sustainable processes, also due to the launch of new, more restrictive laws for environmental protection and pollution remediation. This concept is known as "Green Chemistry" and, according to the definition by Paul Anastas (US Environmental Protection Agency, EPA), there are 12 guiding Principles for the design of innovative environmentally benign processes and products.[1]

These principles can be considered as an overall series of reductions/limitation, claiming at the economic, environmental and social improvements, as represented in Figure 1.1.[2]

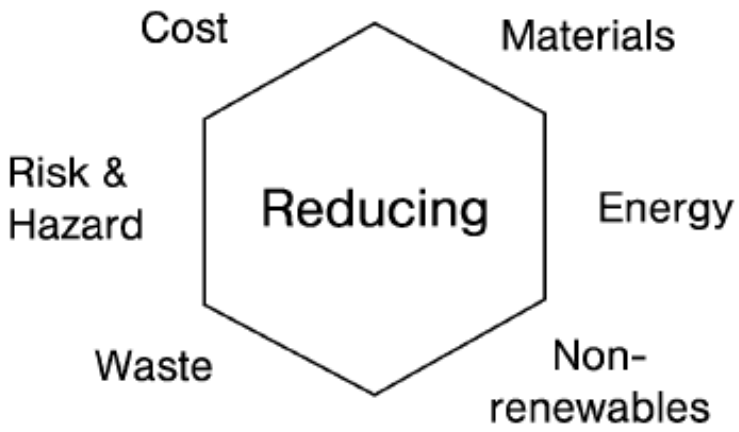

Figure 1.1. "Reducing": The heart of Green Chemistry.[2]

Waste prevention/minimization represents one of the main concerns, together with the need to exclude of the use of toxic and/or hazardous reagents in the manifacture of chemical products.

Making processes more efficient, by reducing material and energy consumption and increasing the use of renewable resources, is another of the strategies of Green Chemistry towards a sustainable manufacturing industry.[3]

Green Chemistry is thus leading us towards the "ideal synthesis" (Fig. 1.2).[2, 4]

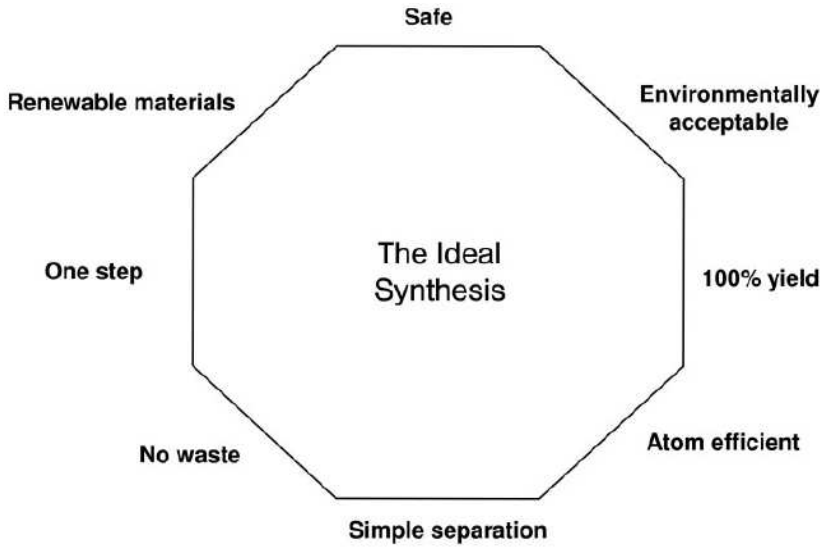

Figure 1.2. Features of the "ideal synthesis".[2]

The "yield" parameter usually provides a simple and understandable way in chemistry research for measuring and comparing the efficiency of a synthetic route. However, it does not take into account the amount of consumed reagents, the incomplete recovery of solvents and catalysts and, above all, the energy-consuming separation stages (such as solvent separations, distillations, recrystallizations and so on). Green Chemistry metrics[5] are rather based on the "atom efficiency" concept, i.e. the maximization of the number of atoms introduced into a process into the final product.[1]

Also the technologies to be applied must be as "clean" as possible. Some of them are summarized in Fig. 1.3 and they range from well-established technologies to new and largely unproven ones.

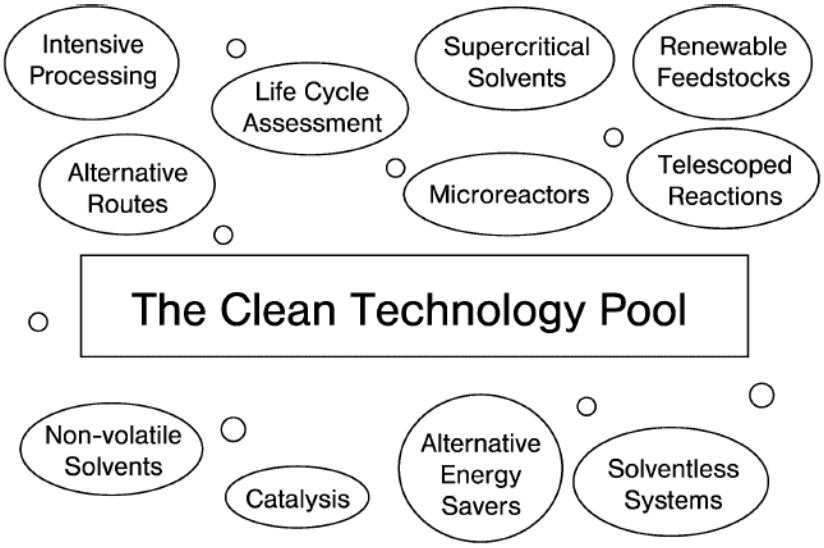

Figure 1.3. The major clean technologies.[2]

Among "clean" strategies, one of the most important targets for chemical companies is the replacement of hazardous volatile organic compounds (VOCs) used as solvents, representing the main source of chemical waste in industry. Some VOCs (e.g. carbon tetrachloride and benzene) have been widely prohibited and replaced, but there is still a widespread use of other problematic solvents, such as dichloromethane. Improvements towards greener processes have included the use of alternative reaction media (e.g. supercritical carbon dioxide[6], water[7] and ionic liquids[8]), but also the total removal of the solvent (i.e. solvent-free processes[9]).

Recently, a lot of environmentally friendly protocols, contemplating the use of alternative reactors (such as continuous flow, membrane and microchannel reactors), have also been reported in literature. In particular, microchannel reactors have been intensively studied,[10] because they reduce hazards and risks (by using small reaction volumes) and are less energy-consuming with respect to traditional batch processes, which often suffer of poor heat transfer and mixing. Nowadays, energy has become an important parameter to take into account in developing new processes, as its cost is increasing. Great efforts are addressed not only to design better reactors (such as those mentioned above), but also to use alternative energy sources, such as microwaves[11] and ultrasounds.[12] Both of these techniques exploit an intensive direct radiation to activate chemical reactions, and their application often allows shortening reaction times and increasing product yields and selectivities.

Last but not least, one of the main statements of the 12 principles of Green Chemistry indicates that "*catalytic rather than stoichiometric reagents*" have to be used, as catalysts are used in small amounts and can carry out a single reaction many times. Nowadays, many chemical processes continue to operate using stoichiometric reagents (e.g. in oxidations) or, even when catalysts are used, they often show low turnover numbers (due to rapid catalyst poisoning or decomposition) and cannot be recycled. So there is a strong need in developing efficient catalytic processes, able to afford high yields and selectivities, together with an easy products separation, in order to recover (and reuse) the catalyst itself. With this aim, heterogenized catalysts, as well as alternative catalyst technologies (e.g. catalytic phases or membranes), are intensively studied.

The aim of this Thesis is directed to the design of innovative and sustainable catalytic systems, with good performance in terms of yields, selectivities and recycling, together with the use of benign reaction conditions.

All the investigated systems deal with the use of catalysts belonging to the family of polyoxometalates.

1.2 Polyoxometalates in catalysis

1.2.1 Polyoxometalates: a general introduction

The history of polyoxometalates (POMs) can be traced back to early XIX century,[13] when it was discovered that metals belonging to early transition series such as niobium, vanadium, tantalum, molybdenum and tungsten, in their higher oxidation states (configuration d^0 or d^1), can form in aqueous solution (at suitable pH, concentration and temperature) discrete polynuclear oxoanions of variable sizes (from few Ångströms to tens of nanometers).[14, 15, 16, 17, 18] Such complexes are known as polyoxometalates.

They can be classified on the basis of their chemical composition, being represented by two types of general formulas:[14-18]

a) $[M_mO_y]^{p-}$

b) $[X_xM_mO_y]^{q-}$

where M is the transition metal constituent the polyoxometalate and X can be a non-metal atom (P, Si, As, Sb or another element of the p-block), or a different transition metal. In the first case (a), polyoxometalates are called isopolyanions, while in the second case (b), heteropolyanions.

In Figure 1.4, some examples of polyoxometalate structures are represented.

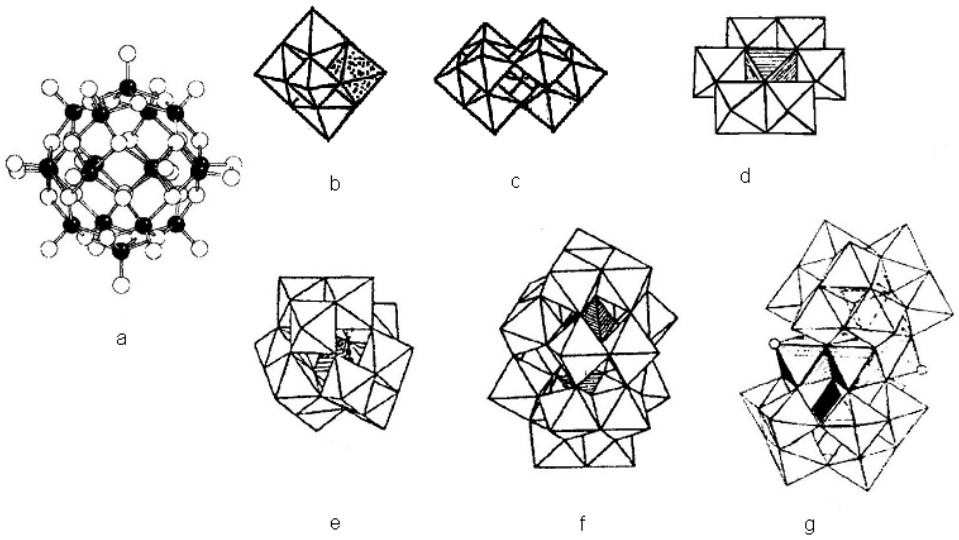

Figure 1.4. Different structures of polyoxometalates: a) *ball-and-stick* representation for the isopolyvanadate $[V_{18}O_{42}]^{12-}$, in which the black spheres are V^{IV} atoms. b) Lindqvist $[M_6O_{19}]^{2-}$ structure (M = Mo, W) and its dimeric $[W_{10}O_{32}]^{4-}$ decatungstate derivative (c). d) Anderson-Evans heteropolyanion $[XMo_6O_{24}]^{m-}$ (X = P, As). e) α-Keggin $[XM_{12}O_{40}]^{n-}$ structure (X = P, Si, B, Al, Ge; M = Mo, W). f) α-Wells-Dawson $[X_2M_{18}O_{62}]^{n-}$ structure (X = P, Si; M = Mo, W). g) Krebs $[M'_4(H_2O)_y(XW_9O_{33})]^{n-}$ structure (X = Bi, As, Sb, Te; M' = Zn, Al, W).

In most cases, POMs structure derives from formal aggregation of octahedral units MO_6, in which the metal M is surrounded by 6 oxygen atoms. Condensation of such octahedra occurs by oxygens sharing, with the formation of M-O-M μ-oxo bridges. Two octahedra usually share one or two oxygens (corner- or edge-sharing respectively, Figure 1.5), while sharing three oxygens (face-sharing) is quite rare.

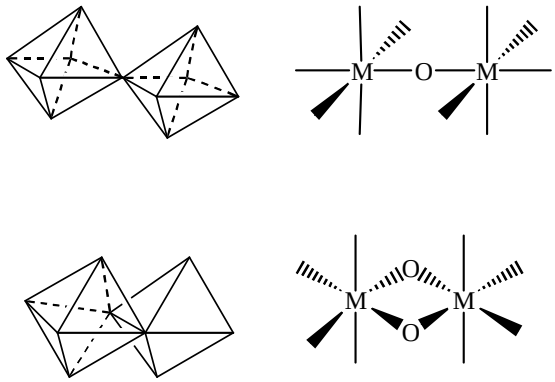

Figure 1.5. Condensation of octahedral units in polyoxometalates by corner- or edge-sharing.

Oxygens that are not shared with other metal atoms within the complex are called terminal oxygens (O_t) and they form short and strong (double) bonds with the metal itself (Lipscomb's law[19]). In Figure 1.6, two kinds of octahedra constituting POMs structures are represented.[14] The first one (a) is a mono-oxo type octahedron, with one O_t and five oxygens shared with other metal atoms within the POM structure. The second one (b) is a *cis*-di-oxo type octahedron, having two terminal oxygens in *cis* position, while the remaining four oxygens are shared with other metal atoms within the POM structure.

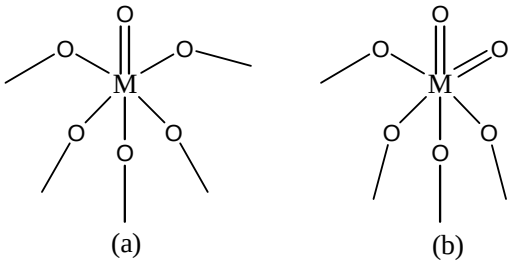

Figure 1.6. Two kinds of octahedra constituting the most common structures of the polyoxometalates.

Hence, the main features a metal must possess to originate polyoxometalate are:[14]

i) cationic radius compatible with an octahedral coordination;

ii) presence of empty and available d orbitals, in order to form the terminal metal–oxygen double bond.

The first feature explains, for example, the absence of a polyanionic chemistry for Cr^{VI}: its small cationic radius (0.58 Å) can bear a maximum of four coordinating oxygens.

The presence of terminal oxygen atoms is instead responsible for the aggregation into discrete structures and not into an extended material (as for most common metal oxides, silicates, germanates and tellurates). Since terminal oxygens are less basic, they do not condense with other units, thus providing a barrier towards the linear polymerization and finally yielding discrete molecular units.[14]

One of the most studied classes of polyoxometalates is constituted by Keggin heteropolyanions, with general formula $[XM_{12}O_{40}]^{n-}$ (X = Si^{IV}, P^{V}, Ge^{IV}, As^{V} and M = Mo^{VI} or W^{VI}). In 1934, Keggin reported the structure of the dodecatungstophosphoric acid $[PW_{12}O_{40}]^{3-}$, by powder X-ray investigation.[20] This structure is known as α-Keggin and consists of a central PO_4 tetrahedron surrounded by 12 mono-oxo WO_6 octahedra. Such octahedra are arranged in four groups (triplets W_3O_{13}), each of them derived from the aggregation of three octahedral units by edge-sharing. The four different triplets are condensed together by corner-sharing.

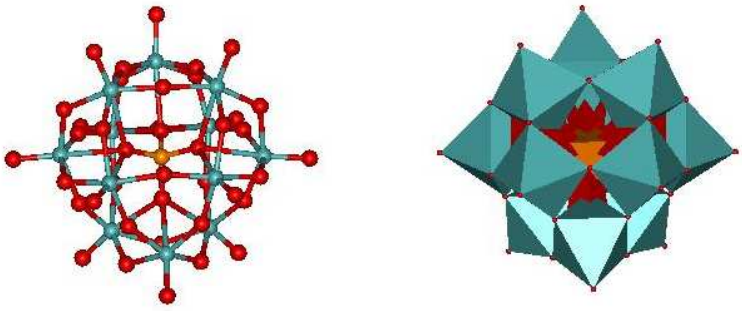

Figure 1.7. Two representations of the same α-Keggin structure of the $[PW_{12}O_{40}]^{3-}$ heteropolyanion. On the left side, a *ball-and-stick* model in which the red spheres are oxygen atoms, the blue are tungsten atoms and the orange one is the central phosphorous atom. On the right side, a polyhedral model is represented: the blue octahedra are centred on tungsten atoms, while the orange tetrahedron is centered on the phosphorous atom.

Structure and symmetry of α-Keggin polyanions have also been confirmed in solution by ^{17}O-, ^{29}Si-, ^{31}P- and ^{183}W-NMR spectroscopies.[21, 22, 23, 24] NMR characterizations of $[\alpha\text{-}PW_{12}O_{40}]^{3-}$ and $[\alpha\text{-}SiW_{12}O_{40}]^{4-}$ are reported in Table 1.1.

Table 1.1. Heteronuclear NMR characterizations of heteropolyanions with α-Keggin structure.

Polyoxoanion	**^{183}W-NMR[a] δ, ppm**	**^{31}P-NMR[b] δ, ppm**	**^{29}Si-NMR[c] δ, ppm**	**^{17}O-NMR[d] δ, ppm**
$[\alpha\text{-}PW_{12}O_{40}]^{3-}$	-99.4	-14.9	---	769 (O_t), 431, 405 (O_B, O_C), n.d. (O_A)
$[\alpha\text{-}SiW_{12}O_{40}]^{4-}$	-103.8	---	-85.3	761 (O_t), 427, 405 (O_B, O_C), 27 (O_A)

[a] ref.: 1 M WO_4^{2-} in D_2O; [b] ref.: 85% H_3PO_4; [c] ref.: $Si(CH_3)_4$; [d] ref.: H_2O.

The chemical equivalence of the 12 tungsten atoms leads to a single signal in both the ^{183}W-NMR spectra.[21] One signal is also observed for the central atom (Si or P),[22, 23] while four different resonances are observed in ^{17}O-NMR spectra.[24] Indeed, the 40 oxygen atoms of the α-Keggin structure can be distinguished in: (i) 4 oxygens bonded to the central atom (O_A); (ii) 12 terminal oxygens (O_t); (iii) 12 oxygens bridging different triplets by corner-sharing (O_B); (iv) 12 oxygens bridging octahedra which belong to the same triplet by edge-sharing (Oc).

Keggin polyoxometalates possess also structural isomers, formally obtained from the α structure by 60° rotation of one (β isomer), two (γ isomer), three (δ isomer) or four (ε isomer) W_3O_{13} triplets.[14, 15] These isomers show lower symmetry and a decreased thermodynamic stability with respect to the α structure.

The heteropolyoxotungstates described above are also called "saturated" structures, due to the high symmetry, the low anionic charge and the stability of the structure itself. However, starting from them, it is possible to synthesize derivatives with defects in the structure, the so called "vacant" (or "lacunary") polyoxometalates. Such complexes derive from saturated POMs by formal loss of one or more octahedral units, thus creating vacancies on the surface. As an example, the structure of the monovacant polyoxotungstate $[\alpha\text{-}XW_{11}O_{39}]^{n-}$ ($X = Si^{IV}$, P^{V}, …), derived from the α-Keggin saturated structure, is reported in Figure 1.8.[25]

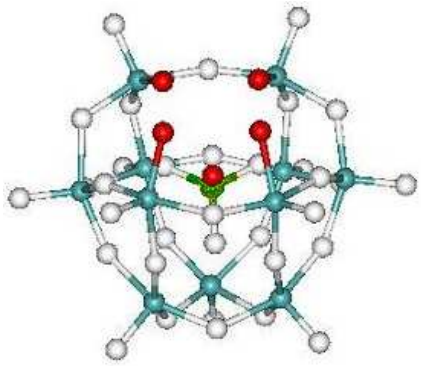

Figure 1.8. *Ball-and-stick* representation of the structure of the monovacant α-Keggin $[XW_{11}O_{39}]^{n-}$. The blue spheres are tungsten atoms, the white are oxygens and the green one is the central heteroatom X. The red spheres are the nucleophilic oxygen atoms around the vacant site (see Paragraph 1.2.2).

Synthetic procedures and experimental conditions to yield these species are strictly related to the thermodynamic and kinetic stability of the lacunary complexes themselves.

Monovacant $[XW_{11}O_{39}]^{n-}$ ($X = Si^{IV}$, P^{V}) POMs are stable and can be isolated.

Di- ($[XW_{10}O_{36}]^{m-}$) and tri-vacant species ($[XW_9O_{34}]^{p-}$), resulting from the formal loss of two or three octahedra respectively, can also be prepared (see Fig. 1.9).[26]

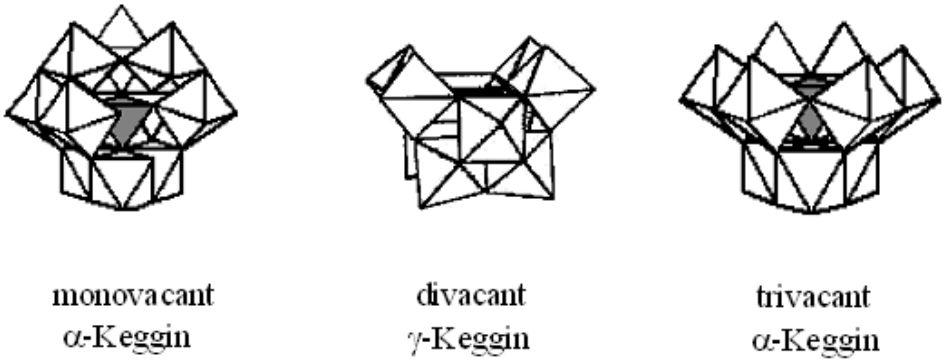

Figure 1.9. Polyhedral structures of mono-, di- and tri-vacant Keggin polyoxotungstates.

Taking into account what said above, a great variety of structures belongs to the family of POMs and they can be obtained by tuning specific parameters like concentration, reactants stoichiometric ratios, temperature and pH. Noteworthy, isostructural polyoxometalates may also display different properties depending both on the heteroatom X and the associated countercation. Moreover, the choice of a suitable counterion allows to solubilize POMs in a wide range of solvents, from apolar ones (toluene, dichloromethane), by using lipophylic cations such as tetraoctylammonium, to water, by using alkaline counterions or protons.

Furthermore, since they are constituted by metal atoms in their highest oxidation states, polyoxometalates result more stable towards the oxidative degradation than generic organic compounds.

The widespread use of polyoxometalates in catalysis is also related to their appealing ability to act as ligands for different transition metals[14-16] and to the possibility of covalently functionalizing their surfaces with organic moieties.[27-29] Both these aspects of POMs chemistry will be discussed in the following Paragraphs.

1.2.2 Transition metal-substituted polyoxometalates

As anticipated above, polyoxometalates can act as ligands for different transition metals, such as chromium, iron, manganese, cobalt and ruthenium. The coordination of heterometals by a polyoxometalate complex can take place essentially in two ways:[14-16]

i) through superficial coordination of the metal cation with the anionic oxygens on the surface of the POM by electrostatic interaction (*Supported Complexes*);

ii) by incorporating the transition metal in the polyoxometalate framework (*Transition Metal-Substituted Polyoxometalates, TMSPs*).

While *Supported Complexes* are preferentially formed through weak interactions in organic solvents and in the presence of highly charged POMs, *Transition Metal-Substituted Polyoxometalates* show high stability also in water, since the transition metal becomes an effective constituent of the whole polyanion structure.

The synthesis of *TMSPs* requires the use of "vacant" polyoxometalates, e.g. the monovacant Keggin polyanion described in the previous Paragraph (see Fig. 1.8). This complex possesses five "lacunary" oxygens, highlighted in red in Figure 1.8 and in Scheme 1.1. Reaction of such vacant POM with a suitable transition metal precursor (M'L) yields the incorporation of this metal into the POM structure, thus forming the *TMSP* (see Scheme 1.1). In the resulting complex, lacunary oxygens act as a polydentate binding site, able to coordinate a large variety of transition metals M'.

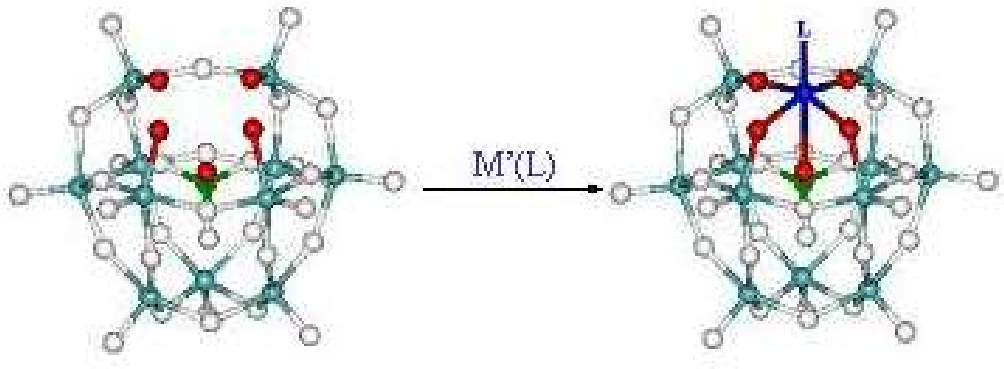

Scheme 1.1. Incorporation of a heterometal M' into the "lacuna" of the monovacant polyoxometalate $[XW_{11}O_{39}]^{n-}$.

Beside the "in pocket" coordination mode of transition metal M' described above, *TMSPs* can be also obtained with an "out of pocket" structural motif, or as *sandwich-like* dimeric structures, as represented in Figure 1.10.

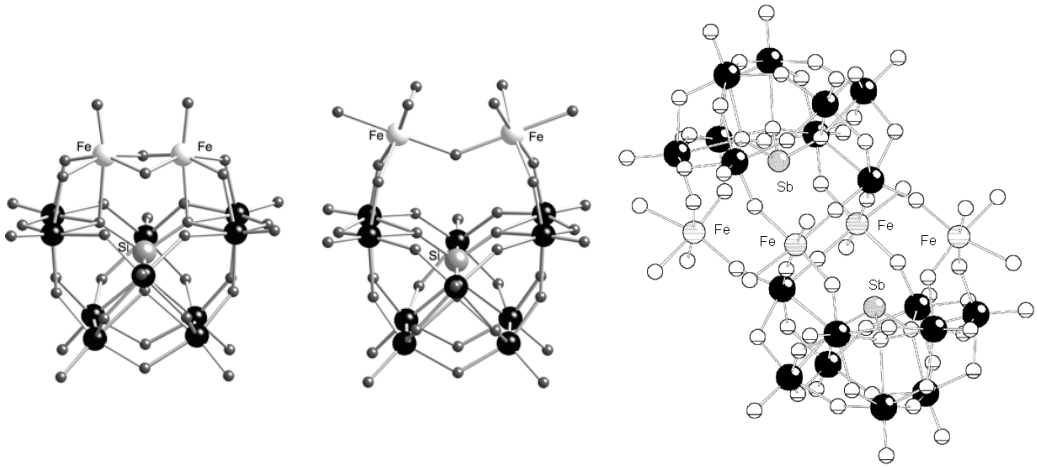

a b c

Figure 1.10. Structural motifs for iron-substituted polyoxotungstates: a) “in pocket”, b) “out of pocket”, c) *sandwich-like*.

Considering the high versatility in terms of structure, chemical composition, electron density and polyanionic charge, it is easy to explain why polyoxometalates are such good candidates as catalysts.

1.2.3 Hybrid polyoxometalates

As already mentioned, vacant POMs feature reactive, coordinatively unsaturated, nucleophilic oxygen atoms. Then, they can also react with electrophilic organic moieties to yield organic-inorganic hybrid complexes (see Scheme 1.2).[27, 28, 29]

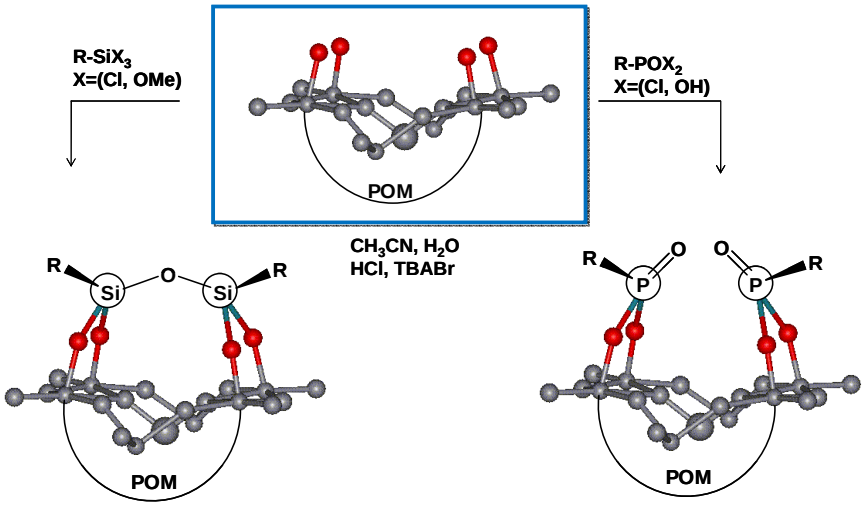

Scheme 1.2. Functionalization of vacant polyoxometalates with organic moieties to yield hybrid POMs. Lacunary oxygens are highlighted in red.

Different procedures have been optimized in order to synthesize organic–inorganic POM-based hybrid complexes, starting from both organosilyl (SiX_3, X = Cl, OMe) and organophosphonyl (POX_2, X = Cl, OH) compounds as electrophilic reagents. The covalent functionalization of different lacunary POMs has been achieved with yields ranging from 65 up to 90%.[30]

The functionalization of the divacant Keggin complex $[\gamma\text{-}SiW_{10}O_{36}]^{8-}$ is particularly effective, due to the high hydrolytic stability of the polyanion in the acidic medium needed for the reaction. $[\gamma\text{-}SiW_{10}O_{36}]^{8-}$ has indeed four equivalent nucleophilic oxygen atoms on the lacuna, which can react with two or four equivalents of the electrophilic compound, yielding respectively the *bis*- and the *tetra*-functionalized hybrids, with high selectivities (Figure 1.11).[31]

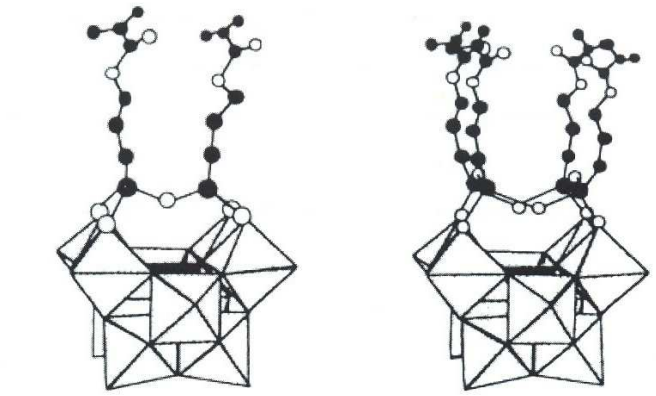

Figure 1.11. Structures of the *bis*- and *tetra*-substituted decatungstosilicate derivatives.

The covalent functionalization of the vacant polyoxoanion improves the stability of the overall molecule and may induce further catalyst diversity, possibly including the high desirable chiral up-grade. The derivatization of polyoxometalates is useful to: (i) stabilize molecular structures which can otherwise give isomerization or decomposition;[32] (ii) support organic molecules and organometallic catalysts, by using the vacant POM as a scaffold; (iii) tune the solubility of the POM in different reaction media (flourinated phases, ionic liquids, etc.); (iv) introduce polyfunctional groups to be used as spacers between polyoxometalates, thus allowing the synthesis of dendrimeric[29] or polymeric hybrid materials.[31]

The support of organometallic catalysts onto the POM scaffold will also be presented in this Thesis, starting from the synthesis of hybrid polyoxometalates decorated with imidazolium moieties. The latter are indeed well-known precursors for *N*-heterocyclic carbenes (NHC).[33] Hence, we have been able to covalently bind a palladium-NHC complex to the lacuna of $[\gamma\text{-}SiW_{10}O_{36}]^{8-}$, thus generating a hybrid catalyst. This compound has displayed a synergistic interaction between the organic and inorganic frameworks, instrumental to perform efficient Suzuki-Miyaura and dehalogenation reactions.[34] This chemistry will be discussed in Chapter 4 of this Thesis.

Finally, hybrid polyoxometalates have been used also as building blocks evolving to self-assembled supramolecular aggregates and to nanostructured systems.[35] The aggregation can lead to spherical vesicles, thus providing an interesting microenvironment for catalytic application, as well as a system to be exploited as molecular carrier.[36]

1.2.4 Activation of H_2O_2 by polyoxometalates

Over the past two decades, the research about applications of polyoxometalates in material science, analytical chemistry, surface chemistry, medicine, electrochemistry and photochemistry has become very important, as reflected by the number of excellent papers and reviews devoted to this topic.[16, 36a, 37] However, the main applications of polyoxometalates are related to catalysis, where their use as Brönsted acids and homogeneous oxidation catalysts has been firmly established since the late 1970s. The development of novel ideas and concepts is moving the use of POMs towards new frontiers, leading to important practical applications in hydrogenations,[38] click chemistry,[39] carbon-carbon bond formation.[40] Moreover, relationships between structure, reactivity and selectivity, which trace the way to the understanding of reaction mechanisms, are often relevant for further improving POMs performance.[14, 17]

In the specific field of oxidation catalysis, polyoxometalates show a distinct advantage over the widely investigated organometallic compounds, that is their relevant stability in the presence of several oxidants, including the environmentally benign H_2O_2.

An overview of oxidation catalysis by polyoxometalates, activating hydrogen peroxide, will be presented in this paragraph and developed in the following chapters of this Thesis.

Among oxidation processes using hydrogen peroxide, those catalyzed by high valent d^0 transition metals (such as Ti^{IV}, V^{V}, W^{VI}, Mo^{VI}) are between the most useful and selective.[41] Experimental evidences on the nature of the intermediates have proven that H_2O_2 association to these d^0 transition metals leads to the formation, in solution, of highly reactive metallo-peroxidic species, acting as the competent oxidants in the catalytic cycles (Scheme 1.3).

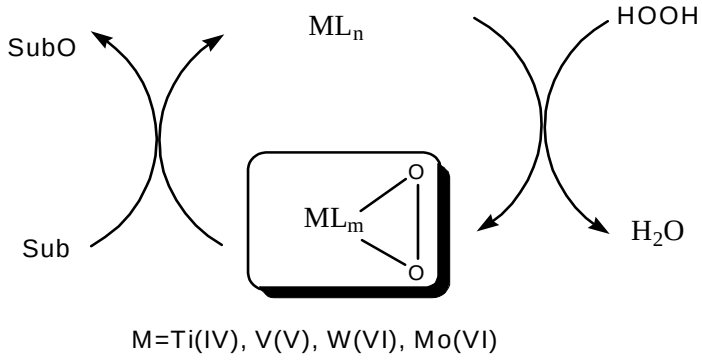

Scheme 1.3. Catalytic cycle for H_2O_2 activation by d^0 metals.

Several research groups studied the interaction of lacunary polyoxometalates (or their parent Keggin anions) and hydrogen peroxide.[42] Peroxotungstates were used by Ishii[43, 44, 45] and co-workers to perform selective epoxidation of olefins with hydrogen peroxide, under phase transfer conditions. In this system, the competent oxidant species in solution are dimeric peroxotungstate complexes, such as $\{PO_4[WO(O_2)_2]_4\}^{3-}$, [46] also obtained by Venturello,[47, 48, 49] Mimoun[50] and Noyori.[51, 52] Jacobs and co-workers reported a biphasic system for the epoxidation of acid sensitive olefins catalyzed by $\{PO_4[WO(O_2)_2]_4\}^{3-}$ in the presence of (aminomethyl)phosphonic acid.[53]

In contrast to monomeric or dimeric peroxo species, polynuclear peroxo species are expected to show specific reactivity and selectivity because of their electronic and structural features. Keggin polyoxometalates, namely $[XW_{12}O_{40}]^{n-}$, $[XW_{11}O_{39}]^{m-}$, $[XW_{11}VO_{40}]^{p-}$ and $[XW_{11}M^{III}(H_2O)O_{40}]^{q-}$ (where X = Si^{IV}, P^{V} and M = Fe, Mn) bearing lipophylic tetrabutylammonium cations, have been used for the oxidation of cyclooctane with H_2O_2, yielding cyclooctyl hydroperoxide with high selectivity.[54]

A lipophylic decatungstate, namely $(n\text{Bu}_4\text{N})_4W_{10}O_{32}$, was used for the selective oxidation of alcohols to carboxylic acids and ketones using hydrogen peroxide.[46f, 55, 56]

$[H_2ZnSiW_{11}O_{40}]^{6-}$ [57] and a polyfluorooxometalate complex, namely $[Ni(H_2O)NaH_2W_{17}O_{55}F_6]^{9-}$,[58] were also used respectively to oxidize alcohols and olefins with hydrogen peroxide.

In some cases, one or more peroxidic η^2-groups can be formed on different transition metal ions, as in the titanium peroxo complex $(n\text{Bu}_4\text{N})_5[PTi(O_2)W_{11}O_{39}]$, isolated by Poblet and Kholdeeva.[59] On the other hand, epoxidation of olefins and allylic alcohols was performed using *sandwich-like* polyoxometalates containing Fe^{III},[42d] Zn^{II},[60] Pt^{II}, Pd^{II}, Rh^{III},[61] Ru^{III} and Mn^{II},[62] showing only a little dependence on the nature of the heterometal, thus supporting the hypothesis of the formation of W-peroxo groups. Formation of peroxotungstic groups was also confirmed by Neumann and co-workers by FT-IR and ^{183}W-NMR analyses.

The most promising epoxidation catalysts belong to the family of vacant polyoxotungstates. Acerete[63] and co-workers synthesized and characterized by X-ray the first peroxo-polyoxometalate complex: the vacant Keggin polyanion $[Co^{III}W_{11}O_{39}]^{9-}$, grafted by four peroxo moieties to yield $[\beta_3\text{-}Co^{II}W_{11}O_{35}(O_2)_4]^{10-}$.

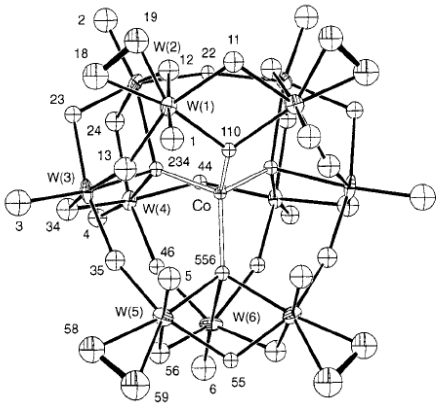

Figure 1.12. Structure of $[\beta_3\text{-}Co^{II}W_{11}O_{35}(O_2)_4]^{10-}$.

This complex was used to epoxidize 2-cyclohexenol with hydrogen peroxide in a biphasic $CHCl_3$ / CH_3CO_2H (aq) system and the results are reported in Scheme 1.4.

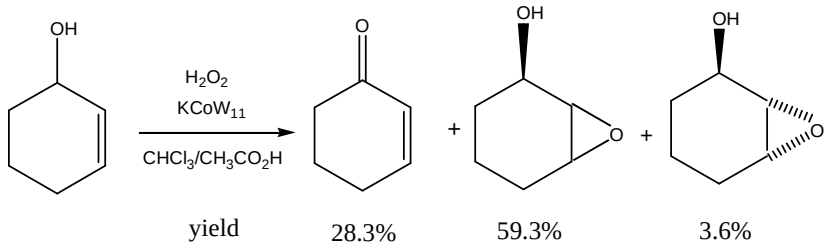

Scheme 1.4. Oxidation of 2-cyclohexenol by $[\beta_3\text{-}Co^{II}W_{11}O_{35}(O_2)_4]^{10-}$ (indicated as $KCoW_{11}$ in the Scheme).

Recently, lacunary $[SbW_9O_{33}]^{9-}$ was proposed as an efficient catalyst for the selective epoxidation of alkenes with H_2O_2 (yields up to 99%) in organic solvent-free conditions, using a phase transfer agent.[64]

In 2003, Mizuno[65] and co-workers presented the benchmark performances of the divacant decatungstosilicate $[\gamma\text{-}SiW_{10}O_{34}(H_2O)_2]^{4-}$ for efficient and selective epoxidation of olefins. The proposed catalytic system shows an interesting regioselectivity when applied to diolefins.[66] The same complex was used by Ren[67] and co-workers to perform sulfoxidations, promoting the oxidation to sulfone in the presence of imidazole.

Both cyclic olefins, such cyclohexene, 1-methyl-1-cyclohexene, *cis*-cyclooctene, cyclododecene and 2-norbornene, and non-activated terminal C_3-C_8 olefins, such as propylene, 1-butene and 1-octene, can be transformed into the corresponding epoxides with ≥ 99% selectivity and ≥ 99% efficiency of hydrogen peroxide utilization.[68] 1,3-butadiene was epoxidized selectively to give the corresponding mono-epoxide, without the epoxidation of the second C=C fragment (i.e. no diepoxide was formed).[68] The decomposition of hydrogen peroxide to form molecular oxygen was reported to be negligible, reducing the risk of

building an explosive atmosphere and simplifying the security measurements. Thus, the catalytic performance of $[\gamma\text{-}SiW_{10}O_{34}(H_2O)_2]^{4-}$ raises to the perspective of industrial application.

The opportunity of using lacunary polyoxometalates as precursors for polynuclear peroxo species is an important issue, since the vacant sites are able to activate hydrogen peroxide.[63] The epoxidation of 1-octene with hydrogen peroxide catalyzed by a series of tungstosilicates in acetonitrile at 32°C was also examined.[65] The mono-, di- and trivacant Keggin tungstosilicates (see Fig. 1.9), as well as the saturated one, were converted into the corresponding tetrabutylammonium salts, by cation metathesis. The divacant decatungstosilicate $[\gamma\text{-}SiW_{10}O_{36}]^{8-}$ (**I**) showed a moderate catalytic activity, whereas the mono- and trivacant compounds, together with the non lacunary dodecatungstosilicate, were almost inactive. The catalytic activity of **I** strongly depends on the pH values used during the synthesis of the corresponding tetrabutylammonium salts. For example, for 1-octene epoxidation, the following yields after 6 h were reported: 75% (pH 2), 52% (pH 1), >51% (pH 3, 4), >32% (pH 0). Hence, the catalyst prepared at pH 2 (compound **I***) exhibited the highest activity. By X-ray crystallographic structural analysis, performed on the tetramethylammonium salt, the formulation of **I*** could be determined as $[\gamma\text{-}SiW_{10}O_{34}(H_2O)_2]^{4-}$, involving two terminal W-(OH_2) (*aquo* ligand) groups. Therefore, four protons are associated with the anionic cluster of **I***, as later confirmed by our research group by means of DFT calculations (see Fig. 1.13, A and B).[69]

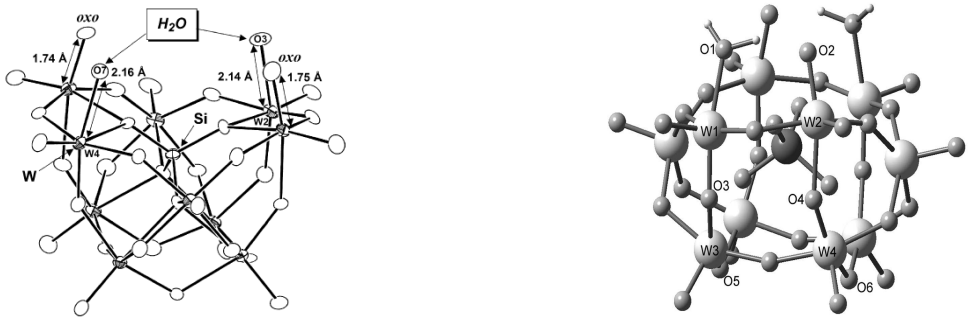

A B

Figure 1.13. $[\gamma\text{-}SiW_{10}O_{34}(H_2O)_2]^{4-}$: X-ray crystallographic molecular structure determined by Mizuno et al. (A)[65] and DFT optimized structure (B).[69]

The catalytic activity of **I*** for 1-octene epoxidation was then compared with that of $[PO_4\{WO(O_2)_2\}_4]^{3-}$ and $[\{WO(O_2)_2(H_2O)\}_2(\mu\text{-}O)]^{2-}$, both reported to be effective catalysts for H_2O_2-based epoxidations.[47-49, 70, 71] In each case, using the same tungsten loading, the selectivity towards 1,2-epoxyoctane is ≥ 99% but **I*** showed the highest activity among the

screened catalysts (yields after 10 h; **I***: 90%, $[PO_4\{WO(O_2)_2\}_4]^{3-}$: 38%, $[\{WO(O_2)_2(H_2O)\}_2(\mu\text{-}O)]^{2-}$: 25%).[65]

Moreover, no substantial changes of FT-IR spectral pattern of **I*** were observed during the catalytic epoxidation with hydrogen peroxide, thus confirming the structural stability of **I*** under turnover regime. On the other hand, a mixture of hydrogen peroxide, the olefin and the saturated Keggin complex $[PW_{12}O_{40}]^{3-}$ exhibited a drastic change of FT-IR spectral pattern, due to the conversion of $[PW_{12}O_{40}]^{3-}$ to $[PO_4\{WO(O_2)_2\}_4]^{3-}$. The contrast shows that the analogous silicon derivative (i.e. $[SiO_4\{WO(O_2)_2\}_4]^{4-}$) was not formed in the catalytic system of **I***, hydrogen peroxide, olefin and acetonitrile. Kinetic study revealed the first-order dependence of the reaction rate on the concentration of **I***, also supporting this idea. Furthermore, catalyst **I*** can be easily recovered.

Another interesting aspect of such catalytic system concerns the oxidation of *Z*- and *E*-2-octenes, for which a retention of the C=C bond configuration was observed in the corresponding epoxides. Moreover, in competitive reactions, *Z*-2-octene was oxidized faster than the *E*- isomer, being the *E/Z* experimental ratio 2,3-epoxyoctane = 11.5. This value is higher than those obtained for other tungstate-H_2O_2 systems[52] and for the stoichiometric epoxidation with organic oxidants such as *m*-chloroperbenzoic acid (*m*-CPBA)[72] and dimethyldioxirane,[73] as shown in Table 1.2.

Table 1.2. Comparison of R_Z/R_E values for the competitive epoxidation of *Z*- and *E*-olefins.

System	**Olefin**	$\mathbf{R_Z / R_E}$
(nBu$_4$N)-**I***/H_2O_2 [65]	*Z*-2-octene/*E*-2-octene	11.5 [a]
$H_3PW_{12}O_{40}/H_2O_2$ [45]	*Z*-2-octene/*E*-2-octene	3.7 [b]
$NH_2CH_2PO_3H_2/WO_4^{2-}/H_2O_2$ [52]	*Z*-3-octene/*E*-3-octene	7.3
m-CPBA [72]	*Z*-2-octene/*E*-2-octene	1.2
Dimethyldioxirane [73]	*Z*-3-hexene/*E*-3-octene	8.3

[a] (nBu$_4$N)-**I*** (8 μmol), *Z*-2-octene (5 mmol), *E*-2-octene (5 mmol), 30% aq. hydrogen peroxide (1 mmol), CH_3CN (6 mL), 32 °C. [b] $H_3PW_{12}O_{40}$ (8 μmol), cetylpyridinium chloride (24 μmol), *Z*-2-octene (1 mmol), *E*-2-octene (1 mmol), 30% aq. hydrogen peroxide (3 mmol), $CHCl_3$ (5 mL), 60°C.

Such a high stereospecificity suggests the contribution of a structurally rigid, non-radical oxidant generated on **I***. The authors could indeed isolate the di-peroxo species, where the two aquo ligands W-(OH_2) were substituted by W(O_2) groups.[74]

Another interesting approach in POM-based oxidation catalysts is the possibility of preparing novel hybrid complexes (see Paragraph 1.2.3) with extended architectures,[75] in which the merging of organic and inorganic domains produces a functional synergistic effect, with the final goal of improving the catalytic performance.

The analysis of isostructural hybrids reactivity shows that their catalytic performance is strongly dependent on the structure/composition of the inorganic framework, as well as on the nature of the organic moiety decorating the POM surface.[28a] Between the screened catalysts, the hybrid polyoxoanion $[\gamma\text{-}SiW_{10}O_{36}(PhPO)_2]^{4-}$ (in which two phenylphosphonic moieties are covalently linked to the lacunary POM) showed a good catalytic activity for the oxidation of different classes of substrates in halide-free solvent[28a] and in ionic liquids.[28b] Furthermore, the functionalization of the vacant site prevents the rearrangement of the POM structure:[76] indeed stability studies by means of heteronuclear NMR, FT-IR and ESI-MS analyses revealed that the complex is stable at high temperature and under microwave (MW)-irradiation.[28]

MW-induced dielectric heating is efficiently absorbed by these polycharged catalysts, behaving as MW-activated molecular heat carriers.[77] With $[\gamma\text{-}SiW_{10}O_{36}(PhPO)_2]^{4-}$ and under MW-irradiation, the oxidation scope was expanded to include highly reactive substituted olefins, alcohols and sulfides, as well as electron-poor alkenes, ketones and sulfoxides. Indeed, the best performances were obtained in the oxidation of internal olefins, organosulfur compounds, secondary and benzylic alcohols. Good to excellent H_2O_2 conversions after 10-50 minutes of MW-irradiation were observed, using 0.8% of catalyst loading.[28a] A mechanistic study was carried out in order to define the catalyst behaviour. Competitive epoxidation of isomeric 2-hexenes showed a *Z*/*E* reactivity ratio > 9. Such *Z* preference speaks in favour of a POM-based peroxide as the actual oxidant.[78] Finally, the formation of a transient η^1-hydroperoxo intermediate via association equilibria of H_2O_2 to the POM precursor[79] was also suggested to explain the atypical biphilic behaviour found in Hammett linear free energy correlations.[28a, 80, 81]

Hybrid $[\gamma\text{-}SiW_{10}O_{36}(PhPO)_2]^{4-}$ was also tested in the epoxidation of olefins with H_2O_2, using ionic liquids (ILs) as alternative reaction media to replace hazardous volatile organic solvents (VOCs).[28b] ILs were successfully used as solvents for metal-catalyzed oxidations with peroxides[82, 83, 84] and, moreover, the IL embedding of catalytically active polyanions, by a straightforward metathesis strategy, is expected to yield tailored functional phases.[85]

Furthermore, the polyelectrolytic nature of the catalytic phase (hybrid POM + IL) guarantees negligible vapour pressure, as well as fast and selective MW-induced heating by ionic conduction mechanism, even at low power (4-10 watt). Using MW-activation, a

noteworthy implementation of the system has been achieved and quantitative epoxidation of *cis*-cyclooctene has occurred in 1 minute, incrementing the TOF value by ca. 35 times with the respect to the conventional heating.[28b] The development of this innovative strategy for catalyst immobilization, activation and recovery will be discussed more in details in Chapter 2 of this Thesis.

Another interesting POM-based oxidation system was recently proposed by Wang[86] and co-workers for the selective oxidation of alcohols with H_2O_2 by $[SiW_9Al_3(H_2O)_3O_{37}]^{7-}$ in solvent-free conditions. Under the given mild conditions, secondary alcohols were highly chemoselectively oxidized to the corresponding ketones in good yields, also in the presence of primary hydroxyl group or double bonds within the same molecule. Benzylic alcohols were selectively oxidized to the corresponding benzaldehydes with good yields, without producing over-oxidation compounds. This selectivity may be due to the introduction of an amphoteric element, such as aluminum, into the polyoxometalate, leading to a peculiar changing in the charges distribution.

Inspired by this work, in our research group we have synthesized new aluminum-substituted POMs, namely the complexes $[Al_4(H_2O)_{10}(\beta\text{-}XW_9O_{33})_2]^{6-}$ ($X = As^{III}$, Sb^{III}) with Krebs *sandwich-like* structures (see Fig. 1.10, c). The catalytic activity of the arsenic derivative towards alcohols, sulfides and alkenes oxidation with H_2O_2 has also been studied[87] and the results will be discussed in details in Chapter 5 of this Thesis.

1.3 Ionic Liquids in catalysis

1.3.1 Ionic Liquids: a general introduction

Since the introduction of cleaner technologies started to be a major concern throughout both industry and academia, the search for alternative solvents has become a high priority. On the list of damaging chemicals, solvents are top-ranking for two simple reasons: (i) they are used in huge amounts for dissolving, mixing and separating; (ii) they are usually volatile liquids that are difficult to contain, in fact they represent the bulk of hazardous substances lost to the atmosphere from chemical industries, by incineration or disposal.

Strategies to reduce or eliminate solvent waste from chemical industries include solvent-free synthesis and the use of more benign reaction media, such as water,[7] supercritical fluids[6] or ionic liquids (ILs).[8]

Ionic liquids are a fascinating class of novel solvents, attracting attention in recent years as a possible green alternative to the commonly used volatile organic solvents (VOCs). The rising interest about ILs is underlined by the large number of reviews and articles devoted to this topic.[8, 88] A wide range of ILs applications has been investigated and nowadays they are studied also for the specific improvements they can afford in yields, rates and selectivities of chemical reactions, rather then for simple VOCs replacement.

In a broad sense, ionic liquids are liquids entirely composed by ions.[88] Nevertheless, they are different from the classical, high-melting, high viscous and corrosive molten salts, because they are liquid at low temperatures (< 100°C), low viscous and easy to handle .

The first ionic liquid reported by chemists was a "red oil" formed during an $AlCl_3$-catalyzed Friedel-Crafts alkylation in the mid-19th century.[89] This compound was later identified by NMR as a salt, with the intermediate sigma complex as the cation and the heptaclorodialuminate as the anion (see Fig. 1.14).[90]

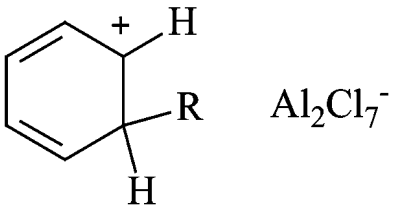

Figure 1.14. Structure proposed for the "red oil": the heptachlorodialuminate salt of the sigma complex.

In the early 20th century, many examples of quaternary ammonium liquid salts were reported, such as ethylammonium nitrate in 1914,[91] although most of them were undesired by-products, so they were not studied in depth.

In the same period, liquid salts composed by heterocyclic cations (such as pyridinium and imidazolium) in combination with tetrachloroaluminate anion were reported as electrolytes in batteries[92] and as solvents for the electroplating of metals.[93]

However, chloroaluminate salts display a limited applicability due to their moisture sensitiveness. In the early 1990s, the first examples of low-melting halide-based ILs have been reported, together with different air- and water-stable ILs, containing suitable anions, such as hexafluorophosphate, tetrafluoroborate, trifluoromethanesulfonate (triflate), *bis*(trifluoromethanesulfonyl)amide, etc.[94]

Ionic liquids are usually prepared by simple *N*-alkylation of the amine compound with alkyl halides, to form quaternary ammonium salts, followed by metathesis reactions in the presence of a metal salt of the desired anion (see Scheme 1.5).

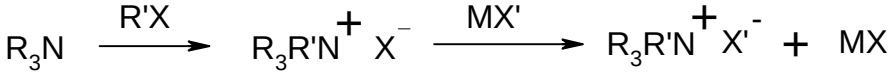

Scheme 1.5. General scheme for the synthesis of ionic liquids.

This classical route suffers from some drawbacks, e.g. incomplete metathesis and possible presence of halide impurities in the product. The latter can be a serious problem while using ILs as solvents for transition metal-catalyzed reactions, as halides are highly coordinating ions, which can severely inhibit the catalytic performance. Halide-free synthesis of ILs has been recently developed.[95]

Ionic liquids show a wide diversity of applications as their physicochemical properties depend on the nature of the ions composing the IL itself (see next paragraph). The number of different ionic liquids obtainable just varying the ions has been estimated to be 10^{12}, each of them with its unique set of properties.[96] This number grows further, considering also the possible synthesis of chiral[97] or task-specific ILs,[98] i.e. ionic liquids in which a functional group is covalently tethered to the cation, anion or both. It is clearly needed, then, to determine how ILs properties vary as a function of anion/cation substitution patterns, in order to establish which, if any, properties change in a systematic, and thus predictable, way. In the following paragraph some of these concepts will be discussed, but it is evident that ILs offer opportunities unobtainable with molecular solvents.

1.3.2 Ionic Liquids: physicochemical properties

As already mentioned in the previous paragraph, the physicochemical properties of ionic liquids can be specifically varied selecting suitable cations and anions. This possibility allows the design of specific ILs.

In this section the relationships between structural features of ILs and some of their physicochemical properties (such as melting point, polarity and miscibility) will be illustrated.

Ionic liquids mainly comprise organic cations such as tetraalkylammonium,[99] tetraalkylphoshonium,[100] trialkylsulphonium,[101] 1,3-dialkylimidazolium,[94] *N*-alkylpyridinium,[102] *N*-alkylthiazolium,[103] *N*, *N*-dialkylpyrrolidinium,[104] and others (see Fig. 1.15).

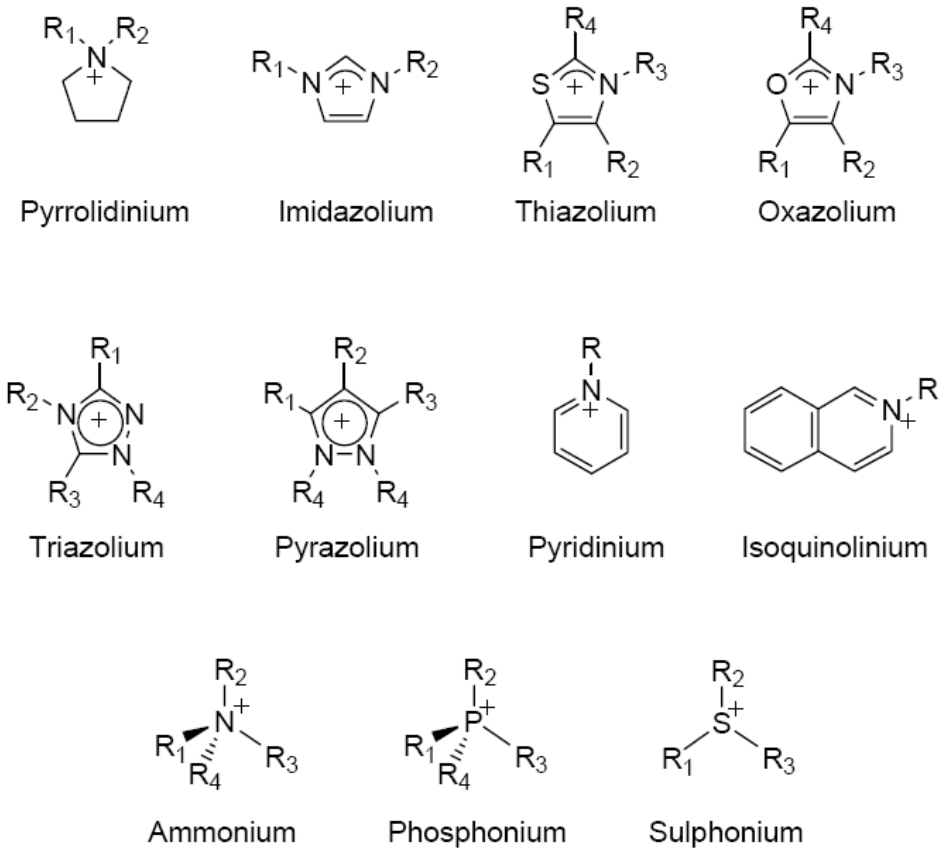

Figure 1.15. Examples of cations commonly used for the formation of ionic liquids.

The common anions are: BF_4^-, PF_6^-, SbF_6^-, $CF_3SO_3^-$ (triflate), $(CF_3SO_2)_2N^-$ (*bis*-(triflyl)amide), $(C_2F_5SO_2)N_2^-$, $(CF_3SO_2)_3C^-$ and $CF_3CO_2^-$. Another class of polynuclear anions, comprising $Al_2Cl_7^-$, $Al_3Cl_{10}^-$ and others, leads instead to air- and water-sensitive ionic liquids.

1.3.2.1 Liquid range and melting point

Liquid temperature range for an ionic liquid can be much greater that those of the common molecular solvents. Dichloromethane, for example, has a liquid range of 145°C (from -95 to 40°C), while for water it is 100°C (from 0 to 100°C).

The upper liquid limit for ILs is usually that of their thermal decomposition (mainly by dealkylation), rather than vaporization (as for the classical molecular solvents), because ILs display relatively weak ion–ion pairing (in comparison to molten salts), so they have little or no measurable vapor pressure. The lower temperature limit corresponds instead to the melting point and is related to solidification (either as crystallization or glassification).[8b]

Melting point is one of the main parameters used to classify a solvent. Comparing the melting points of different chloride salts, it is clearly shown that the nature of the cation deeply influence this property.[88] Alkali metal chlorides show very high melting points, while chlorides of suitable organic cations can melt at temperatures below 150°C (see Tab. 1.3).

Table 1.3. Melting point of different chlorides.[88]

Salt	Melting point (m.p.), °C
NaCl	803
KCl	772
[mmim][Cl] [a]	125
[emim][Cl] [b]	87
[bmim][Cl] [c]	65

[a] [mmim] = 1,3-dimethylimidazolium; [b] [emim] = 1-ethyl-3-methylimidazolium; [c] [bmim] = 1-butyl-3-methyl-imidazolium.

In particular, organic cations with low symmetry, weak intermolecular interactions and good charge distribution originate low-melting salts.

The nature of the anion also influences the melting point, as shown in Table 1.4.[88] Comparing different 1-ethyl-3-methylimidazolium (indicated as [emim] in the text) salts, it was shown that, in most cases, increasing the anion size leads to a decreasing of the melting point.

Table 1.4. Influence of different anions on the melting point of imidazolium salts.[88]

Salt	Melting point, °C	Reference
[emim][Cl]	87	92a
[emim][NO_2]	55	105
[emim][NO_3]	38	105
[emim][$AlCl_4$]	7	106
[emim][BF_4]	6*	107
[emim][CF_3SO_3]	- 9	94
[emim][CF_3CO_2]	- 14	94

* glass transition

Also the upper liquid limit strongly depends on the nature of the anion, since, for example, [emim][BF_4] and [emim][$(CF_3SO_2)_2N$] are reported to be stable up to 300°C [108] and 400°C [94] respectively. Hence, for [emim][$(CF_3SO_2)_2N$], the liquid range is more then 400°C (m.p. = - 3°C).

1.3.2.2 Polarity

Polarity is the most commonly used parameter for solvent classification. The simplest qualitative definition of a polar solvent is related to its ability to dissolve and stabilize dipolar or charged solutes. According to this definition, ionic liquids would be highly polar solvents. Instead, overall polarity measures have shown that ILs can be located in the range of short- or medium-chain alcohols.[8a]

The polarity of ionic liquids can be modified functionalizing the cation with different groups, such as perfluorinated chains (known to lower considerably the polarity of the IL).[109]

However, ionic liquids can be generally considered as polar phases and their solvent properties largely depend on their ability to act as a hydrogen-bond donor/acceptor, as well as by the degree of charge localization on the anion.[8a]

1.3.2.3 Miscibility in water and in organic solvents

Water miscibility of ionic liquids is dramatically affected by the nature of the anion. Even subtle changes, like replacing a tetrafluoroborate with a hexafluorophosphate, have significant effects on the hydrophilicity, as PF_6^- is typically more hydrophobic than BF_4^-. Hydrophobic ILs always involve perfluorinated anions, thus showing the importance of negligible hydrogen bonding on this property.[110] For example, *bis*-(trifluoromethanesulfonyl)amide and hexafluorophosphate anions afford hydrophobic ionic liquids with most of *N*-alkylpyridinium, 1,3-dialkylimidazolium and tetraalkylammonium cations.[111] Instead, tetrafluoroborate and triflate anions originate hydrophobic ILs only if the cation has a long (> 4 C) *N*-alkyl chain, providing evidence of some cation influence too.

It must be noted, however, that also hydrophobic ILs are hygroscopic and water is omnipresent in ionic liquids, unless special drying procedures are applied. For example, hydrophobic [bmim][$(CF_3SO_2)_2N$] saturates with a significant 1.4 mass % of water.[94] As regards more hydrophilic ionic liquids, water up-take from air can be much greater. Imidazolium halide salts are especially known to be extremely hygroscopic.[8b]

However, the presence of water in ionic liquids may be a problem for some applications. One should be aware that water in the ionic liquid may not be inert and, furthermore, that its presence can significantly influence the physicochemical properties of the ionic liquid itself, including its stability (some wet ionic liquids may undergo hydrolysis with formation of protic impurities), as well as reactivity of the catalysts dissolved in it.[8b]

It should also be noted that, in general, polar organic solvents (such as dichloromethane and acetone) are fully miscible with ionic liquids, low polarity solvents (like ethyl acetate) show only partial miscibility, while non-polar solvents (such as hexane and diethylether) are immiscible with them.

As regards to supercritical fluids and, in the specific, to supercritical carbon dioxide ($scCO_2$), it should be noted that ionic liquids show a very little solubility in it, while $scCO_2$ results totally miscible in ILs.[112] This particular behaviour paves the way to the development of “green” biphasic catalytic systems, in which the catalyst retains in the IL phase, while reactants and products in the $scCO_2$ phase, thus allowing their addition and removal in an easy and clean way.

1.3.3 Ionic Liquids as solvents in catalysis

The synthesis of ambient-temperature, air- and moisture-stable ionic liquids has provided a new impetus for the use of these compounds as solvents for transition metal based catalysts.

As mentioned above, ionic liquids display a variety of special properties allowing them to outperform other solvents in many organic reactions. Some of these properties are listed below.[113]

- Ionic liquids have essentially no vapour pressure, thus they can potentially replace volatile organic solvents in the chemical industry, eliminating many containment problems and reducing pollution. They also may be used in high-vacuum systems.
- They are often composed of poorly coordinating ions, so they have the potential to be highly polar, yet non-coordinating, solvents. This feature implies that solvated catalytic intermediates are unlikely to form, thus generally enhancing the reactivity both in terms of yields and selectivities.
- They are able to dissolve a wide range of organic, inorganic and organometallic compounds, thus making them suitable as solvents for homogeneous catalysis.
- They are immiscible with a number of organic solvents and provide a non-aqueous, polar alternative for two-phase systems (hydrophobic ionic liquids can also be used as immiscible polar phases with water).
- They are “designer solvents”, as their physical-chemical properties can be modified according to the nature of the desired reactions by altering the nature of their cations and anions (see Paragraph 1.3.2).
- They possess good thermal stability and do not decompose over a large temperature range, enabling to conveniently perform in them reactions requiring high temperatures.
- Reactions carried out in ionic liquids display different thermodynamic and kinetic behaviour, which often leads to improved process performance. Their ionic character, indeed, enhances the reaction rates to a great extent in many reactions, including microwave-assisted syntheses.[114]
- They generally do not coordinate to metal complexes, enzymes and different organic substrates.
- Their polar and non-coordinating properties can significantly affect the reactivity and enantioselectivity of several reactions. In addition, chiral ionic liquids have been

synthesized and used to control the stereoselectivity.

- Most of them can be stored without decomposition for a long period of time.
- They solubilise gases, such as H_2, CO, O_2 and CO_2. Many reactions reported in the literature are performed using supercritical CO_2 ($scCO_2$) as the extracting solvent for ionic liquid phase, due to the fact that ILs do not dissolve in carbon dioxide, so pure product (without any contamination) can be recovered quantitatively.[112] Moreover, the dissolution of CO_2 in the ionic liquid is completely reversible, thus allowing the recovering of the pure IL after the extraction of the product and depressurization.

All the features listed above contribute in making ionic liquids good candidates as solvents for catalytic reactions and actually almost all kinds of reactions have been performed in them, both homogeneously and under biphasic conditions.[8, 109, 113, 115]

The latter case is probably the most attractive from an industrial point of view, as homogeneous catalytic processes often suffer of disadvantages, such as products separation from the reaction mixture and catalyst recovery. In order to overcome these problems, various approaches have been proposed. Among them, liquid–liquid biphasic catalysis has emerged, as biphasic systems can combine the advantages of both homogeneous catalysis (such as greater catalytic efficiency and mild reaction conditions) and heterogeneous catalysis (such as easy separation of the products and recycling). Ionic liquids are widely used in biphasic condition, because in general the catalyst is fully immobilized in the IL phase, thus providing an actual catalytic phase, which can be extracted at the end of the reaction (using a non-miscible solvent) and reused in consecutive cycles.

This aspect will be discussed more in detail in Chapter 2 of this Thesis, where an innovative and efficient IL-based catalytic system for the epoxidation of olefin with H_2O_2 by a hybrid polyoxometalate will be presented.

Moreover, the results of an extensive investigation of Friedel-Crafts acylation of ferrocene in ILs will be described in Chapter 3.

Finally, it is worth to note that, when used as solvents, ionic liquids must not contain impurities, as halide anions (from incomplete metathesis reaction), undesired cations (inefficiently separated from the final product) or water (see Paragraph 1.3.2). The presence of such impurities can have an extremely detrimental effect on the performance of the ionic liquid, particularly if its application involves transition metal catalysts, which are often deactivated by halide ions.

1.4 Aim of the Ph.D. Thesis: New catalytic systems for the selective functionalization of organic molecules

The green chemistry revolution is providing a number of challenges to chemists working in industry, education and research, in order to develop new processes, products and services able to achieve the now required social, economic and environmental targets. Together with these challenges, there are also opportunities to discover and apply new chemistry, to improve processes, manufacturing and also the tarnished image of chemistry.

The achievement of these goals needs new approaches, in order to reduce materials and energy required for chemical processes, through the discovery and the development of innovative synthetic pathways, using renewable feedstocks and more selective chemistry, but also identifying alternative reaction conditions and media, in order to design less toxic and safer chemicals. As discussed in the Paragraph 1.1, the ideal synthesis combines environmental, health, safety and economic targets (see Fig. 1.2).

In the chemical industry, there is a strong drive towards the development of innovative and clean systems (with particular emphasis on the reduction of waste), because mature chemical processes are often based on technologies developed in the first half of the 20th century, that are no longer acceptable in these environmentally conscious days.

In this context, lots of efforts are aimed to the development of innovative methodologies for industrially relevant chemical processes, such as oxidations, C-C bond formation and dehalogenation reactions.

In this Thesis, different strategies have been used to implement benchmark oxidative transformations (see Chapters 2 and 5) and in all cases the research approach has been based on some key issues, which involves:

i) the use of bulk oxidants with low environmental impact (in the specific case, hydrogen peroxide);
ii) sustainable reaction media, such as ionic liquids and water;
iii) non conventional activation techniques, as microwave (MW)-irradiation;
iv) alternative reactors, as microchannel reactors;
v) multi-metallic catalysts with high thermal, hydrolytic and oxidative resistance, tailored functionality and solubility, able to be heterogenized on solid supports (in the specific case, polyoxometalates).

Moreover, another appealing system employing ILs as solvents has been developed for Friedel-Crafts acylation of ferrocene catalyzed by scandium triflate under MW-irradiation (see Chapter 3).

As regards to the C-C bond formation and dehalogenation reactions (Chapter 4), the research approach has been focused onto different aspects, i.e.:

i) the synthesis of tailored hybrid multi-metallic catalysts, providing a synergistic interaction between the organic and inorganic frameworks and a fine tuning of the stereo-electronic properties of the resulting complexes, both instrumental to access multi-turnover catalysis;

ii) an accurate design of the covalently bound organic moieties, in order to afford a binding site to other transition metals, such as palladium;

iii) the enhancement of the catalytic performances using non conventional activation techniques, as microwave irradiation;

iv) the possibility of a further evolution to heterogeneous catalysis, including Supported Ionic Liquid Catalysis (SILPC) techniques.[116]

Developing new concepts or improving the existing ones is therefore more than just selecting the best of each field: it is the challenge to pick in each field the concepts that will lead to the best combination. This is the goal of this Ph.D. Thesis and it will be developed in the following chapters.

1.5 References and notes

[1] P. T. Anastas, J. C. Warner, in *Green Chemistry: Theory and Practice*, Oxford University Press – Oxford – England, printed in Great Britain, **1998**.

[2] J. H. Clark, in *Green Separation Processes*, Wiley-VCH Verlag GmbH & Co. KGaA, Weinheim, **2005**.

[3] C. V. Stevens, R. G. Vertie in, *Renewable Resources*, J. Wiley & Sons, Chichester, **2004**.

[4] J. H. Clark *Green Chem.* **1998**, *1*, 1.

[5] D. J. C. Constable, A. D. Curzons, V. L. Cunningham *Green Chem.* **2002**, *4*, 521.

[6] W. Leitner, in *Topics in Current Chemistry - Modern Solvents in Organic Synthesis*, Springer-Verlag Berlin Heidelberg, printed in Germany, **1999**, 107.

[7] A. Lubineau, J. Augò, in *Topics in Current Chemistry - Modern Solvents in Organic Synthesis*, Springer-Verlag Berlin Heidelberg, printed in Germany, **1999**, 1.

[8] a) T. Welton *Chem. Rev*. **1999**, *99*, 2071. b) P. Wasserscheid, T. Welton (Eds.) *Ionic Liquids in Synthesis*, Wiley-VCH, Weinheim, **2003**.

[9] A. Loupy, in *Topics in Current Chemistry - Modern Solvents in Organic Synthesis*, Springer-Verlag Berlin Heidelberg, printed in Germany, **1999**, 153.

[10] a) S. J. Haswell, P. Watts *Green Chem.* **2003**, *5*, 240. b) B. P. Mason, K. E. Price, J. L. Steinbacher, A. R. Bogdan, D. T. McQuade *Chem. Rev.* **2007**, *107*, 2300.

[11] a) A. Loupy (Ed.), in *Microwaves in Organic Synthesis*, Wiley-VCH Verlag GmbH & Co. KGaA, Weinheim, printed in the Federal Republic of Germany, **2002**. b) C. O. Kappe *American Laboratory* **2001**, *33*, 13.

[12] K. S. Suslick, S. E. Skrabalak, in *Handbook of Heterogeneous Catalysis – Sonocatalysis*, Wiley-VCH Verlag GmbH & Co. KGaA, Weinheim, printed in the Federal Republic of Germany, **2008**.

[13] A. Hiskia, A. Mylonas, E. Papaconstantinou *Chem. Soc. Rev.* **2001**, *30*, 62.

[14] M. T. Pope, A. Müller, in *Heteropoly and Isopoly Oxometalates*, Springer Verlag, New York, **1983**.

[15] M. T. Pope, A. Müller *Angew. Chem. Int. Ed.* **1991**, *30*, 34.

[16] C. L. Hill *Polyoxometalates, Chem. Rev.* (Special Issue) **1998**, 98, 1.

[17] D. L. Kepert, in *The Early Transition Metals*, Academic Press Inc., London, **1972**.

[18] Y. P. Jeannin *Chem. Rev.* **1998**, *98*, 51.

[19] W. N. Lipscomb, *Inorg. Chem.* **1965**, *4*, 132.

[20] J. F. Keggin *Proc. R. Soc. London Scr. A.* **1934**, *144*, 75.

[21] R. Acerete, C. F. Hammer, L. C. W. Baher *J. Am. Chem. Soc.* **1982**, *104*, 5384.

[22] R. Massart, R. Contant, J. M. Fruchart, J. P. Ciabrini *Inorg. Chem.* **1977**, *11*, 2916.

[23] P. Judeinstein, C. Deprum, L. Nadjo *J. Chem. Soc. Dalton Trans.* **1991**, 1991.

[24] M. Filowitz, R. K. C. Ho, W. G. Klemperer, W. Shum *Inorg. Chem.* **1979**, *18*, 93.

[25] F. Zonnevijlle, C. M. Tournè, G. F. Tournè *Inorg. Chem.* **1982**, *21*, 2742.

[26] J. Canny, A. Tézé, R. Thouvenot, G. Hervé *Inorg. Chem.* **1986**, *25*, 2114.

[27] A. Müller, P. Kögerler *Coord. Chem. Rev.* **1999**, *182*, 3.

[28] a) M. Carraro, L. Sandei, A. Sartorel, G. Scorrano, M. Bonchio *Org. Lett.* **2006**, *8*, 3671. b) S. Berardi, M. Bonchio, M. Carraro, V. Conte, A. Sartorel, G. Scorrano *J. Org. Chem.* **2007**, *72*, 8954. c) M. Bonchio, M. Carraro, G. Scorrano, E. Fontananova, E. Drioli *Adv. Synth. Catal.* **2003**, *345*, 1119. d) M. Bonchio, M. Carraro, G. Scorrano, A. Bagno *Adv. Synth. Catal.* **2004**, *346*, 648.

[29] H. Zeng, G. R. Newkome, C. L. Hill *Angew. Chem. Int. Ed.* **2000**, *39*, 1772.

[30] P. Mason *Master degree thesis*, Università degli studi di Padova, a.a. **1998/1999.**

[31] C. R. Mayer, I. Fournier, R. Thouvenot *Chem Eur. J.* **2000**, *6*, 105.

[32] A. Proust, P. Gouzerh, F. Robert *Inorg. Chem.* **1993**, *32*, 5291.

[33] a) W. A. Herrmann *Angew. Chem. Int. Ed.* **2002**, *41*, 1290-1309. b) O. Schuster, L. Yang, H. G. Raubenheimer, M. Albrecht *Chem. Rev.* **2009**, *109*, 3445-3478. c) S. Nolan, in *N-Heterocyclic Carbenes in Synthesis*, Wiley-VCH Verlag GmbH & Co. KGaA, Weinheim, printed in the Federal Republic of Germany, **2006**. d) E. A. B. Kantchev, C. J. O' Brien, M. G. Organ *Angew. Chem. Int. Ed.* **2007**, *46*, 2768-2813.

[34] S. Berardi, M. Carraro, M. Iglesias, A. Sartorel, G. Scorrano, M. Albrecht, M. Bonchio *submitted*.

[35] M. Carraro, A. Sartorel, G. Scorrano, C. Maccato, M. H. Dickman, U. Kortz, M. Bonchio *Angew. Chem. Int. Ed.* **2008**, *47*, 7275.

[36] a) I. V. Kozhevnikov, in *Catalysis by Polyoxometalates*, Wiley-VCH, Chichester, **2002**. b) E. L.–M. Wong, R. W.–Y. Sun, N. P.–Y. Chung, C.–L. S. Lin, N. Yong, C.–M. Che *J. Am. Chem. Soc.* **2006**, *128*, 4938.

[37] a) M. T. Pope, in *Isopoly and Heteropoly Anions*, Springer, Berlin, **1983**. b) A. Müller in, *Polyoxometalate Chemistry*, Kluwer Academic, Dordrecht, **2001**. c) C. L. Hill, C. M. Prosser-McCartha *Coord. Chem. Rev.* **1995**, *143*, 407. d) N. Mizuno, M. Misono *Chem. Rev.* **1998**, *98*, 171. e) R. Neumann *Prog. Inorg. Chem.* **1998**, *47*, 317.

[38] I. Bar-Nahum, R. Neumann *Chem. Commun.* **2003**, 2690.

[39] K. Yamaguchi, M. Kotani, K. Kamata, N. Mizuno *Chem. Lett.* **2008**, *37*, 1258.

[40] V. Kogan, Z. Aizenshtat, R. Popovitz-Biro, R. Neumann *Org. Lett.* **2002**, *4*, 3529.

[41] B. S. Lane, K. Burgess *Chem. Rev.* **2003**, *103*, 2457 and references cited therein.

[42] a) A. M. Khenkin, C. L. Hill *Mendeleev Commun.* **1993**, 140. b) X. Zhang, Q. Chen, D. C. Duncan, R. J. Lachicotte, C. L. Hill *Inorg. Chem.* **1997**, *36*, 4381. c) X. Zhang, Q. Chen, D. C. Duncan, C. F. Campana, C. L. Hill *Inorg. Chem.* **1997**, *36*, 4208. d) X. Zhang, T. M. Anderson, Q. Chen, C. L. Hill *Inorg. Chem.* **2001**, *40*, 418. e) N. Mizuno, C. Nozaki, I. Kiyoto, M. Misono *J. Am. Chem. Soc*. **1998**, *120*, 9267. f) Y. Seki, J. S. Min, M. Misono, N. Mizuno *J. Phys. Chem. B* **2000**, *104*, 5940. g) N. Mizuno, Y. Seki, Y. Nishiyama, I. Kiyoto, M. Misono *J. Catal.* **1999**, *184*, 550. h) N. Mizuno, I. Kiyoto, C. Nozaki, M. Misono *J. Catal.* **1999**, *181*, 171.

[43] Y. Ishii, K. Yamawaki, T. Yoshida, T. Ura, H. Yamada, M. Ogawe *J. Org. Chem.* **1987**, *52*, 1868.

[44] Y. Ishii, H. Tanaka, Y. Nishiyama *Chem. Lett.* **1994**, *1*, 1.

[45] Y. Ishii, K. Yamawaki, T. Ura, H. Yamada, T. Yoshida, M. Ogawa *J. Org. Chem.* **1988**, *53*, 3587.

[46] a) L. J. Csanyi, K. Jaky *J. Mol. Catal.* **1990**, *61*, 75. b) L. J. Csanyi, K. Jaky *J. Catal.* **1991**, *127*, 42. c) L. Salles, C. Aubry, R. Thouvenot, F. Robert, C. Dorémieux-Morin, G. Chottard, H. Ledon, Y. Jeannin, J.-M.Brégeault *Inorg. Chem.* **1994**, *33*, 871. d) A. C. Dengel, W. P. Griffith, B. C. Parkin, *J. Chem. Soc. Dalton Trans.* **1993,** 2683. e) A. J. Bailey, W. P. Griffith, B. C. Parkin *J. Chem. Soc. Dalton Trans.* **1995**, 1833. f) D. C. Duncan, R. C. Chambers, E. Hecht, C. L. Hill, *J. Am. Chem. Soc.* **1995**, *117*, 681.

[47] C. Venturello, E. Alneri, M. Ricci *J. Org. Chem.* **1983**, *48*, 3831.

[48] C. Venturello, R. D'Aloisio, J. C. Bart, M. Riai *J. Mol. Catal.* **1985**, *32*, 107.

[49] C. Venturello, R. D'Aloisio *J. Org. Chem.* **1988**, *53*, 1553.

[50] J. Prandi, H. B. Kagan, H. Mimoun *Tetrahedron Lett.* **1986**, *27*, 2617.

[51] K. Sato, M. Aoki, M. Ogawa, T. Hashimoto, R. Noyori *J. Org. Chem.* **1996**, *61*, 8310.

[52] K. Sato, M. Aoki, M. Ogawa, T. Hashimoto, D. Panyella, R. Noyori *Bull. Chem. Soc. Jpn.* **1997**, *70*, 905.

[53] A. L. Villa de P., B. F. Sels, D. E. De Vos, P. A. Jacobs *J. Org. Chem.* **1999**, *64*, 7267.

[54] M. S. Balula, I. C. M. S. Santos, M. M. Q. Simões, M. G. P. M. S. Neves, J. A. S. Cavaleiro, A. M. V. Cavaleiro *J. Mol. Catal. A: Chem.* **2004**, *222*, 159.

[55] M.-L. Guo *Green Chem.* **2004**, *6*, 271.

[56] M. Schwegler, M. Floor, H. van Bekkum *Tetrahedron Lett.* **1988**, *29*, 823.

[57] J. Wang, L. Yan, G. Li, X, Wang, Y. Ding, J. Suo *Tetrahedron Lett.* **2005**, *46*, 7023.

[58] R. Ben-Daniel, A. M. Khenkin, R. Neumann *Chem. Eur. J.* **2000**, *6*, 3722.

[59] O. A. Kholdeeva, T. A. Trubitsina, R. I. A. V. Golovin, W. A. Neiwert, B. A. Kolesov, X. López, J. M. Poblet *Inorg. Chem.* **2004**, *43*, 2284.

[60] P. T. Witte, P. L. Alsters, W. Jary, R. Mullner, P. Pochlauer, D. Sloboda-Rozner, R. Neumann *Org. Process Res. Dev.* **2004**, *8*, 524.

[61] R. Neumann, A. M. Khenkin *J. Mol. Catal. A: Chem.* **1996**, *114*, 169.

[62] W. Adam, P. L. Alsters, R. Neumann, C. R. Saha-Möller, D. Sloboda-Rozner, R. Zhang *J. Org. Chem.* **2003**, *68*, 1721.

[63] J. Server-Carrió, J. Bas-Serra, M. E. Gonzàlez-Nuñez, A. Garcìa-Gastaldi, G. B. Jameson, L. C. W. Baker, R. Acerete *J. Am. Chem. Soc.* **1999**, *121*, 977.

[64] R. H. Ingle, N. K. Kala Raj *J. Mol. Cat. A: Chem.* **2008**, *294*, 8.

[65] N. Mizuno, K. Kamata, K. Yonehara, Y. Sumida, K. Yamaguchi, S. Hikichi *Science* **2003**, *300*, 964.

[66] K. Kamata, Y. Nakagawa, K.Yamaguchi, N. Mizuno *J. Catal.* **2004**, *224*, 224.

[67] T. D. Phan, M. A. Kinch, J. E. Barker, T. Ren *Tetrahedron Lett.* **2005**, *46*, 397.

[68] K. Kamata, M. Kotani, K. Yamaguchi, S. Hikichi, N. Mizuno *Chem. Eur. J.* **2007**, *13*, 639.

[69] A. Sartorel, M. Carraro, A. Bagno, G. Scorrano, M. Bonchio *Angew. Chem. Int. Ed.* **2007**, *46*, 3255.

[70] A. J. Bailey, W. P. Griffith, B. C. Parkin *J. Chem. Soc. Dalton Trans.* **1995**, 1833.

[71] K. Kamata, K. Yamaguchi, S. Hikichi, N. Mizuno *Adv. Synth. Catal.* **2003**, *345*, 1193. b) K. Kamata, K. Yamaguchi, N. Mizuno *Chem. Eur. J.* **2004**, *10*, 4728.

[72] S. Ueno, K. Yamaguchi, K. Yoshida, K. Ebitani, K. Kaneda *Chem. Commun.* **1998**, 295.

[73] A. L. Baumstark, P. C. Vasquez *J. Org. Chem.* **1998**, *53*, 3437.

[74] N. Mizuno, K. Kamata, M. Kotani, K. Yamaguchi, S. Hikichi *Chem. Eur. J.* **2007**, *13*, 639.

[75] a) M. Antonietti, M. Niederberger, B. Smarsly *Dalton Trans*. **2008**, 18. b) C. Sanchez, G. J. de A. A. Soler-Illa, F. T. Ribot, T. Lalot, C. R. Mayer, V. Cabuil *Chem. Mater.* **2001**, *13*, 3061. c) C. Sterb, D. L. Long, L. Cronin *Chem. Commun.* **2007**, 471.

[76] Non functionalized lacunary POMs evolve to saturated XW_{12}-derivatives under MW-assisted catalysis.

[77] B. A. Roberts, C. R. Strauss *Acc. Chem. Res.* **2005**, *38*, 653.

[78] This value is similar to that obtained with the parent catalyst $[\gamma\text{-}SiW_{10}O_{34}(H_2O)_2]^{4-}$ (13.9).[66] See also: Y. Goto, K. Kamata, K. Yamaguchi, K. Uehara, S. Hikichi, N. Mizuno *Inorg. Chem.* **2006**, *45*, 2347.

[79] R. Prabhakar, K. Morokuma, C. L. Hill, D. G. Musaev *Inorg. Chem.* **2006**, *45*, 5703.

[80] V. Conte, F. Di Furia, G. Modena, in *Organic Peroxides,* John Wiley & Sons, Cheichester, **1992**, 559.

[81] a) M. Bonchio, S. Campestrini, V. Conte, F. Di Furia, S. Moro *Tetrahedron* **1995**, *51*, 12363. b) K. A. Vassell, J. H. Espenson *Inorg. Chem.* **1994**, *33*, 5491.

[82] J. Muzart *Adv. Synth. Catal.* **2005**, *348*, 275 and references cited therein.

[83] V. Conte, B. Floris, P. Galloni, A. Silvagni *Pure Appl. Chem.* **2005**, *77*, 1575.

[84] V. Conte, B. Floris, P. Galloni, A. Silvagni *Adv. Synth. Catal.* **2005**, *347*, 1341.

[85] W. Miao, T. H. Chan *Acc. Chem. Res.* **2006**, *39*, 897.

[86] J. Wang, L. Yan, G. Qian, S. Li, K. Yang, H. Liu, X. Wang *Tetrahedron* **2007**, *63*, 1826.

[87] M. Carraro, S. Berardi, A. Sartorel, G. Scorrano, M. H. Dickman, U. Kortz, M. Bonchio *manuscript in preparation.*

[88] P. Wasserscheid, W. Keim *Angew. Chem. Int. Ed.* **2000**, *39*, 3772.

[89] N. O. Calloway *Chem. Rev.* **1935**, *17*, 327.

[90] J. S. Wilkes *Green Chem.* **2002**, *4*, 73.

[91] P. Walden *Bull. Acad. Imper. Sci. (St. Petersburg)* **1914**, 1800.

[92] a) J. S. Wilkes, J. A. Lewisky, R. A. Wilson, C. L. Hussey *Inorg. Chem.* **1982**, *21*, 1263. b) C. L. Hussey, T. B. Scheffler, J. S. Wilkes, A. A. Fannin Jr. *J. Electrochem. Soc.* **1986**, *133*, 1389.

[93] a) G. E. McManis III, A. N. Fletcher, D. E. Bliss *U. S. Patent 4624755*, **1986**. b) X. H. Xu, C. L. Hussey *J. Electrochem. Soc.* **1992**, *139*, 1295.

[94] P. Bonhôte, A. P. Dias, N. Papageorgiou, K. Kalyanasundaram, M. Grätzel *Inorg. Chem.* **1996**, *35*, 1168.

[95] J. D. Holbrey, W. M. Reichert, R. P. Swatloski, G. A. Broker, W. R. Pitner, K. R. Seddon, R. D. Rogers *Green Chem.* **2002,** *4***,** 407.

[96] J. D. Holbrey, K. R. Seddon *Clean Technol. Environ. Pol.* **1999**, 223.

[97] P. Wasserscheid, A. Bösmann, C. Bolm *Chem. Commun.* **2002**, 200.

[98] S. Lee *Chem. Commun.* **2006**, 1049.

[99] J. Sun, M. Forsyth, D. R. MacFarlane *J. Phys. Chem. B* **1998**, *102*, 8858.

[100] H. S. Kim, Y. J. Kim, J. Y. Bae, S. J. Kim, M. S. Lah, C. S. Chin *Organometallics* **2003**, *22*, 2498.

[101] K. Mujatake, K. Yamamoto, K. Endo, E. Tsuchida *J. Org. Chem.* **1998**, *63*, 7522.

[102] S. Tait, R. A. Osteryoung *Inorg. Chem.* **1984**, *23*, 4352.

[103] J. H. Davis, K. J. Forrester *Tetrahedron Lett.* **1999**, *40*, 1621.

[104] D. R. MacFarlane, P. Meakin, J. Sun, N. Amini, M. Forsyth *J. Phys. Chem. B* **1999**, *103*, 4164.

[105] J. S. Wilkes, M. J. Zaworotko *J. Chem. Soc. Chem. Commun.* **1992**, 965.

[106] A. A. Fannin Jr., D. A. Floreani, L. A. King, J. S. Landers, B. J. Piersma, D. J. Stech, R. L. Vaughn, J. S. Wilkes, J. L. Williams *J. Phys. Chem.* **1984**, *88*, 2614.

[107] J. D. Holbrey, K. R. Seddon *J. Chem. Soc. Dalton Trans.* **1999**, 2133.

[108] M. L. Mutch, J. S. Wilkes *Proc. Electrochem. Soc.* **1998**, *98*, 254.

[109] P. J. Dyson, T. J. Geldbach (Eds.) *Metal Catalysed Reactions in Ionic Liquids*, Springer, Dordrecht, The Netherlands, printed in the Netherlands, **2005**.

[110] J. M. Pringle, J. Golding, K. Baranyai, C. M. Forsyth, G. B. Deacon, J. L. Scott, D. R. MacFarlane *New. J. Chem.* **2003**, *27*, 1504.

[111] S. A. Forsyth, J. M. Pringle, D. R. MacFarlane *Austr. J. Chem.* **2004**, *57*, 113 and references cited therein.

[112] L. A. Blanchard, D. Hancu, E. J. Beckman, J. F. Brennecke *Nature* **1999**, *399*, 28.

[113] N. Jain, A. Kumar, S. Chauhan, S. M. S. Chauhan *Tetrahedron* **2005**, *61*, 1015.

[114] N. E. Leadbeater, H. M. Torenius, H. Tye *Comb. Chem. High Throughput Screen.* **2004**, *7*, 511.

[115] V. I. Pârvulescu, C. Hardacre *Chem. Rev.* **2007**, *107*, 2615.

[116] H. Hagiwara, K. H. Ko, T. Hoshi, T. Suzuki *Chem. Commun.* **2007**, 2838.

2. H_2O_2-based epoxidations catalyzed by [γ-$SiW_{10}O_{36}(PhPO)_2]^{4-}$ in Ionic Liquids

2.1 Catalytic epoxidations: introduction and state of art

Olefins are one of the most important raw materials used in industry, as they are susceptible of many key synthetic reactions, such as addition, polymerisation and oxidative processes. The latters represent a major research field in organic chemistry, as they include combustion, biological oxidation, production of specific organic and inorganic compounds. Olefin oxidations can be performed with stoichiometric oxidants, eventually using transition metals as catalysts, both in homogeneous and heterogeneous processes.

In particular, catalytic epoxidation of olefins plays an important role in the synthesis of several commodity compounds, intermediates, fine chemicals and pharmaceuticals, leading to the production of tons of oxygenated compounds per year (mainly, ethylene and propylene oxides).[1] Moreover, epoxides can be also be used as epoxy resins, paints, surfactants,[2] but also as building blocks for polymers (e.g. polyesters and polyurethanes) and as key intermediates in the functionalization of more complex molecules, due to the broad range of ring-opening possibilities.

The main methods for the direct epoxidation of alkenes in industrial applications use oxygen, peroxides and peracids. For example, ethylene oxide is widely produced by vapour phase oxidation of ethylene with oxygen or air, using a supported silver catalyst.[3] However, this catalytic procedure can only be applied to olefins without C-H allylic bonds, such as ethylene, 1,3-butadiene and styrene. For all the other olefins (e.g. propylene), low yields of the desired product are obtained, due to the competing oxidation of allylic C-H bonds, which leads to numerous by-products.[4] Indeed, propylene oxide is traditionally produced by the "chlorohydrin route", in which propylene is reacted with aqueous chlorine to form propylene chlorohydrin, followed by base induced dehydrochlorination of the latter to yield propylene oxide (Scheme 2.1).[5]

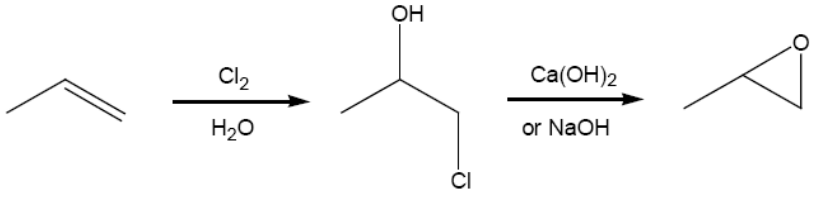

Scheme 2.1. The "chlorohydrin route".

This process is currently object of increasing environmental pressing, due to the use of expensive, toxic and corrosive chlorine as reagent and to the production of highly toxic by-products. Therefore alternative catalytic processes have been developed. For example, homogeneous[6] Mo^{VI} and heterogeneous[7] Ti^{IV} have been efficiently used as catalysts for the epoxidation of olefins, using *tert*-butyl hydroperoxide and ethylbenzene hydroperoxide as oxidants. Even though these methods have been widely used, they still suffer from the formation of the alcoholic by-product (*tert*-butanol and 1-phenylethanol, respectively).

In alternative routes, the epoxidation of substituted alkenes is successfully achieved using stoichiometric amounts of peracids (such as peracetic acid and *m*-chloroperbenzoic acid).[8] This approach also suffers from many disadvantages, since the reagents are expensive, corrosive and non-regenerable, while equivalent amounts of acid waste are produced. Moreover, safety issues associated with handling peracids must be taken into account.

Therefore, it is clear that there is a strong request for developing new epoxidation methods which employ safer oxidants and produce little waste. The employment of hydrogen peroxide as oxidant is an attractive option both on environmental and economic grounds. H_2O_2 is cheap, readily available and can oxidize organic compounds with relatively high atom efficiency, giving water as the only by-product.[8]

Many catalytic systems based on different transition metals, such as tungsten,[9] manganese,[10] rhenium[11] and iron[12], have been reported for the epoxidation of a wide range of alkenes using hydrogen peroxide. Robust polyoxometalates (POMs, Paragraph 1.2) can also promote H_2O_2 based epoxidation of internal and terminal double bonds with outstanding catalytic performance, with >99% of H_2O_2 utilization and selectivity.[13, 14, 15] Moreover, the use of hybrid polyoxotungstates (Paragraph 1.2.3) in such reactions has been recently proposed by our research group as a catalyst up-grade.[16, 17] In particular, it has been shown that the phenyl phosphonate hybrid derivative of the γ-Keggin divacant anion, namely $[\gamma\text{-}SiW_{10}O_{36}(PhPO)_2]^{4-}$ (Figure 2.1)[18], displays an improved thermal stability, higher yields and turnover frequencies (TOFs)[16] when compared to the non-functionalized precursor $[\gamma\text{-}SiW_{10}O_{34}(H_2O)_2]^{4-}$.[14]

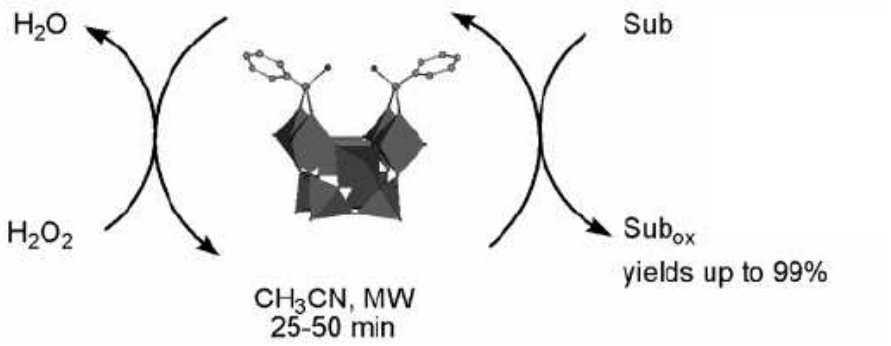

Figure 2.1. Oxidation of different substrates with H_2O_2 by the hybrid polyoxometalate [γ-$SiW_{10}O_{36}(PhPO)_2]^{4-}$.

In the presence of [γ-$SiW_{10}O_{36}(PhPO)_2]^{4-}$, under microwave (MW)-irradiation, oxidation of alkenes by H_2O_2, can be accomplished in 25-50 min with yields up to 99%.[16]

A further innovation of the proposed catalytic system toward environmental sustainability should also consider the replacement of hazardous volatile organic solvents (VOCs) by alternative reaction media. In particular, ionic liquids (ILs, Paragraph 1.3) are widely used as green alternatives to volatile solvents for many organic reactions.[19] In most of the cases, the catalysts are immobilized in the ionic liquid, rather than dissolved, thus yielding an actual and tailored catalytic phase,[20] which can be recycled after products extraction with an immiscible solvent. Furthermore, a rate acceleration effect has been observed for some catalytic reactions performed in ionic liquids.[21]

Recently, many publications on the catalytic epoxidation of alkenes with H_2O_2 in ionic liquids have been reported in the literature. For example, Bortolini and co-workers reported the quantitative epoxidation of electrophilic alkenes (whose structures resemble the vitamin K class) in both [bmim][BF_4] and [bmim][PF_6] (bmim = 1-butyl-3-methylimidazolium) using hydrogen peroxide as oxidant and NaOH as basic catalyst. Yields of epoxides range from 80-99% for all the substrates under examination, while the nature of the IL does not influence the reaction course, despite the difference in their hydrophilicity.[22]

Yang and co-workers reported the epoxidation of electron-deficient α,β-unsaturated carbonyl compounds in ionic liquid/water biphasic systems at room temperature, using hydrogen peroxide as oxidant and a basic catalyst (in the specific case, NaOH, Na_2CO_3 or $NaHCO_3$).[23] A mass transfer model has been proposed, suggesting that a small quantity of the IL, dissolved into water, is associated to the anionic peroxide, yielding Q^+OOH^- (being Q^+ the cation of the IL itself). The latter is then transferred into the IL phase to initiate the epoxidation reaction the reverse transport of OH^- follows in the catalytic cycle (Scheme 2.2).

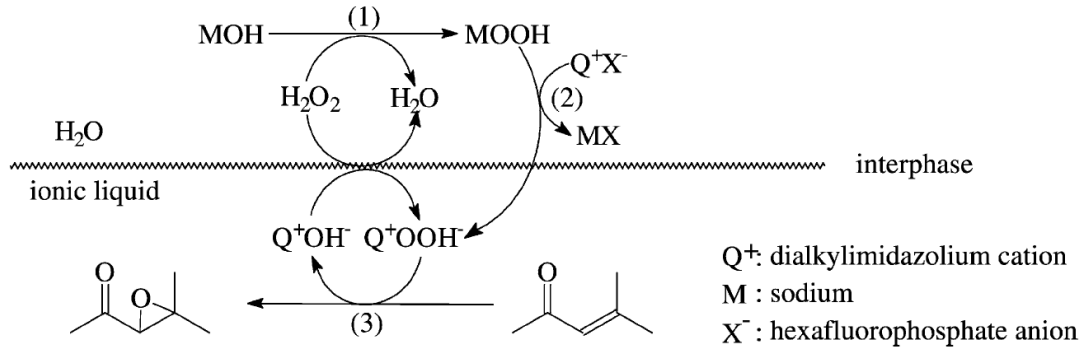

Scheme 2.2. Mass transfer model of epoxidation of mesityl oxide in the IL/H_2O biphasic system.

A similar system was described by Bernini and co-workers for epoxidation of chromone, isoflavone and chalcone derivatives using [bmim][BF_4] as the solvent and alkaline hydrogen peroxide as oxidant.[24] All reactions proceed in good yields and faster than in conventional solvents, without evidence of by-products formation, deriving form opening of the epoxide ring.

Effective epoxidation of lipophilic alkenes was accomplished at room temperature in [bmim][BF_4] with aqueous hydrogen peroxide, in the presence of catalytic amounts of manganese sulfate and a stoichiometric quantity of tetramethylammonium hydrogen carbonate.[25] Good reactivities and high selectivities were generally obtained, except for unactivated terminal alkenes, such as 1-decene. Recycling experiments can be performed adding some $MnSO_4$ and $(Me_4N)HCO_3$ to restore the activity of the system.

Owens and Abu-Omar reported the efficient epoxidation of alkenes and allylic alcohols in [emim][BF_4] (emim = 1-ethyl-3-methylimidazolium), using urea-hydrogen peroxide adduct (UHP) as oxidant and methyltrioxorhenium (MTO) as catalyst.[26] Under these conditions, good conversions and selectivities for the epoxides of a wide number of substrates were observed. When 30% aqueous H_2O_2 was used instead of UHP, the MTO-catalyzed oxidation in [emim][BF_4] afforded mainly the corresponding diol, due to the ring-opening of sensitive epoxides in the presence of large amount of water.

A recent work by Mizuno and co-workers should also be mentioned, although their method does not use strictly ILs as solvent. A dinuclear peroxotungstate has been immobilized onto SiO_2 covalently functionalised with ionic liquid moieties (Fig. 2.2).[27] The proposed system is able to heterogeneously epoxidize a wide range of olefins, using H_2O_2 as oxidant, maintaining the catalytic activity of the homogeneous analogue.

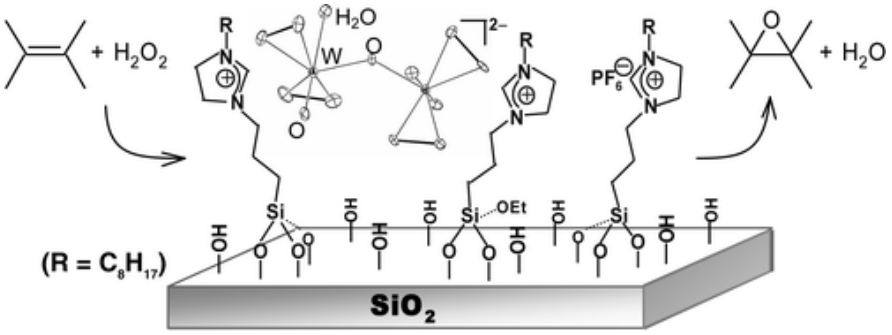

Figure 2.2. Immobilization of a peroxotungstate onto ionic-liquid modified silica.

The epoxidation immediately stopped by removal of the catalyst, while no tungsten species has been found in the filtrate due to adventitious leaching of the catalyst, thus proving the actual heterogeneous nature of the catalysis. Furthermore, the catalyst is reusable without the loss of the catalytic performance.

This work follows the new concept of supported ionic liquid phase catalysis (SILPC),[28] inspired by the capability of ILs of retaining and immobilizing catalysts. The concept of SILPC involves the modification of the surface of a support material (generally silica) with a monolayer of covalently bonded ionic liquid fragments. The resulting material is then treated with additional IL, in order to obtain a multiple layer of free IL onto the support. This phase, in which the homogeneous catalyst is dissolved, is the actual reaction phase (Fig. 2.3).

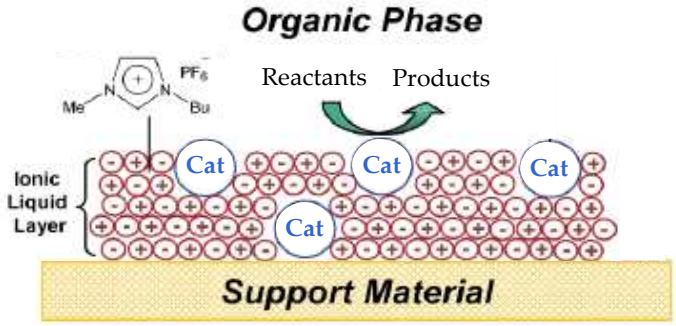

Figure 2.3. General representation of the SILPC concept.

The resulting material is a solid, performing as a homogeneous catalyst, yet maintaining the advantages of the heterogenization (e.g. easy catalyst/product separation). Furthermore, in this system the amount of ionic liquid is minimized with respect of using ILs as solvents in biphasic reaction systems, thus lowering the costs of the entire process.

On the basis and perspectives described above, we have decided to study the combined use of the hybrid polyoxometalate [γ-$SiW_{10}O_{36}(PhPO)_2]^{4-}$ and ILs for the catalytic epoxidation of olefins with H_2O_2, as an implementation of a previous work within the group.[16] The experimental results obtained will be reported and described in the following paragraphs.

2.2 Results and discussion [17]

2.2.1 Preparation and characterization of the catalytic phase

The ionic liquids used in this work are represented in Figure 2.4 and are constituted by 1-butyl-3-methylimidazolium (indicated as [bmim] in the text) as cation, and by four different anions, i.e. BF_4^-, PF_6^-, $CF_3SO_3^-$ (triflate) and $(CF_3SO_2)_2N^-$ (*bis*-(triflyl)amide).

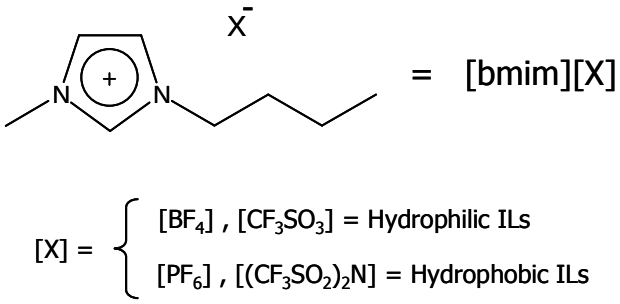

Figure 2.4. Ionic liquids synthesised and used in this work.

They have been synthesised in collaboration with the group of prof. Conte at the University of Rome – Tor Vergata, following literature two-step procedures,[29] consisting in the quaternization of the alkyl-substituted imidazole with an alkyl-bromide, followed by metathesis exchange with a suitable anion (see also Experimental Part).

These four ionic liquids can be classified on as hydrophilic (if they are fully miscible with water) or hydrophobic (if they form a biphasic system with water). As already mentioned in the Paragraph 1.3.2, this property is mainly related to the nature of the anion. In our particular case, BF_4^- and $CF_3SO_3^-$ originate hydrophilic ILs, while PF_6^- and $(CF_3SO_2)_2N^-$ lead to hydrophobic ones.

The catalytic phase has been prepared by dissolving the hybrid POM $[\gamma\text{-}SiW_{10}O_{36}(PhPO)_2]^{4-}$ (previously prepared according to literature procedures,[18, 30] see Experimental Part) in the appropriate ionic liquid, which thereby acts as a solvating/immobilization medium for the hybrid organic-inorganic polyelectrolyte.

Characterization of the resulting phase has been performed by UV-vis, FT-IR and ^{31}P-NMR techniques. Combining the evidences from all these analyses, it has been shown that both the inorganic framework and the organic domain of $[\gamma\text{-}SiW_{10}O_{36}(PhPO)_2]^{4-}$ are preserved within the IL environment.

In particular, ^{31}P-NMR of the catalyst in both CD_3CN and [bmim][$(CF_3SO_2)_2N$] has been recorded, showing the presence of one signal, at δ = 14.8 and 15.7 ppm respectively (Fig. 2.5), due to the phosphorous atom in the phenyl phosphonic moieties linked to the POM.

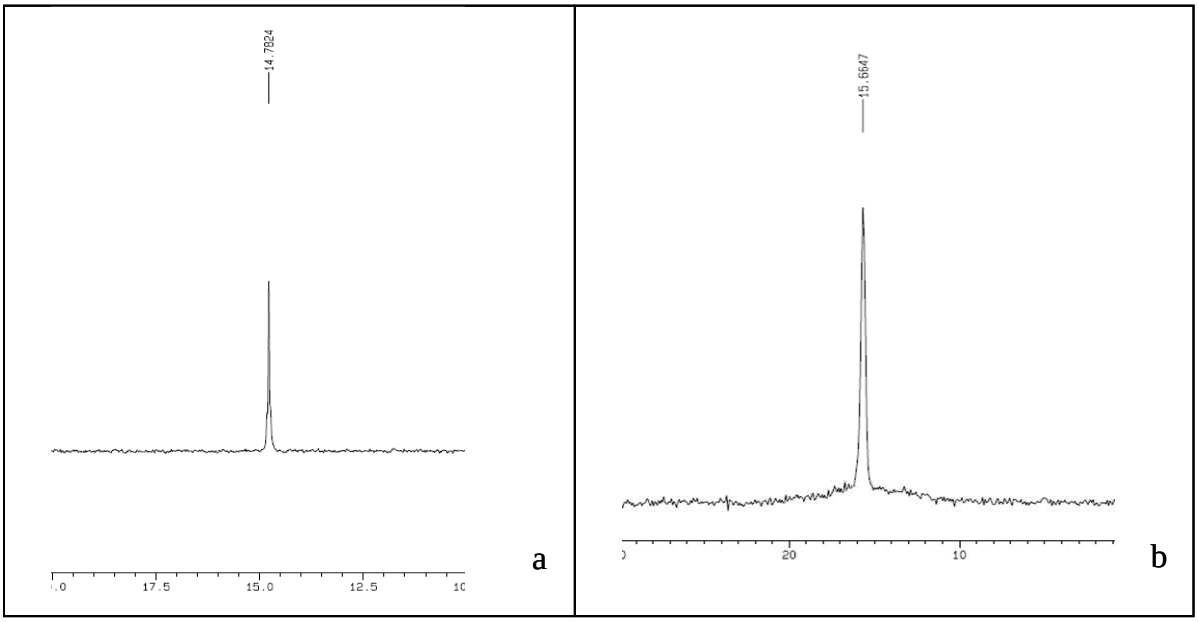

Figure 2.5. a) $^{31}P\{^1H\}$-NMR (121.5 MHz, CD_3CN, 301 K) of [γ-$SiW_{10}O_{36}(PhPO)_2]^{4-}$; b) $^{31}P\{^1H\}$-NMR (121.5 MHz, 301 K) of [γ-$SiW_{10}O_{36}(PhPO)_2]^{4-}$ in [bmim][$(CF_3SO_2)_2N$].

Spectroscopic analyses have been conveniently used also to assess the catalyst stability under turnover regime and to rule out its washing off by extraction procedures during reaction sampling and/or recycling. In particular, FT-IR analyses of [γ-$SiW_{10}O_{36}(PhPO)_2]^{4-}$ (black line in Fig. 2.6) and of the catalytic phase after the reaction (red line in Fig. 2.6), have shown a complete overlap of the bands in the range 850<ν<1000 cm^{-1}, where the peculiar absorptions of both the Si-O and W-O-W *stretchings* appear. In the remaining part of the spectral window, the bands of the catalytic phase match to ionic liquid absorptions. The catalyst does not isomerise or degrade under catalytic regime, thus showing the actual stabilization given by the functionalization of the vacant site of the POM.

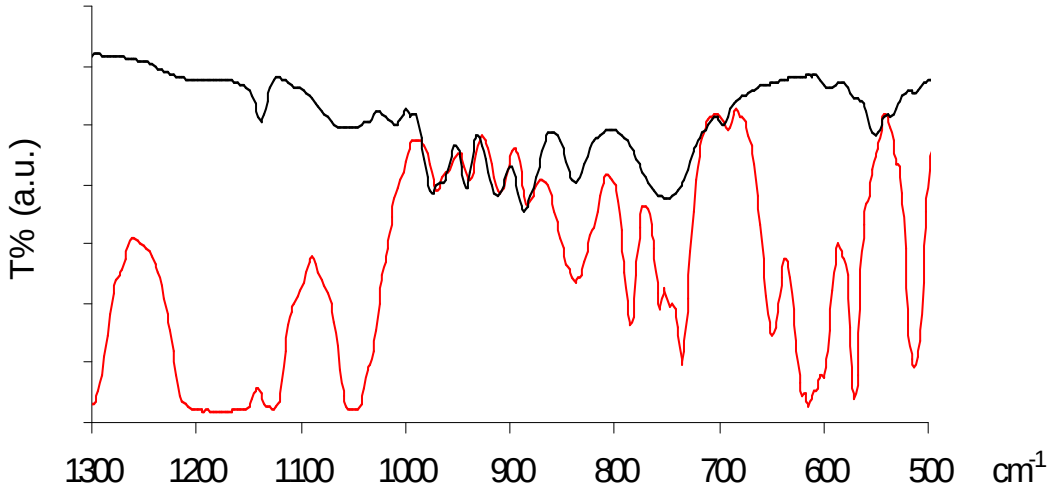

Figure 2.6 Superimposed FT-IR spectra ($1300<\nu<500$ cm^{-1}) of $[\gamma\text{-}SiW_{10}O_{36}(PhPO)_2]^{4-}$ as solid (KBr pellet, black line) and in $[bmim][(CF_3SO_2)_2N]$ after the reaction (NaCl windows, red line).

Finally, UV-vis analysis has confirmed that no catalyst leaching occurs upon extraction and washing of the catalytic phase (Fig. 2.7).

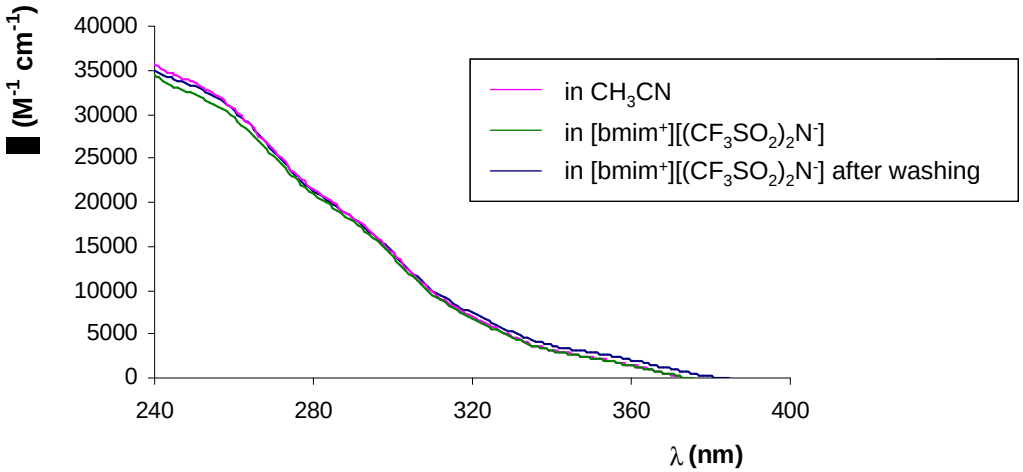

Figure 2.7 UV-vis spectra ($240<\lambda<400$ nm) of $[\gamma\text{-}SiW_{10}O_{36}(PhPO)_2]^{4-}$ in CH_3CN (pink line), in $[bmim][(CF_3SO_2)_2N]$ (green line) and in the latter after extraction of unreacted reagent and product followed by washing of the catalytic phase (blue line). No leaching of the catalyst was observed during work-up procedure.

2.2.2 Epoxidation of *cis*-cyclooctene with H_2O_2 in the catalytic phase

After ensuring the effective stability of [γ-$SiW_{10}O_{36}(PhPO)_2$]$^{4-}$ in the IL phase, catalytic tests have been performed, using *cis*-cyclooctene as the model substrate, in both hydrophilic and hydrophobic ILs (Scheme 2.3).

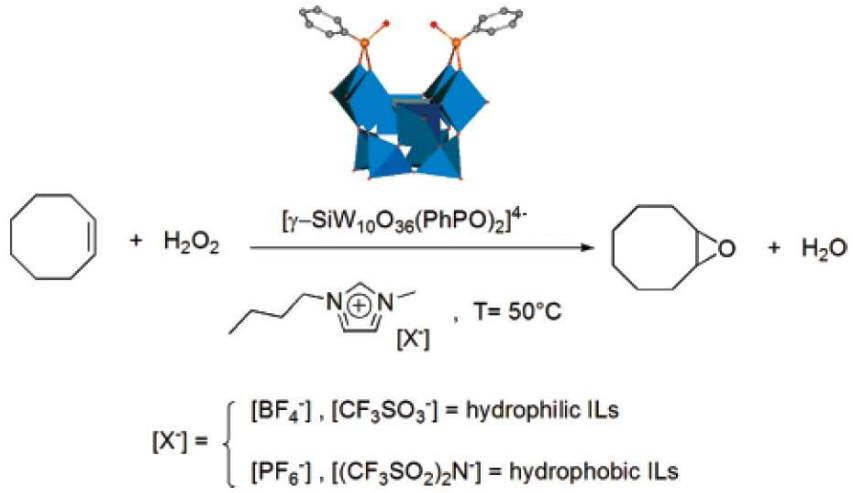

Scheme 2.3. Catalytic epoxidation of *cis*-cyclooctene by [γ-$SiW_{10}O_{36}(PhPO)_2$]$^{4-}$ with H_2O_2 in ILs.

The reactions have been performed in a two-phases set-up (see Table 2.1, footnote "a" for the experimental details). A hydrocarbon reservoir provides a stationary concentration of the olefin within the IL catalytic phase, thus fostering maximum rates at substrate saturation conditions.[i]

Quantitative GC analysis, performed during the reaction, indicates that the limiting olefin amount in the IL-phase is 1.5 M. Epoxidation occurs upon addition of aqueous hydrogen peroxide under vigorous stirring. H_2O_2 is fully soluble in all hydrophilic ILs, while a highly dispersed emulsion is formed within hydrophobic ILs. Both the supply of the peroxidic reagent and its evolution under catalysis result in H_2O accumulation in the system, which varies in the range 11-45% calculated with respect to the IL medium (Table 2.1).

According to the water content determined after high vacuum drying at 70°C for 4-30 h, hydrophobicity of the selected ILs is reported to increase in the order [bmim][BF_4]~ [bmim][CF_3SO_3]< [bmim][PF_6] < [bmim][$(CF_3SO_2)_2N$].[31]

[i] In particular, under conditions of stoichiometric olefin and H_2O_2, slower reaction rates were generally observed (99% yield of cyclooctene epoxide after 18 h and 51% of 1,2-epoxyoctane after 66 h, results to be compared with those of Tables 2.1 and 2.2).

Table 2.1. Catalytic epoxidation of *cis*-cyclooctene by $[\gamma\text{-}SiW_{10}O_{36}(PhPO)_2]^{4-}$ with aqueous H_2O_2 in ILs at 50°C.[a]

Entry	IL	H_2O[b] (%)	Time (min)	Epoxide yield[c] (%)	TOF[d] (min^{-1})
1	[bmim][BF_4]	23	300	62	0.6
2	[bmim][CF_3SO_3]	23	240	81	0.7
3	[bmim][PF_6]	23	180	>99	0.8
4		11	90	>99	3.5
5		45	90	17	0.1
6	[bmim][$(CF_3SO_2)_2N$]	23	120	92	1.2
7		11	45	>99	5.7
8[e]		11	1	>99	210
9[e,f]		22	2	94	100
10[g]		11	2	10	6.3

[a] Reactions performed in the presence of a layered hydrocarbon phase, *cis*-cyclooctene (3.0 mmol); H_2O_2 (0.60 mmol), provided by aqueous solutions with concentrations in the range 7-24 M; $[\gamma\text{-}SiW_{10}O_{36}(PhPO)_2]^4$ (4.80 μmol); 200 μl of IL. Substrate:oxidant:catalyst = 625:125:1. [b] Total amount of water (v/v %) introduced and formed during turnovers. [c] Calculated with respect to H_2O_2. [d] Turnover frequency (TOF) calculated as epoxide(mol)/catalyst (mol) per minute, and determined at < 60% conversion. [e] MW-irradiation at W= 10 watt, under stirring and simultaneous cooling with compressed air at 40 psi; T_{bulk} = 80°C. [f] Entry 8 recharged with H_2O_2 (0.60 mmol). [g] microflow-reaction at 0.017 mL/min (see Fig. 2.13).

Inspection of data in Table 2.1 reveals that selective epoxidation and quantitative conversion of H_2O_2 (epoxide yields up to >99%) is achieved in the hydrophobic ILs, namely [bmim][PF_6] and [bmim][$(CF_3SO_2)_2N$] (entries 3 and 6). Instead, slower to sluggish reactions occur in hydrophilic media, [bmim][CF_3SO_3] and [bmim][BF_4] (entries 1 and 2). Thus, optimization of the catalytic performance has been evaluated in ILs with high hydrophobicity.

The extent of water content in ILs is an often overlooked parameter for the optimization of the catalytic protocol. This instance has been further addressed by evaluating the impact of water addition/accumulation on the epoxidation kinetics and on the resulting turnover frequency (TOF) (Table 2.1 and Fig. 2.8).

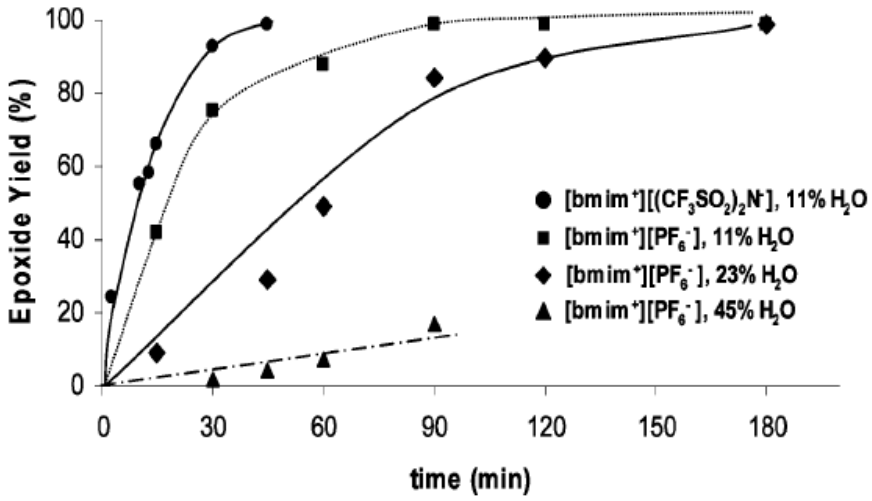

Figure 2.8. Kinetics of *cis*-cyclooctene epoxidation by [γ-$SiW_{10}O_{36}(PhPO)_2]^{4-}$ with aqueous H_2O_2 in hydrophobic ILs, at 50 °C.

Faster epoxidation profiles are obtained by using higher concentrated H_2O_2 in hydrophobic [bmim][$(CF_3SO_2)_2N$] and [bmim][PF_6] (● and ■ in Fig. 2.8), yielding respectively a maximum TOF of 5.7 and 3.5 turnovers per minute (entries 7 and 4 in Table 2.1). Addition of more diluted H_2O_2 solutions in [bmim][PF_6] results in a remarkable abatement of the oxidation rate with TOF values decreasing below unity (◆ and ▲ in Fig. 2.8 and entries 3 and 5 in Table 2.1). Anhydrous H_2O_2, in the form of urea complex (UHP), has been also tested as alternative oxidant but, under the particular conditions explored, it is not fully soluble in the IL-phase.

Therefore, water has a detrimental effect on the proposed system, because it modifies the physico-chemical properties of the ionic liquid itself. Pure 1,3-dialkylimidazolium ionic liquids can be in fact described as polymeric hydrogen-bonded supramolecules[32] (i.e. highly ordered hydrogen bonded materials), showing the structural trend of one imidazolium hydrogen bonded to at least three anions and one anion hydrogen bonded to at least three cations (Fig. 2.9 A). This structural pattern is a general trend for both the solid and the liquid phase.

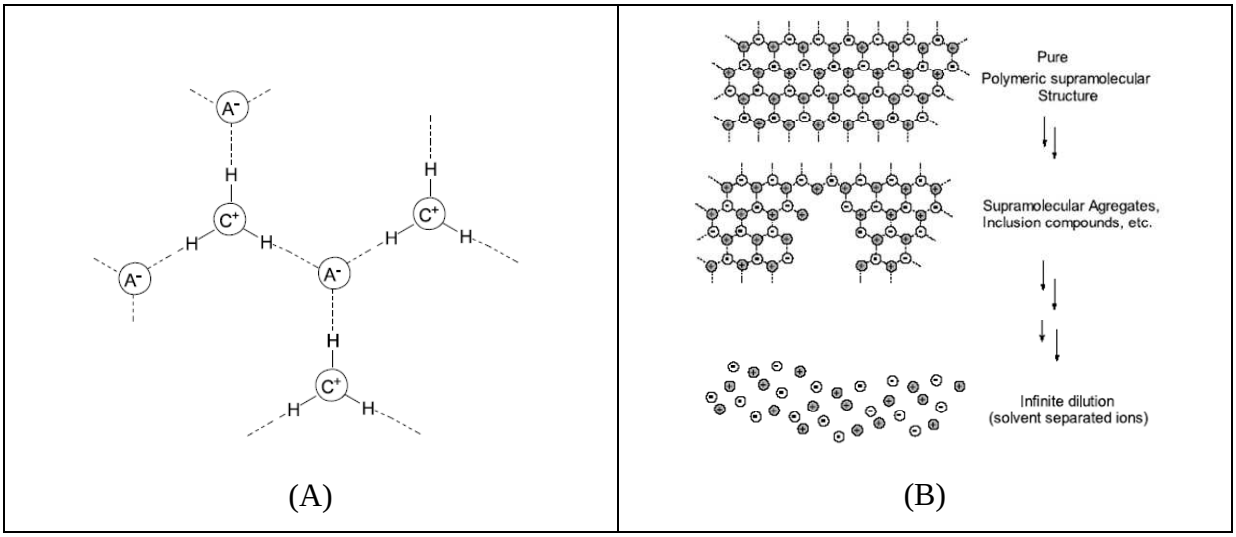

Figure 2.9. (A) Two-dimensional simplified solid-state model of the polymeric supramolecular structure of 1,3-dialkylimidazolium ionic liquids, showing the hydrogen bonds between the imidazolium cation (C^+) and the anions (A^-): one cation is surrounded by three anions and vice-versa. (B) Simplified two-dimensional model of the structural features of 1,3-dialkylimidazolium ionic liquids from hydrogen-bonded polymeric supramolecules (pure form) to solvent separated ion pairs (infinite dilution). Dashed lines represent the hydrogen bonds.

The incorporation of other molecules into the ionic liquid network causes changes to its physico-chemical properties, due to the disruption of the hydrogen bond network. In the case of water, the observed variation of the diffusion coefficient for neutral and ionic species in wet ionic liquids[33] may be explained by considering the ILs themselves no more as homogeneous solvents, but as nano-structures with polar and non-polar regions.[32] These nano-inhomogeneties allow neutral molecules to reside in less polar regions and ionic species to undergo faster diffusion in the more polar or wet regions.[32]

Moreover, the delivery of water is expected to impact the mass-transfer processes within the substrate/ILs/water multiphase system. Reactivity and physical-chemical properties of POMs are also known to be driven and influenced by protonation equilibria and ion-pair association, which can be strongly affected by the composition of the medium under turnover regime.[15, 34] Consequently, a direct, on-site, recharge of the system with additional portions of aqueous H_2O_2 fails to restore the pristine catalytic efficiency, leading to lower TOF values (recharge of reactions 2, 3, and 6 in Table 2.1, TOF < 0.5 min^{-1}) and overall epoxide yields <60%. Furthermore, at long reaction time, H_2O_2 decomposition becomes a competing process.

Nevertheless, a good recycling performance has been obtained after extraction of the spent catalytic phase (IL+POM) with hexane and water followed by vacuum anhydrification over P_2O_5. With this treatment, the epoxide has been recovered in quantitative yield, after at least four consecutive runs (total turnover numbers, TONs = 500, Fig. 2.10).

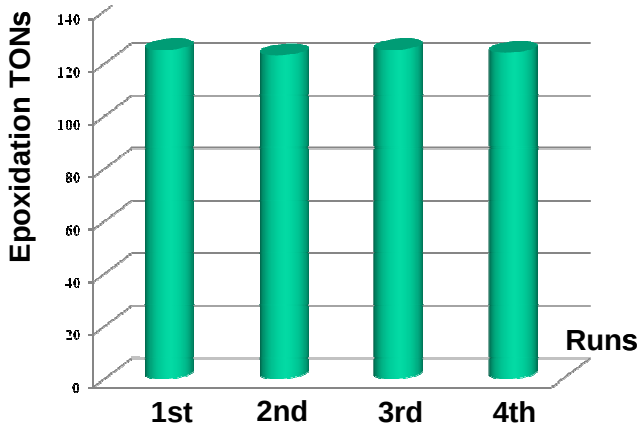

Figure 2.10. Turnover numbers (TONs) obtained in the four consecutive runs of the catalytic epoxidation of *cis*-cyclooctene with [γ-$SiW_{10}O_{36}(PhPO)_2]^{4-}$ and H_2O_2 in [bmim][$(CF_3SO_2)_2N$] at 50°C.

As already mentioned above, FT-IR and quantitative UV-vis analyses of the recovered catalytic phase confirm that both the POM structure and its loading are preserved upon extraction and recycling procedures (see Fig. 2.6 and 2.7).

As a corollary, *cis*-cyclooctene epoxidation by the non hybrid precursor [γ-$SiW_{10}O_{34}(H_2O)_2]^{4-}$ (Fig. 1.13) has been screened in [bmim][PF_6], [bmim][$(CF_3SO_2)_2N$] and [bmim][CF_3SO_3]. In these reactions, the epoxide has been obtained only in moderate yields (44-74%), while the exhausted catalyst precipitates out of the solution. FT-IR analyses indicate a major structural rearrangement of the lacunary POM.[35]

Therefore, further optimization of the reaction protocol and of the substrate scope has been performed only with [γ-$SiW_{10}O_{36}(PhPO)_2]^{4-}$, which exhibits a superior stability.

In particular, the implementation of the system has been achieved by:

- using microwave irradiation as heating source;
- performing the reaction in a microflow apparatus.

Both these aspects will be presented and discussed in the following paragraph.

2.2.3 Exploring new approaches: Microwave irradiation and microflow technique

A noteworthy implementation of the reaction protocol can be achieved using microwave (MW)-irradiation, as already established for a similar system in a recent publication by our research group.[16]

Microwave heating has become a widely accepted non-conventional energy source to perform organic synthesis, as shown by the increasing number of related publications in the recent years.[36]

In the electromagnetic spectrum, microwave radiation occurs between infrared radiation and radiofrequencies (Fig. 2.11).

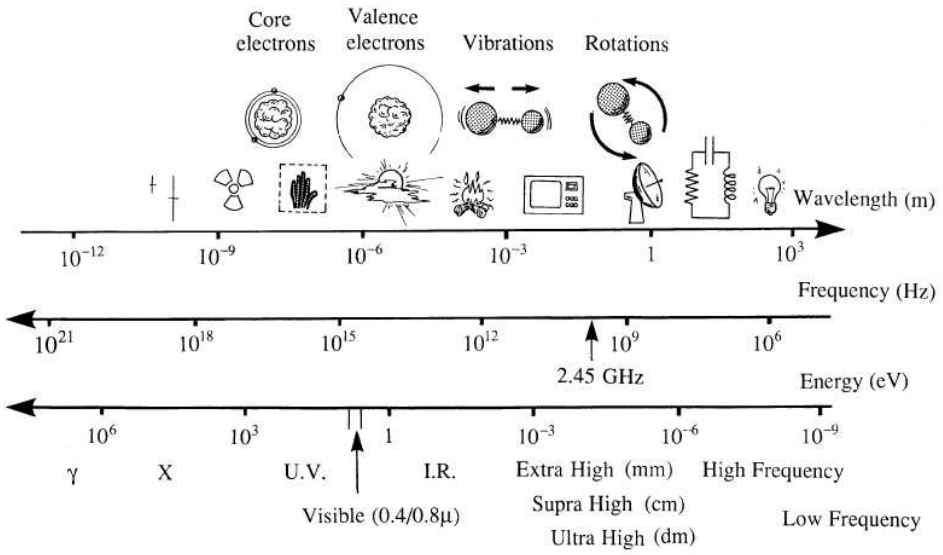

Figure 2.11. The electromagnetic spectrum.

MW frequencies are between 30 GHz and 300 MHz, but domestic ovens and laboratory systems generally work at 2.45 GHz. This energy is not sufficient to break any chemical (or hydrogen) bond and it is not transferred by conduction or convection (as in the case of conventional heating), but by dielectric loss.[37] The two main mechanisms by which materials dissipate microwave energy are indeed:

- dipole rotation, i.e. the alignment of the molecules possessing permanent or induced dipoles with the alternating electric field. In this case, energy is lost by molecular friction and collision, generating dielectric heating.
- ionic conduction, i.e. the migration of ions under the influence of the oscillating electric field. In this other case, heat generation is instead due to frictional losses, depending on size, charge and conductivity of the ions.[38]

Also in the case of an ionic sample, the initial heating, resulting from MW-irradiation, depends mainly from the dielectric loss by dipole rotation. The contribution from ionic conduction becomes relevant when temperature rises and predominates when ionic liquids are used as solvents.[39]

Spectacular accelerations, higher yields under milder reaction conditions, shorter reaction times, higher product purities and also increased selectivities (chemo-, regio- and stereoselectivity) have been reported for many MW-assisted organic reactions.[36d]

These evidences are mainly due to thermal effects. Such effects arise from the different features of microwave dielectric heating and conventional heating. As already mentioned above, microwave heating is related to the ability of some compounds (liquids or solids) to transform electromagnetic energy into heat. This feature allows absorption of the radiation and heating to be performed selectively. Moreover, microwave irradiation is rapid and volumetric, because the whole material is heated simultaneously; in contrast, conventional heating is slow and is transferred to the sample from the vessel wall (Fig. 2.12).

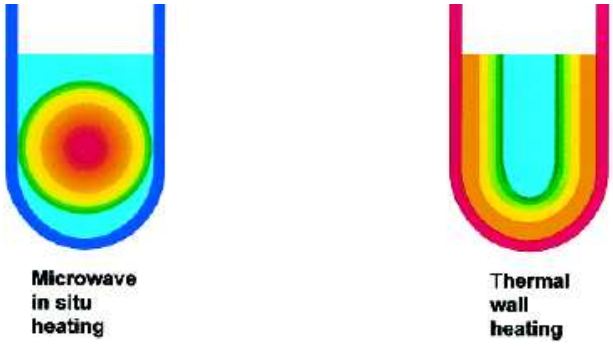

Figure 2.12. Schematic illustration of microwave in-situ heating (A): the heat is transferred directly into the reaction mixture. Classic wall heating (B): the heat energy must be transferred via the vessel wall.

A part from the heating rate, thermal effects arise also from:[36d]

- overheating of polar liquids, above their normal boiling point. This effect can be explained by the ‘‘inverted heat transfer’’ effect (from the irradiated medium towards the exterior), to which the enhancement in reaction rates observed in organic and organometallic chemistry can be addressed.
- ‘‘hot spots’’ effect. It arises from the inhomogeneity of the applied field, resulting in the raising of the temperature in certain zones within the sample, above the macroscopic (bulk) temperature. These regions are not representative of the reaction conditions as a whole.
- selective absorption of radiation by polar substances (both solvents and catalysts, reagents and products) in the presence of apolar ones.

All these effects can be used and tuned efficiently to improve processes, accelerate reactions (or even to perform reactions that do not occur under classical conditions) and avoid decomposition of thermally unstable compounds.[36]

Acceleration or changes in reactivity and selectivity of chemical reactions have also been addressed to non thermal effects, but this is still a controversial matter. Non-thermal effects (also called "specific microwave effects") can be addressed to the fact that microwave radiation is a very polarizing field and it may thus stabilize polar transition states and intermediates.[40]

During our study on the epoxidation of olefins with H_2O_2 catalyzed by $[\gamma\text{-}SiW_{10}O_{36}(PhPO)_2]^{4-}$, we have been interested in studying the combination of ionic liquids and microwaves. Indeed, it has already been demonstrated that the hybrid catalyst itself is stable under these conditions.[16]

Recently, many publications about the concomitant use of MW and ILs have been reported in literature, where ILs are used as solvents, reagents, but also as heating aids.[39]

The efficiency of these approaches is due to the extraordinary properties of ionic liquids, such as:

- ionic composition. Being composed entirely by ions, ILs can efficiently absorb MW energy, heading very fast to high temperatures. Efficient stirring is thus essential to distribute the heat evenly, avoiding the formation of hot spots.
- good thermal stability.
- negligible vapor pressure. The risk of explosion caused by rapid increase of vapor pressure of the solvent can then be avoided.

Encouraged by these perspectives, we have studied the catalytic epoxidation of *cis*-cyclooctene with H_2O_2 and $[\gamma\text{-}SiW_{10}O_{36}(PhPO)_2]^{4-}$ in $[bmim][(CF_3SO_2)_2N]$, the IL displaying the best results under conventional heating, and having also the highest thermal stability.

Indeed, the polyelectrolytic nature of the catalytic phase (POM+IL) guarantees fast and selective MW-induced heating, even at low power (4-10 watt). In our study, continuous MW-irradiation has been applied with simultaneous cooling (T_{bulk} < 80 °C). Here, the reaction vessel is cooled from the outside by a stream of compressed air, allowing a higher level of microwave power to be directly administered to the reaction mixture, while preventing bulk overheating.[41] Due to the fast and efficient response of ILs to MW-induced dielectric heating, a careful optimization of both the supplied MW power and the cooling flow is crucial to promote selective epoxidation versus unproductive H_2O_2 decomposition. Under the conditions

explored, quantitative epoxidation occurs in 1 minute, thus incrementing the TOF value obtained using conventional heating by ca. 35 times (entries 7 and 8, Table 2.1 in Paragraph 2.2.2). On the other hand, in the absence of simultaneous cooling, the yield of epoxide was negligible.

Considering the experimental set-up, the epoxide productivity amounts to ca. 7500 mol/h per mol of catalyst.

Moreover, the in-situ recharge of the reaction mixture with a second H_2O_2 aliquot provides a second epoxidation run with a reduced, but still remarkable TOF of 100 min^{-1} (entries 8 and 9, Table 2.1 in Paragraph 2.2.2).

The fast turnover regime achieved under MW-irradiation is amenable to flow type operations and microfluidic technology, responding to process intensification issues.

Recently, microfluidic technology has received a great deal of attention, because it offers a sustainable alternative to traditional methods.[42] Microreactors generally consist of a series of small (10-1000 μm) channels connected in various geometries, allowing the spatial and temporal manipulation of small amounts of fluids and reagents, infused in the channels by syringe or peristaltic pumps.

Continuously flowing microreactors can afford several advantages, such as increasing yield, selectivity, safety and efficiency of the chemical process, because they provide:[42a]

- a non-convective, laminar flow, wherein only diffusion affects mixing;
- rapid (millisecond scale), efficient and homogeneous mass-transfer, due to the high surface-to-volume ratio resulting from the narrow channel dimensions. This aspect is instrumental to avoid turbulence, chaotic mixing and inhomogeneities created by the stirring mechanism in classical reactors. These inhomogeneities lead indeed to concentration gradients, poor heat transfer and “hot spots” in the reaction environment, so, ultimately, to inefficient chemistry.
- rapid and efficient heat transfer and dissipation, with narrow temperature profiles, thus reducing the access to multiple pathways.
- better control by using small volumes of reactants, thus increasing the safety of the process especially when toxic or explosive compounds are used. For the same reason (but also because highly concentrated reagent streams can be used), microreactors minimize significantly waste production with the respect of using traditional reactors.
- elimination of scale-ups. The output is instead increased by “numbering up” with many reactors running in parallel, thus increasing safety and enhancing production by avoiding large reactors.[43]

- a powerful method for process optimization and library generation, that can be done rapidly on small scale, further reducing waste.

On these bases, the application of microreactors for multiphase systems can be an interesting implementation of our system, also considering the potentially harmful peroxide run-over.

Epoxidation of *cis*-cyclooctene with H_2O_2 catalyzed by $[\gamma\text{-}SiW_{10}O_{36}(PhPO)_2]^{4-}$ has been performed under flow conditions in a polytetrafluoroethylene (PTFE) microchannel tube (300 μm x 400 mm), placed in a thermostated (T = 50°C) reactor.

Reactants feeding was achieved using two syringes, connected to two different syringe-pumps, providing an experimentally determined flow of 0.017 mL/min (see Fig. 2.13, A). The first syringe was filled with the catalytic phase (i.e. the catalyst immobilized in [bmim][$(CF_3SO_2)_2N$]) and aqueous H_2O_2, while the second one with *cis*-cyclooctene and the internal standard (dodecane). The two phases were forced in the two different microtubes connected with the syringes, until they came into laminar contact in the actual reaction microchannel (Fig. 2.13, B). The exiting mixture was finally collected in a vial placed at the end of the tube, diluted with CH_2Cl_2 and analyzed (see Chapter 6 for the details).

Using this apparatus, epoxidation of *cis*-cyclooctene interestingly occurs with similar TOFs with the respect of the same reaction performed in batch (entries 7 and 10, Table 2.1 in Paragraph 2.2.2).

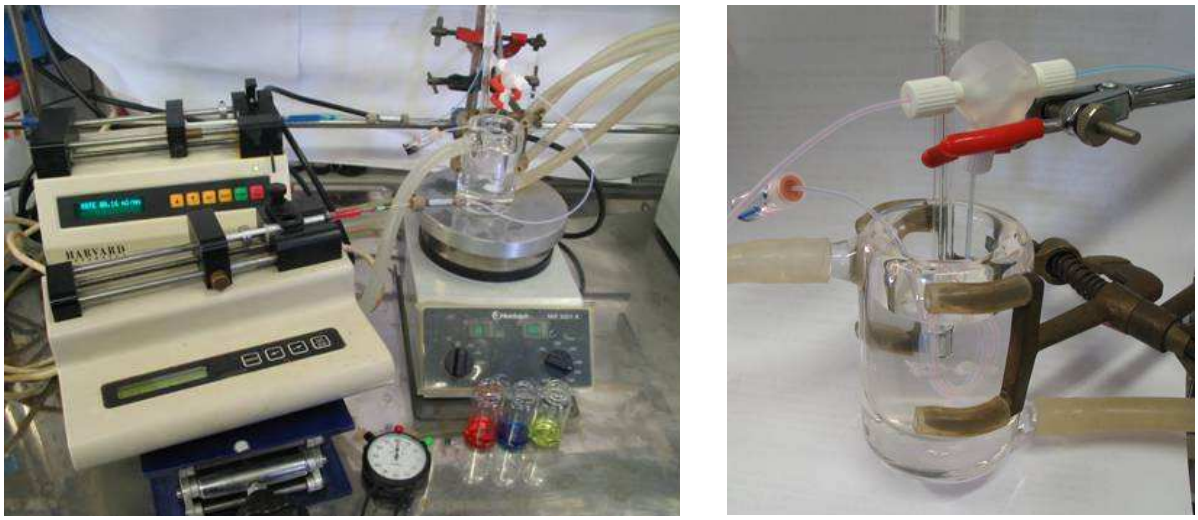

(A) (B)

Figure 2.13. Microflow-reaction apparatus (A) and a detail of the microchannel tube, where the reaction takes place (B). In the photos, the two syringes are filled with two dyes.

2.2.4 Scope of the reaction

The substrate scope of the optimized reaction protocol among the class of olefins is addressed in Table 2.2, including also the results obtained under MW-heating (results in parentheses).

In all these reactions the amount of water is kept below 1%, in order to prevent the epoxide conversion to diol and to over-oxidation products.

Under MW-irradiation, the registered bulk temperature (T_{bulk}) depends both on the substrate nature and on its concentration. For less reactive substrates (such as terminal alkenes), at high temperature, decomposition of H_2O_2 strongly competes with catalytic epoxidation, giving low epoxide yields. Optimization of the MW-assisted protocol requires the presence of a layered substrate phase and a higher catalyst loading, both instrumental for higher epoxide yields.

Table 2.2 Catalytic epoxidation by [γ-$SiW_{10}O_{36}(PhPO)_2]^{4-}$ with aqueous H_2O_2 in [bmim][$(CF_3SO_2)_2N$] at 50°C[a] and under MW-irradiation (results in parentheses)[b].

Entry	Olefin	Time, h	Epoxide yield,[c] %
1	cyclohexene	4 (0.25)	>99
2	*E*-2-octene	15 (0.75)	>99
3	1-octene	40 (3)	75 (54)
4	1-hexene	40 (2)	85 (99)
5	*Z*-2-hexene	15 (0.5)	77 (97)
6	*E*-2-hexene	15 (1)	89 (99)
7	*Z*-stilbene	15 (0.5[d])	89 (44)

[a] In all reactions: olefin (0.20 mmol), H_2O_2 (40 μmol) provided by 24M aqueous solution;[γ-$SiW_{10}O_{36}(PhPO)_2]^{4-}$ (0.32 μmol); 200 μl of [bmim][$(CF_3SO_2)_2N$]; T=50°C. [b] Reactions performed in the presence of a layered hydrocarbon phase (2.0 mmol); H_2O_2 (40 μmol), provided by 24 M aqueous solution; [γ-$SiW_{10}O_{36}(PhPO)_2]^{4-}$ (3.2 μmol); 200 μl of [bmim][$(CF_3SO_2)_2N$]. MW-irradiation at 5 watt, under stirring and simultaneous cooling; T_{bulk}=57-65°C. [c] Calculated with respect to H_2O_2. [d] MW-irradiation at 4 watt; T_{bulk}=58-73°C.

Oxidation of both internal and terminal olefins has proceeded with 99% selectivity towards epoxides. Internal olefins have been smoothly converted into the corresponding epoxides (yields up to 99%), using both conventional and MW-induced heating (entries 1-2, 5-7 in Table 2.2). Interestingly, high (up to quantitative) epoxide yields have been also achieved for less reactive terminal olefins, such as 1-octene and 1-hexene (entries 3 and 4 in Table 2.2).

A further point concerns the steric constrains of stereospecific oxygen transfer to *Z*- and *E*-alkenes. Competitive epoxidation of diastereomeric 2-hexenes shows a reactivity ratio *Z*/*E* of 6 (at 50 °C) and 5 (under MW-irradiation) at conversion of H_2O_2 <30%. Such *Z* preference is similar to that reported for other tungstate-based catalysts.[16, 44]

2.3 Conclusions

The combined use of a hybrid polyoxometalate, ionic liquids and MW-irradiation represents an innovative strategy for the immobilization, recycling and activation of an innovative and efficient catalytic phase for the epoxidation of olefins, within a solvent-free reaction set-up and using a sustainable oxidant (such as hydrogen peroxide).

Our results include the following:

- the screening of different ionic liquids in order to optimize catalytic efficiency of the system;
- the study of catalyst speciation and stability in the IL environment;
- the recovery and recycling of the catalytic phase (IL+POM), yielding quantitative production of cyclooctene epoxide in four consecutive runs (total TON = 500);
- the advantageous use of microwaves, which are readily absorbed by the totally ionic catalytic phase, to promote unprecedented turnover frequencies (TOF > 200 min^{-1} for the epoxidation of *cis*-cyclooctene);
- the miniaturization of the process, through microreactor technology coupled with continuous flow processing of the reaction mixture;
- the general applicability of the proposed catalytic system among the class of the olefins, leading to noteworthy selectivities and good/excellent yields (44-99%) in epoxide, also for less reactive terminal alkenes.

Further improvements of the reaction performances will be aimed to optimize its water tolerance, using of tailor-made, water-proof, IL phases which might be instrumental for catalytic oxidation with H_2O_2.

2.4 References and notes

[1] H. Adolfsson, in *Modern Oxidation Methods*, Wiley-VCH, Weinheim, **2004**, 21.

[2] R. A. Sheldon, J. K. Kochi, in *Metal Catalyzed Oxidations of Organic Compounds*, Academic Press, New York, **1981**.

[3] R. A. Van Santen, H. P. C. E. Kuipers *Adv. Catal.* **1987**, *35*, 265.

[4] H. B. Kagan, H. Mimoun, C. Marc, V. Schurig *Angew. Chem. Int. Ed. Engl.* **1979**, *18*, 485.

[5] T. Katsuki, K. B. Sharpless *J. Am. Chem. Soc.* **1980**, *102*, 5974.

[6] R. Landau, G. A. Sullivan, D. Brown *CHEMTECH*, **1979**, 602.

[7] R. A. Sheldon *J. Mol. Catal.* **1980**, *7*, 107.

[8] C. L. Hill, C. M. Prosser-McCartha *Coord. Chem. Rev.* **1995**, *143*, 407.

[9] a) C. Venturello, E. Alneri, M. Ricci *J. Org. Chem.* **1983**, *48*, 3831. b) C. Venturello, R. D'Aloisio, J. C. Bart, M. Riai *J. Mol. Catal.* **1985**, *32*, 107. c) C. Venturello, R. D'Aloisio *J. Org. Chem.* **1998**, *53*, 1553. d) K. Sato, M. Aoki, M. Ogawa, T. Hashimoto, R. Noyori *J. Org. Chem.* **1996**, *61*, 8310. e) K. Sato, M. Aoki, M. Ogawa, T. Hashimoto, D. Panyella, R. Noyori *Bull. Chem. Soc. Jpn.* **1997**, *70*, 905.

[10] a) P. Battioni, J.-P. Renaud, J. F. Bartoli, M. Reina-Artiles, M. Fort, D. Mansuy *J. Am. Chem. Soc.* **1988**, *110*, 8462. b) P. L. Anelli, L. Banfi, F. Legramandi, F. Montanari, G. Pozzi, S. Quici *J. Chem. Soc. Perkin Trans.* **1993**, *1*, 1345. c) A. Berkessel, M. Frauenkron, T. Schwenkreis, A. Steinmetz, G. Baum, D. Fenske *J. Mol. Catal. A: Chem.* **1996**, *113*, 321. d) R. Irie, N. Hosoya, T. Katsuki *Synlett.* **1994**, 255.

[11] a) W. A. Herrmann, R. W. Fischer, D. W. Marz *Angew. Chem. Int. Ed. Engl.* **1991**, *30*, 1638. b) J. Rudolph, K. L. Reddy, J. P. Chiang, K. B. Sharpless *J. Am. Chem. Soc.* **1997**, *119*, 6189. c) W.-D. Wang, J. H. Espenson *J. Am. Chem. Soc.* **1998**, *120*, 11335.

[12] a) T. G. Traylor, S. Tsuchiya, Y.-S. Byun, C. Kim *J. Am. Chem. Soc.* **1993**, *115*, 2775. b) M. C. White, A. G. Doyle, E. N. Jacobsen *J. Am. Chem. Soc.* **2001**, *123*, 7194.

[13] a) W. Adam, P. L. Alsters, R. Neumann, C. R. Saha-Möller, D. Sloboda-Rozner, R. Zhang *J. Org. Chem.* **2003**, *68*, 1721. b) D. Sloboda-Rozner, P. L. Alsters, R. Neumann *J. Am. Chem. Soc.* **2003**, *125*, 5280. c) D. Sloboda-Rozner, P. Witte, P. L. Alsters, R. Neumann *Adv. Synth. Catal.* **2004**, *346*, 339.

[14] a) N. Mizuno, K. Kamata, K. Yonehara, Y. Sumida *Science* **2003**, *300*, 964. b) N. Mizuno, K. Yamaguchi, K. Kamata *Coord. Chem.Rev.* **2005**, *249*, 1944. c) K. Kamata, Y. Nakagawa, K. Yamaguchi, N. Mizuno *J. Catal.* **2004**, *224*, 224. d) K. Kamata, M. Kotani, K. Yamaguchi, S. Hikichi, N. Mizuno *Chem. Eur. J.* **2007**, *13*, 639.

[15] A. Sartorel, M. Carraro, A. Bagno, G. Scorrano, M. Bonchio *Angew. Chem. Int. Ed.* **2007**, *46*, 3255.

[16] M. Carraro, L. Sandei, A. Sartorel, G. Scorrano, M. Bonchio *Org. Lett.* **2006**, *8*, 3671.

[17] S. Berardi, M. Bonchio, M. Carraro, V. Conte, A. Sartorel, G. Scorrano *J. Org. Chem.* **2007**, *72*, 8954.

[18] a) C. R. Mayer, R. Thouvenot. *J. Chem. Soc. Dalton Trans.* **1998**, 7. b) C. R. Mayer, P. Herson, R. Thouvenot *Inorg. Chem.* **1999**, *38*, 6152.

[19] a) T. Welton *Chem. Rev.* **1999**, *99*, 2071. b) P. Wasserscheid, T. Welton (Eds.) *Ionic Liquids in Synthesis*, Wiley-VCH, Weinheim, **2003**. c) P. Wasserscheid, W. Keim *Angew. Chem. Int. Ed.* **2000**, *39*, 3772. d) V. I. Pârvulescu, C. Hardacre *Chem. Rev.* **2007**, *107*, 2615.

[20] W. Miao, T. H. Chan *Acc. Chem. Res.* **2006**, *39*, 897.

[21] a) J. D. Revell, A. Ganesan *Org. Lett.* **2002,** *4***,** 3071. b) B. C. Ranu, A. Saha, S. Banerjee *Eur. J. Org. Chem.* **2008**, 519.

[22] O. Bortolini, V. Conte, C. Chiappe, G. Fantin, M. Fogagnolo, S. Maietti *Green Chem.* **2002**, *4*, 94.

[23] B. Wang, Y.-R. Kang, L.-M. Yang, J.-S. Suo *J. Mol. Catal. A: Chem.* **2003**, *203*, 29.

[24] R. Bernini, E. Mincione, A. Coratti, G. Fabrizi, G. Battistuzzi *Tetrahedron* **2004**, *60*, 967.

[25] K.-H. Tong, K.-Y. Wong, T. H. Chan *Org. Lett.* **2003**, *5*, 3423.

[26] G. S. Owens, M. M. Abu-Omar *Chem. Commun.* **2000**, 1165.

[27] Y. Kazuya, C. Yoshida, S. Uchida, N. Mizuno *J. Am. Chem. Soc.* **2005**, *127*, 530.

[28] a) C. P. Mehnert, R. A. Cook, N. C. Dispenziere, M. Afeworki *J. Am. Chem. Soc.* **2002**, *124*, 12932. b) C. P. Mehnert, E. J. Mozeleski, R. A. Cook *Chem. Commun.* **2002**, 3010. c) A. Riisager, R. Fehrmann, M. Haumann, P. Wasserscheid *Eur. J. Inorg. Chem.* **2006**, 695.

[29] a) G. S. Owens, M. M. Abu-Omar *J. Mol. Catal. A*: *Chem.* **2002**, *187*, 215. b) P. Bonhôte, A. P. Dias, N. Papageorgiou, K. Kalyanasundaram, M. Grätzel *Inorg. Chem.* **1996**, *35*, 1168. c) K. R. Seddon, A. Stark, M. J. Torres *Pure Appl. Chem.* **2000**, *72*, 2275.

[30] J. Canny, A. Tézé, R. Thouvenot, G. Hervé *Inorg. Chem.* **1986**, *25*, 2114.

[31] a) J. G. Huddleston, A. E. Visser, W. M. Reichert, H. D. Willauer, G. A. Broker, R. D. Rogers *Green Chem.* **2001**, *3*, 156. b) M. Kanakubo, Y. Hiejima, K. Minami, T. Aizawa, H. Nanjo *Chem. Commun.* **2006**, 1828.

[32] J. Dupont *J. Braz. Chem. Soc.* **2004**, *15*, 341.

[33] U. Schroder, J. D. Wadhawan, R. G. Compton, F. Marken, P. A. Z. Suarez, C. S. Consorti, R. F. de Souza, J. Dupont *New J. Chem.* **2000**, *24*, 1009.

[34] a) D. G. Musaev, K. Morokuma, Y. V. Geletii, C. L. Hill *Inorg. Chem.* **2004**, *43*, 7702. b) V. A. Grigoriev, D. Cheng, C. L. Hill, I. A. Weinstock *J. Am. Chem. Soc.* **2001**, *123*, 5292.

[35] Evolution of $[\gamma\text{-}SiW_{10}O_{34}(H_2O)_2]^{4-}$ to dimeric complexes has been reported to occur in non-aqueous environment. See also: A. Yoshida, M. Yoshimura, K. Uehara, S. Hikichi, N. Mizuno *Angew. Chem., Int. Ed.* **2006**, *45*, 1956.

[36] a) A. Loupy, in *Microwaves in Organic Synthesis*, Wiley-VCH, Weinheim, **2002**. b) B. L. Hayes, in *Microwave Synthesis: Chemistry at the Speed of Light*, CEM Publishing, Matthews, NC, **2002**. c) C. O. Kappe, *American Laboratory* **2001**, *33*, 13. d) A. de la Hoz, A. Díaz-Ortiz, A. Moreno *Chem. Soc. Rev.* **2005**, *34*, 164.

[37] J. E. Gerling *J. Microwave Power Electromagnetic Energy* **1987**, *22*, 199.

[38] S. Washisu, I. Fukai *J. Microwave Power* **1980**, *15*, 59.

[39] N. E. Leadbeater, H. M. Torenius, H. Tye *Comb. Chem. High Throughput Screen.* **2004**, *7*, 511.

[40] A. Loupy, F. Maurel, A. Sabatié-Gogova *Tetrahedron* **2004**, *60*, 1683.

[41] M. Hosseini, N. Stiasni, V. Barbieri, C. O. Kappe *J. Org. Chem.* **2007**, *72*, 1417.

[42] a) B. P. Mason, K. E. Price, J. L. Steinbacher, A. R. Bogdan, D. T. McQuade *Chem. Rev.* **2007,** *107*, 2300 and references cited therein. b) B. Ahmed, D. Barrow, T. Wirth *Adv. Synth. Catal.* **2006**, *348*, 1043 and references cited therein. c) T. N. Glasnov, C. O. Kappe *Macromol. Rapid Commun.* **2007**, *28*, 395.

[43] T. Bayer, J. Jenck, M. Matlosz *Chem. Eng. Technol.* **2005**, *28*, 431.

[44] Y. Goto, K. Kamata, K. Yamaguchi, K. Uehara, S. Hikichi, N. Mizuno *Inorg. Chem.* **2006**, *45*, 2347 and references cited therein.

3. Friedel-Crafts acylation of ferrocene in Ionic Liquids

3.1 Friedel-Crafts acylation of ferrocene: an introduction

During my Ph.D., a collaboration with prof. Conte of the University of Rome – Tor Vergata, has regarded the MW-assisted Friedel-Crafts acylation of ferrocene catalyzed by scandium triflate in ionic liquids.[1]

Friedel-Crafts acylation represents a useful method for the functionalization of arenes, using a suitable acylating agent (aryl/alkyl halide or the corresponding anhydride) in presence of a Lewis acid catalyst, such as $AlCl_3$, $FeCl_3$, $ZnCl_2$, HF or H_3PO_4, in stoichiometric amounts. The Lewis acid is indeed complexed to the formed ketone, thus requiring a hydrolysis step to isolate the product.[2]

These reactions have been also performed in chloroaluminate ILs, which have the advantage of being simultaneously the reaction catalyst and the solvent, but at the same time the disadvantage of being extremely sensitive to water.[3] Air- and moisture-stable pyridinium based ILs have been later successfully employed as reaction media.[3, 4]

More sustainable reaction protocols have reported the use of catalytic amounts of scandium or lanthanides triflates as the Lewis acid.[5]

Also metal triflate catalyzed Friedel-Crafts acylation reactions have been performed in ILs.[6]

In this section, only the Friedel-Crafts acylation of ferrocene (FcH) in ionic liquids will be discussed, since FcH is an excellent aromatic substrate for this reaction, being ca. 10^6 times more reactive than benzene.[7]

Moreover, such reaction represents one of the more versatile methods to functionalize FcH. In general, the reaction proceeds under relatively mild conditions with both acyl halides and anhydrides and affords excellent yields of mono- and diacylferrocenes, both useful intermediates for the preparation of less accessible derivatives. Generally the main (if not the only) product of Friedel-Crafts acylations is the monoacyl derivative, due to the deactivating effect of the conjugated ketone moiety. In the case of FcH, however, formation of the corresponding 1,1'-diacylderivate is also observed, when performing the reaction in presence of an excess of Lewis acid. Such anomalous change in the relative reactivities of the substrate and its monoacyl derivative is due to FcH protonation by HCl in presence of an excess of $AlCl_3$ (Scheme 3.1).[7b]

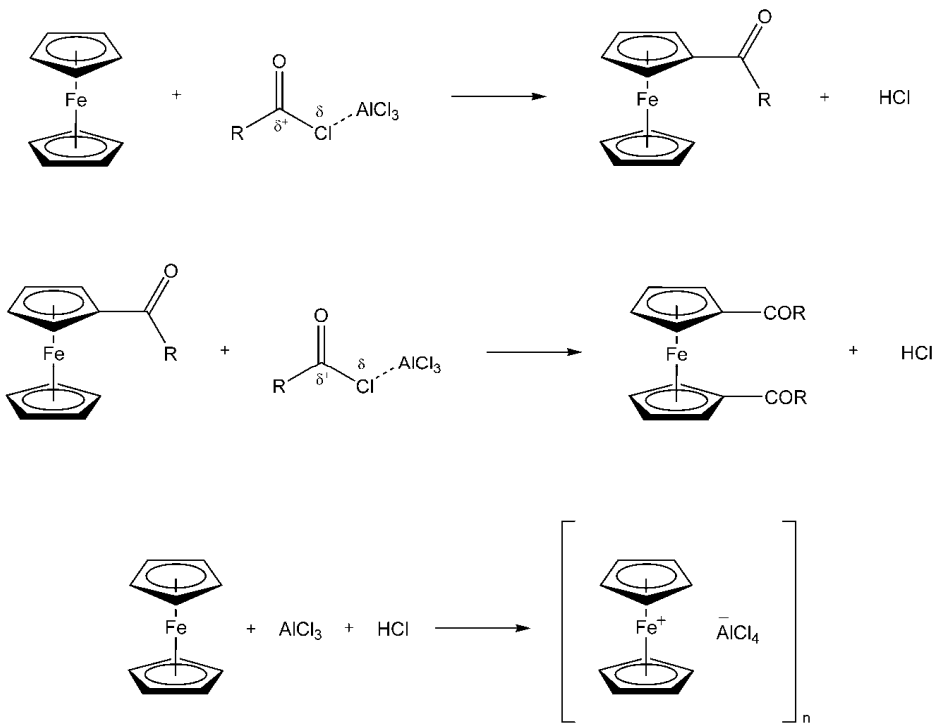

Scheme 3.1. Mono- *vs.* diacylation of FcH in Friedel-Crafts acylations with an excess of $AlCl_3$.

The cation resulting from HCl protonation is indeed inert toward acylation, and, by this reactivity pattern, removed from competition with the monoacyl derivative.

In molecular solvents (e.g. dichloromethane, chloroform of carbon disulfide), this reaction is usually carried out at room temperature or at 0°C in the presence of a stoichiometric amount of Lewis acid ($AlCl_3$, $SnCl_4$, BF_3, H_3PO_4, HF). Reaction progress is evidenced by the formation of a dark red or purple solution, characteristic of the acylferrocene-Lewis acid complex.[7b]

Friedel-Crafts acylation of FcH has also been studied in ILs, using stoichiometric or catalytic amounts of Lewis acids.[8]

Our work has regarded the investigation of scandium triflate catalyzed FcH acylation performed in ILs, using both conventional and MW-induced heating. The reaction parameters have been optimized (when possible) in order to maximize the formation of monosubstituted species. Results will be presented and discussed in the following paragraphs.

3.2 Results and Discussion

3.2.1 Friedel-Crafts acylation of ferrocene with acetic anhydride

Reaction conditions, such as the Lewis acid used, the IL choice, catalyst loading and reaction temperature have been optimized for the Friedel-Crafts acylation of ferrocene (FcH) with acetic anhydride (Ac_2O) (Scheme 3.2).

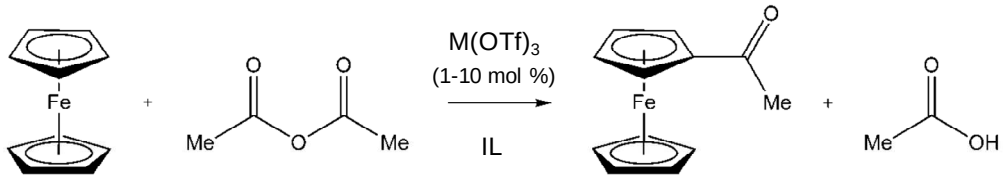

M = Sc^{III}, Y^{III}, Yb^{III}

Scheme 3.2. Lewis acid catalyzed Friedel-Crafts acylation of ferrocene with acetic anhydride.

Effect of the solvent

First attempts of performing FcH acetylations with scandium triflate ($Sc(OTf)_3$) have regarded the use of molecular solvents. Using nitromethane, dichloromethane or acetonitrile, led to FcH conversion at 25°C of 42%, 10% and 21% respectively. Increasing the temperature led to an improvement of conversion (38% in CH_3CN at 50°C). Acetylation reaction improved slightly when performed using Ac_2O as the solvent at 50°C, as a 66% conversion of FcH was observed after 2.5 h.

These disappointing results notwithstanding, investigation has been extended to ILs as solvents, where improved reactivity is often observed. Results are reported in Table 3.1.

Table 3.1. Sc^{III} catalyzed acetylation of ferrocene in ILs (FcAc = acetylferrocene).[a]

#	IL	T, °C	t, h	FcH:Ac_2O:$Sc(OTf)_3$ ratio	Conversion, %[b]	FcH:FcAc relative ratio[c]	Yield, %[d]
1	[bmim][CF_3SO_3]	25	96	1 : 1 : 0.1	1	99 : 1	<1
2	[bmim][PF_6]	25	4	1 : 1 : 0.1	79	75 : 25	21
3	[bmim][PF_6]	50	3	1 : 1 : 0.1	67	20 : 80	57
4	[bmim][PF_6]	50	2.5	1 : 5 : 0.1	73	32 : 68	64
5	[bmim][$(CF_3SO_2)_2N$]	50	2.5	1 : 5 : 0.1	94	7 : 93	78
6	[hmim][$(CF_3SO_2)_2N$]	50	2.5	1 : 1.3 : 0.1	17	93 : 3	2
7	[bupy][$(CF_3SO_2)_2N$]	50	2.5	1 : 1.3 : 0.1	89	15 : 85	75

[a] FcH 1 M in IL (1 mL). [b] Calculated from recovered FcH. [c] GC analysis (internal standard = tetradecane). [d] Isolated FcAc, yield relative to conversion.

Hydrophilic 1-butyl-3-methylimidazolium triflate, [bmim][CF_3SO_3], dissolves well $Sc(OTf)_3$, but almost no reaction has occurred after days (1% acetylferrocene, FcAc, entry 1, Table 3.1). Most likely, $CF_3SO_3^-$ exerts a common ion effect and interferes with scandium triflate dissociation, thus inhibiting the catalyst.

In hydrophobic 1-butyl-3-methylimidazolium hexafluorophosphate, [bmim][PF_6], interesting conversions have been obtained (67-79%, entries 2-4, Table 3.1). Isolated yields of acetylferrocene were up to 64% on the basis of reacted ferrocene (47% *vs*. initial FcH).

Excess Ac_2O (entry 3, Table 3.1) did not yield any disubstituted product, but allows reducing reaction time and, consequently, ferrocene decomposition due to prolonged exposure to acid.[9] Moreover, reduced decomposition has been observed raising the temperature from 25°C to 50°C, also resulting in shorter reaction time (entries 2 and 3, Table 3.1).

Even better results were obtained in hydrophobic [bmim][$(CF_3SO_2)_2N$] (entry 5, Table 3.1), with 93% FcH conversion and 78% FcAc isolated yield (73% *vs*. initial FcH). However, ferrocene is not much soluble in [bmim][$(CF_3SO_2)_2N$] and therefore other *bis*-triflylimide-based ILs have been tested, in an attempt to improve solubility. In particular, *N*-butylpyridinium ([bupy][$(CF_3SO_2)_2N$], entry 7, Table 3.1) and 1-hexyl-3-methylimidazolium ([hmim][$(CF_3SO_2)_2N$], entry 6, Table 3.1) cations have been tested. Still, [bmim][$(CF_3SO_2)_2N$] is the solvent where higher FcH conversion and lower decomposition are observed, thus the following experiments have been performed in such IL.

The following experimental conditions were chosen for subsequent throughout investigations: 1 mmol FcH in 1 mL [bmim][$(CF_3SO_2)_2N$] in presence of a five-fold excess of Ac_2O at 50°C. Excess of acylating agent is advisable, because it helps in solubilizing FcH in the IL and speeding up the reaction; moreover, it does not interfere with the reaction outcome, since production of 1,1'-diacetylferrocene was never observed. Moreover, no oxidation of ferrocene occurred in [bmim][$(CF_3SO_2)_2N$].

The effects of the metal catalyst and of its loading have also been evaluated. Results will be discussed in the following paragraph.

Effects of the metal catalyst and its loading

Catalytic performances of different Lewis acid catalysts have been investigated, under the above mentioned optimized reaction. Results are reported in Table 3.2.

Table 3.2. Acetylation of ferrocene in [bmim][$(CF_3SO_2)_2N$] at 50°C, catalyzed by different metal triflates.[a]

#	Catalyst	t, h	FcH:Ac_2O:$M(OTf)_3$ ratio	Conversion, %[b]	FcH:FcAc ratio[c]	Yield, %[d]
1	$Y(OTf)_3$	2.5	1 : 5 : 0.1	94	12 : 88	66
2	$Y(OTf)_3$	8.0	1 : 5 : 0.1	100	0 : 100	67
3	$Yb(OTf)_3$	2.5	1 : 5 : 0.1	95	17 : 83	59
4	$Yb(OTf)_3$	5.5	1 : 5 : 0.1	95	5 : 95	64
5	$Sc(OTf)_3$	2.5	1 : 5 : 0.1	94	7 : 93	78

[a] FcH 1 M in [bmim][$(CF_3SO_2)_2N$] (1 mL). [b] Calculated from recovered FcH. [c] GC analysis (internal standard = tetradecane). [d] Isolated FcAc, yield relative to conversion.

After comparable reaction times (2.5 h), scandium triflate has resulted more efficient than the corresponding yttrium and ytterbium salts (entries 5, 1 and 3, Table 3.2), giving the highest isolated yield of FcAc, whereas FcH conversion was slightly lower.

With longer reaction times, the yttrium catalyst caused quantitative disappearance of FcH, without any increase of FcAc yield (Entry 2, Table 3.2).

As to the ytterbium catalyst, FcH conversion is the same as that with scandium, but yields are definitely lower (Entry 4, Table 3.2). Thus, the less expensive $Sc(OTf)_3$ results a better Friedel-Crafts catalyst for ferrocene acetylation than the corresponding lanthanides triflates.

Scandium-catalyzed acetylation of ferrocene was then performed using different catalyst loadings. Results are summarized in Table 3.3.

Table 3.3. Acetylation of ferrocene in [bmim][$(CF_3SO_2)_2N$] at 50°C, with different amounts of $Sc(OTf)_3$.[a]

#	$Sc(OTf)_3$, mol%	t, h	FcH:Ac_2O:$Sc(OTf)_3$ ratio	Conversion, %[b]	FcH:FcAc ratio[c]	Yield, %[d]
1	10	2.5	1 : 5 : 0.1	94	7 : 93	76
2	5	2.5	1 : 5 : 0.05	89	32 : 69	43
3	5	9.0	1 : 5 : 0.05	94	14 : 86	55
4	5	2.5 (60°C)	1 : 5 : 0.05	100	0 : 100	60
5	1	2.5	1 : 5 : 0.01	32	90 : 10	20
6	1	29.5	1 : 2.5 : 0.01	95	83 : 17	37

[a] FcH 1 M in [bmim][$(CF_3SO_2)_2N$] (1 mL). [b] Calculated from recovered FcH. [c] GC analysis (internal standard = tetradecane). [d] Isolated FcAc, yield relative to conversion.

Although 10% molar for the Lewis acid is an improvement with respect of the stoichiometric $AlCl_3$, it is still a considerable amount of a precious catalyst. Therefore, experiments have been performed reducing the catalyst. 5% molar $Sc(OTf)_3$ is still efficient in terms of catalysis, but requires higher temperature (60°C), in order to avoid prolonged reaction times and consequent decomposition of FcH (entries 2-4, Table 3.3). When the catalyst loading was lowered to 1% molar of $Sc(OTf)_3$, efficiency decreased sharply and increasing reaction times did not improve significantly FcH conversion, nor isolated quantity of ketone (entries 5 and 6, Table 3.3).

To summarize results, acetylferrocene can be obtained in good yields using 5% scandium triflate as Lewis acid, [bmim][$(CF_3SO_2)_2N$] as solvent and a five-fold excess of acylating agent Ac_2O. Using such optimized conditions, the scope of the Friedel-Crafts acylation has been then investigated. Results will be reported in the following paragraph.

3.2.2 Scope of the reaction

In order to establish the scope of the reaction, different acylating reagents were used. Experiments with acyl chlorides were abandoned after some initial attempts with disappointing results, clearly due to the formation of HCl, that causes extensive decomposition of ferrocene, especially in ILs. When using propanoic anhydride ($(EtCO)_2O$) as acylating agent good yields of propanoylferrocene (FcCOEt) have been obtained. Results are summarized in Table 3.4.

Table 3.4. Sc^{III}-catalyzed Friedel-Crafts acylation of ferrocene with propanoic anhydride $(EtCO)_2O$.[a]

#	Fc:$(EtCO)_2O$:cat ratio	t, h	T, °C	Work-up method	Conversion, %[b]	Yield, %[c]
1	1 : 3 : 0.1	2.5	50	extraction	78	63
2	1 : 3 : 0.1	2	60	extraction	71	71
3	1 : 1 : 0.1	48	50	extraction	57	52
4	1 : 1 : 0.1	48	50	distillation	57	52
5[d]	1 : 1 : 0.1	96	50	distillation	38	6
6	1 : 2 : 0.1	17	60	extraction	98	72
7[e]	1 : 2 : 0.1	17	60	distillation	97	2.4

[a] FcH 1 M in [bmim][$(CF_3SO_2)_2N$] (1 mL). [b] Calculated from recovered FcH. [c] Isolated FcCOEt, yield relative to conversion. [d] Recycle of entry 4. [e] Recycle of entry 6.

Propanoylferrocene was isolated either by extraction with diethyl ether, or by direct distillation under vacuum from the reaction mixture. After the latter work-up, a recycle of the IL phase was attempted, re-loading it with FcH and propanoic anhydride. Unfortunately, even after prolonged reaction times, only small amounts of propanoylferrocene have been obtained (Entry 5, Table 3.4), thus confirming that prolonged exposure to acidic medium is detrimental for FcH and/or the catalyst.

An aromatic anhydride, namely benzoic anhydride ($(PhCO)_2O$), has been also tested as acylating agent. Unfortunately, it resulted scarcely reactive, since 24 h heating produced, at best, only 25% isolated benzoylferrocene.

3.2.3 Sc^{III}-catalyzed Friedel-Crafts acylation of ferrocene in [bmim][$(CF_3SO_2)_2N$] under MW-irradiation

To complete the exploration of reaction parameters, we have decided to perform the reaction using microwave (MW)-induced dielectric heating. Microwave should indeed be readily absorbed by the ionic solvent, thus eventually leading to a drastic reduction of reaction times (see Chapter 2, Paragraph 2.2.3).

Friedel-Crafts acylation of ferrocene has been then performed under MW-irradiation, using different aliphatic and aromatic anhydrides (Scheme 3.3).

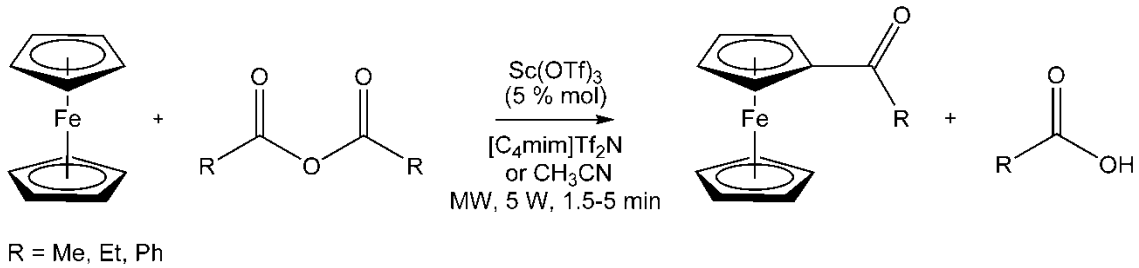

Scheme 3.3. Sc^{III}-catalyzed Friedel-Crafts acylation of ferrocene under MW-irradiation.

Results are summarized in Table 3.5.

Table 3.5. Sc^{III}-catalyzed Friedel-Crafts acylation of FcH under MW-irradiation.[a]

#	Anhydride (A)	FcH:A:cat ratio	T_{bulk}, °C	t, min	Conversion, %[b]	Yield, %[c]
1	Ac_2O	1 : 5 : 0.05	80	3.5	80	77
2[d]	Ac_2O	1 : 10 : 0.05	105-110	3.5	94	93
3[d,e]	Ac_2O	1 : 5 : 0.05	105-110	7.0	88	79
4[f]	Ac_2O	1 : 5 : 0.05	95	4.5	100	100
5	Ac_2O	1 : 5 : 0.05	115	1.5	100	100
6[g]	Ac_2O	1 : 5 : 0.05	72-74	2.0		30
7[g]	Ac_2O	1 : 5 : 0.05	65	5.0		38
8	$(EtCO)_2O$	1 : 5 : 0.05	116-120	4.5[h]	92	84[i]
9	$(EtCO)_2O$	1 : 5 : 0.05	92-96	2.0[j]	>99	86[k]
10	$(PhCO)_2O$	1 : 5 : 0.05	127-155	4.5	98	42

[a] 1 M FcH in [bmim][$(CF_3SO_2)_2N$] (1 mL); MW-irradiation at W = 5 watt (40 watt in Entries 6-7), under stirring and simultaneous cooling with compressed air (30-50 psi). [b] GC analysis (internal standard=dodecane). [c] Isolated monoacetylated product, yield relative to conversion. [d] 0.5 M FcH. [e] Catalyst added in two portions. [f] 0.25 M FcH. [g] CH_3CN as solvent. [h] 3 irradiation cycles, 1.5 min each. [i] After column chromatography, 72% propanoylferrocene was recovered, together with 18% disubstituted ketone. [j] Single irradiation cycle. [k] After column chromatography, 84% propanoylferrocene was recovered, together with 13% disubstituted ketone.

Blank experiments in presence of ferrocene and Ac_2O in [bmim][$(CF_3SO_2)_2N$] without $Sc(OTf)_3$ gave no product under both conventional and MW-assisted heating. Addition of the catalyst in two portions did not improve the yield (entry 3, Table 3.5).

Under best conditions for the MW-assisted acetylation of FcH in [bmim][$(CF_3SO_2)_2N$], 5% molar catalyst loading has quantitatively yielded acetylferrocene in 1.5 min (entry 5, Table 3.5). On the other hand, no appreciable improvement has been observed when performing the reaction in molecular solvent under MW-irradiation with respect to conventional heating (entries 6 and 7, Table 3.5). Despite the higher irradiation power used (40 watt in CH_3CN *vs.* 5 watt in IL), T_{bulk} in CH_3CN remains lower than in [bmim][$(CF_3SO_2)_2N$]. This can be ascribed to the more efficient MW-absorption by ionic species (see Chapter 2, Paragraph 2.2.3).

Improved results have also been obtained performing FcH acylation with propanoic anhydride under MW-irradiation (entries 9 and 10, Table 3.5). In all cases, fast quantitative conversion of ferrocene has been accompanied with high yield of propanoylferrocene. The reaction mixture has been purified by column chromatography and isolated yields were similar to GC ones (e.g. see entry 10, Table 3.5: 84% of isolated propanoylferrocene, together with 13% 1,1'-dipropanoylferrocene; total isolated products account for 97% of initial ferrocene, thus confirming that decomposition is due to prolonged heating).

MW-irradiation was also beneficial for Friedel-Crafts acylation with less reactive anhydrides, such as benzoic anhydride. Benzoylferrocene yield has indeed improved from isolated 25%, under conventional heating, to 42% (entry 10, Table 3.5).

3.3 Conclusions

An extensive investigation of Friedel-Crafts acylation of ferrocene in ILs has been accomplished.

Catalytic performances in alkylmethylimidazolium-based ILs as solvents resulted superior to pyridinium ones, and scandium triflate resulted a better (and cheaper) catalyst with respect to yttrium or ytterbium triflates.

A major improvement has been realized using microwaves as heating source, producing ferrocenylketones in quantitative GC and isolated yields within minutes. Thus, the results presented above clearly show that the catalytic protocol IL-MW-$Sc(OTf)_3$ is, at present, the most efficient in ferrocene acylation.

3.4 References and notes

[1] S. Berardi, V. Conte, G. Fiorani, B. Floris, P. Galloni *J. Organomet. Chem.* **2008**, *693*, 3015.

[2] a) M. Bejblová, D. Procházková, J. Čejka *Chem. Sus. Chem.* **2009**, 2, 486. b) P. Goodrich, C. Hardacre, H. Mehdi, P. Nancarrow, D. W. Rooney, J. M. Thompson *Ind. Eng. Chem. Res.* **2006**, *45*, 6640.

[3] M. J. Earle, in *Ionic Liquids in Synthesis, 2nd ed.*, Wiley-VCH: Weinheim, **2008**, *1*, 292.

[4] Y. Xiao, S. V. Malhotra *J. Mol. Cat. A: Chem.* **2005**, *230*, 129.

[5] a) A. Kawada, S. Mitamura, S. Kobayashi *Synlett.* **1994**, 545. b) S. Kobayashi *Eur. J. Org. Chem.* **1999**, 15.

[6] a) K. Binnemans *Chem. Rev.* **2007**, *107*, 2592. b) J. Ross, J. Xiao *Green Chem.* **2002**, *4*, 129. c) S. Gmouh, H. Yang, M. Vaultier *Org. Lett.* **2003**, *5*, 2219. d) M. J. Earle, U. Hakala, B. J. McAuley, M. Nieuwenhuyzen, A. Ramani, K. R. Seddon *Chem. Commun.* **2004**, 1368. e) M. J. Earle, U. Hakala, C. Hardacre, J. Karkkainen, B. J. McAuley, D. W. Rooney, K. R. Seddon, J. M. Thompson, K. Wähälä *Chem. Commun.* **2005**, 903. f) F. Zayed, L. Greiner, P. S. Schulz, A. Lapkin, W. Leitner *Chem. Commun.* **2008**, 79.

[7] a) M. Rosenblum, in *Chemistry of iron group metallocenes: ferrocene, ruthenocene, osmocene*, John Wiley & Sons New York, **1965**, 120. b) M. Rosenblum, J. O. Santer, W. G. Howells *J. Am. Chem. Soc.* **1963**, *85*, 1450.

[8] a) A. Stark, B. L. MacLean, R. D. Singer *J. Chem. Soc., Dalton Trans.* **1999**, 63. b) J. Li, W. Su, J. Lin, M. Chen, J. Li *Synth. Commun.* **2005**, *35*, 1929.

[9] a) M. Aly, R. Bramley, J. Upadhyay, A. Wassermann, P. Woolliams *Chem. Commun. (London)* **1965**, 404. b) M. Castagnola, B. Floris, G. Illuminati, G. Ortaggi *J. Organomet. Chem.* **1973**, *60*, C17. c) J. Silver *J. Chem. Soc., Dalton Trans.* **1990**, 3513.

4. Polyoxometalate-based *N*-heterocyclic carbenes as ligands for palladium

4.1 Palladium in catalysis

Palladium (Pd), named after the asteroid Pallas, is one of the most versatile and ubiquitous metal in modern organic synthesis.[1]

Palladium-mediated processes are, in fact, essential tools in the hands of the chemists and its application goes from the syntheses of natural products to those of polymers, pharmaceuticals and also agrochemicals. Such versatility of palladium is due to its ability to participate in catalytic transformations and to its high functional group tolerance. Palladium can be used to catalyze manifold transformations, including Heck, Suzuki-Miyaura, Stille and Buchwald-Hartwig cross-couplings,[1] the Wacker process[2] and the Tsuji-Trost allylation (cfr. Scheme 4.1).

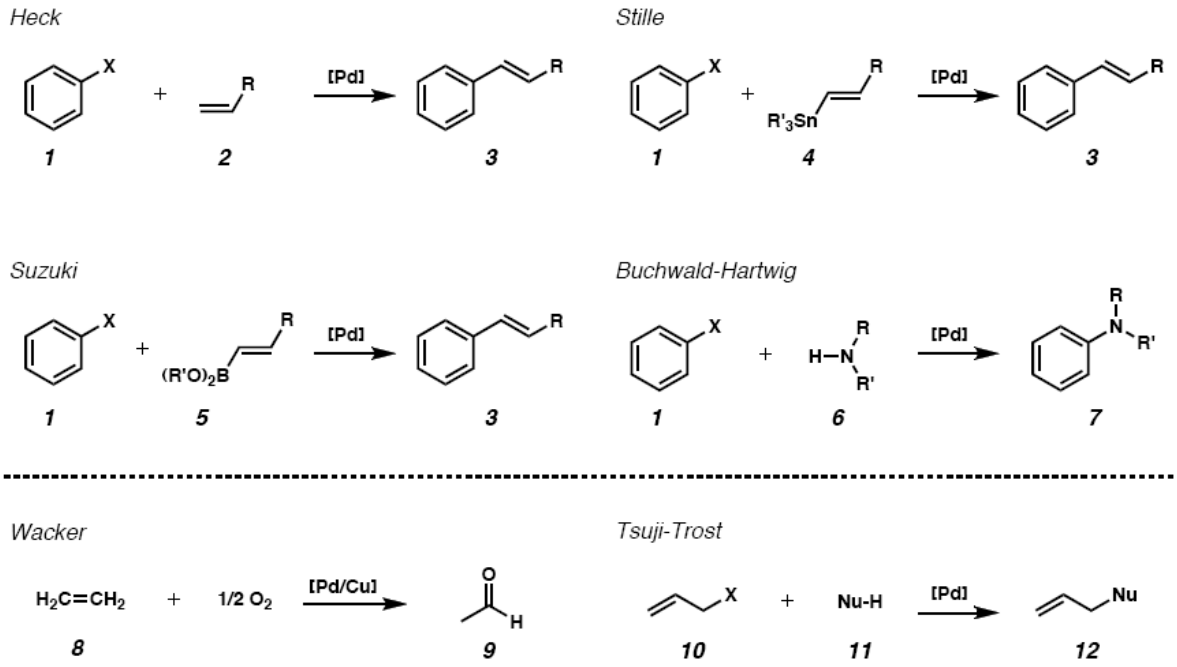

Scheme 4.1. Some of the palladium-catalyzed organic transformations.

In addition, palladium can also catalyze dehalogenations, hydrogenations, hydrogenolysis reactions, carbonylations, formation of C–C, C–O, C–N and C–S bonds, cycloisomerization and even pericyclic reactions.[1] Palladium-based methods often proceed under mild conditions and afford high yields, with excellent levels of stereo-, regio-, and chemoselectivity. Domino catalysis, where multiple Pd-catalyzed transformations are carried out in a single operation, is also a powerful extension of this chemistry.[3]

The prominent role of palladium in catalysis and synthesis is due to its electronegativity (2.2), which facilitates the formation of relatively strong Pd–H and Pd–C bonds, but also gives rise to polarized Pd–X bonds.[4]

Although palladium can exist in a number of different oxidation states, useful organic methods are dominated by the use of Pd^0 and Pd^{II},[1] although the utility of Pd^{IV} has been steadily emerging.[5] Other oxidation states have still not found practical applications and their observation remains rare.[6]

The increased stability of the even-numbered oxidation states (e.g. 0, II, IV) can be rationalized by the low tendency of palladium to undergo one-electron or radical processes; conversely, it readily participates in two-electron oxidations or reductions.[1a] Palladium ability to undergo facile and reversible two-electron processes has contributed to its widespread use as catalyst, since each oxidation state presents different chemistry.

In Figure 4.1 a simplified and general cycle for palladium-catalyzed reactions is represented.

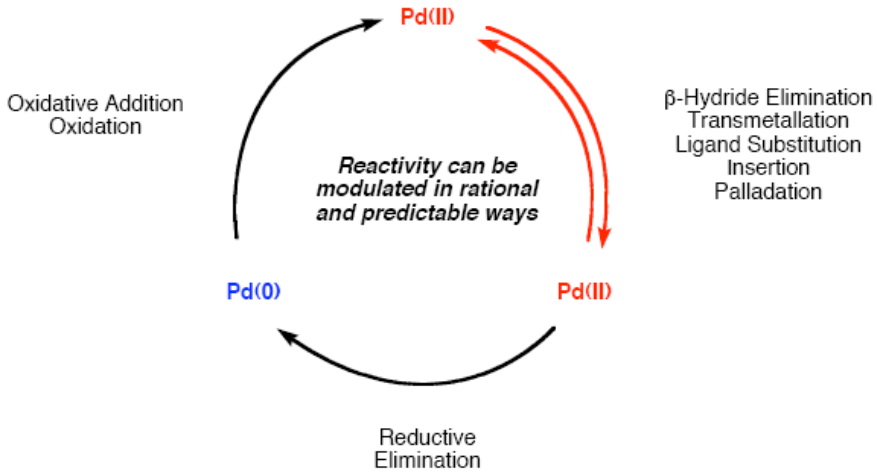

Figure 4.1. General cycle for palladium-catalyzed reactions.

Pd^0 can undergo either oxidation or oxidative addition, affording a Pd^{II} complex. The latter can generate different Pd^{II} complexes via several processes, such as β-hydride elimination, transmetalation, ligand substitution, insertion or palladation. Finally, reductive elimination converts the Pd^{II} complex back to Pd^0. This mechanistic understanding, combined with the modulation of palladium reactivity by changing the reaction parameters and ligands ability, has paved the way for the rational design in this field.

Among the palladium-catalyzed reactions, cross-coupling are the most general and selective.

In this kind of reactions, an organic and electrophilic molecule (generally an aryl halide) and a suitable hard or soft organometallic nucleophile are coupled together with the formation of a new C-C bond in the product (Scheme 4.2).

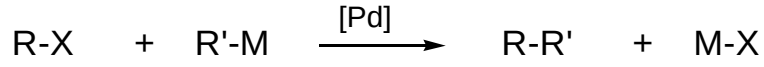

Reaction	**R'-M**		**R-X**	**Catalyst**	**Remarks**
Corriu-Kumada	R-MgBr	sp^2, sp^3	sp^2	Pd (or Ni)	---
Negishi	R-Zn-X	sp^3, sp^2, sp	sp^3, sp^2	Pd (or Ni)	---
Stille	R-SnR_3	sp^3, sp^2, sp	sp^3, sp^2	Pd	---
Suzuki -Miyaura	R-$B(OR)_2$	sp^3, sp^2	sp^3, sp^2	Pd	requires base
Hiyama	R-SiR_3	sp^2	sp^3, sp^2	Pd	requires base

Scheme 4.2. General scheme of palladium-catalyzed cross-coupling reactions.

Among C-C coupling reactions, the Suzuki-Miyaura (i.e. the palladium-catalyzed cross-coupling of an aryl halide Ar-X with a boronic acid Ar'-$B(OR')_2$, in the presence of a base) plays a leading role, due to: (i) the easy access and stability of a broad variety of organoboron compounds, (ii) the tolerance for different functional groups and (iii) the simple and mild experimental conditions.

The proposed catalytic cycle is reported in Scheme 4.3. The first step is the oxidative addition of the aryl halide to the Pd^0L_2 complex, yielding Ar-Pd^{II}-XL_2, which then undergoes transmetalation with the organoboron compound. In particular, the latter is actually a more reactive borate, formed by coordination of the base (RO^- in Scheme 4.3) with the Ar'-$B(OR')_2$. Transmetalation yields the Ar-Pd^{II}-Ar'L_2 complex, which finally reductively eliminates the cross-coupling product (Ar-Ar'), regenerating the active catalyst Pd^0L_2.

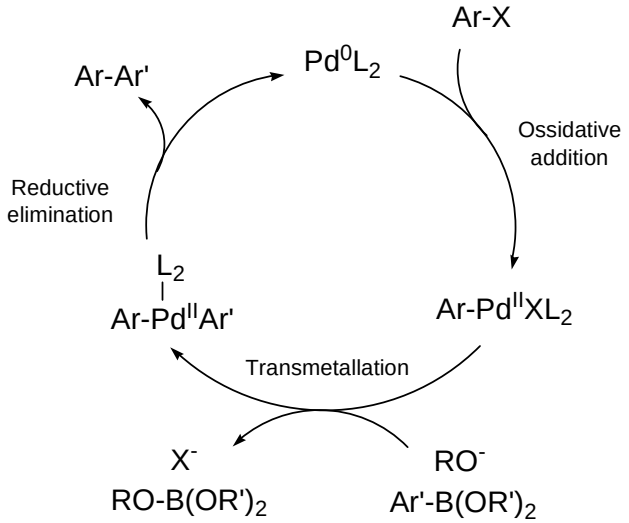

Scheme 4.3. Catalytic cycle for the Suzuki-Miyaura reaction (L = ancillary ligands on Pd).

Amatore and Jutand[7] have recently reported an anionic version of the Pd^0/Pd^{II} catalytic cycle described above. Their observation can rationalize several empirical findings reported in the literature, concerning reactivity and selectivity which cannot be accounted for by usual mechanisms.[7]

$Pd^{II}/^{IV}$ catalytic cycles have also been proposed to be active in cross-coupling reactions by several scientists over the years.[8] Although disproved in the majority of cases, such catalytic cycles are not ill-conceived in reactions employing palladacycles.[9]

Meanwhile, several scientists have also shown the importance of Pd colloids/clusters in this kind of catalysis, especially if ligand-free palladium is used as catalyst.[10] Recently, De Vries[11] has proposed the presence of active monomeric or dimeric molecular Pd species in equilibrium with soluble Pd clusters (Scheme 4.4).

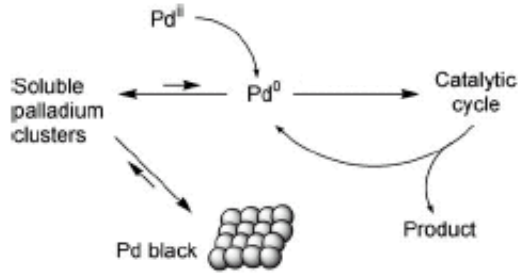

Scheme 4.4. Catalytic cycle for a cross-coupling reaction, involving active molecular Pd species in equilibrium with soluble Pd clusters.

Colloidal palladium nanoparticles have, indeed, been revealed by TEM analyses[12] and they are supposed to be involved as a reservoir of catalytically active species. Moreover, if not opportunely stabilized, they aggregate to yield inactive metallic palladium (known as Pd-black).

In recent publications, the scope of Suzuki-Miyaura reaction has been extended also to alkyl halides and pseudohalides (as the electrophilic component), which can now be coupled with aryl, vinyl and alkynyl nucleophiles.[13] The coupling of a nucleophile and an electrophile involving the formation sp^3-sp^3 carbon-carbon bonds has also been recently developed.[14]

Finally, it should be noted that the choice of palladium as the catalyst for cross-coupling reactions is a good compromise because this metal is sufficiently noble to favor reductive elimination, without impairing its ability to undergo a sufficiently fast oxidative addition. All the steps of the catalytic cycle must, indeed, proceed at comparable reaction rates, in order to avoid accumulation of intermediates and deactivation of the catalyst (see also Paragraph 4.1.1). For example, using nickel (a less expensive metal) in Suzuki-Miyaura reaction slows down the reductive elimination step, decreasing the catalytic efficiency, by favoring competitive pathways that lead to undesired by-products.

In the following paragraphs, some of the still open problems relating to C-C coupling reactions will be presented, together with our strategies to overcome them.

4.1.1 Open problems in C-C coupling reactions

Catalytic efficiency is a crucial issue in developing new strategies and designing an ideal catalyst require a precise knowledge of the behaviour of the actual catalytic species.

A common inhibition of palladium-catalyzed reactions arises from the aggregation of Pd^0, finally heading to the formation and precipitation of inert metal, the so-called "palladium black", which limits the lifetime of the active species (see Scheme 4.4, Paragraph 4.1).[15]

In order to overcome this problem, an accurate selection of the coordination sphere of palladium must be accomplished. In particular, innovative ligands or supports must (i) stabilize Pd^0 (or its colloidal forms) until the quantitative reoxidation to Pd^{II} is achieved, preventing agglomeration processes and avoiding losses of active catalyst during each cycle; (ii) concerting all the different catalytic steps in order to avoid the unproductive accumulation of the reactive intermediate (and consequent parallel reactions). To accomplish to these aspects, both electronic and steric factors must be taken into account in the choice of the suitable ligand system for palladium.

In particular, sterically hindered ligands have been designed and synthesized in order to avoid the aggregation of the nanoclusters of Pd^0 formed during the catalytic cycle.[15] For example, Fu and co-workers[16] have reported the use of sterically demanding electronrich organophosphines (such as $P(^tBu)_3$, ^tBu = *tert*-butyl) as efficient ligands for palladium. In the reported conditions, the coupling reaction has been effective also for less reactive substrates, such as aryl chlorides.

Nowadays, the design of an efficient catalytic system should also consider the sustainability of the whole process (Chapter 1, Paragraph 1.1). Thus, the development of a phosphine-free protocol is a topic of enormous interest, since organic phosphines are generally toxic, expensive, sensitive to air and unrecoverable.[17]

N-based ligands, such as *N*-heterocyclic carbenes (NHC),[18] *N*,*O*- [19] or *N*,*N*- [20] bidentate ligands, aryloximes,[21] arylimines,[22] *N*-acylamidines,[23] guanidines[17] and simple amines[24] have been efficiently used as phosphine alternatives in the Suzuki-Miyaura cross-coupling reaction.

In the following paragraph, the use of *N*-heterocyclic carbenes will be discussed.

4.2 *N*-heterocyclic carbenes

The discovery of *N*-heterocyclic carbenes (NHC) as ligands for transition metals has attracted a broad interest, since Arduengo's pioneristic work on stable and isolable imidazol-2-ylidenes.[25]

In the structure of this kind of carbenes, the two methylene hydrogen atoms are substituted with σ-electron-withdrawing, π-electron-donating nitrogens, leading to stabilization of the singlet, nucleophilic state of the carbene (Figure 4.2 a).[26] Further stabilization (by resonance) is conferred upon incorporation of the carbene itself into an aromatic heterocyclic framework (e.g. imidazol-2-ylidenes, the most widely used NHC in catalysis, Figure 4.2 b).[26] Bulky substituents R on the nitrogen atoms are also crucial for the stabilization of thermodynamically less stable carbenes, in order to avoid their dimerization.

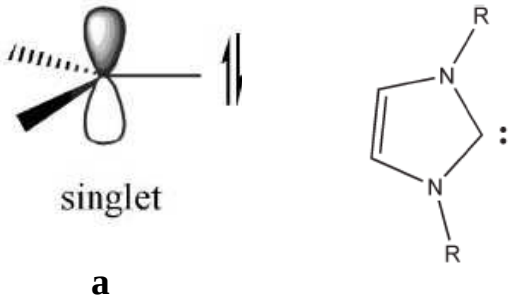

Figure 4.2. Singlet state of a carbene (a) and structure of an imidazol-2-ylidene (b).

N-heterocyclic carbenes behave like typical σ-donor ligands,[27] able to substitute classical 2e⁻donor ligands such phosphines, amines and ethers. They form robust metal-carbene sigma bonds with a variety of transition metals M, leading to M-NHC metal complexes with extraordinary stability toward temperature, oxidation and hydrolysis.[18, 27]

Steric and electronic tuning of the NHC ligand may be optimized in order to improve the catalytic performance of the resulting M-NHC complexes, which are often reported to surpass the activity of phosphine analogues, not only in cross-coupling reactions.[18, 28, 29]

In the following paragraphs, our strategy, based on the synthesis of molecular hybrid POM-appended NHC palladium complexes, will be described, together with the application in catalysis.

4.3 Results and discussion [30]

4.3.1 Hybrid POMs containing imidazole-like moieties as ligands for palladium

The design of novel ligands for transition metals is a major goal in catalysis, in order to obtain better performances in terms of yields, selectivities and sustainability of the reaction. Molecular hybrids are of particular interest in catalysis, due to the interplay of joint organic-inorganic domains with very diverse functional environments. The hybrid strategy is expected to allow for fine-tuning of the stereo-electronic properties of the catalyst through a tailored choice of the interacting organic-inorganic moieties. Such hybrid up-grade of the catalytic system can be readily accessed, through the covalent functionalization of molecular polyoxometalates (POMs, Chapter 1, Paragraph 1.2).[31] Indeed, covalent POM hybrids are characterized by discrete, nanosized, multi-metal-oxides as polyanionic scaffolds, which allow for anchoring on-surface organic pendants, including also chiral residues.[31]

We focused our attention towards the synthesis of novel hybrid POMs, able to act as ligands for palladium. To this end, imidazolium-like moieties have been successfully grafted on the defect site of the Keggin polyanions.

In addition to the specifically designed binding site for palladium, such POM-based hybrids display an extended polyanionic surface. This set-up is expected to contribute sterically and by virtue of electrostatic repulsions to prevent agglomeration of incipient Pd^0, which generally deteriorates the turnover efficiency of the system.[32] The molecular nature of such composite structures is a further point of interest, offering a single-site model for extended materials. Specifically, the defined molecular structure of the hybrid allows for selective tailoring of the active site, as well as for detecting subtle changes by solution characterization techniques, including heteronuclear NMR and ESI-MS.

In particular, we have synthesized two hybrid POMs functionalized with imidazole-like moieties, reacting both the divacant[33] $[\gamma\text{-}SiW_{10}O_{36}]^{8-}$ and the monovacant[34] $[\alpha\text{-}SiW_{11}O_{39}]^{8-}$ Keggin anions with 1-octyl-3-(3-triethoxysilylpropyl)-4,5-dihydroimidazolium bromide **1** (prepared in a previous step, see Chapter 6). The synthetic route, reported in Scheme 4.5, involves the reaction of the organosilane reagent **1** with the nucleophilic oxygens of the POMs defect sites upon hydrolysis and condensation reaction in the presence of

tetrabutylammonium bromide (as phase transfer agent), in order to promote the solubilization of the POM in CH_3CN by countercation metathesis.[35]

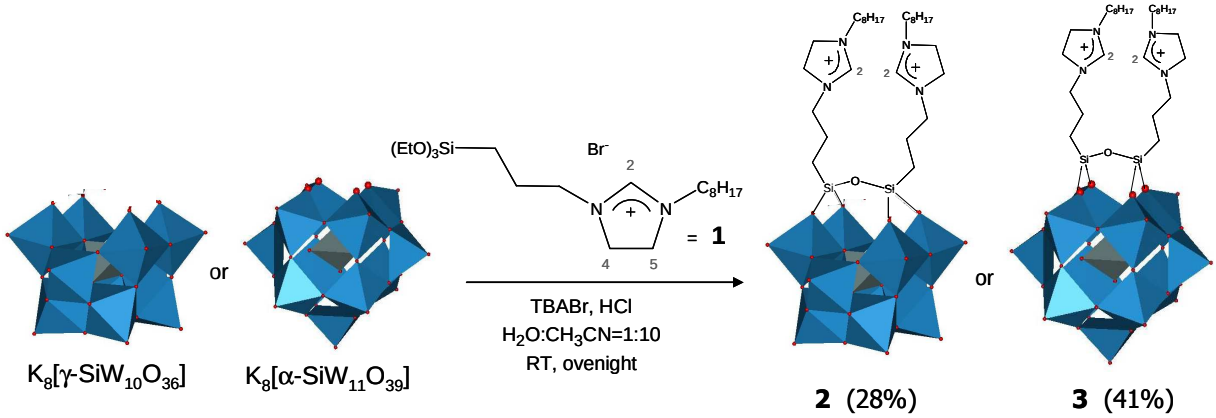

Scheme 4.5. Synthesis of hybrid POMs **2** and **3**: lacunary $[\gamma\text{-}SiW_{10}O_{36}]^{8-}$ and $[\alpha\text{-}SiW_{11}O_{39}]^{8-}$ have been functionalized with 1-octyl-3-(3-triethoxysilylpropyl)-4,5-dihydroimidazolium bromide **1**.

We have successfully grafted the organic moieties onto the POM frameworks in a covalent fashion, as confirmed by the characterization in solution (^{1}H-, ^{13}C-, ^{29}Si- and ^{183}W-NMR) and in the solid state (FT-IR). All the spectroscopic analyses are in agreement with the expected *bis*-functionalized hybrid structures[31g] (see Table 4.1, where some results have been reported, and Chapter 6 for the spectra).

Table 4.1. ^{29}Si-, ^{183}W- and ^{13}C-NMR chemical shifts of compounds **1**, **2** and **3**, compared with those of the lacunary POM precursors.

Compound	**^{29}Si-NMR: δ, ppm (integration)**	**^{183}W-NMR: δ, ppm (integration)**	**^{13}C-NMR: δ, ppm**
1	- 47.5	---	158.4, *58.6*, 53.5, 50.5, 48.5, 48.2, 31.7, 29.1, 29.0, 27.5, 26.4, 22.6, 21.2, *18.3*, 14.0, 7.2
$[\gamma\text{-}SiW_{10}O_{36}]^{8-}$ [a]	- 83.5	-99.3 (4), -140.4 (4), -161.2 (2)	---
2[b]	- 62.1 (2), - 88.0 (1)	-107.0 (4), -134.2 (2), -141.6 (4)	158.3, 59.3, 58.2, 50.9, 49.5, 49.0, 32.6, 29.9, 28.0, 27.1, 24.4, 23.4, 22.5, *21.9*, 20.4, 14.5, 14.1, 12.4
$[\alpha\text{-}SiW_{11}O_{39}]^{8-}$ [a]	- 84.5	-100.8 (2), -116.1 (2), -121.3 (1), -127.9 (2), -143.2 (2), -176.1 (2)	---
3[b]	- 52.0 (2), - 84.5 (1)	-107.1 (2), -108.0 (2), -112.7 (1), -124.8 (2), -174.2 (2), -248.5 (2)	158.1, 59.3, 58.1, 50.2, 49.4, 49.0, 32.5, 29.9, 29.8, 27.9, 27.1, 24.5, 23.4, *21.7*, 20.4, 14.5, 14.0, 9.7

[a] K^+ salt; [b] tetrabutylammonium $(n\text{-}Bu)_4N^+$ salt. Countercation's signals underlined.

^{29}Si- and ^{183}W-NMR analyses have confirmed the preservation of the structure of the inorganic domains upon functionalization. No isomerization nor other structural modifications have occurred, as the NMR patterns are consistent with the simmetry of the two anions (C_{2v} and C_s for $[\gamma\text{-}SiW_{10}O_{36}]^{8-}$ and $[\alpha\text{-}SiW_{11}O_{39}]^{8-}$ respectively).[33, 34] The FT-IR spectra for **2** and **3** are also in agreement with those of analogous hybrid derivatives of the same lacunary POMs.[31g] Moreover, ^{13}C- and ^{1}H-NMR analyses have confirmed the effective covalent grafting of the organic moieties.

First attempts of palladation of these hybrid structures have been made on complex **3** (see Scheme 4.6). Unfortunately all the known strategies to form the Pd-NHC, i.e. (i) direct metalation using $Pd(OAc)_2$;[36] (ii) base-mediated palladation with $PdCl_2(CH_3CN)_2$ in the presence of potassium *bis*-(trimethylsilyl)-amide (KHMDS) or NaH;[37] (iii) transmetalation using Ag_2O,[38] have met little success, as evidenced by the persistence of ^{1}H-NMR resonance of the C_2-bound protons of the dihydroimidazolium ring (δ_H = 8.1 ppm, see Chapter 6).

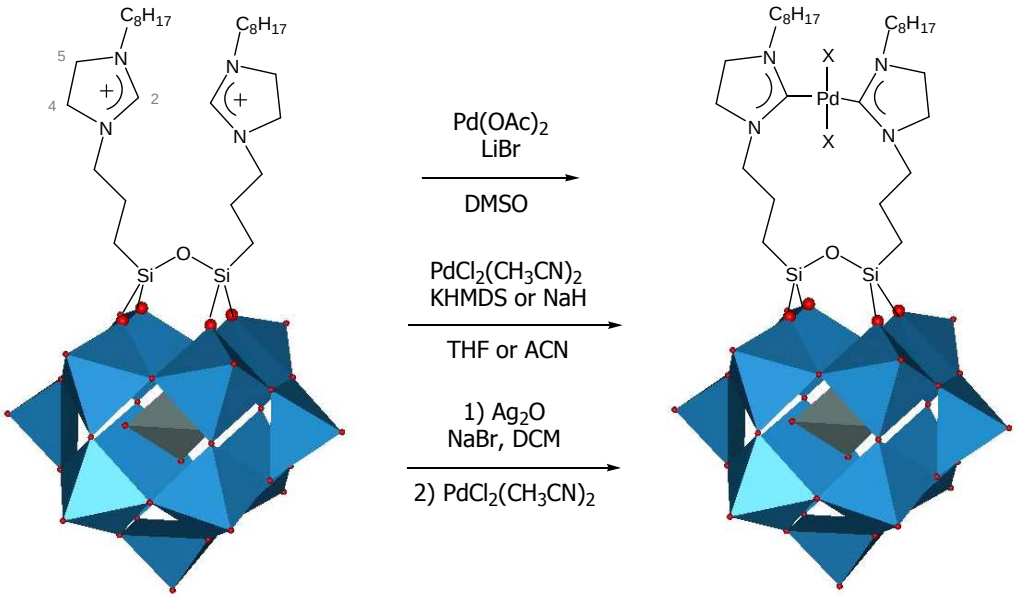

Scheme 4.6. Synthetic strategies for the formation of the Pd-NHC complex on the hybrid POM **3**. Numeration of the dihydroimidazolium ring is also reported.

Analysis of the palladation reaction by UV-Vis spectrophotometric titration suggests a possible electrostatic association of Pd^{2+} ions to the anionic POM surface.[i]

[i] UV/Vis spectrophotometric titration (λ < 450 nm), of **3** upon addition of $Pd(OAc)_2$ in DMSO and incubation at 50°C for 4 h and at 100 °C for 30 min indicates a 1:1 Pd^{2+}: **3** association stoichiometry.

To avoid such complications, we have focused on a convergent approach involving the immobilization of preformed Pd-NHC complex on the POM. Hence, the triethoxysilyl-tagged imidazolium precursor **4**, containing an unsaturated[ii] heterocycle and a less hindered *n*-butyl substituent at the nitrogen atom[18, 39] has been synthesized, under strictly anhydrous conditions, from (3-chloropropyl)-triethoxysilane and 1-butylimidazole (Scheme 4.7).

Reaction of **4** with Ag_2O, followed by transmetallation with $PdCl_2(CH_3CN)_2$ [38] has afforded the palladium *bis*-carbene complex **5** (Scheme 4.7).

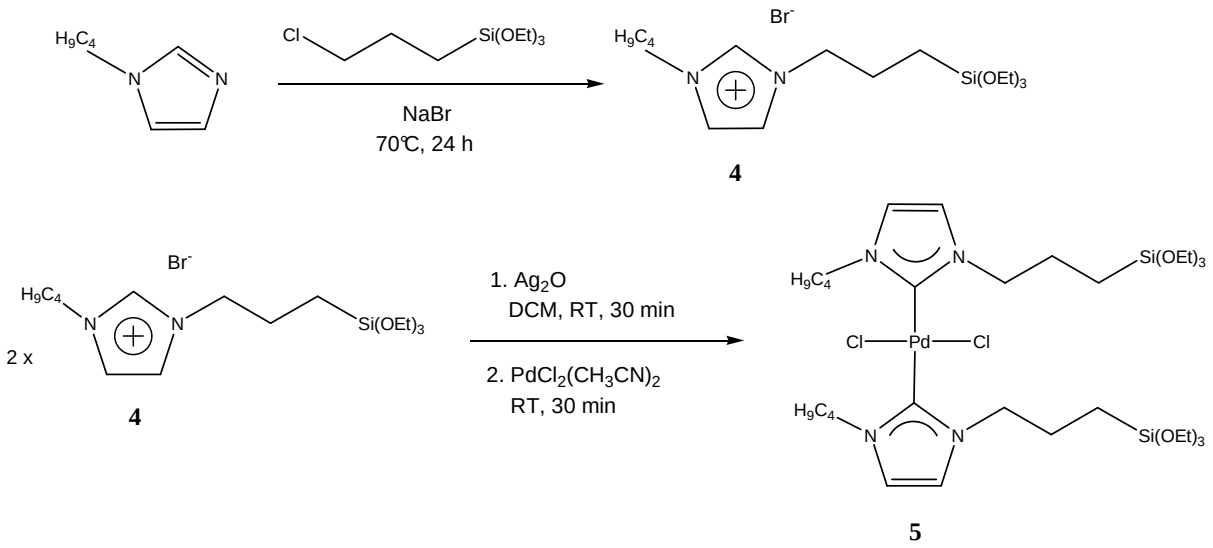

Scheme 4.7. Synthesis of 1-butyl-3-(3-triethoxysilylpropyl)imidazolium bromide **4** and of the palladium *bis*-carbene complex **5**.

Complex **5** has been characterized by ^{1}H-, ^{13}C-NMR and ESI-MS analyses.

The absence of the resonance due to the C_2-bound imidazolium proton (δ_H = 10.3 ppm) is corroborated by the appearance of a new signal at δ_C = 170.6 ppm, featuring the formation of a palladium-carbene bond (see Figures 4.3 and 4.4).

[ii] Using a saturated ring have led to hydrolysis and decomposition of the carbene to give by-products (i.e. aldehydes, identified by the presence of ^{1}H-NMR signals at $\delta > 9$ ppm), even keeping strictly anhydrous reaction conditions. In particular, in the case of the silver-route, a molecule of water is formed during the reaction, which is likely enough to decompose the saturated NHC.

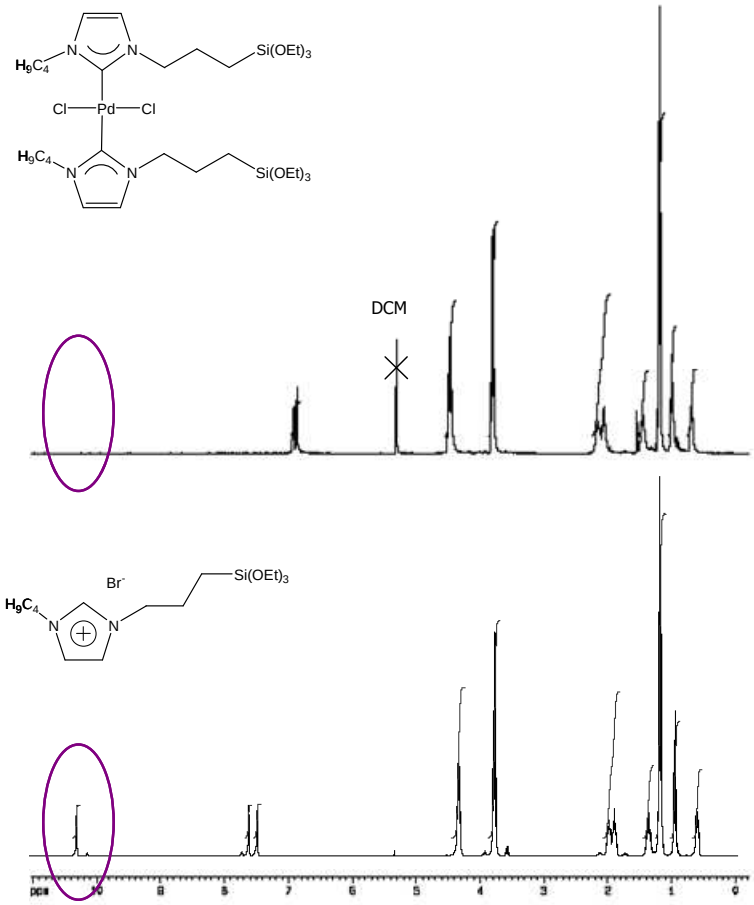

Figure 4.3. ^{1}H-NMR of the complex **5** (top) and the starting material **4** (bottom). In the circles, the disappearance of the C_2-bound imidazolium proton resonance is underlined.

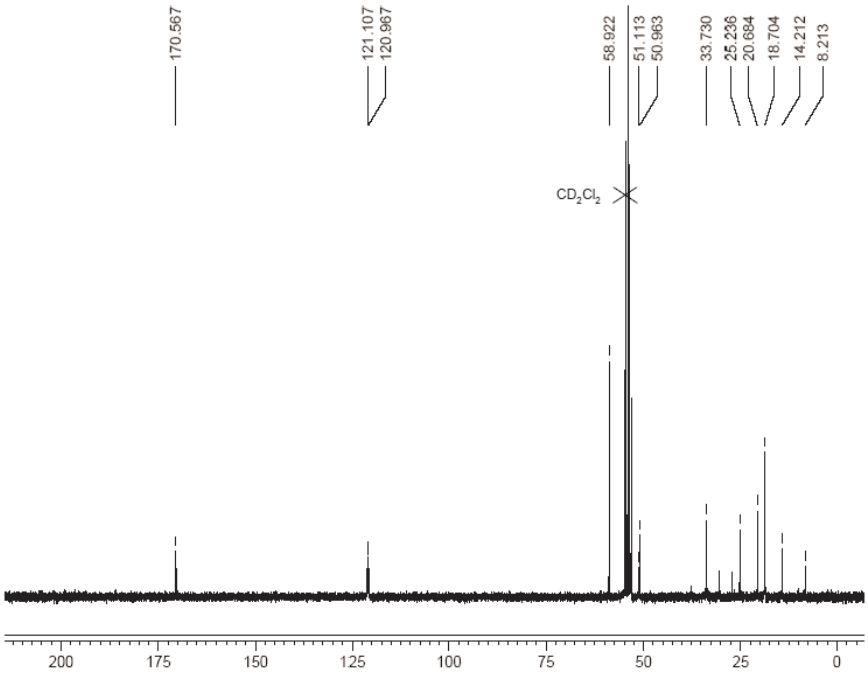

Figure 4.4. ^{13}C-NMR of complex **5**. The signal at δ_C = 170.6 ppm is characteristic of a palladium-carbene bond.

ESI-MS (positive mode) analysis of complex **5** shows two signals centred at *m/z* = 799.3 and 843.3, corresponding to the monochloride and monobromide cationic fragments, $[\{C_{10}H_{17}N_2Si(OEt)_3\}_2PdCl]^+$ and $[\{C_{10}H_{17}N_2Si(OEt)_3\}_2PdBr]^+$ respectively (Fig. 4.5).

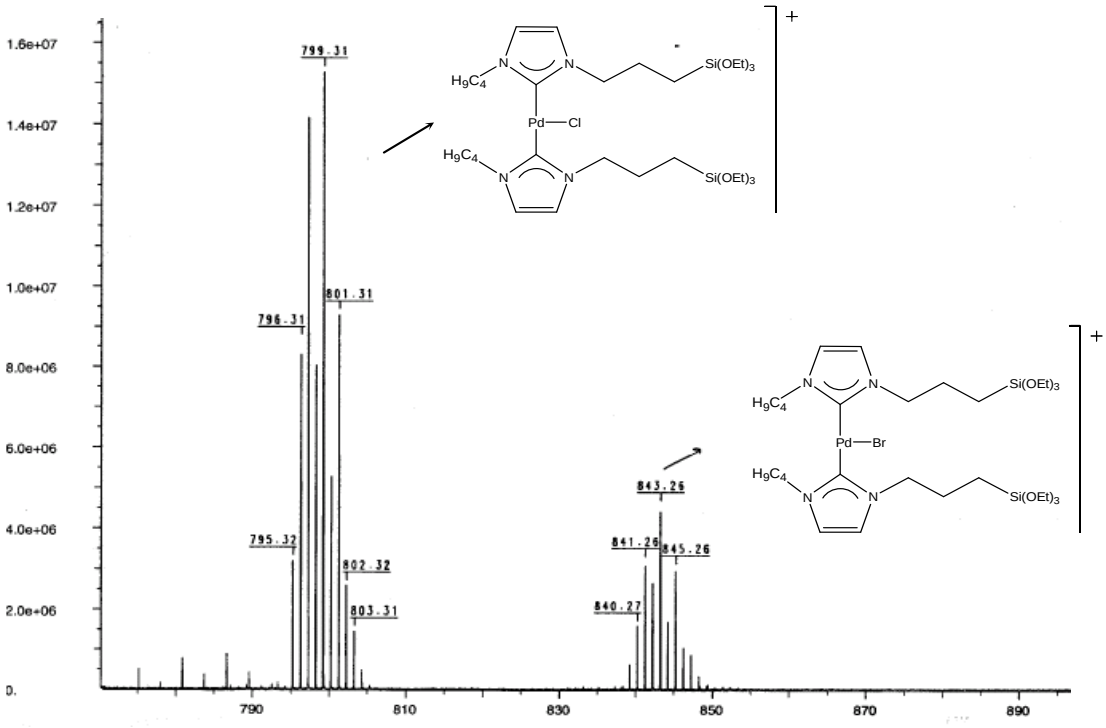

Figure 4.5. ESI-MS spectrum of the complex **5**.

Complex **5** has been finally reacted with the divacant Keggin POM, namely $[\gamma\text{-}SiW_{10}O_{36}]^{8-}$, in acetonitrile, under phase transfer conditions[35] (Scheme 4.8), leading to the functionalized hybrid **6** in 75% yield.

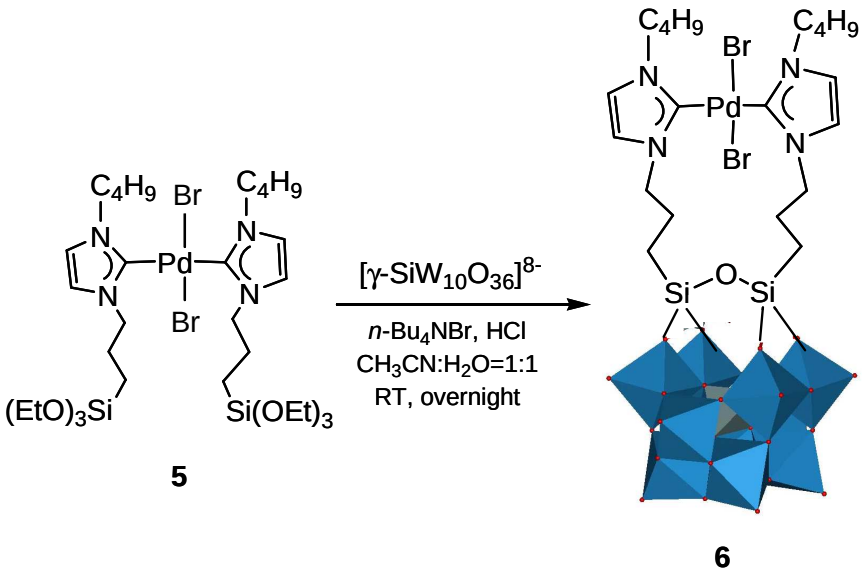

Scheme 4.8. Functionalization of $[\gamma\text{-}SiW_{10}O_{36}]^{8-}$ with palladium *bis*-carbene complex **5**.

Complex **6** has been characterized both in the solid state (by FT-IR and elemental analysis) and in solution (^{1}H-, ^{13}C-, ^{29}Si- and ^{183}W-NMR, ESI-MS). All spectroscopic results have confirmed the proposed structure. The ^{183}W-NMR spectrum (Fig. 4.6) shows three resonances at -107.4, -135.8, and -142.1 ppm in 2:1:2 ratio, in agreement with the expected C_{2v} symmetry.

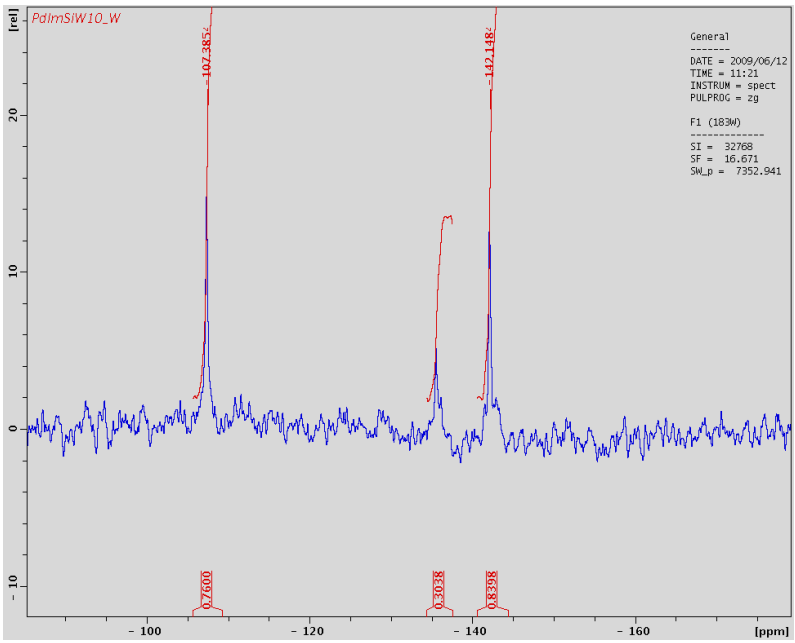

Figure 4.6. ^{183}W NMR spectrum of complex **6**.

The ^{29}Si-NMR spectrum (Fig. 4.7) reveals two signals at -62.8 and -88.4 ppm with integration ratio 2:1. Both these results are consistent with a *bis*-substitution of the POM surface.

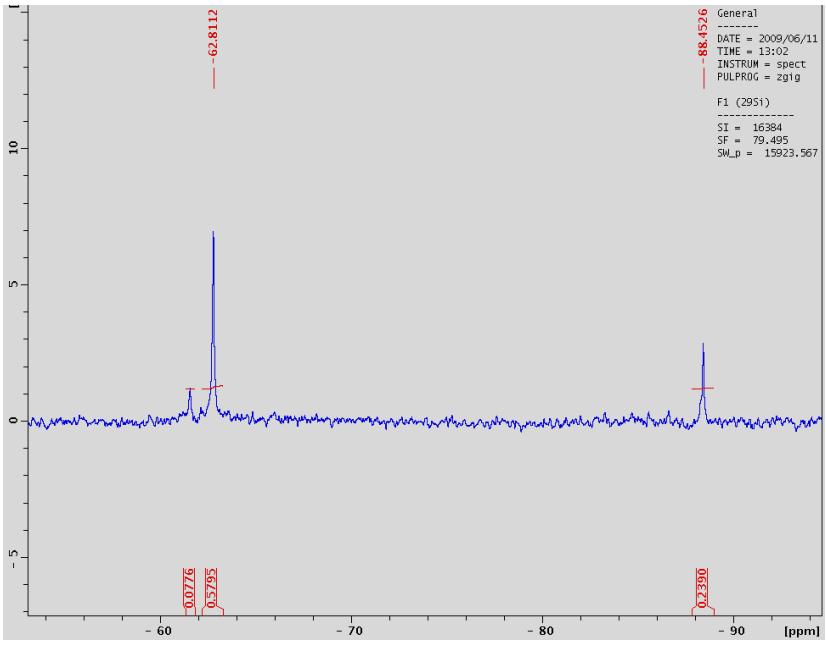

Figure 4.7. ^{29}Si NMR spectrum of complex **6**.

The DFT optimized structure of complex **6**, reported in Figure 4.8, suggests a planar distorted coordination for Pd, with *trans* halide ligands and bond lengths around 2.07-2.11 Å (Pd-C) and 2.59 Å (Pd-Br) (see Chapter 6).

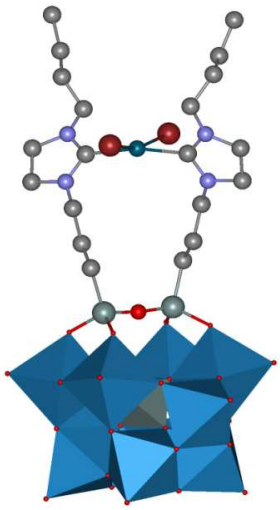

Figure 4.8. DFT optimized structure of complex **6**.

The POM-appended *N*-heterocyclic carbene palladium complex **6** has been then tested in Suzuki-Miyaura and dehalogenation reactions and has showed remarkable performances. The experimental results will be discussed in details in the following paragraphs.

4.3.2 Suzuki-Miyaura cross-coupling reaction catalyzed by a POM-based Palladium-NHC complex

Complex **6** has been tested in the palladium-catalyzed cross-coupling of aryl halides with phenylboronic acids, according to established Suzuki-Miyaura protocols (Scheme 4.9).

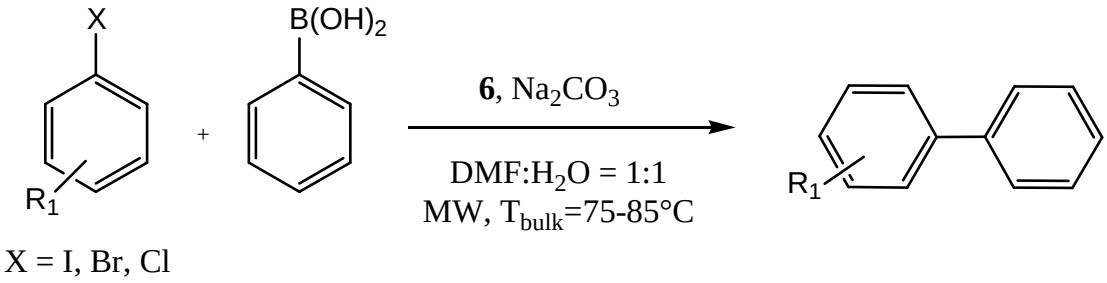

Scheme 4.9. Suzuki-Miyaura cross-coupling catalyzed by **6** under MW-irradiation.

The performance of catalyst **6** in this chemistry has been screened in 1:1 DMF/H_2O mixtures and under microwave (MW)-induced dielectric heating (Table 4.2).[40, 41] This latter method is particularly efficient for poly-charged catalysts, which behave as MW-activated molecular heat-carriers (see also Chapter 2, Paragraph 2.2.3).[42] Indeed, hybrid POMs, are known to display a remarkable thermal stability and high catalytic efficiency in microwave (MW)-assisted processes.[31d, f]

The cross-coupling catalytic activity of **6** has been initially evaluated using a representative range of aryl halides as substrates and MW irradiation at 10 watt for 10–30 min (Table 4.2).

Table 4.2. Suzuki-Miyaura cross-coupling catalyzed by **6** under MW-irradiation (Scheme 4.9). In all reactions: aryl halide, ArX (0.25 mmol), phenylboronic acid, $PhB(OH)_2$ (1.1 eq, 0.275 mmol), Na_2CO_3 (2 eq, 0.5 mmol), DMF:H_2O =1:1 (0.45:0.45 ml); MW-irradiation: W = 10 watt, compressed air at 30-40 psi; T_{bulk} = 75-85°C.

#	X	R_1	6 loading, %	% product (time, min)
1[a]	I	*p*-$COCH_3$	0.05%	99 (10)
2	I	H	0.05%	85 (30)
3	I	*p*-CH_3	0.05%	80[c] (20)
4	I	*p*-OCH_3	0.05%	95[c] (20)
5	Br	*p*-$COCH_3$	0.1%	99 (10)
6	Br	*p*-NO_2	0.1%	93[c] (10)
7[b]	Br	H	0.1%	94 (35)
8[b]	Br	*p*-CH_3	0.1%	87[c] (30)
9[b]	Cl	*p*-$COCH_3$	1%	98[c] (30)
10[b]	Cl	*o*-$COCH_3$	1%	10[d] (150)
11[b]	Cl	*p*-CHO	1%	20[c] (30)
12	Cl	*p*-NO_2	1%	38[e] (30)
13[b]	Cl	H	1%	57 (60)
14[b]	Cl	*p*-CH_3	1%	33[f] (60)

[a] under analogous conditions, the coupling reaction catalyzed by **5** proceeds with 32% yield; [b] ArX (0.25 mmol), $PhB(OH)_2$ (1.3 eq, 0.325 mmol), Na_2CO_3 (3 eq, 0.75 mmol), DMF:H_2O =1:1 (0.45:0.45 ml); [c] biphenyl (1-7%) and dehalogenation products (traces) observed; [d] biphenyl (4%) and acetophenone (14%) also formed; [e] biphenyl (18%) also formed; [f] biphenyl (9%) and toluene (6%) also formed.

Under these conditions, both activated and deactivated aryl iodides react smoothly with 0.05 mol% catalyst loading, leading to the corresponding substituted biphenyl products with up to 99% yield, 1980 turnover numbers (TON) and frequencies (TOF) up to 11880 h^{-1} (entries 1-4, Table 4.2). In all reactions, the bulk temperature is kept at ca. 80°C by simultaneous cooling with compressed air. Control experiments, performed with iodobenzene and phenylboronic acid, indicate no coupling product in the Pd free reaction, nor in the presence of the imidazolium functionalized POM **2** alone. Noticeably, the POM-free NHC complex **5** deactivates rapidly under analogous catalytic regime, thus yielding poor conversion and turnover efficiency (see Footnote "a" in Table 4.2). Addition of Na_2CO_3 (2 or 3 equivalents) is an essential prerequisite of the catalytic protocol, in agreement with the generally accepted mechanism involving a reactive borate anion for the transmetalation step.[1]

Coupling of aryl bromides is readily achieved by increasing the catalyst loading to 0.1 mol%, with similar yields and reaction time (yield up to 99%, TON = 990; TOF = 5940 h^{-1}, entry 5, Table 4.2). A remarkable 87% yield of 4-methylbiphenyl has been obtained after 30

min irradiation when using the unactivated 4-bromotoluene as substrate, (TOF = 1740 h^{-1}, entry 8, Table 4.2).[iii, 43] The POM-based system has also been effective in coupling aryl chlorides, which are known to be poorly reactive but synthetically highly appealing and cheaper.[16b, iv] An increased catalyst loading (1.0 mol%), and a larger excess of phenylboronic acid and Na_2CO_3 (1.3 and 3 equivalents with respect to aryl chloride), have been pivotal for ensuing reactivity. Under such conditions, 4-chloroacetophenone has given the corresponding coupling product in 98% yield when MW-irradiated for 30 minutes (TON = 98, TOF = 196 h^{-1}, entry 9, Table 4.2).[v, 44] *Ortho*-substituted, 2-chloroacetophenone has been converted only sluggishly, presumably due to steric factors (entry 10, Table 4.2). The POM residue may be sufficiently bulky to hamper the oxidative addition and/or transmetalation step of the catalytic cycle.[45] Other activated aryl chlorides reacted with less success, as for 4-chloronitrobenzene, affording a significant amount (18%) of biphenyl originating from homo-coupling[vi] together with 38% of cross-coupled 4-nitrobiphenyl (entry 12, Table 4.2). In this case, the selectivity of the process has not been improved upon increasing the amount of base.[46]

Interestingly, the reaction of the unactivated 4-chlorotoluene has turned out to yield 33% of the desired product, with concurrent homo-coupling (<9%) and dehalogenation to toluene (<10%).[47]

[iii] Average TON and TOF values in the range 1100-1900 and 314-543 h^{-1} respectively, have been reported for classic NHC-ligands employed in the homogeneous Suzuki coupling of deactivated aryl bromides.

[iv] Ligand **3** in combination with $Pd(OAc)_2$ (1 eq.) was found to be inactive with chloroaryl substrates, thus confirming the superior performance of the POM-based NHC-ligand in this chemistry.

[v] Literature TON and TOF values, for Suzuki coupling of aryl chlorides by Pd-NHC catalysts are in the range 40-100 h^{-1}.

[vi] Homo-coupling of arylboronic acids is a well-known side reaction while performing Suzuki-Miyaura cross-couplings with less reactive substrates, such as aryl chlorides, under normal air atmosphere. For these compounds, the oxidative addition step is generally slower, so also the arylboronic acid can be oxidatively added to palladium, thus yielding the symmetric biaryl after the transmetalation step (see also endnote 47).

4.3.3 Dehalogenation of aryl chlorides catalyzed by a POM-based Palladium-NHC complex

Catalytic dehalogenation has been previously reported as a parallel reaction in SuzukiMiyaura cross-coupling of less reactive substrates (as aryl chlorides), but few papers provide details on this topic.[48] Such reaction is of major importance from an environmental point of view, in particular with regards to the degradation of highly toxic halogenated organic compounds.[49]

The proposed mechanism of palladium-catalyzed dehalogenation involves the oxidative addition of the aryl halide to the Pd^0-L intermediate (L = NHC), and the formation of a Pd^{II}-hydride species, generated by a strong base, such as an alkoxide (see Scheme 4.10).[49, 50]

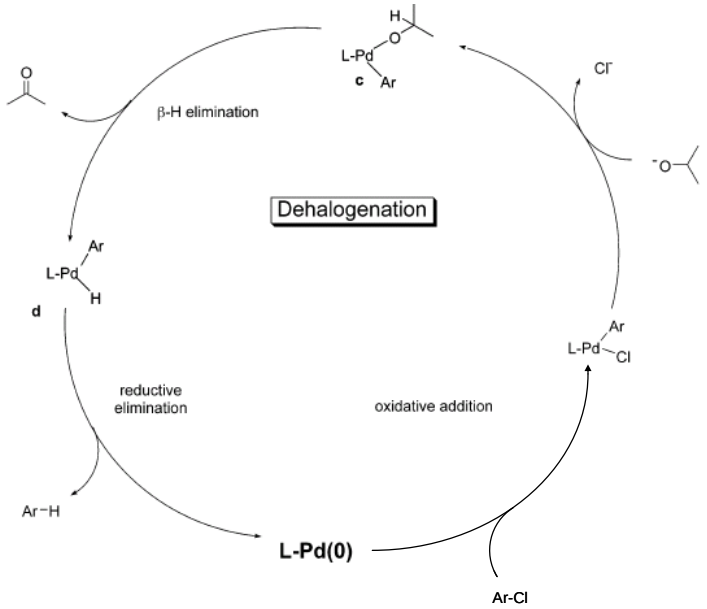

Scheme 4.10. Catalytic cycle for the dehalogenation of aryl chlorides in the presence of isopropoxide.

In line with this proposal, the dehalogenation reaction is strongly promoted upon changing the base from Na_2CO_3 to *n*-Bu_4NOH. Under these conditions, otherwise identical to the Suzuki-Miyaura protocol, catalytic dehalogenation of aryl chlorides has been readily accomplished. In the presence of *n*-Bu_4NOH as the base in the Suzuki-Miyaura coupling protocol of 4-chloroacetophenone with phenyl boronic acid, dehalogenated acetophenone has been formed as the major product (63% yield), together with 4-acetylbiphenyl in 35% yield.

The competitive dehalogenation reaction has thus been investigated in more detail, performing the reaction in the absence of phenylboronic acid. Highest selectivities have been achieved when using 2 equivalents of *n*-Bu_4NOH in DMF, under MW-irradiation (Table 4.3). Under these conditions, a formate ion is surmised to be generated from DMF and hydroxide, as the hydrogen donor.[51]

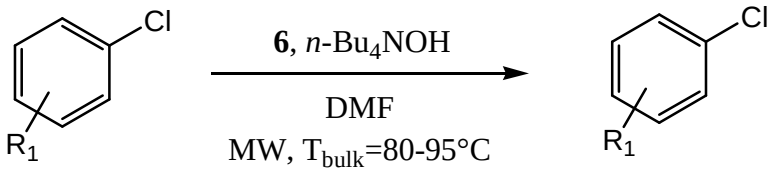

Table 4.3. Dehalogenation of aryl chlorides (ArCl) catalyzed by **6** under MW-irradiation.[a]

#	ArCl	ArH Yield, % (time, min)
1	4-chloroacetophenone	>99 (30)
2	2-chloroacetophenone	57 (120[b])
3	3-chloroacetophenone	86 (60)
4	4-chloronitrobenzene	>99 (40)
5	4-chlorophenol	12 (60)
6	4-chlorotoluene	43 (60)
7	1-chloronaphthalene	87 (60)

[a] ArCl (0.25 mmol), *n*-$Bu_4NOH{\cdot}30H_2O$ (2 eq, 0.5 mmol), **6** (1 mol%, 0.0025 mmol), DMF (0.5 ml); MW-irradiation: W = 10 watt, compressed air at 30 psi; T_{bulk} = 80-95°C. [b] after 3 cycles (2 x 30 min + 1 x 60 min).

Dehalogenation of activated aryl chlorides occurs smoothly and quantitative yields have been reached within 30-40 min (entries 1 and 4, Table 4.3). Noteworthy, thermal and photo-redox carbon-halogen bond cleavage by POM catalysts has been reported to proceed by radical mechanisms.[52] However, under the explored condition, no reaction has been observed using the Pd-free complex **3**.

Sterically hindered 2-chloroacetophenone and 3-chloroacetophenone have been converted at a slower rate and afforded respectively 57% and 86% acetophenone after 2 and 1 h (entries 2 and 3, Table 4.3).

Aryl chlorides with electron-donating substituents have been dehalogenated less efficiently (entries 5 and 6, Table 4.3). Nevertheless, 4-chlorotoluene yielded appreciable 43% of toluene after irradiation for 1 h (entry 6, Table 4.3).

4.4 Conclusions and future goals

A novel synthetic route to hybrid Pd catalysts has been developed through decoration of a POM surface with an imidazolium-based NHC palladium complex.

Our results include the following:

- the interplay of the Pd binding domains with the inorganic POM scaffold provides new opportunities to access multi-turnover catalysis while preserving good to excellent performance under MW-assisted protocols;
- both Suzuki-Miyaura and dechlorination reactions of aromatic compounds are efficiently accomplished, depending on the reaction conditions. The generation of new reactivity patterns illustrates the potential of hybrid materials and POMs as active supports.

Further studies will be addressed to evaluate the possibility to recover the catalyst upon heterogeneization. An up-grade of the system, using ionic liquid phases, can also be envisaged, due to the likely implemented affinity of such POM-based hybrid systems for these media.[53]

The covalent functionalization of POM vacant sites with other M-NHC complexes will be also evaluated. In particular, the synthesis of hybrid POMs, covalently binding Ru-NHC moieties is now in progress. This kind of complexes will be tested as catalysts for the hydrogenation of ketones.

4.5 References and notes

[1] a) E. Negishi, in *Handbook of Organopalladium Chemistry for Organic Synthesis*, Wiley-Interscience, New York, **2002**. b) J. Tsuji, in *Palladium Reagents and Catalysts: Innovations in Organic Synthesis*, Wiley and Sons, New York, **1995**. c) J. Tsuji Palladium *Reagents and Catalysts: New Perspectives for the 21st Century*, Wiley and Sons, New York, **2003**. d) J. Tsuji, in *Palladium in Organic Synthesis*, Springer, Berlin, **2005**. e) A. de Meijere, F. Diederich, in *Metal Catalyzed Cross-Coupling Reactions*, Wiley-VCH Verlag GmbH & Co. KGaA, Weinheim, Federal Republic of Germany, **2004**.

[2] For a recent review, see: T. Punniyamurthy, S. Velusamy, J. Iqbal *Chem. Rev.***2005**, *105*, 2329 and references cited therein.

[3] G. Poli, G. Giambastiani, A. Heumann *Tetrahedron* **2000**, *56*, 5959.

[4] I. J. S. Fairlamb *Tetrahedron* **2005**, *61*, 9661.

[5] a) L. V. Desai, M. S. Sanford *Angew. Chem. Int. Ed.* **2007**, *46*, 5737. b) J. Q. Yu, R. Giri, X. Chen *Org. Biomol. Chem.* **2006**, *4*, 4041. c) O. Daugulis, V. G. Zaitsev, D. Shabasov, O.-N. Pham, A. Lazareva *Synlett.* **2006**, 3382. d) C. Bressy, D. Alberico, M. Lautens *J. Am. Chem. Soc.* **2005**, *127*, 13148.

[6] a) J. J. Escobar-Nuricumbo, C. Campos-Alvarado, G. Ríos-Moreno, D. Morales-Morales, P. J. Walsh, M. Parra-Hake, M. *Inorg. Chem.* **2007**, *46*, 6182. b) W. Chen, S. Shimada, M. Tanaka *Science* **2002**, *295*, 308.

[7] C. Amatore, A. Jutand *Acc. Chem. Res.* **2000**, *33*, 314.

[8] a) B. L. Shaw *New. J. Chem.* **1998**, *22*, 77. b) B. L. Shaw, S. D. Perera *Chem. Commun.* **1998**, 1863.

[9] a) I. P. Beletskaya, A. V. Cheprakov *J. Organomet. Chem.* **2004**, *689*, 4055. b) J. Dupont, C. S. Consorti, J. Spencer *Chem. Rev.* **2005**, *105*, 2527.

[10] a) M. T. Reetz, J. G. de Vries *Chem. Commun.* **2004**, 1559. b) T. I. Wallow, B. M. Novak *J. Org. Chem.* **1994**, *59*, 5034. c) R. B. Bedford, M. E. Blake, C. P. Butts, D. Holder *Chem. Commun.* **2003**, 466. d) C. C. Cassol, A. P. Umpierre, G. Machado, S. I. Wolke, J. Dupont *J. Am. Chem. Soc.* **2005**, *127*, 3298.

[11] J. G. de Vries *Dalton Trans.* **2006**, 421.

[12] A. H. M. de Vries, F. J. Parlevliet, L. Schmieder-van de Vondervoort, J. H. M. Mommers, H. J. W. Henderickx, M. A. M. Walet, J. G. de Vries *Adv. Synth. Catal.* **2002**, *344*, 996.

[13] A. Suzuki *Chem. Commun.* **2005**, 4759.

[14] a) T.-Y. Luh, M.-K. Leung, K.-T. Wong *Chem. Rev.* **2000,** *100*, 3187. b) B. Saito, G. C. Fu *J. Am. Chem. Soc.* **2007**, *129*, 9602.

[15] N. T. S. Phan, M. Van Der Sluys, C. W. Jones *Acc. Chem. Res.* **2006**, *348*, 609.

[16] a) A. F. Littke, G. C. Fu *J. Org. Chem.* **1999**, *64*, 10. b) A. F. Littke, G. C. Fu *Angew. Chem. Int. Ed.* **2002**, *41*, 4176.

[17] S. Li, Y. Lin, J. Cao, S. J. Zhang *J. Org. Chem.* **2007**, *72*, 4067.

[18] O. Navarro, N. Marion, J. Mei, S. P. Nolan *Chem. Eur. J.* **2006**, *12*, 5142.

[19] Y.-C. Lai, H.-Y. Chen, W.-C. Hung, C.-C. Lin, F.-E. Hong *Tetrahedron* **2005**, *61*, 9484.

[20] W.-Y. Wu, S.-N. Chen, F.-Y. Tsai *Tetrahedron Lett.* **2006**, *47*, 9267.

[21] D. A. Alonso, C. Nájera, M. C. Pacheco *Org. Lett.* **2000**, *2*, 1823.

[22] R. B. Bedford, C. S. J. Cazin *Chem. Commun.* **2001**, 1540.

[23] J. K. Eberhardt, R. Fröhlich, E.-U. Würthwein *J. Org. Chem.* **2003**, *68*, 6690.

[24] J.-H. Li, W.-J. Liu, Y.-X. Xie *J. Org. Chem.* **2005**, *70*, 5409.

[25] A. J. Arduengo III, R. L. Harlow, M. Kline *J. Am. Chem. Soc.* **1991**, *113*, 361.

[26] E. A. B. Kantchev, C. J. O'Brien, M. G. Organ *Angew. Chem. Int. Ed.* **2007**, *46*, 2768.

[27] a) W. A. Herrmann *Angew. Chem. Int. Ed.* **2002**, *41*, 1290. b) O. Schuster, L. Yang, H. G. Raubenheimer, M. Albrecht *Chem. Rev.* **2009**, *109*, 3445. c) S. Nolan, in *N-Heterocyclic Carbenes in Synthesis*, Wiley-VCH Verlag GmbH & Co. KGaA, Weinheim, Federal Republic of Germany, **2006**. d) D. Bourissou, O. Guerret, F. P. Gabbaï, G. Bertrand *Chem. Rev.* **2000**, *100*, 39. e) K. J. Cavell, D. S. McGuinness *Coord. Chem. Rev.* **2004**, *248*, 671.

[28] M.-T. Lee, C.-H. Hu *Organometallics* **2004**, *23*, 976.
[29] a) J. Huang, H.-J. Schanz, E. D. Stevens, S. P. Nolan *Organometallics* **1999**, *18*, 5375. b) M. Scholl, T. M. Trnka, J. P. Morgan, R. H. Grubbs *Tetrahedron Lett.* **1999**, *40*, 2247. c) M. Heckenroth, E. Kluser, A. Neels, M. Albrecht *Angew. Chem. Int. Ed.* **2007**, *46*, 6293.
[30] S. Berardi, M. Carraro, M. Iglesias, A. Sartorel, G. Scorrano, M. Albrecht, M. Bonchio *submitted*.
[31] a) M. T. Pope, A. Müller, in *Heteropoly and Isopoly Oxometalates*, Springer Verlag, New York, **1983**. b) M. T. Pope, A. Müller *Angew. Chem. Int. Ed.* **1991**, *30*, 34. c) C. L. Hill *Polyoxometalates, Chem. Rev.* (Special Issue) **1998**, 98, 1. d) S. Berardi, M. Bonchio, M. Carraro, V. Conte, A. Sartorel, G. Scorrano *J. Org. Chem.* **2007**, *72*, 8954. e) M. Carraro, A. Sartorel, G. Scorrano, C. Maccato, M. H. Dickman, U. Kortz, M. Bonchio *Angew. Chem. Int. Ed.* **2008**, *47*, 7275. f) M. Carraro, L. Sandei, A. Sartorel, G. Scorrano, M. Bonchio, *Org. Lett.* **2006**, *8*, 3671. g) M. Carraro, G. Modugno, A. Sartorel G. Scorrano, M. Bonchio *Eur. J. Inorg. Chem.* **2009**, 5164.
[32] M. De bruyn, R. Neumann *Adv. Synth. Catal.* **2007**, *349*, 1624.
[33] J. Canny, A. Tézé, R. Thouvenot, G. Hervé *Inorg. Chem.* **1986**, *25*, 2114.
[34] C. Rocchiccioli-Deltcheff, R. Thouvenot *J. Chem. Research (S)* **1977**, 46.
[35] C. R. Mayer, I. Fournier, R. Thouvenot *Chem. Eur. J.* **2000**, *6*, 105.
[36] I. Özdemir, M. Yiğit, E. Çetinkaya, B. Çetinkaya *Appl. Organomet. Chem.* **2006**, *20*, 187.
[37] T. Weskamp, V. P. W. Bölm, W. A. Herrmann *J. Organomet. Chem.* **2000**, *600*, 12 and references cited therein.
[38] a) C. K. Lee, J. C. C. Chen, K. M. Lee, C. W. Liu, I. J. B. Lin *Chem. Mater.* **1999**, *11*, 1237. b) D. S. McGuinness, K. J. Cavell *Organometallics* **2000**, *19*, 741. c) M. C. Perry, X. Cui, K. Burgess *Tetrahedron: Asymm.* **2002**, *13*, 1969.
[39] M. B. Andrus, C. Song *Org. Lett.* **2001**, *3*, 3761.
[40] H. Qiu, S. M. Sarkar, D.-H. Lee, M.-J. Jin *Green Chem.* **2008**, *10*, 37.
[41] a) R. K. Arvela, N. E. Leadbeater *Org. Lett.* **2005**, *7*, 2101. b) M. Marco, N. E. Leadbeater *J. Org. Chem.* **2003**, *68*, 888. c) R. K. Arvela, N. E. Leadbeater, M. S. Sangi, V. A. Williams, P. Granados, R. D. Singer *J. Org. Chem.* **2005**, *70*, 161.
[42] a) I. Guryanov, F. M. Toma, Al. Montellano Lopez, M. Carraro, T. Da Ros, G. Angelini, E. D'Aurizio, A. Fontana, M. Maggini, M. Prato, M. Bonchio *Chem. Eur. J.* **2009**, 15, 12837. b) I. Guryanov, A. Montellano Lopez, M. Carraro, T. Da Ros, G. Scorrano, M. Maggini, M. Prato, M. Bonchio *Chem Commun.* **2009**, 3940.
[43] N. Marion, O. Navarro, J. Mei, E. D. Stevens, N. M. Scott, S. P. Nolan *J. Am.Chem. Soc.* **2006**, *128*, 4101.
[44] a) Z. Jin, S.-X. Guo, X.-P. Gu, L.-L. Qiu, H.-B. Song, J.-X. Fang *Adv. Synth. Catal.* **2009**, *351*, 1575. b) R. Singh, M. S. Viciu, N. Kramareva, O. Navarro, S. P. Nolan *Org. Lett.* **2005**, *7*, 1829.
[45] a) O. Diebolt, P. Braunstein, S. P. Nolan, C. S. J. Cazin *Chem. Commun.***2008**, 3190. b) G. Altenhoff, R. Goddard, C. W. Lehmann, F. Glorius *Angew. Chem. Int. Ed.* **2003**, *42*, 3690.
[46] a) M. J. Burns, I. J. S. Fairlamb, A. R. Kapdi, P. Sehnal, R. J. K. Taylor *Org. Lett.* **2007**, 9, 5397. b) R. Rodríguez González, L. Liguori, A. Martinez Carrillo, H.-R. Bjørsvik *J. Org. Chem.* **2005**, *70*, 9591. c) G. Dyker, A. Kellner *J. Organomet. Chem.* **1998**, *555*, 141.
[47] M. Moreno-Mañas, M. Pérez, R. Pleixats *J. Org. Chem.* **1996**, *61*, 2346.
[48] S. T. Handy, H. Bregman, J. Lewis, X. Zhang, Y. Zhang *Tetrahedron Lett.* **2003**, *44*, 427.
[49] a) O. Hutzinger, S. Safe, V. Zitko, in *The Chemistry of PCBs*, CRC Press: Cleveland, OH, **1974**. b) O. Navarro, H. Kaur, P. Mahjoor, S. P. Nolan *J. Org. Chem.* **2004**, *69*, 3173.
[50] F. Alonso, I. P. Beletskaya, M. Yus *Chem. Rev.* **2002**, *102*, 4009.
[51] a) E. Buncel, E. A. Symons *J. Chem Soc. D.: Chem. Commun.* **1970**, 164. b) Y. Ben-David, M. Gozin, M. Portnoy, D. Milstein *J. Mol. Catal.* **1992**, *73*, 173.
[52] D. Sattari, C. L. Hill *J. Am. Chem. Soc.* **1993**, *115*, 4649.
[53] H. Hagiwara, K. H. Ko, T. Hoshi, T. Suzuki *Chem. Commun.* **2007**, 2838.

5. Aluminum-substituted polyoxometalates for H_2O_2-based oxidations

5.1 Aluminum in catalysis: some perspectives

Aluminum is electron-deficient, thus it displays a marked tendency to complete the electron octet and high Lewis acidity.[1]

Aluminum can strongly bond electronegative atoms (such as oxygen and halogens), as well as alkyl groups, thus originating organoaluminum compounds. An accurate selection of the groups bonded to aluminum can be exploited in order to tune the reactivity of the organometallic reagent according to needs.[1, 2]

Neutral Al^{III} compounds tend indeed to form 1:1 complexes by covalent or coordination bond, especially with neutral bases, such as ethers. Covalent bonds are formed with anionic (and more reactive) species, while coordination bonds are usually formed by interaction with neutral Lewis bases, such as carbonyl compounds, ethers, and nitrogen containing molecules.[1,2] Regardless to the bond formed, Al^{III} species can undergo easily tetracoordination (sometimes also penta- or hexa- coordination), forming anionic ("ate") aluminum compounds.[1, 2]

Cationic aluminum species are of synthetic interest as well; due to their positively charged nature they are excellent Lewis acids and are widely used in catalysis, mainly in polymerization/oligomerization processes.

Chiral aluminum complexes have also been synthesized and efficiently employed as Lewis acids in asymmetric transformations.[1b]

Another growing field of study in which Al-based catalysts are employed is that of catalytic oxidations. Among this kind of transformations, Baeyer-Villiger reaction, i.e. the conversion of ketones into esters and lactones, is one the more investigated.[3]

As an example, Lei and co-workers[4] recently reported an environmentally benign protocol for Baeyer-Villiger oxidation of ketones, using cheap $AlCl_3$ as catalyst and H_2O_2 as oxidant.

The system provides excellent catalytic activity (up to 100% substrate conversion) and good selectivity (up to 99%) for the oxidation of general cyclic and acyclic ketones. Coordination of the carbonyl group of the ketone to the hard Lewis-acid Al^{3+}, as well as the formation of $Al(H_2O)_5(H_2O_2)^{3+}$ (or even $Al(H_2O)_5(OOH)^{2+}$) have been postulated.

On the other hand, asymmetric oxidation catalysis by aluminum complexes has been still scarcely developed. As a rare example, Bolm and co-workers[5] reported the asymmetric Al-catalyzed Baeyer–Villiger oxidation with cumyl hydroperoxide as oxidant. Chiral BINOL-

type ligands (BINOL = 1,1'-binaphthalen-2,2'-diol) were used in combination with Me_2AlCl, increasing the Lewis-acidity of the metal center, thus leading to high enantioselectivities. Mechanistic investigations led to hypothesize that a chiral aluminum intermediate is formed in-situ and that the ketone is coordinated to the metal site of such complex (see Fig. 5.1). Subsequent oxygen transfer and stereoselective rearrangement yield the Baeyer–Villiger product.

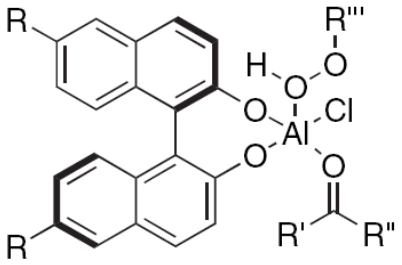

Figure 5.1. Pentacoordinated BINOL-aluminum intermediate, coordinating the substrate (i.e. the ketone) and the cumyl hydroperoxide (i.e. the oxidant).

Recently, Katsuki and co-workers reported the first example of asymmetric oxidation of sulfide with hydrogen peroxide catalyzed by a water-compatible chiral Al(salalen) complex (see Fig. 5.2).[6]

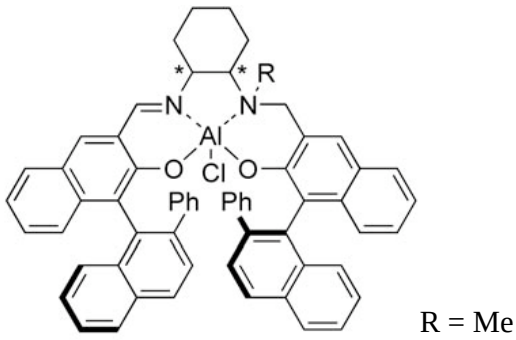

Figure 5.2. Chiral BINOL-based salalen ligand for aluminum, used for asymmetric oxidation of sulfides.

The catalytic activity of this complex was evaluated in the asymmetric oxidation of different aryl methyl sulfides with H_2O_2 in methanol.

High chemoselectivities towards sulfoxide were achieved (overoxidation to sulfone <10%). Moreover, excellent enantioselectivities (ee > 97%) were observed, irrespective of the position and the electronic nature of the substituent on the aromatic ring.

Such highly enantioselective oxidation of sulfides towards the production of the S enantiomer is followed by an oxidative kinetic resolution process. Indeed, enantiomer differentiation in the oxidation of racemic methyl phenyl sulfoxide showed that the R sulfoxide was oxidized preferentially to the sulfone. Such synergistic combination is explains the gradual increase in the ee value of the sulfoxide as the reaction proceeds.

5.2 Aluminum-substituted polyoxometalates: state of art

As already mentioned above, aluminum cations are electron-deficient.[1] Since their chemical properties and reactivities are strongly dependent on their structures, the synthesis of aluminum compounds with structurally well-defined sites is a key issue.

In order to reach this goal, a possible synthetic strategy can be the incorporation of aluminum into the robust inorganic structure of a polyoxometalate (POM, see Chapter 1, Paragraph 1.2), with the formation of a Transition Metal Substituted Polyoxometalate (*TMSP*, see Chapter 1, Paragraph 1.2.2).

Although some examples of aluminum-substituted polyoxometalates have been reported in the literature, structurally characterized (by X-ray crystallographic analysis) Al-POMs are still one of the least reported compounds.[7]

Recently, Mizuno and co-workers[8] reported the synthesis of a novel dialuminum-substituted silicotungstate $[\gamma\text{-}SiW_{10}O_{36}\{Al(OH_2)\}_2(\mu\text{-}OH)_2]^{4-}$, by reacting the divacant Keggin anion $[\gamma\text{-}SiW_{10}O_{36}]^{8-}$ with 2 equivalents of $Al(NO_3)_3$ in an acidic aqueous medium.

X-ray crystallographic analysis of this dialuminum-substituted silicotungstate compound showed the presence of a $\{Al_2(\mu\text{-}OH)_2\}$ diamond core in it (Fig. 5.3).

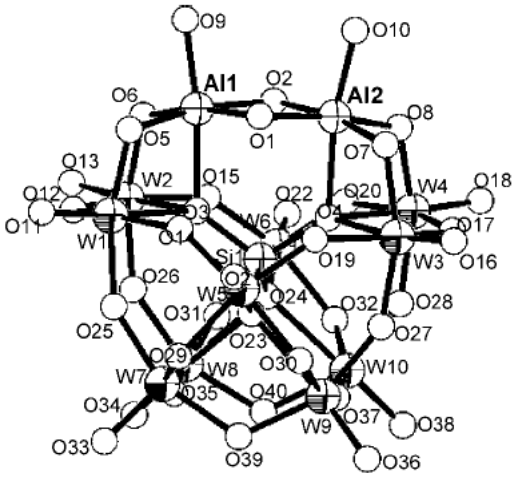

Figure 5.3. Molecular structure of $[\gamma\text{-}SiW_{10}O_{36}\{Al(OH_2)\}_2(\mu\text{-}OH)_2]^{4-}$.

Such compound showed high catalytic activity for the intramolecular diasteroselective cyclization of citronellal derivatives, such as (+)-citronellal (**3**) (see Scheme 5.1), without formation of by-products resulting from etherification or dehydration.

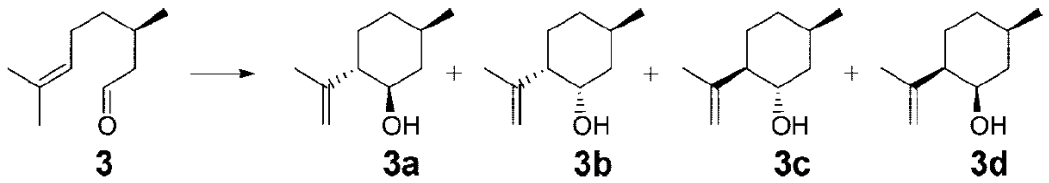

Scheme 5.1. Intramolecular cyclization of (+)-citronellal (**3**) by $[\gamma\text{-}SiW_{10}O_{36}\{Al(OH_2)\}_2(\mu\text{-}OH)_2]^{4-}$.

The observed high diastereoselectivity toward (-)-isopulegol (**3a**) (a precursor of the industrially relevant (-)-menthol), together with other experimental and computational results, speaks in favour of a Lewis-acid catalysis promoted by the Al-centres of the POM.

Recently, Wang and co-workers[9] reported the environmentally benign oxidation of alcohols with H_2O_2 by another aluminum-substituted POM, namely $[SiW_9Al_3(H_2O)_3O_{37}]^{7-}$, in solvent-free conditions. Such complex gave the best results when compared with the analogous complexes containing Tl, In and Ga.

Control experiments indicate no oxidation products in the absence of the catalyst, or in the presence of both the saturated Keggin anion $[SiW_{12}O_{40}]^{4-}$ and the trivacant derivative $[SiW_9O_{34}]^{10-}$. Neither using $AlCl_3$ or $Al(NO_3)_3$ as catalysts, the reaction takes place.

Under the explored mild conditions, $[SiW_9Al_3(H_2O)_3O_{37}]^{7-}$ was able to catalyze the chemoselective oxidation of secondary alcohols to the corresponding ketones in good yields, also in the presence of primary hydroxyl group or double bonds within the same molecule. Benzylic alcohols have also been selectively converted to the corresponding benzaldehydes with good yields, without producing over-oxidation compounds. Such selectivity may be due to the introduction of an amphoteric element, such as aluminum, into the polyoxometalate, leading to a peculiar change in the charges distribution.

Also in our research group, a recent collaboration with prof. Kortz of Jacobs University of Bremen, regarded the synthesis and the evaluation of the catalytic activity of novel Al-substituted POMs.[10] Results will be presented and discussed in the following paragraphs.

5.3 Results and discussion [10]

5.3.1 Synthesis and characterization of aluminum-substituted polyoxometalates

Amongst transition metal-substituted polyoxometalates (*TMSPs*), the sandwich-type species are one of the larger families. They are usually composed of transition metal ions and a trivacant Keggin $[XM_9O_{33-34}]^{n-}$ ($X = P^V$, Si^{IV}, Ge^{IV}) or Wells-Dawson $[X_2W_{15}O_{56}]^{12-}$ ($X = P^V$, As^V) polyanionic ligands. Furthermore, dimeric species based on two lone-pair containing β-Keggin fragments $[\beta\text{-}XW_9O_{33}]^{n-}$ ($X = As^{III}$, Sb^{III}, Bi^{III}, Te^{IV}, Se^{IV}) have led to several isostructural derivatives in which the presence of a lone pair on the heteroatom does not allow the closed Wells-Dawson structure to form. The first report on these polyoxometalates was described by Krebs in 1997.

Even if 3rd group metal polyoxometalates are known,[11] little work on aluminum-containing polyanions has been reported to date.[7, 9]

We synthesized the first two sandwich-type aluminum containing polyoxotungstates, namely the dimeric tungstoarsenate $[Al_4(H_2O)_{10}(\beta\text{-}AsW_9O_{33})_2]^{6-}$ (**I**) and tungstoantimonate $[Al_4(H_2O)_{10}(\beta\text{-}SbW_9O_{33})_2]^{6-}$ (**II**).

Polyoxometalates **I** and **II** originated from the interaction of Al^{III} ions with the trivacant $[\alpha\text{-}XW_9O_{33}]^{9-}$ ($X = As^{III}$, Sb^{III}) precursors in aqueous acidic medium, upon heating at 70°C for one hour. The synthetic strategy is reported in Scheme 5.2.

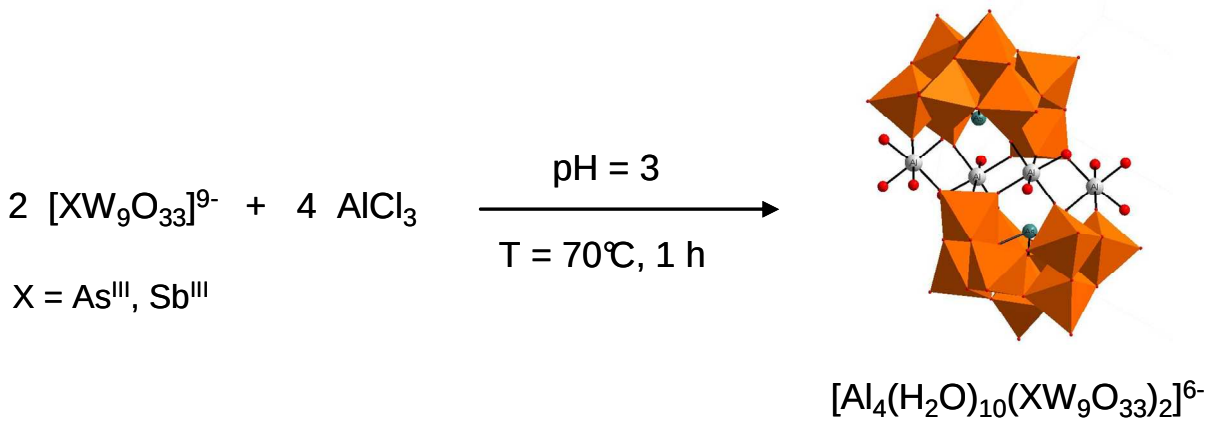

Scheme 5.2. Synthesis and structure of $[Al_4(H_2O)_{10}(XW_9O_{33})_2]^{6-}$ ($X = As^{III}$, Sb^{III}). Orange octahedra centred on W atoms; O (red spheres), As or Sb (dark blue), Al (grey).

The introduction of Al^{III} ions is followed by an expected isomerization (α → β) of the trivacant subunits.

The amorphous salt of $[Al_4(H_2O)_{10}(\beta\text{-}XW_9O_{33})_2]^{6-}$ polyanions can be obtained upon addition of an excess of KCl to the reaction mixture. Lipophylic derivatives can be obtained by cation metathesis reaction, adding *n*-Bu_4NBr to the potassium salts.

FT-IR analyses of both the K^+ and the *n*-Bu_4N^+ salts of complex **I** are reported as an example in Figure 5.4.

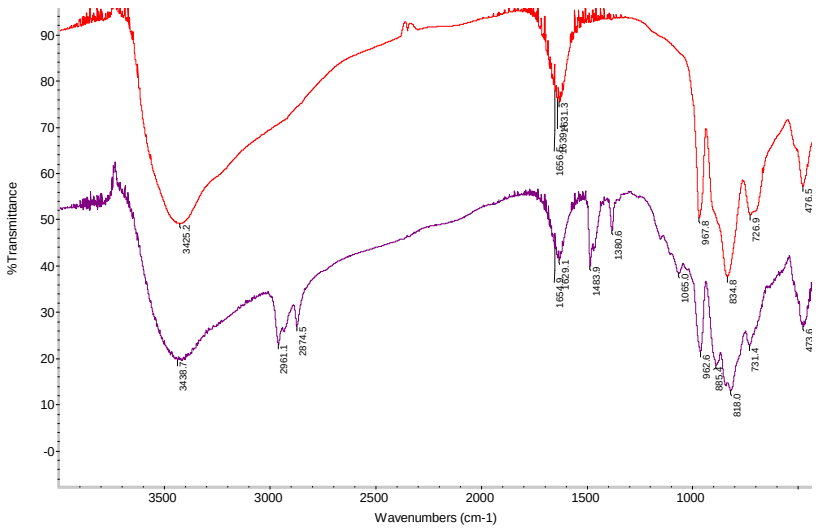

Figure 5.4. FT-IR spectra of K^+ (top) and *n*-Bu_4N^+ (bottom) salts of complex **I**.

The inorganic structure of the polyoxometalate is retained during the metathesis reactions, as confirmed by the overlapping of the bands in the range $850 < \nu < 1000$ cm^{-1}, where the peculiar stretching modes absorptions of the Krebs structure appear.

The effectiveness of the metathesis reaction is confirmed by the appearance of new bands in the range $2800 < \nu < 3000$ cm^{-1}, due to the absorptions of the tetrabutylammonium C-H bonds, as well as by the solubility of the resulting complexes in organic solvent (such as CH_3CN, DMSO and DMF).

Crystallization of both the complexes **I** and **II** can be accomplished by slow evaporation of water in the presence of Rb^+ and NH_4^+ respectively. X-ray structural analyses revealed that the two polyanions are isostructural (see Fig. 5.5). In agreement with previously reported *TMSPs* containing trivalent metal ions, the expected tetra-substituted complex has formed.[11, 12] In particular, the structures of **I** and **II** consist in two trivacant $[\beta\text{-}XW_9O_{33}]^{9-}$ ($X = As^{III}$, Sb^{III}) Keggin units, bridged *via* four octahedral Al^{III} ions, resulting in a sandwich-type structure with formal C_{2h} symmetry (see Fig. 5.5).

In both these structures, the two external and the two internal Al^{III} ions display respectively three and two terminal aquo ligands.

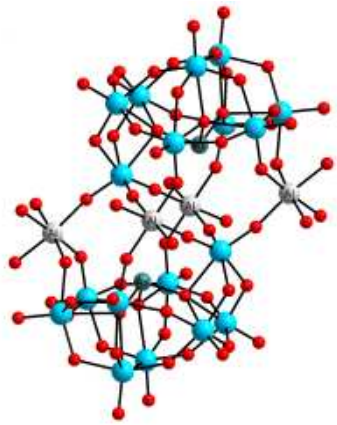

Figure 5.5. Crystal structure of both complexes **I** and **II**. O (red), Al (grey), W (blue), As or Sb (dark blue).

From the crystallographic analysis we could indeed identify only 2.5 Rb^+ (for complex **I**) or protons (for complex **II**) as countercations.

As expected, As–O bond lengths are shorter (1.80-1.82 Å) than Sb–O bonds (2.01-2.02 Å) and the heteroatom X···X separations within **I** (As···As = 5.92 Å) and **II** (Sb···Sb = 5.54 Å) are consistent with this observation. Instead, the heteroatom does not affect the Al–O bond lengths (1.85-1.93 Å in **I** and 1.86-1.95 Å in **II**). The small Al^{III} ioni radius (0.67 Å) results in shorter X···O and X···X distances in comparison with the previously reported Fe^{III} and In^{III} Krebs-type derivatives.[11, 12]

Catalytic activity of complex **I** has been tested for the oxidation of different classes of substrates in the presence of hydrogen peroxide. The results will be discussed in the following Paragraph.

5.3.2 $[Al_4(H_2O)_{10}(\beta\text{-}AsW_9O_{33})_2]^{6-}$ as catalyst for oxidation reactions

Polyoxotungstate complexes have been widely used as oxidation catalysts in the presence of sustainable oxidants.[13] Both transition metal substituted polyoxoanions and hybrid organic inorganic polyoxometaltes have indeed proven to be useful to achieve hydrogen peroxide activation.[14] As already introduced, even if the interest in using aluminum derivatives is mainly due to their Lewis acidity, they have recently successfully used as catalysts for alcohol oxidation[9] and for the asymmetric oxygen transfer to sulfides.[6]

Complex **1**, with different countercations, has thus been used as oxidation catalysts in the presence of hydrogen peroxide.

The lipophylic tetrabutylammonium derivative has been used for the oxidation of different classes of substrates with H_2O_2 in acetonitrile, in a temperature range of 30-70°C. Results are summarized in Table 5.1.

Table 5.1. Reactivity of complex **I** (*n*-Bu_4N^+ salt) in acetonitrile.

#	Substrate	Product	T, °C	Yield[a], % (time, h)	TOF, h^{-1}
1	Methyl-*p*-tolylsulfide	Methyl-*p*-tolylsulfoxide	30	100 (1)	125
2	*Cis*-cyclooctene	Cyclooctene oxide	70	98 (1)	123
3	Cyclohexene	Cyclohexene oxide[b]	70	58 (1)	73
4	1-octene	1,2-epoxyoctane	70	26 (1)	33
5	1-decene	1,2-epoxydecane	70	28 (1)	35
6	Cyclohexanol	Cyclohexanone	35 70	100 (24) 96 (1)	5 120
7	Cyclopentanol	Cyclopentanone	70	60 (1)	75
8	2-nonanol	2-nonanone	70	81 (1)	100
9	Benzylic alcohol	Benzaldehyde	70	73 (1)	91
10	2-cyclohexen-1-ol	2-cyclohexen-1-one	70	90 (2)	56

Reaction conditions: 35% aqueous H_2O_2 (0.1 mmol); **I** (0.8 μmol), substrate (0.5 mmol), CH_3CN (0.6 mL).
[a] calculated with respect to H_2O_2. [b] 2-cyclohexen-1-ol (traces) also formed.

An interesting reactivity with high yields and selectivities has been observed for oxidation of olefins, sulfides and alcohols.

Methyl-*p*-tolylsulfide was oxidized to the corresponding sulfoxide in quantitative yield in 1 h (turnover frequency, TOF = 125 h^{-1}, entry 1, Tab. 5.1), without overoxidation to sulfone.

The proposed system was also effective for the epoxidation of cyclic and terminal olefins. While cyclooctene epoxide was selectively produced in high yield (98%, entry 2, Tab. 5.1), oxidation of cyclohexene yielded a 58% of the corresponding epoxide, together with traces of the allylic oxidation product (i.e. 2-cyclohexen-1-ol, entry 3, Tab. 5.1). Less reactive terminal olefins (such as 1-octene and 1-decene) could also be epoxidized, but yields remain low (26% and 28% respectively, entries 4 and 5, Tab. 5.1).

Secondary alcohols were efficiently converted into the corresponding ketones, with >99% selectivity and good yields (60-100%, entries 6-8, Tab. 5.1), while oxidation of benzylic alcohol yielded benzaldehyde as the only product, in 73% yield (entry 9, Tab. 5.1).

Interestingly, a high chemoselectivity has been found for 2-cyclohexen-1-ol, leading to the corresponding α,β-unsaturated ketone with 90% yield (entry 10, Tab. 5.1). No oxidation of the C=C bond was observed.

A first attempt of performing Baeyer-Villiger oxidation of cyclopentanone showed that catalyst **I** is inactive toward this kind of reaction, since no formation of the corresponding lactone was observed.

Another interesting aspect about catalytic activity of complex **I** concerns the possibility of using water as the reaction media. In the presence of ammonium or alkaline countercations (such as Rb^+ or K^+), the resulting POM is indeed soluble in water. Results obtained for the oxidation of ciclohexanol in H_2O catalyzed by water-soluble **I** salts are reported in Table 5.2.

Table 5.2. Reactivity of water-soluble **I** salts toward cyclohexanol oxidation with H_2O_2.

#	$Al_4(AsW_9O_{33})_2^{6-}$ salt	T, °C	Yield,[a] % (time, h)	TOF, h^{-1}
1	NH_4	70	100 (2)	63
2	K	70	33 (1) 64 (2) 95 (4)	41
3	Rb	70	54 (1) 98 (2.5)	50

Reaction conditions: Cyclohexanol (0.5 mmol), 35% H_2O_2 (0.1 mmol); **I** (0.8 μmol), H_2O (1.2 mL). [a] calculated with the respect of H_2O_2.

Cyclohexanol can be efficiently oxidized in water at 70°C, producing the corresponding ketone in quantitative yields with high turnover frequencies (entries 1-3, Tab. 5.2). Further experiments will be addressed to evaluate the effect (if any) of the countercation.

In all reactions, both performed in organic solvent and in water, POM stability has been assessed upon precipitation of the catalyst at the end of the reaction, by addition of a non-solvent. FT-IR analyses have revealed that all the spectroscopic features of complex **I** are preserved when it is used in acetonitrile (Fig. 5.6).

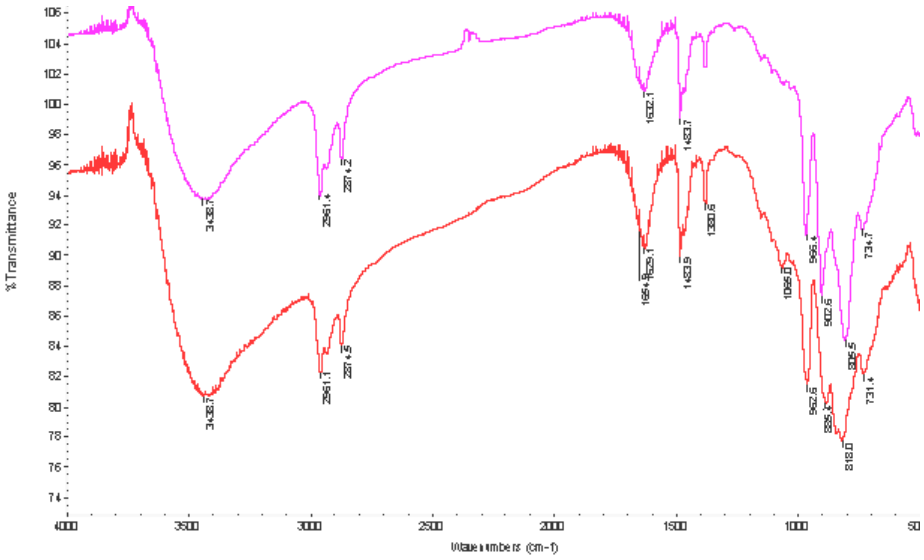

Figure 5.6. FT-IR (1% in KBr) spectra of $[Al_4(AsW_9O_{33})_2]^{6-}$ (n-Bu_4N^+ salt) before (top) and after (bottom) the sulfoxidation of methyl-*p*-toylsulfide in CH_3CN (entry 1, Tab. 5.1).

Spectral changes have instead been observed when recovering the catalyst from the aqueous solution (Fig. 5.7).

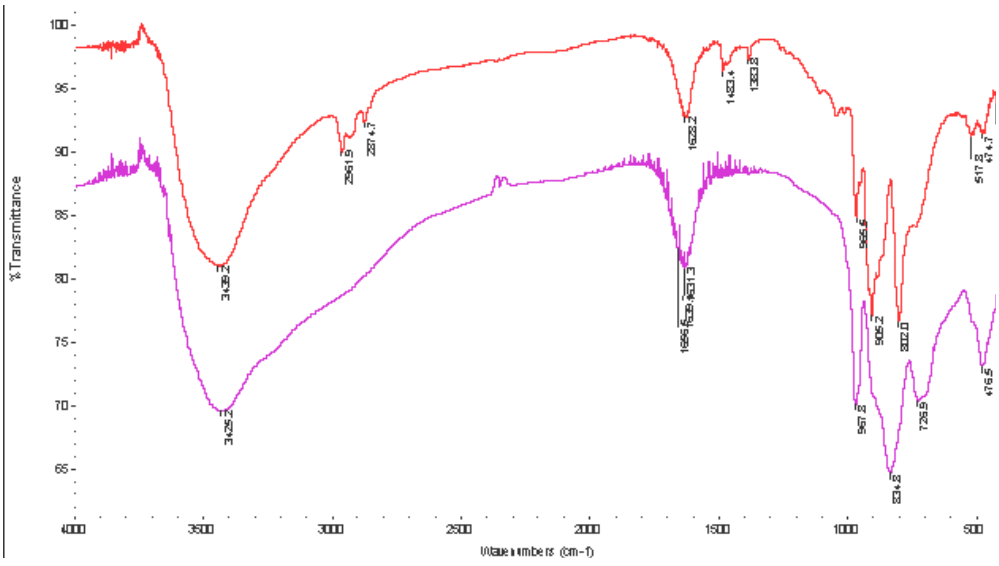

Figure 5.7. FT-IR (1% in KBr) spectra of $[Al_4(AsW_9O_{33})_2]^{6-}$ (K^+ salt) before (bottom) and after (top) the oxidation of cyclohexanol in H_2O (entry 2, Tab. 5.2).

On the basis of this latter observation, a kinetic study of cyclohexanol oxidation in H_2O has been performed. In Figure 5.8 the profile of the cyclohexanone formation during the time is reported.

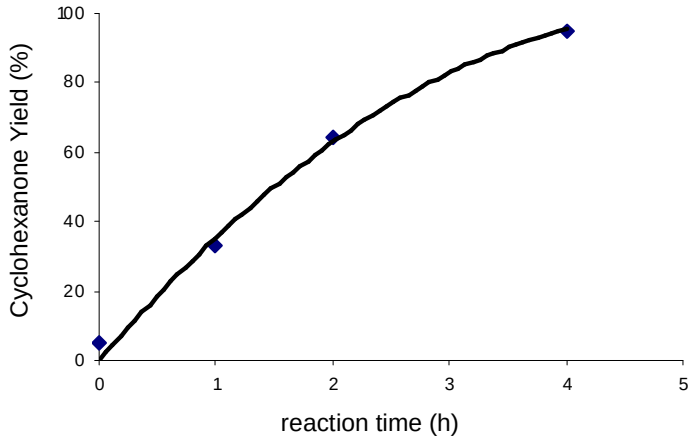

Figure 5.8. Kinetic profile for cyclohexanol oxidation with H_2O_2, catalyzed by $[Al_4(AsW_9O_{33})_2]^{6-}$ (K^+ salt) (entry 2, Tab. 5.2).

The observed kinetic profile is regular, without induction periods. We can thus hypothesize that catalyst modification happens since the beginning of the reaction, leading to the formation of a different active specie. In order to assess this hypothesis and to optimize consequently the reaction, further studies on both the speciation of the catalyst under turnover regime and the pH effect on complex stability will be performed.

A preliminary evaluation of the possible coordination of hydroxylic moieties to the Al-sites of the POM has been studied. Modifications of the UV-vis spectrum of complex **1** have been evaluated upon addition of increasing amounts of *S*-(-)-1,1'-binaphthalen-2,2'-diol (later called BINOL) to a solution of **I** in CH_3CN. Similar ligands have been indeed used to perform asymmetric Baeyer-Villiger oxidations in a recent work by Bolm and co-workers,[5] in which the formation of an intermediate such as that depicted in Figure 5.1 has been postulated.

However, preliminary UV-vis analyses did not show this kind of coordination of the BINOL ligand to complex **I**, since simple linear correlations between absorbance (at different wavelengths, i.e. λ = 320 and 334 nm) and number of equivalents of the added BINOL have been observed (see Fig. 5.9).

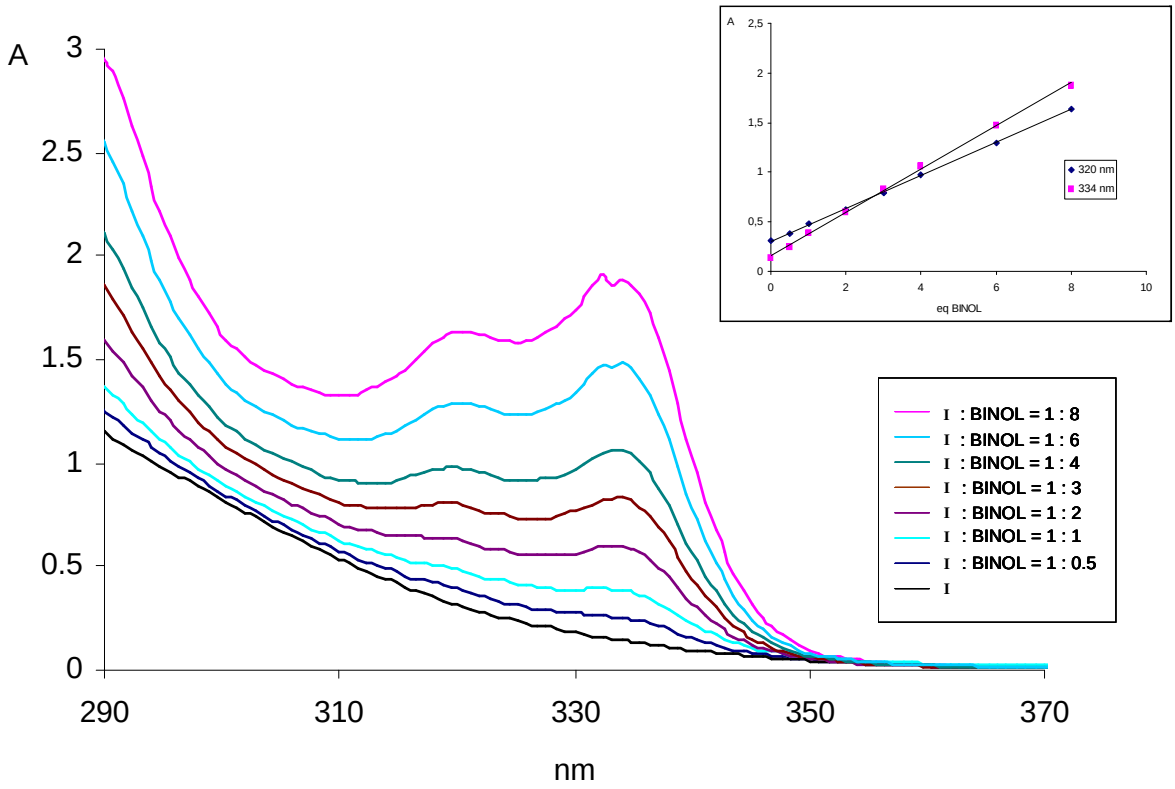

Figure 5.9. UV-vis spectra of **I** (10^{-4} M in CH_3CN) in the presence of increasing amounts of BINOL. Inset: Absorbance at λ = 320 and 334 nm *vs.* number of equivalents of added BINOL.

Also performing the reactions in which POM:BINOL = 1:1 and 1:8 at 70°C for 30 minutes, did not lead to the coordination of BINOL to complex **I**, since UV-vis spectra resulted identical to those of the analogous reactions performed at room temperature.

Further experiments will be addressed to evaluate the possible coordination of other ligands to the aluminum centres, in order to tune their Lewis acidity and to modulate the catalytic sites, also introducing chiral moieties.

5.4 Conclusions and future perspectives

In conclusion we have synthesized and fully characterized two aluminum-substituted POMs, namely the tungstoarsenate $[Al_4(H_2O)_{10}(\beta\text{-}AsW_9O_{33})_2]^{6-}$ and the tungstoantimonate $[Al_4(H_2O)_{10}(\beta\text{-}SbW_9O_{33})_2]^{6-}$. These complexes are two of the few examples of structurally characterized (by X-ray analysis) POMs incorporating this metal.

Both these complexes possess a sandwich-like structure, in which two trivacant Keggin units are bridged *via* four Al^{III} ions, two external and two internal, displaying respectively three and two terminal aquo ligands.

Future experiments will be addressed to evaluate the possible exchanging of these ligands with different (also chiral) ones, in order to exploit the Lewis acidity of the aluminum centres by fine tuning the catalytic site.

Up to now, $[Al_4(H_2O)_{10}(\beta\text{-}AsW_9O_{33})_2]^{6-}$ has displayed an interesting catalytic activity for oxidation of different substrates (alcohols, olefins, sulfides) with benign H_2O_2 in acetonitrile. Good yields and >99% selectivities have been observed in almost all the cases. Interestingly, high chemoselectivity has been observed for 2-cyclohexen-1-ol oxidation, yielding the corresponding α,β-unsaturated ketone as the only product, without oxidation of the C=C bond.

POMs particular feature of tuning their solubility by changing the countecation has been also exploited and water-soluble $[Al_4(H_2O)_{10}(\beta\text{-}AsW_9O_{33})_2]^{6-}$ salts have been used to catalyze cyclohexanol oxidation in water. High yields have been achieved in an environmentally friendly set-up, thus making this system very promising. Further studies on both the speciation of the catalyst in water under turnover regime and the pH effect on complex stability will be performed.

5.5 References and notes

[1] a) T. Ooi, K. Maruoka, in *Lewis Acids in Organic Synthesis*, H. Yamamoto Ed., Wiley-VCH: Weinheim, **2000**, 191. b) W. D. Wulff, in *Lewis Acids in Organic Synthesis*, H. Yamamoto Ed., Wiley-VCH: Weinheim, **2000**, 283. c) S. Saito, in *Main Group Metals in Organic Synthesis*, H. Yamamoto, K. Oshima Eds., Wiley-VCH: Weinheim, **2004**, 189.

[2] H. Yamamoto, in *Organometallics in Synthesis: A Manual*, M. Schlosser Ed., John Wiley & Sons Ltd., Chichester, **1994**, 509.

[3] a) G. R. Krow, in *Comprehensive Organic Synthesis*, B. M. Trost, I. Fliming Eds., Pergamon: Oxford, **1991**, *7*, 671. b) C. Bolm, in *Advances in Catalytic Processes*, M. P. Doyle Ed., JAI: Greenwich, **1997**, *2*, 43. c) M. Renz, B. Meunier *Eur. J. Org. Chem.* **1999**, 737.

[4] Z. Lei, G. Ma, L. Wei, Q. Yang, B. Su *Catal. Lett.* **2008**, *124*, 330.

[5] J.-C. Frison, C. Palazzi, C. Bolm *Tetrahedron* **2006**, *62*, 6700 and references cited therein.

[6] T. Yamaguchi, K. Matsumoto, B. Saito, T. Katsuki *Angew. Chem. Int. Ed.* **2007**, *46*, 4729.

[7] a) F. Zonnevijlle, C. M. Tournè, G. F. Tournè *Inorg. Chem.* **1982**, *21*, 2742. b) J. Liu, F. Ortéga, P. Sethuraman, D. E. Katsoulis, C. E. Costello, M. T. Pope *J. Chem. Soc., Dalton Trans.* **1992**, 1901. c) Q. H. Yang, D. F. Zhou, H. C. Dai, J. F. Liu, Y. Xing, Y. H. Lin, H. Q. Jia *Polyhedron* **1997**, *16*, 3985. d) J. J. Cowan, A. J. Bailey, R. A. Heintz, B. T. Do, K. I. Hardcastle, C. L. Hill, I. A. Weinstock *Inorg. Chem.* **2001**,
40, 6666. e) W. H. Casey *Chem. Rev.* **2006**, *106*, 1.

[8] Y. Kikukawa, S. Yamaguchi, Y. Nakagawa, K. Uehara, S. Uchida, K. Yamaguchi, N. Mizuno *J. Am. Chem. Soc.* **2008**, *130*, 15872.

[9] J. Wang, L. Yan, G. Qian, S. Li, K. Yang, H. Liu, X. Wang *Tetrahedron* **2007**, *63*, 1826.

[10] M. Carraro, S. Berardi, A. Sartorel, G. Scorrano, M. H. Dickman, U. Kortz, M. Bonchio *manuscript in preparation*.

[11] F. Hussain, M. Reicke, V. Janowski, S. de Silva, J. Futuwi, U. Kortz *Compt. Rend. Chim.* **2005**, *8*, 1045.

[12] a) U. Kortz, M. G. Savelieff, B. S. Bassil, B. Keita, L. Nadjo *Inorg. Chem.* **2002**, *41*, 783. b) M. Prinz, A. Takács, J. Schnack, I. Balasz, E. Burzo, U. Kortz, K. Kuepper, M. Neumann *J. Appl. Phys.* **2006**, *99*, 08J505.

[13] a) Y. Ishii, K. Yamawaki, T. Yoshida, T. Ura, H. Yamada, M. Ogawe *J. Org. Chem.* **1987**, *52*, 1868. b) Y. Ishii, H. Tanaka, Y. Nishiyama *Chem. Lett.* **1994**, *1*, 1. c) C. Venturello, E. Alneri, M. Ricci *J. Org. Chem.* **1983**, *48*, 3831. d) C. Venturello, R. D'Aloisio, J. C. Bart, M. Riai *J. Mol. Catal.* **1985**, *32*, 107. e) J. Prandi, H. B. Kagan, H. Mimoun *Tetrahedron Lett.* **1986**, *27*, 2617. f) K. Sato, M. Aoki, M. Ogawa, T. Hashimoto, R. Noyori *J. Org. Chem.* **1996**, *61*, 8310. g) J. Server-Carrió, J. Bas-Serra, M. E. Gonzàlez-Nuñez, A. Garcìa-Gastaldi, G. B. Jameson, L. C. W. Baker, R. Acerete *J. Am. Chem. Soc.* **1999**, *121*, 977 h) N. Mizuno, K. Kamata, K. Yonehara, Y. Sumida, K. Yamaguchi, S. Hikichi *Science* **2003**, *300*, 964. i) K. Kamata, M. Kotani, K. Yamaguchi, S. Hikichi, N. Mizuno *Chem. Eur. J.* **2007**, *13*, 639 j) A. Sartorel, M. Carraro, A. Bagno, G. Scorrano, M. Bonchio *Angew. Chem. Int. Ed.* **2007**, *46*, 3255. k) M. Bonchio, M. Carraro, A. Farinazzo, A. Sartorel, G. Scorrano, U. Kortz *J. Mol. Cat. A: Chem.* **2007**, *262*, 36. l) M. Bonchio, M. Carraro, A. Sartorel, G. Scorrano, U. Kortz *J. Mol. Catal. A: Chem.* **2006**, *251*, 93. m) M. Bonchio, M. Carraro, G. Scorrano, U. Kortz *Adv. Synth. Cat.*, **2005,** *347*, 1909.

[14] M. Carraro, L. Sandei, A. Sartorel, G. Scorrano, M. Bonchio *Org. Lett.* **2006**, *8*, 3671. b) S. Berardi, M. Bonchio, M. Carraro, V. Conte, A. Sartorel, G. Scorrano *J. Org. Chem.* **2007**, *72*, 8954.

Experimental Part

6. Experimental part

6.1 Instruments and apparatus

- *^{1}H-NMR* spectra were recorded using Bruker AC250, AV300 and AV360 instruments operating, respectively, at 250.18 MHz, 300.13 MHz and 360.13 MHz. Chemical shifts were determined using $Si(CH_3)_4$ as reference (δ ^{1}H-NMR = 0 ppm). For protonic spectra, the following symbolism has been used: s: singlet; d: doublet; t: triplet; q: quartet; m: multiplet.

- *^{13}C-NMR* spectra were recorded with a Bruker Avance AV300 spectrometer operating at 75.47 MHz. Chemical shifts were determined using $Si(CH_3)_4$ as reference (δ ^{13}C-NMR = 0 ppm).

- *^{29}Si-NMR* spectra were recorded with a Bruker Avance DRX 400 spectrometer operating at 79.49 MHz, using a 10 mm tube. Chemical shifts were determined using $Si(CH_3)_4$ in $CDCl_3$ as external reference (δ ^{29}Si-NMR = 0 ppm).

- *^{183}W-NMR* spectra were recorded with a Bruker Avance DRX 400 spectrometer operating at 16.67 MHz. using a 10 mm tube. 2 M Na_2WO_4 in D_2O was used as external reference (δ ^{183}W-NMR = 0 ppm).

- *^{31}P-NMR* spectra were recorded with a Bruker Avance AV300 spectrometer operating at 121.49 MHz, using 85% H_3PO_4 as external reference (δ ^{31}P-NMR = 0 ppm).

- *FT-IR* spectra were recorded with a Nicolet 5700-Thermo Electron Corporation instrument.

- *UV-Vis* spectra were recorded with a Lambda 45 Perkin-Elmer spectrophotometer. Molar extinction coefficients ε are expressed in M^{-1} x cm^{-1}.

- *Gas-chromatographic GLC analyses* were performed using: (i) a Hewlett Packard 6890 series instrument equipped with a flame ionisation detector (FID) using a 30 m (internal diameter = 0.32 mm, film thickness = 0.25 μm) HP-5 capillary column; (ii) a Hewlett

Packard 5890 series II instrument equipped with a FID, using a 60 m (internal diameter = 0,53 mm, film thickness = 1 μm) Alcohols Stabilwax® (Restek) capillary column; (iii) a Shimadzu GC-2100 instrument for GLC flash chromatography equipped with a FID, using a 15 m (internal diameter = 0.10 mm, film thickness = 0.10 μm) Equity™-5 capillary column (composition = 5% biphenyl and 95% dimethylsiloxane).

- *GC-MS* spectra were recorded on a Agilent GC6850 series coupled with a Agilent 5973 Network Mass Selective Detector. GC system is equipped with a 30 m (internal diameter = 0.32 mm, film thickness = 0.25 μm) HP-5 capillary column.

- *ESI-MS* spectra of polyoxometalates were recorded on a Agilent 1100-LC/MSD Trap SL spectrometer (Capillary potential = + 4500 V; skimmer potential = - 35 V; cap. exit. potential = - 100 V). ESI-MS spectrum of compound **5** (see Chapter 2) was recorded on a Bruker FTMS 4.7T BioAPEX II spectrometer.

- *Temperature* was controlled using a Haake L thermostat with external circulation with a 0.05°C of precision.

- *MW-assisted reactions* were performed using a monomodal CEM-Discover microwave apparatus operating at 2.45 GHz with continuous irradiation power.

- *pH measurements* were performed using a lab 827 pH-meter, Metroohm – Swiss.

- *Elemental Analyses* were performed at Microanalysis Laboratory of Chemical Science Department, University of Padova.

- *X-ray Characterizations* of complexes **1** and **2** (see Chapter 4) were performed at Jacobs University of Bremen. Data were collected at 173 K on a single-crystal X-ray diffractometer (Bruker Kappa Apex II), using MoKα radiation and a graphite monochromator (λ = 0.71073 Å). Data were integrated using SAINT (Bruker AXS) and a multi-scan absorption correction was performed using SADABS. Direct methods were used to locate the heavy atoms (SHELXS97) and the remaining atoms were found from successive Fourier syntheses (SHELXL97).

6.2 Solvents and chemicals

General Remarks: All solvents and reagents were purchased from commercial sources and used as received, without further purification.

MilliQ-deionized water (Millipore) was used as solvent.

Table 6.1. Solvents.

Solvent	**Provenience**
Acetonitrile	Prolabo
Dichloromethane	Prolabo
Diethyl Ether	Aldrich
N, *N*-Dimethylformamide	Prolabo
Dimethylsulfoxide	Lab Scan
Pentane	Aldrich
Anhydrous dichloromethane	Fluka
Anhydrous diethyl ether	Fluka
Anhydrous hexane	Aldrich
Deuterated acetone	Aldrich
Deuterated acetonitrile	Aldrich
Deuterated chloroform	Aldrich
Deuterated dichlorometane	Aldrich
D_2O	Aldrich

Table 6.2. Chemicals.

Product	**Provenience**	**Purity**
Acetic acid (glacial)	Carlo Erba	---
H_2O_2	Aldrich	35%
H_2O_2	Rusimont	70%
KI	J. T. Baker	99%
KIO_3	Carlo Erba	---
$Na_2S_2O_3$	Carlo Erba	99%
Starch indicator for iodometry	Carlo Erba	---
HCl	Carlo Erba	37%
HNO_3	Carlo Erba	65%
KBr	Aldrich	IR grade
KCl	Riedel-de-Haën	99.5%
K_2CO_3	Aldrich	> 99%

Na_2SiO_3	Aldrich	98%
$Na_2WO_4 \cdot 2H_2O$	Riedel-de-Haën	99%
$PhPO(OH)_2$	Aldrich	98%
Tetrabutylammonium bromide	Aldrich	99%
1-methylimidazole	Fluka	99%
1-bromobutane	Acros	99%
KPF_6	Alfa Aesar	97%
$Li[(CF_3SO_2)_2N]$	Fluka	98%
$Li(CF_3SO_3)$	Fluka	99%
$NaBF_4$	Aldrich	98%
Cis-cyclooctene	Aldrich	95%
Cyclohexene	Fluka	≥ 99,5%
Cyclooctene epoxide	Aldrich	99%
Dodecane	Aldrich	> 99%
1-hexene	Fluka	~ 99%
E-2-hexene	Aldrich	97%
Z-2-hexene	Fluka	≥ 99.5%
P_2O_5	Prolabo	> 98%
1-octene	Fluka	> 97%
E-2-octene	Aldrich	97%
Z-stilbene	Janssen	97%
Triphenylphosphine	Aldrich	> 95%
UHP	Aldrich	97%
Acetic anhydride	Carlo Erba	---
Benzoic anhydride	Fluka	95%
Ferrocene	Fluka	98%
Propanoic anhydride	Aldrich	97%
Scandium triflate	Fluka	97%
Ytterbium triflate	Fluka	> 97%
Yttrium triflate	Aldrich	98%
4-acetyl-1,1'-biphenyl	Aldrich	98%
Biphenyl	Aldrich	> 99%
4-bromoacetophenone	Fluka	> 98%
Bromobenzene	Aldrich	99%
4-bromonitrobenzene	EGA Chemie	---
1-bromooctane	Aldrich	99%
4-bromotoluene	Aldrich	98%
1-butylimidazole	Aldrich	98%

Celite	Merck	---
2-chloroacetophenone	Janssen	97%
3-chloroacetophenone	Aldrich	98%
4-chloroacetophenone	Janssen	98%
4-chlorobenzaldehyde	Aldrich	97%
Chlorobenzene	Janssen	99%
1-chloronaphthalene	Aldrich	95%
4-chloronitrobenzene	Carlo Erba	---
4-chlorophenol	Aldrich	> 99%
(3-chloropropyl)-triethoxysilane	Aldrich	95%
4-chlorotoluene	Fluka	≥ 99%
3-(2-imidazolin-1-yl)propyltriethoxysilane	Fluka	≥ 98%
4-iodoacetophenone	Aldrich	98%
4-iodoanisole	Aldrich	98%
Iodobenzene	Fluka	≥ 99%
4-iodonitrobenzene	EGA Chemie	99%
4-iodotoluene	Aldrich	99%
KHMDS	Fluka	≥ 95%
4-methyl-1,1'-biphenyl	Aldrich	98%
Magnesium sulfate	Prolabo	98%
Palladium acetate	Aldrich	99.9+%
Phenylboronic acid	Fluka	> 97%
Sodium bromide	Aldrich	99%
Sodium carbonate	Carlo Erba	---
Silver oxide	Aldrich	≥ 99%
n-$Bu_4NOH \cdot 30H_2O$	Aldrich	98%
$AlCl_3$	Fluka	99%
Ammonium chloride	J. T. Baker	99.5%
Benzylic alcohol	Aldrich	99%
S-(-)-1,1'-binaphthalen-2,2'-diol	Fluka	≥ 99%
Cyclopentanol	Aldrich	99%
Cyclohexanol	Aldrich	99%
2-cyclohexen-1-ol	Fluka	> 95%
1-decene	Aldrich	> 97%
Methyl-*p*-tolylsulfide	Aldrich	99%
2-nonanol	Aldrich	> 97%
Rubidium chloride	Aldrich	99.8%

6.3 Synthesis of polyoxometalates

6.3.1 Synthesis of $K_8[\alpha\text{-}SiW_{11}O_{39}]$ [1]

$$11\ WO_4^{2-} + SiO_3^{2-} + 16\ H^+ + 8K^+ + 6\ H_2O \rightarrow K_8[\alpha\text{-}SiW_{11}O_{39}] \cdot 14\ H_2O$$

Na_2SiO_3 (sodium metasilicate, 1.51 g, 12.4 mmol) was dissolved with magnetic stirring at room temperature in 12 mL of distilled water (if the solution is not completely clear, it must be filtered – Solution A).

In a 250 mL beaker, containing a magnetic stirring bar, $Na_2WO_4{\cdot}2H_2O$ (sodium tungstate bihydrate, 45.48 g, 0.138 mol) was dissolved in 75 mL of boiling water (Solution B).

To the boiling Solution B, a solution of 4 M HCl (40 mL, 0.164 mol) was added dropwise in ~ 30 minutes, while vigorously stirring in order to dissolve the precipitate (tungstic acid). Solution A was then added, followed by quick addition of 12 mL of 4 M HCl (49.3 mmol). Measured pH was in the range 5-6. The solution was allowed to boil for 1 h. After cooling it down to room temperature, solution must be filtered (if not completely clear). KCl (37 g, 0.496 mol) was then added to the solution, while stirring. The white precipitate was collected on a fritted funnel (medium porosity), washed twice with 12 mL of 1 M KCl aqueous solution, then once with 12 mL of cold water and finally dried under vacuum.

Yield: 30.4 g, 82%.

FT-IR <1000 cm^{-1} (KBr, cm^{-1}): 996, 959, 893, 797, 731, 537, 514, 475.

6.3.2 Synthesis of $K_8[\beta_2\text{-}SiW_{11}O_{39}]$ [2]

$$11\ WO_4^{2-} + SiO_3^{2-} + 16\ H^+ + 8\ K^+ + 6\ H_2O \rightarrow K_8[\beta_2\text{-}SiW_{11}O_{39}] \cdot 14\ H_2O$$

Sodium metasilicate (1.50 g, 12.3 mmol) was dissolved in 25 mL of water (Solution A).

Sodium tungstate bihydrate (45.44 g, 0.138 mol) was dissolved in ~ 75 mL of water in a separate 250 mL beaker containing a magnetic stirrer bar. The latter solution was placed in an ice/water bath and cooled down to ~ 5°C. To this solution, 40 mL of 4.1 M HCl (0.16 mmol) were added

dropwise in ~ 30 minutes, under vigorous stirring, in order to dissolve tungstic acid that is locally formed.

Tungstate solution was then left to reach to room temperature and solution A was added to it. pH of the mixture was adjusted to 5.5, by addition of 4 M HCl (~ 10 mL). This pH value was kept for 100 minutes adding small amounts of 4 M HCl. Potassium chloride (22.1 g, 0.296 mol) was then added to the solution, while gently stirring. After 15 minutes, the white precipitate was collected by filtration through a sintered glass filter. Purification was achieved by dissolving the product in 210 mL of water. The insoluble material was quickly removed by filtration on a fine frit and the salt reprecipitated by addition of KCl (19.7 g, 0.264 mol). The precipitate (a white solid) was collected by filtration, washed with 2 M KCl aqueous solution (2 x 12 mL) and dried under vacuum.

Yield: 17.00 g, 45%.

FT-IR <1000 cm^{-1} (KBr, cm^{-1}): 993, 949, 878, 805, 731, 536, 517. **UV-vis** ($4 \cdot 10^{-5}$ M in H_2O): λ_1 = 298 nm, logε = 5.16, λ_2 = 283 nm, logε = 5.92.

6.3.3 Synthesis of $K_8[\gamma\text{-}SiW_{10}O_{36}]$ [3]

$$K_8[\beta_2\text{-}SiW_{11}O_{39}] + 2\ CO_3^{2-} + 13\ H_2O \rightarrow K_8[\gamma\text{-}SiW_{10}O_{36}] \cdot 12\ H_2O + 2\ HCO_3^- + WO_4^{2-}$$

The potassium salt of the β_2 isomer of undecatungstosilicate (9 g, 2.78 mmol), -recently synthesized as described above -, was dissolved in 140 mL of water at 25°C.

Impurities in the $K_8[\beta_2\text{-}SiW_{11}O_{39}]$ salt (mainly paratungstate) result as insoluble materials, which are quickly removed by filtration on a fine frit. pH of the solution was quickly adjusted to 9.1 by addition of a 2 M K_2CO_3 aqueous solution. This pH value was maintained by adding 2 M K_2CO_3 solution for 16 minutes. The potassium salt of the γ-decatungstosilicate was then precipitated by addition of KCl (24.42 g). During the precipitation (10 minutes), pH was kept at 9.1 by addition of small amounts of the K_2CO_3 solution. The solid was finally removed by filtration, washed with 1 M KCl aqueous solution and dried under vacuum.

Yield: 2.94 g, 25%.

FT-IR <1000 cm^{-1} (KBr, cm^{-1}): 987, 942, 905, 866, 820, 742, 656, 556, 530. **^{183}W-NMR** (16.67 MHz, D_2O) δ: -99.4 (4 W), -140.4 (4 W), -161.4 (2 W) ppm.

6.3.4 Synthesis of $Na_9[\alpha\text{-}AsW_9O_{33}]$ [4]

$$18\ WO_4^{2-} + As_2O_3 + 18\ H^+ \rightarrow\ 2\ [\alpha\text{-}AsW_9O_{33}]^{9-} + 9\ H_2O$$

$Na_2WO_4{\cdot}2H_2O$ (33.0 g, 100 mmol) was dissolved in water (35 mL) and the resulting mixture was warmed at 90°C. As_2O_3 (1.10 g, 5.56 mmol) was then added, together with 8.3 mL of 37% HCl (the latter added dropwise). The mixture was refluxed for 10 min, then filtered (yet warm) on a fine frit. The solution was allowed to cool slowly and left at 4°C overnight. The day after, precipitation of the product (as white solid) was observed. The complex is collected on a fine frit, washed with water (2 x 10 mL) and finally dried under vacuum.

Yield: 19.3 g (70%).

FT-IR < 1000 cm^{-1} (KBr, cm^{-1}): 932, 899, 873, 721, 509, 469.

6.3.5 Synthesis of $Na_9[\alpha\text{-}SbW_9O_{33}]$ [5]

$$18\ WO_4^{2-} + Sb_2O_3 + 18\ H^+ \rightarrow\ 2\ [\alpha\text{-}\textit{B}\text{-}SbW_9O_{33}]^{9-} + 9\ H_2O$$

$Na_2WO_4{\cdot}2H_2O$ (8.0 g, 24.2 mmol) was dissolved in water (15 mL) and the resulting mixture was warmed at 100°C. A solution of Sb_2O_3 (392 mg, 1.34 mmol) in 37% HCl (2 mL) was added dropwise. The mixture was refluxed for 1 h and allowed to cool slowly. Colourless crystals of the product were formed after evaporation of one-third of the solution volume, collected on a fine frit and washed with cold water.

Yield: 4.8 g (62%).

FT-IR < 1000 cm^{-1} (KBr, cm^{-1}): 920, 891, 770, 712.

6.3.6 Synthesis of (n-$Bu_4N)_4[\gamma$-$SiW_{10}O_{34}(H_2O)_2]$ [6]

$K_8[\gamma$-$SiW_{10}O_{36}]\cdot 12H_2O$ (0.6 g, 0.2 mmol) was dissolved in H_2O (6 mL) and the pH of this aqueous solution was adjusted carefully to 2 adding HNO_3.The solution was stirred for 15 min at room temperature, then an excess of n-Bu_4NBr (0.646 g, 2 mmol) was added in a single step. The resulting white precipitate of (n-$Bu_4N)_4[\gamma$-$SiW_{10}O_{34}(H_2O)_2]$ was collected by filtration and then washed with an excess of H_2O.The crude product was dried, then purified twice by precipitation (addition of water to a CH_3CN solution of the complex). Analytically pure (n-$Bu_4N)_4[\gamma$-$SiW_{10}O_{34}(H_2O)_2]$ was obtained as a white powder.

Yield: 3.4 g, 54%.

FT-IR <1000 cm^{-1} (KBr, cm^{-1}): 999, 958, 920, 902, 877, 784, 745, 691, 565, 544. **^{29}Si-NMR** (59.6 MHz, CD_3CN/DMSO-d_6 (2:1v/v), 25°C): δ = - 83.5 ppm. **^{183}W-NMR** (16.67 MHz, DMSO/DMSO-d_6, 25°C) δ -94.7 (2W), -98.1 (2W), -115.6 (2W), -118.1 (2W), -193.8 (2W) ppm.

6.3.7 Synthesis of (n-$Bu_4N)_3K[\gamma$-$SiW_{10}O_{36}(PhPO)_2]$ [7]

$K_8[\gamma$-$SiW_{10}O_{36}]\cdot 12H_2O$ (0.12 g, 0.4 mmol) was suspended in an acetonitrile solution (20 mL) of n-Bu_4NBr (0.39 g, 0.12 mmol) and $PhPO(OH)_2$ (0.126 g, 0.8 mmol). A 12 M hydrochloric acid solution (133 µL) was poured dropwise under vigorous stirring and the mixture was stirred overnight at reflux. After separation of the white residue (KBr + a small amount of unreacted $[\gamma$-$SiW_{10}O_{36}]^{8-}$), the white compound (n-$Bu_4N)_3K[\gamma$-$SiW_{10}O_{36}(PhPO)_2]$ was obtained by evaporation of the resulting solution under reduced pressure. The crude compound was washed with distilled water and recrystallized from acetonitrile.

Yield: 0.92 g, 66.5%.

FT-IR <1200 cm^{-1} (KBr, cm^{-1}): 1196, 1137, 1049, 1008, 970, 943, 911, 884, 834, 796, 785, 752, 699. **^{31}P{^{1}H}-NMR** (121.5 MHz, CD_3CN, 25°C) δ 14.9 ppm. **^{31}P{^{1}H}-NMR** (121.5 MHz, [bmim][$(CF_3SO_2)_2N$], 25°C) δ 15.7 ppm. **^{183}W-NMR** (16.67 MHz, CH_3CN/ CD_3CN) δ -106.6 (2 W), -114.4 (4 W), -154.9 (4 W, d, J = 10.9 Hz) ppm. **^{1}H-NMR** (300 MHz, CD_3CN, 25°C) δ 7.95-7.88 (m, 4 H), 7.55-7.49 (m, 6 H), 3.11 (m, 24 H), 1.61 (m, 24 H), 1.37 (m, 24 H), 0.97 (t, J = 7.3 Hz, 36 H) ppm. **UV-vis** ([bmim][$(CF_3SO_2)_2N$]) λ = 244 nm, logε = 4.56. **ESI-MS(-)** (CH_3CN/H_2O) m/z 896.9, $[HSiW_{10}O_{36}(PhPO)_2]^{3-}$.

6.4 H_2O_2-based epoxidations catalyzed by $[\gamma\text{-}SiW_{10}O_{36}(PhPO)_2]^{4-}$ in Ionic Liquids

6.4.1 Synthesis and characterization of ILs

The synthesis of ILs was performed in a two step procedure by quaternization of 1-methylimidazole with 1-bromobutane, followed by anion metathesis in presence of a suitable metal salt (namely $NaBF_4$, $Li[(CF_3SO_2)_2N]$, $Li(CF_3SO_3)$ and KPF_6).[8] The resulting ILs were characterized by ^{1}H-NMR, $^{13}C\{^1H\}$-NMR and FT-IR (see following paragraphs) and their identity was confirmed by comparison with literature data.[9]

6.4.1.1 Spectral data of [bmim][BF_4]

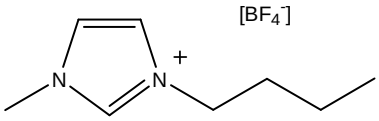

^{1}H-NMR (400 MHz, D_2O, 25°C): δ 8.67 (s, 1 H), 7.46 (s, 1 H), 7.42 (s, 1 H), 4.18 (t, *J* = 7.1 Hz, 2 H), 3.88 (s, 3 H), 1.88-1.79 (m, *J* = 7.1 Hz, 2 H), 1.30 (sextet, *J* = 7.3 Hz, 2 H), 0.90 (t, *J* = 6.9 Hz, 3 H) ppm. **$^{13}C\{^1H\}$-NMR** (400 MHz, D_2O, 25°C): δ 135.8, 123.5, 122.2, 49.3, 35.7, 31.3, 18.8, 12.7 ppm. **FT-IR** (NaCl, cm^{-1}): 3163, 3121, 2965, 2939, 2878, 1576, 1469, 1172, 1054, 850, 755.

6.4.1.2 Spectral data of [bmim][$(CF_3SO_2)_2N$]

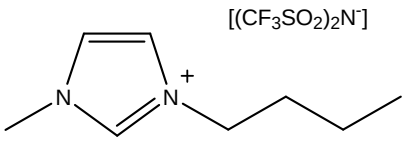

^{1}H-NMR (300 MHz, Acetone-d_6, 25°C): δ 8.89 (s, 1 H), 7.68 (t, *J* = 1.7 Hz, 1 H), 7.62 (t, *J* = 1.7 Hz, 1 H), 4.31 (t, *J* = 7.3 Hz, 2 H), 4.02 (s, 3 H), 1.97-1.87 (m, *J* = 7.4 Hz, 2 H), 1.39 (sextet, *J* = 7.7 Hz, 2 H), 0.95 (t, *J* = 7.4 Hz, 3 H) ppm. **$^{13}C\{^1H\}$-NMR** (400 MHz, Acetone-d_6, 25°C): δ 136.9, 124.3, 123.0, 49.9, 36.2, 32.3, 19.5, 13.2 ppm. **FT-IR** (NaCl, cm^{-1}): 3160, 3121, 2967, 2941, 2881, 1576, 1351, 1191, 844.

6.4.1.3 Spectral data of [bmim][CF_3SO_3]

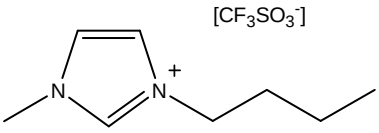

^{1}H-NMR (300 MHz, Acetone-d_6, 25°C): δ 9.12 (s, 1 H), 7.79 (t, *J* = 1.6 Hz, 1 H), 7.71 (t, *J* = 1.6 Hz, 1 H), 4.33 (t, *J* = 7.3 Hz, 2 H), 4.03 (s, 3 H), 1.96-1.86 (m, *J* = 7.4 Hz, 2 H), 1.36 (sextet, *J* = 7.7 Hz, 2 H), 0.93 (t, *J* = 7.4 Hz, 3 H) ppm. **^{13}C{^{1}H}-NMR** (400 MHz, Acetone-d_6, 25°C): δ 137.3, 124.2, 123.0, 49.7, 36.2, 32.4, 19.6, 13.3 ppm. **FT-IR** (NaCl, cm^{-1}): 3155, 3115, 2966, 2941, 2879, 1575, 1262, 1164, 851.

6.4.1.4 Spectral data of [bmim][PF_6]

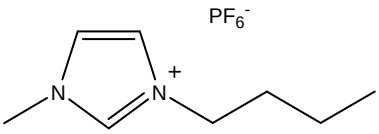

^{1}H-NMR (300 MHz, Acetone-d_6, 25°C): δ 8.79 (s, 1 H), 7.65 (t, *J* = 1.7 Hz, 1 H), 7.59 (t, *J* = 1.7 Hz, 1 H), 4.29 (t, *J* = 7.3 Hz, 2 H), 3.99 (s, 3 H), 1.95-1.85 (m, *J* = 7.5 Hz, 2 H), 1.37 (sextet, *J* = 7.7 Hz, 2 H), 0.93 (t, *J* = 7.3 Hz, 3 H) ppm. **^{13}C{^{1}H}-NMR** (400 MHz, Acetone-d_6, 25°C): δ 136.9, 124.3, 122.9, 49.8, 36.2, 32.3, 19.5, 13.3 ppm. **FT-IR** (NaCl, cm^{-1}): 3171, 3124, 2967, 2940, 2879, 1576, 1468, 836.

6.4.2 General procedures for catalytic epoxidations in Ionic Liquids

6.4.2.1 Epoxidation of *cis*-cyclooctene with H_2O_2 catalyzed by $[\gamma\text{-}SiW_{10}O_{36}(PhPO)_2]^{4-}$ in ILs under conventional and MW-assisted heating

The catalyst (4.8 μmol) was dissolved in the IL phase (200 μL) upon sonication. *Cis*-cyclooctene (3.0 mmol) was added and the biphasic system was placed in an oil bath at 50°C. H_2O_2 (0.60 mmol, 7-24 M aqueous solution) was added under vigorous stirring. The reaction was sampled by quantitative GLC analysis after dilution in CH_2Cl_2 containing dodecane, as internal standard, and Ph_3P as quencher. The catalytic phase was extracted with hexane (5 x 0.5 mL), washed with H_2O (0.5 mL), dried under vacuum over P_2O_5 at 70 °C for 4 h, and then recycled in three more consecutive runs with no loss of catalytic activity. Microwave experiments were performed with continuous irradiation power at 10 watt, under simultaneous cooling with compressed air (60 psi), keeping T_{bulk} < 80 °C.

6.4.2.2 Epoxidation of *cis*-cyclooctene with H_2O_2 catalyzed by $[\gamma\text{-}SiW_{10}O_{36}(PhPO)_2]^{4-}$ in [bmim][$(CF_3SO_2)_2N$] in a microflow apparatus

Epoxidation of *cis*-cyclooctene with H_2O_2 catalyzed by $[\gamma\text{-}SiW_{10}O_{36}(PhPO)_2]^{4-}$ was performed under flow conditions in a PTFE (polytetrafluoroethylene) microchannel tube (internal diameter I.D. = 300 μm, length = 400 mm), placed in a thermostated (T = 50°C) reactor containing water. Two syringes were connected to two different syringe-pumps, providing an experimentally determined flow of 0.017 mL/min. The first syringe was filled with the catalytic phase (4.8 μmol of $[\gamma\text{-}SiW_{10}O_{36}(PhPO)_2]^{4-}$dissolved in 200 μl of [bmim][$(CF_3SO_2)_2N$]) and 0.6 mmol of H_2O_2 (24 M aqueous solution). The second syringe was filled with *cis*-cyclooctene (3.0 mmol) and dodecane (0.6 mmol) as internal standard. The two phases were forced in the two different microtubes connected with the syringes, until they come into laminar contact in the actual reaction microchannel. The exiting mixture is finally collected in a vial placed at the end of the tube, diluted with CH_2Cl_2 and analyzed *via* GLC.

6.4.2.3 H_2O_2-based epoxidation of olefins with catalyzed by $[\gamma\text{-}SiW_{10}O_{36}(PhPO)_2]^{4-}$ in $[bmim][(CF_3SO_2)_2N]$ under conventional and MW-assisted heating

Conventional heating: The catalyst (0.32 μmol) was dissolved under sonication in the IL (200 μL). Alkene (0.2 mmol) and H_2O_2 (40 μmol, 24 M aqueous solution) were added and the mixture was stirred vigorously in an oil bath at 50 °C. At the end of the reaction the mixture was diluted in CH_2Cl_2 containing dodecane as internal standard and monitored by quantitative GLC analysis.

MW-irradiation: The catalyst (3.2 μmol) was dissolved under sonication in the IL (200 μL). Alkene (2.0 mmol) and H_2O_2 (40 μmol, 24 M aqueous solution) were added. The reaction vessel was placed in the single-mode cavity of the instrument and irradiated with W = 4-5 watt, under simultaneous cooling by a stream of compressed air (pressure = 60 psi) and stirring (measured T_{bulk} in the range 57-65°C). At the end of the reaction, the mixture was diluted in CH_2Cl_2 containing dodecane as internal standard and monitored by quantitative GLC analysis.

6.5 Friedel-Crafts acylation of ferrocene in Ionic Liquids

6.5.1 General procedures for Friedel-Crafts acylations

Conventional heating: In a typical experiment, FcH (1 mmol) was weighed in a 10 mL round-bottomed flask and dissolved with known amounts of solvent (either molecular or ionic) and acylating agent. The resulting mixture was heated in a thermostated oil bath and, finally, the weighed amount of catalyst was introduced. The reaction was monitored by TLC. In the work-up, different procedures were followed. For reactions performed in molecular solvents, the solvent was removed under vacuum and the residue separated and purified by column chromatography. For reactions performed in ILs, solvent extraction or distillation was used. Alternatively, the reaction mixture was directly chromatographed on a silica gel column.

Extraction: the reaction mixture was repetitively extracted with Et_2O until colourless organic phase and acylferrocenes were purified by column chromatography (eluent: hexane/Et_2O 99:1 v/v).

Distillation: the reaction flask was introduced into a Kugelrohr distillation apparatus and distilled under reduced pressure. When volatile acids were formed as by-products, pure acylferrocenes were obtained. With less volatile acids, an extraction with aqueous $NaHCO_3$ or a column chromatography are needed to yield pure acylferrocenes.

Purity and identity of products was checked by GC-MS and ^{1}H-NMR analyses and by comparison with authentic samples.

MW-irradiation: In a typical experiment, FcH (1 mmol) was weighed in a vessel, added with known amounts of solvent, the acylating reagent and, finally, the weighed amount of catalyst (0.05 mmol). The reaction vessel was then placed in the single-mode cavity of the instrument and irradiated for the required time with power at 5 watt (when using [bmim][$(CF_3SO_2)_2N$] as solvent) or 40 watt (in the case of acetonitrile) under simultaneous stirring and cooling by a stream of compressed air (30-50 psi). The reaction was sampled by quantitative GLC analysis after dilution in CH_2Cl_2 containing dodecane as external standard. At the end of the reaction, the mixture was chromatographed on a silica gel column.

6.6 Polyoxometalate-based *N*-heterocyclic carbenes as ligands for palladium

6.6.1 Synthesis of 1-octyl-3-(3-triethoxysilylpropyl)-4,5-dihydroimidazolium bromide (1) [10]

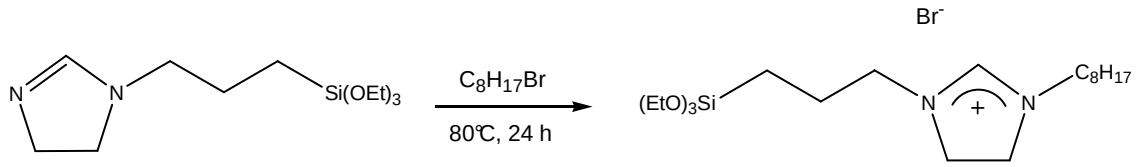

1

A mixture of 3-(2-imidazolin-1-yl)propyltriethoxysilane (0.5 mL, 1.8 mmol) and 1-bromooctane (1 mL, 5.8 mmol) was stirred and heated at 80°C for 24 h in a Schlenk tube, under a nitrogen atmosphere. After the reaction, the mixture was cooled to room temperature and the volatile compounds were removed by the evaporation under reduced pressure. The orange viscous liquid was washed with anhydrous pentane (2 x 3 mL) and evaporated to dryness. The product was redissolved in anhydrous dichloromethane (ca. 5 mL) and filtered with activated carbon. The product, 1-octyl-3-(3-triethoxysilylpropyl)-4,5-dihydroimidazolium bromide (**1**), was dried under vacuum to give a sticky yellow solid.

Yield: 0.82 g (98%).

^{29}Si-NMR (59.6 MHz, $CDCl_3$, 25°C): δ −47.4 ppm. **^{13}C{^{1}H}-NMR** (75.5 MHz, $CDCl_3$, 25°C): δ 158.4 (N<u>C</u>HN), 58.6 (O<u>C</u>H$_2$), 53.5 ($CH_3(CH_2)_6$<u>C</u>H$_2$N), 50.5 (SiCH$_2$CH$_2$<u>C</u>H$_2$N), 48.5 (SiCH$_2$CH$_2$CH$_2$N<u>C</u>H$_2$CH$_2$N), 48.2 (SiCH$_2$CH$_2$CH$_2$NCH$_2$<u>C</u>H$_2$N), 31.7, 29.1, 29.0, 27.5, 26.4, 22.6, 21.2 (methylene groups), 18.3 (OCH$_2$<u>C</u>H$_3$), 14.0 (methyl), 7.2 (SiCH$_2$) ppm. **^{1}H-NMR** (300 MHz, $CDCl_3$, 25°C): δ 9.54 (1H, s, NC<u>H</u>N), 3.95-3.88 (4H, m, C<u>H</u>$_2$ dihydroimidazole), 3.77 (6H, q, *J* = 7.14 Hz, CH$_3$C<u>H</u>$_2$O), 3.65−3.54 (4H, m, SiCH$_2$CH$_2$C<u>H</u>$_2$N, NC<u>H</u>$_2$(CH$_2$)$_6$CH$_3$), 1.76-1.58 (4H, m, SiCH$_2$C<u>H</u>$_2$CH$_2$N, NCH$_2$C<u>H</u>$_2$(CH$_2$)$_5$CH$_3$), 1.27-1.13 (19H, m, methylene, C<u>H</u>$_3$CH$_2$O), 0.83 (3H, t, *J* = 6.98 Hz, C<u>H</u>$_3$(CH$_2$)$_6$CH$_2$N), 0.61−0.52 (2H, m, SiC<u>H</u>$_2$CH$_2$) ppm. **ESI-MS(+)** (CH_3CN): *m/z* 387.3, calcd. for $[C_{20}H_{43}N_2O_3Si]^+$ = 387.3.

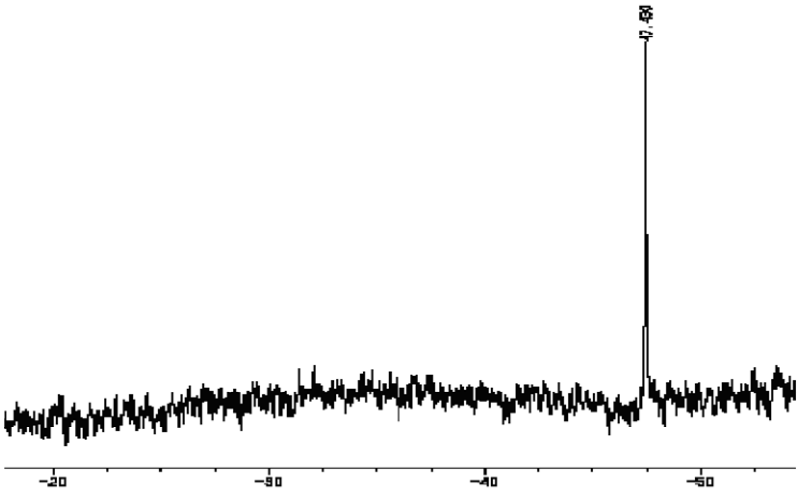

Figure 6.1. ^{29}Si-NMR spectrum of compound **1**.

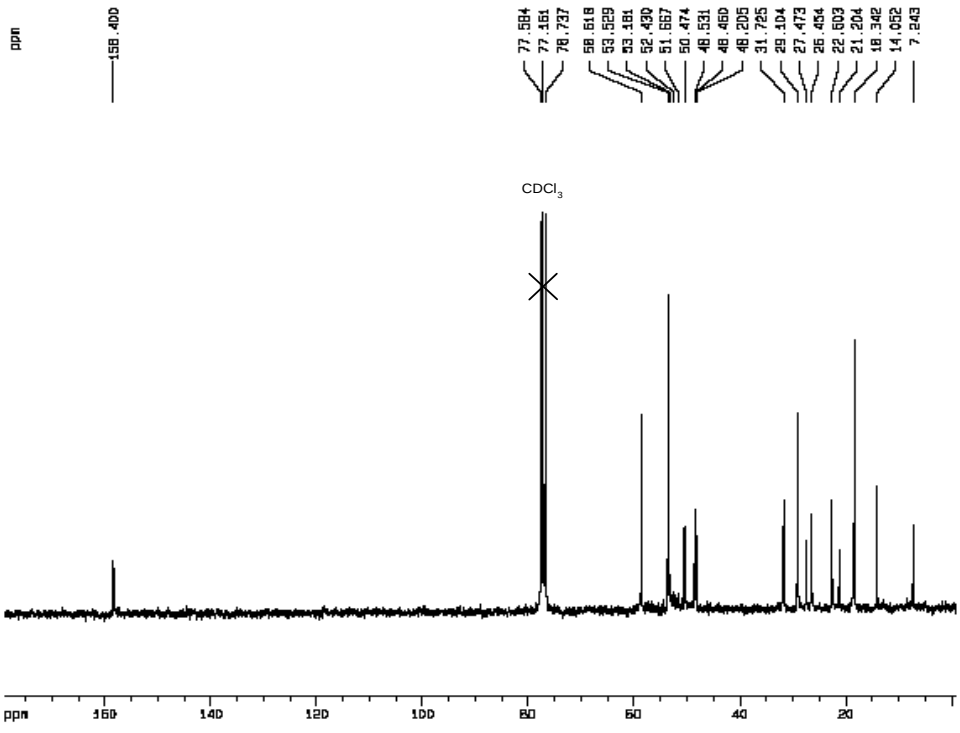

Figure 6.2. ^{13}C{^{1}H}-NMR spectrum of compound **1**.

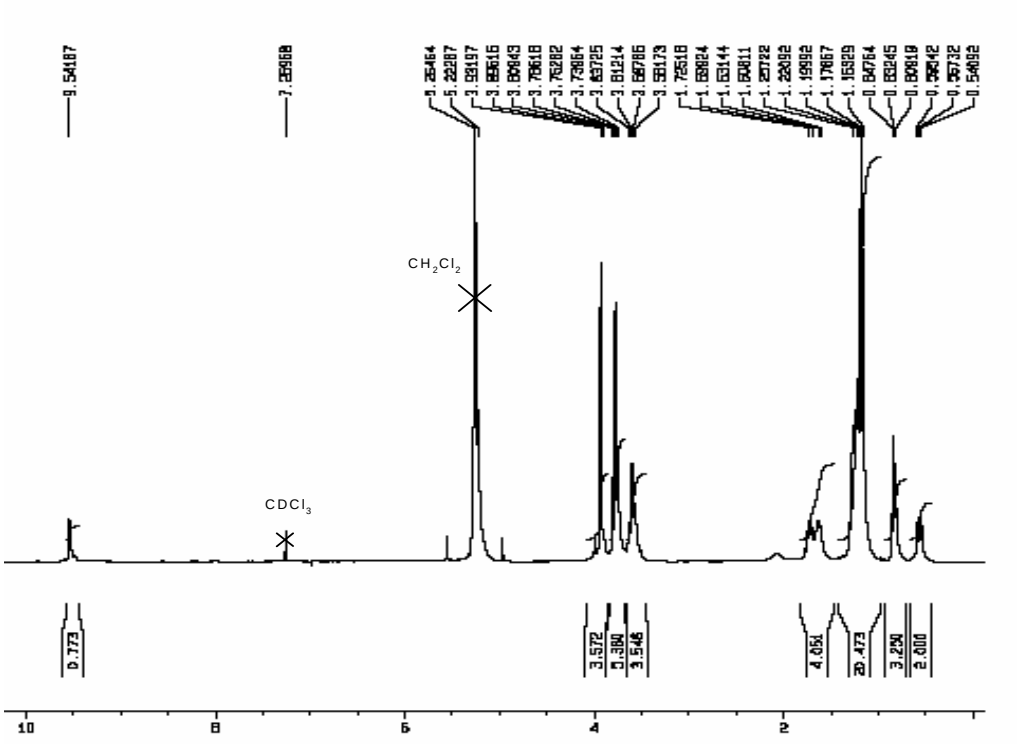

Figure 6.3. ^{1}H-NMR spectrum of compound **1**.

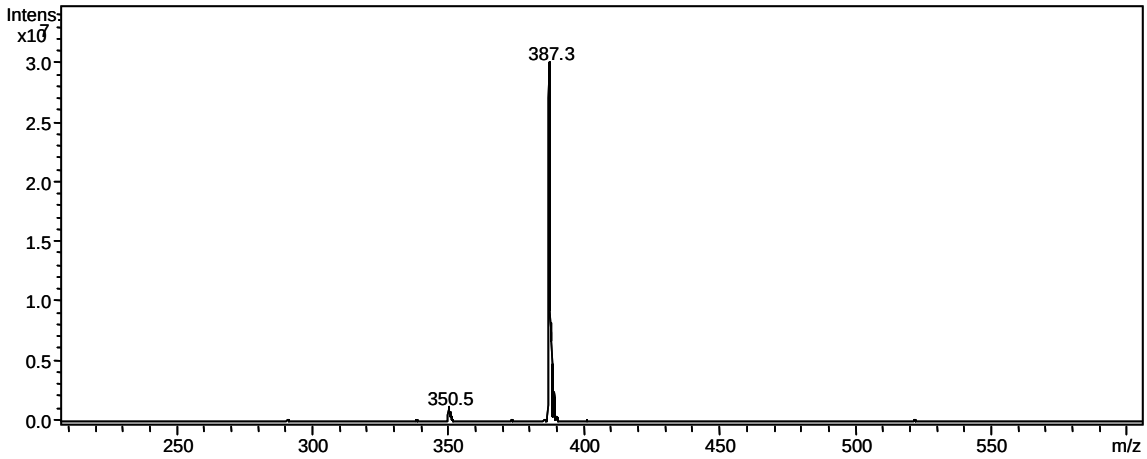

Figure 6.4. ESI-MS(+) spectrum of compound **1**.

6.6.2 Synthesis of $(n\text{-}Bu_4N)_2K_2[Br_2(C_{14}H_{28}N_2Si)_2O(\gamma\text{-}SiW_{10}O_{36})]$ (2) [11]

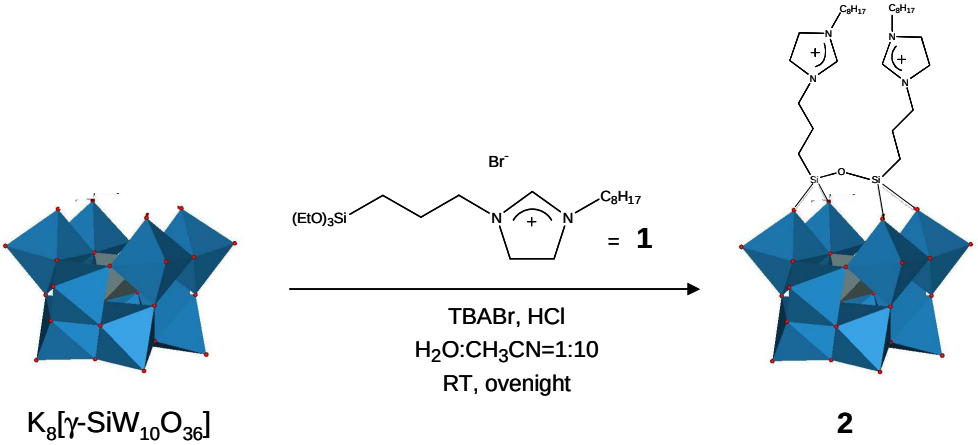

$K_8[\gamma\text{-}SiW_{10}O_{36}]$ (1.2 g, 0.44 mmol) was suspended in H_2O (2 mL). (n-Bu_4N)Br (0.57 g, 1.8 mmol, 4 eq) and CH_3CN (15 mL) were added and the mixture was stirred at room temperature for 20 minutes. 1-octyl-3-(3-triethoxysilylpropyl)-4,5-dihydroimidazolium bromide **1** (0.41 g, 0.88 mmol, 2 eq), dissolved in 5 mL of anhydrous CH_3CN, and HCl 4 M (2.6 mmol, 6 eq) were successively added under vigorous stirring. The mixture was stirred overnight at room temperature. The product was obtained after filtration of the insoluble portion and evaporation of the organic solvent. The crude compound was thoroughly washed with water.

Yield: 0.501 g (31 %).

FT-IR (KBr, cm^{-1}) 3067, 2960, 2931, 2872, 1653, 1483, 1465, 1380, 1304, 1250, 1173, 1154, 1103, 1043, 1004, 965, 903, 886, 818, 781, 734, 668, 545, 511, 482. **^{29}Si-NMR** (79.5 MHz, CD_3CN, 25°C) δ −62.1 (2 Si), -88.0 (1 Si) ppm. **^{183}W-NMR** (16.7 MHz, CD_3CN, 25°C) δ −107.0 (4 W), -134.2 (2 W), -141.6 (4 W) ppm. **^{13}C{^{1}H}-NMR** (75.5 MHz, CD_3CN, 25°C) δ 158.3 (NCHN), 59.3 ($(CH_3CH_2CH_2CH_2)_4N^+$), 58.2 ($CH_3(CH_2)_6CH_2N$), 50.9 ($SiCH_2CH_2CH_2N$), 49.5 ($SiCH_2CH_2CH_2NCH_2CH_2N$), 49.0 ($SiCH_2CH_2CH_2NCH_2CH_2N$), 32.6, 29.9, 28.0, 27.1, 23.4, 22.5, 14.5 (methylene groups), 24.4 ($(CH_3CH_2CH_2CH_2)_4N^+$), 20.4 ($(CH_3CH_2CH_2CH_2)_4N^+$), 14.1 ($(CH_3CH_2CH_2CH_2)_4N^+$), 12.4 ($SiCH_2$) ppm. **^{1}H-NMR** (300 MHz, CD_3CN, 25°C) δ 8.14 (2H, s, NCHN), 4.22-3.87 (8 H, m, $SiCH_2CH_2CH_2NCH_2CH_2N$, $SiCH_2CH_2CH_2NCH_2CH_2N$), 3.76-3.57 (4H, m, $SiCH_2CH_2CH_2N$), 3.56-3.38 (4H, m, $CH_3(CH_2)_6CH_2N$), 3.23-3.15 (16H, m, $(CH_3CH_2CH_2CH_2)_4N^+$), 1.81-1.54 (16H, m, $(CH_3CH_2CH_2CH_2)_4N^+$), 1.38 (16H, sextet, J = 7.1 Hz, $(CH_3CH_2CH_2CH_2)_4N^+$), 1.34-1.17 (28H, m, methylene), 0.98 (24H, t, J = 7.1 Hz,

($C\underline{H}_3CH_2CH_2CH_2)_4N^+$), 0.91-0.85 (6 H, m, $C\underline{H}_3$), 0.71-0.39 (4 H, m, $SiC\underline{H}_2$) ppm. **ESI-MS(-)** (CH_3CN) *m/z* = 1482, calcd. for $\{[(C_{14}H_{28}N_2Si)_2O(\gamma\text{-}SiW_{10}O_{36})]\}^{2-}$ = 1481. **Elemental Analysis** calcd (%) for $C_{60}H_{128}Br_2K_2N_6O_{37}Si_3W_{10}$: C 19.55, H 3.50, N 2.28; found: C 19.43, H 3.42, N 2.07.

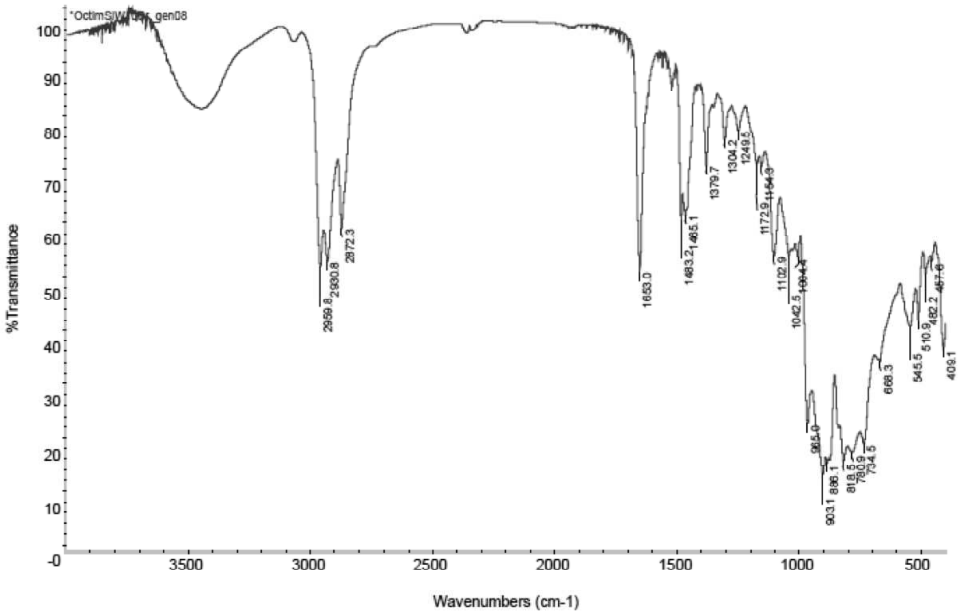

Figure 6.5. FT-IR spectrum of compound **2**.

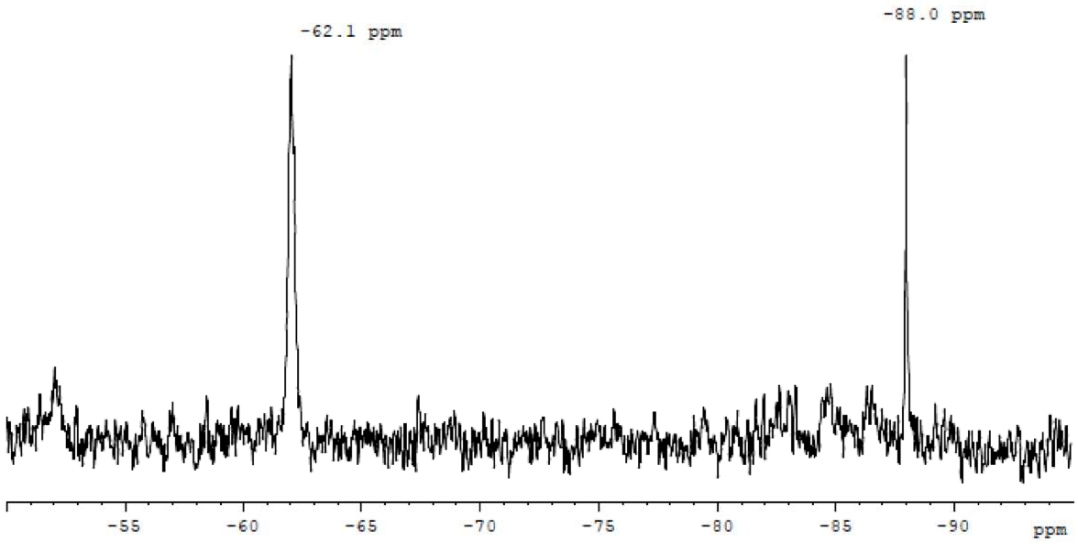

Figure 6.6. ^{29}Si-NMR spectrum of compound **2**.

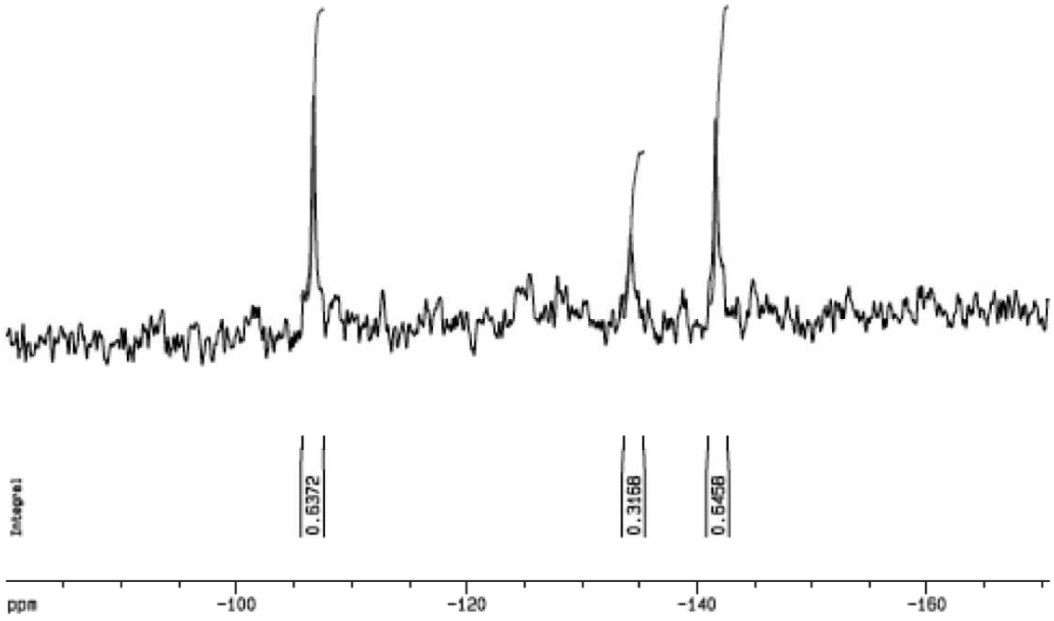

Figure 6.7. ^{183}W-NMR spectrum of compound **2**.

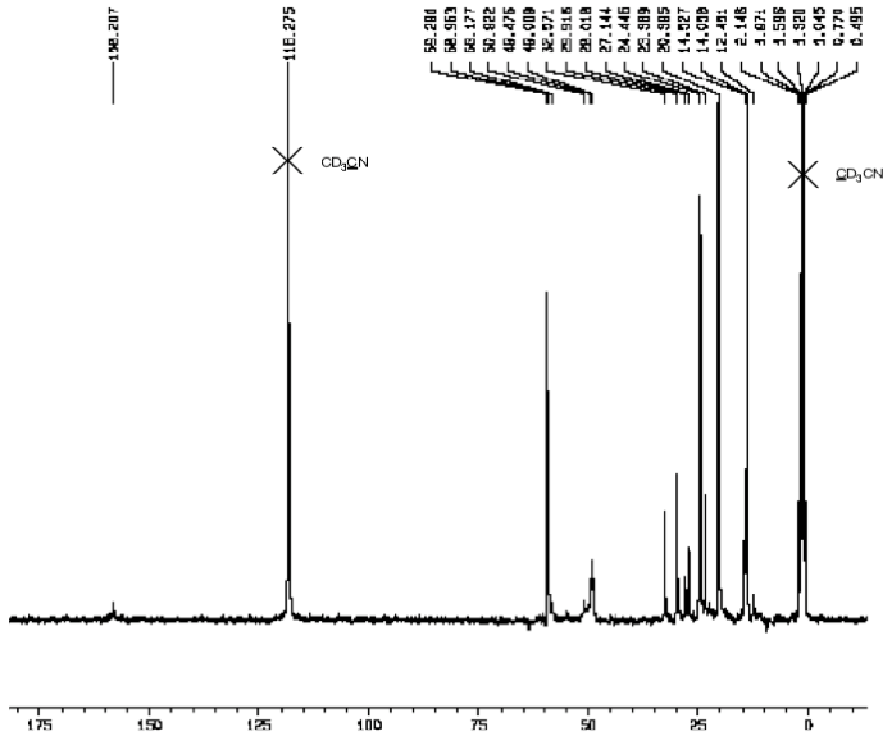

Figure 6.8. $^{13}C\{^{1}H\}$-NMR spectrum of compound **2**.

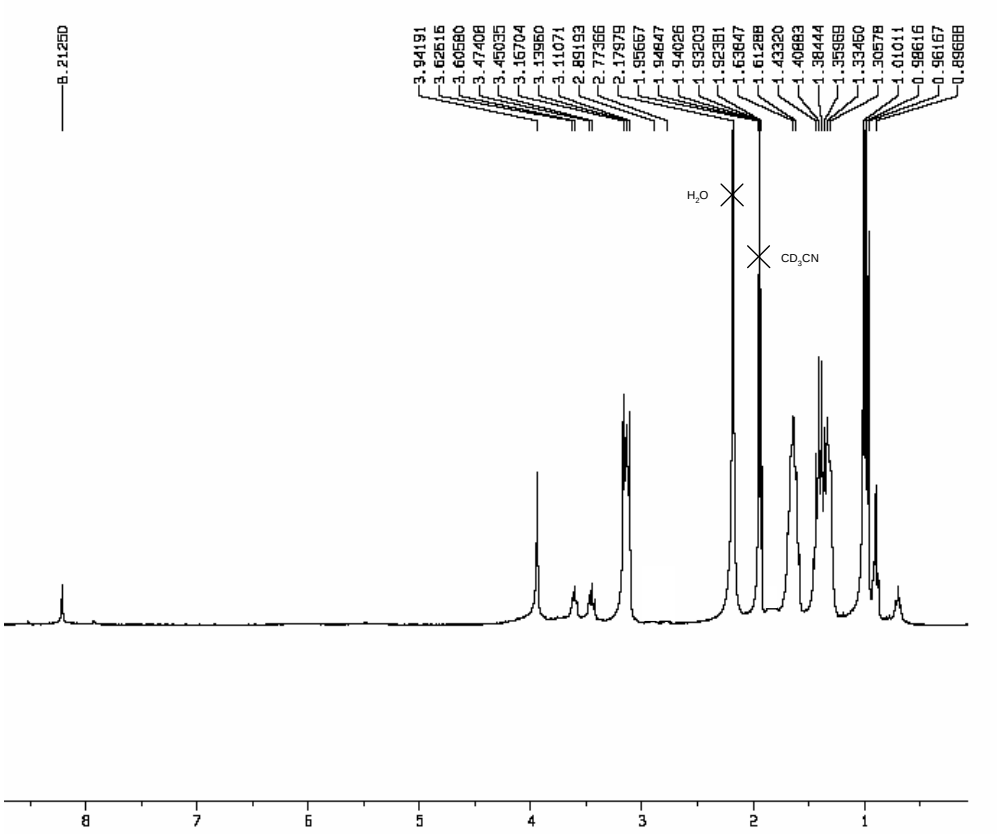

Figure 6.9. ^{1}H-NMR spectrum of compound **2**.

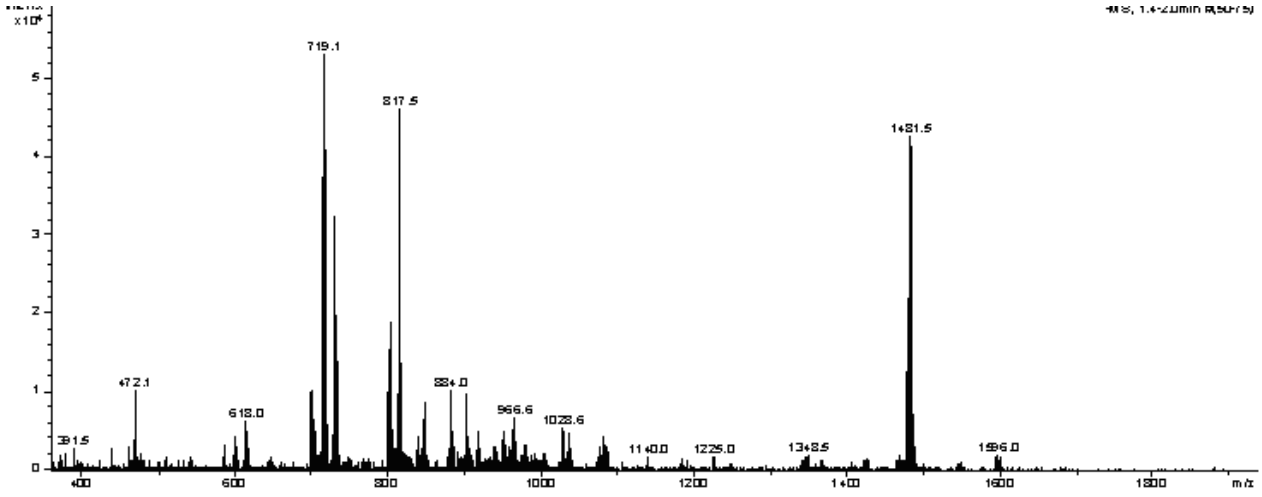

Figure 6.10. ESI-MS(-) spectrum of compound **2**.

6.6.3 Synthesis of $(n\text{-}Bu_4N)_2H_2[Br_2(C_{14}H_{28}N_2Si)_2O(\alpha\text{-}SiW_{11}O_{39})]$ (3) [11]

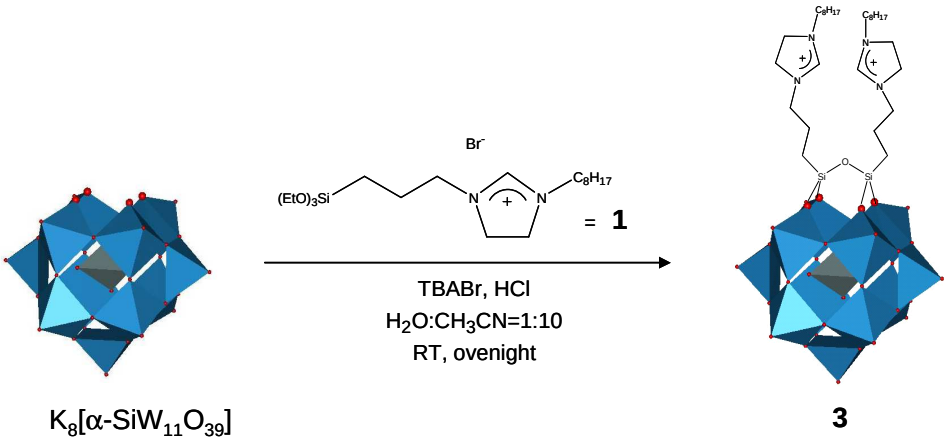

The synthesis follows the same procedure as for the compound **2**, using $K_8[\alpha\text{-}SiW_{11}O_{39}]$ (1.33 g, 0.44 mmol) instead of $K_8[\gamma\text{-}SiW_{10}O_{36}]$.

Yield: 0.774 g (41%).

FT-IR (KBr, cm^{-1}) 3066, 2960, 2930, 2872, 1653, 1522, 1483, 1466, 1380, 1304, 1250, 1175, 1155, 1045, 966, 949, 905, 854, 802, 755, 533, 481. **^{29}Si-NMR** (79.5 MHz, CD_3CN, 25°C) δ −52.0 (2 Si), -84.5 (1 Si) ppm. **^{183}W-NMR** (16.7 MHz, CD_3CN, 25°C) δ −107.1 (2 W), −108.0 (2 W), -112.7 (1 W), - 124.8 (2 W), -174.2 (2 W), -248.5 (2 W) ppm. **^{13}C{^{1}H}-NMR** (75.5 MHz, CD_3CN, 25°C) δ 158.1 (N$\underline{C}$HN), 59.3 ($(CH_3CH_2CH_2\underline{C}H_2)_4N^+$), 58.1 ($CH_3(CH_2)_6\underline{C}H_2N$), 50.2 ($SiCH_2CH_2\underline{C}H_2N$), 49.4 ($SiCH_2CH_2CH_2N\underline{C}H_2CH_2N$), 49.0 ($SiCH_2CH_2CH_2NCH_2\underline{C}H_2N$), 32.5, 29.9, 29.8, 27.9, 27.1, 23.4, 14.5 (methylene), 24.5 ($(CH_3CH_2\underline{C}H_2CH_2)_4N^+$), 20.4 ($(CH_3\underline{C}H_2CH_2CH_2)_4N^+$), 14.0 ($(\underline{C}H_3CH_2CH_2CH_2)_4N^+$), 9.7 ($Si\underline{C}H_2$) ppm. **^{1}H-NMR** (300 MHz, CD_3CN, 25°C) δ 8.17 (2 H, s, NC$\underline{H}$N), 4.15-3.87 (8 H, m, $SiCH_2CH_2CH_2NCH_2C\underline{H}_2N$, $SiCH_2CH_2CH_2NC\underline{H}_2CH_2N$), 3.84-3.62 (4 H, m, $SiCH_2CH_2C\underline{H}_2N$), 3.53-3.35 (4 H, m, $CH_3(CH_2)_6C\underline{H}_2N$), 3.23-3.15 (16 H, m, $(CH_3CH_2CH_2C\underline{H}_2)_4N^+$), 1.68-1.59 (16 H, m, $(CH_3CH_2C\underline{H}_2CH_2)_4N^+$), 1.43 (16 H, sextet, J = 7.0 Hz, $(CH_3C\underline{H}_2CH_2CH_2)_4N^+$), 1.31-1.27 (28 H, m, methylene), 0.99 (24 H, t, J = 7.0 Hz, $(C\underline{H}_3CH_2CH_2CH_2)_4N^+$), 0.88-0.82 (6 H, m, $C\underline{H}_3$), 0.80-0.62 (4 H, m, $SiC\underline{H}_2$) ppm. **ESI-MS(-)** (CH_3CN) *m/z* = 1597, calcd. for $[(C_{14}H_{28}N_2Si)_2O(\alpha\text{-}SiW_{11}O_{39})]^{2-}$ = 1597. **Elemental Analysis** calcd. (%) for $C_{60}H_{130}Br_2N_6O_{40}Si_3W_{11}$: C 18.76, H 3.41, N 2.19; found: C 19.72, H 3.50, N 2.09.

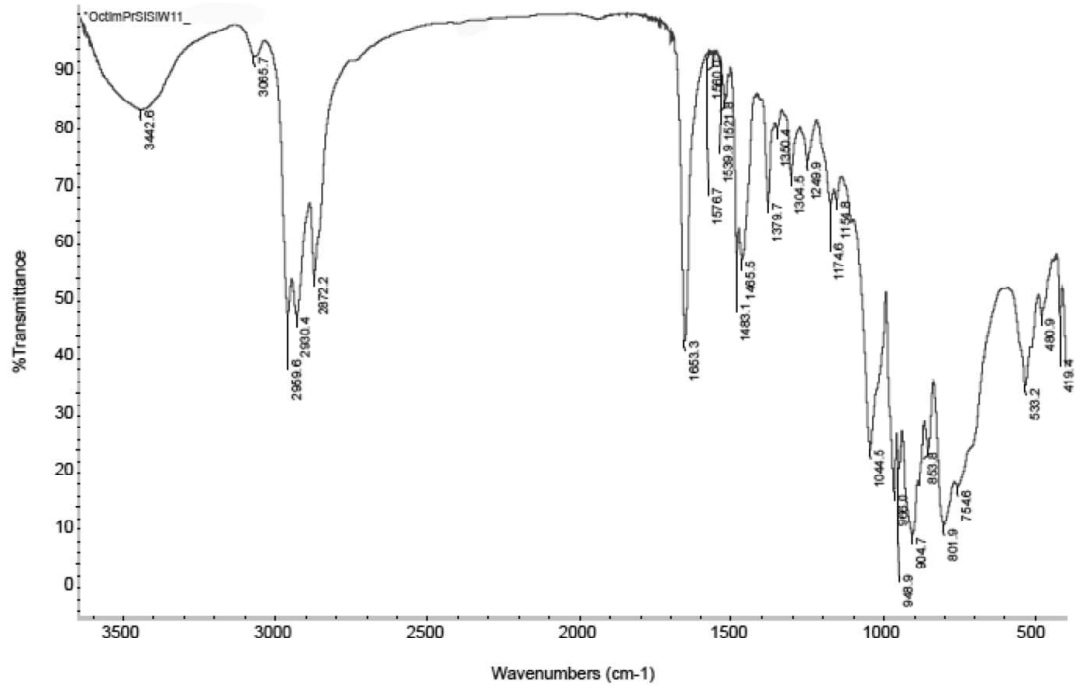

Figure 6.11. FT-IR spectrum of compound **3**.

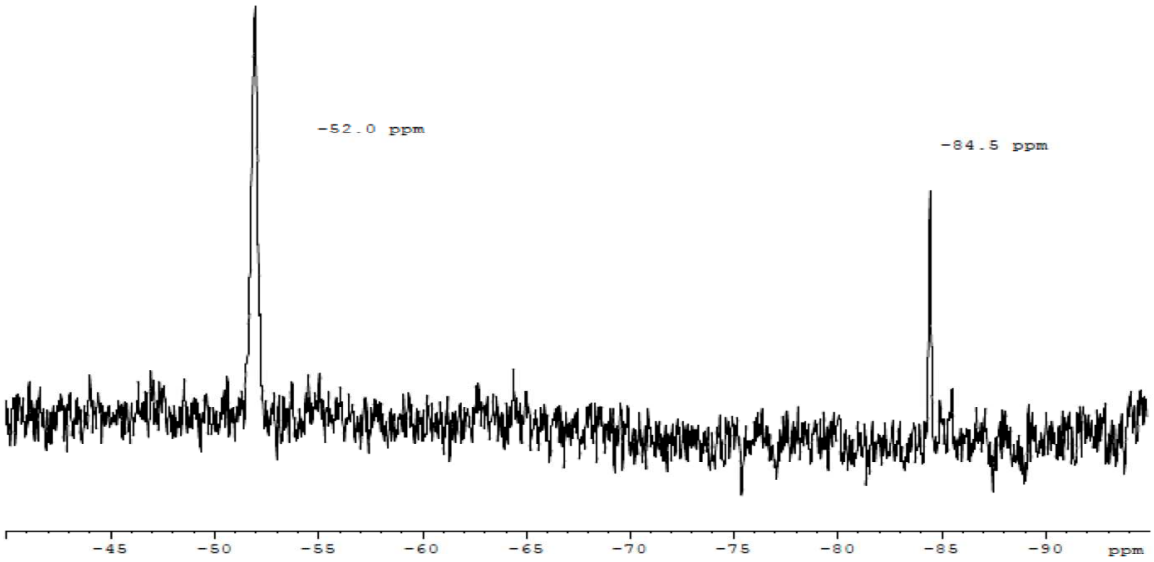

Figure 6.12. ^{29}Si-NMR spectrum of compound **3**.

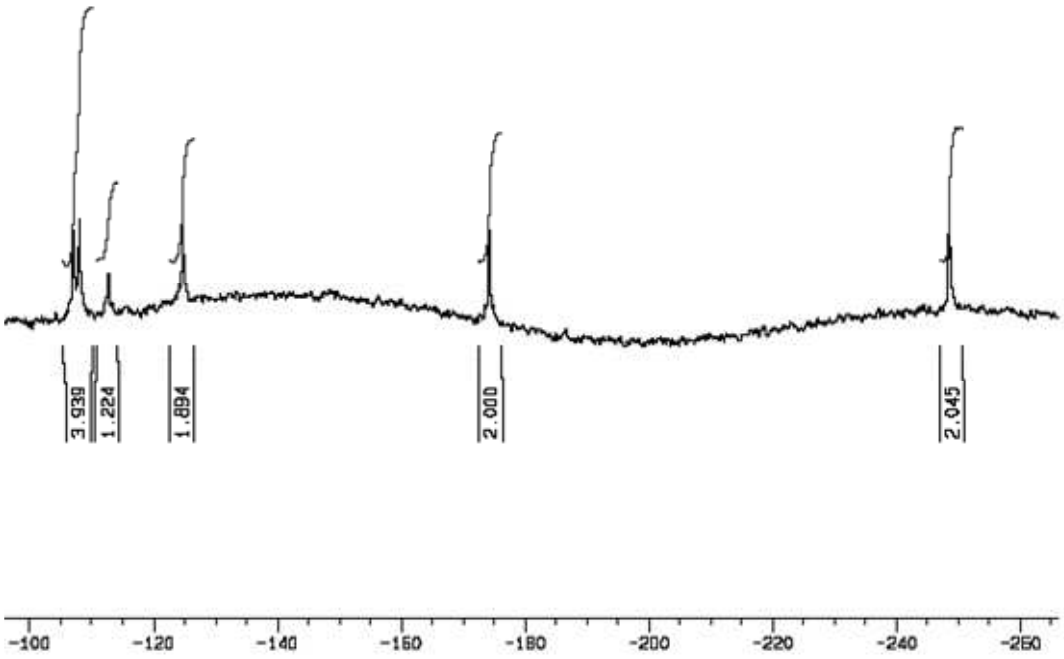

Figure 6.13. ^{183}W-NMR spectrum of compound **3**.

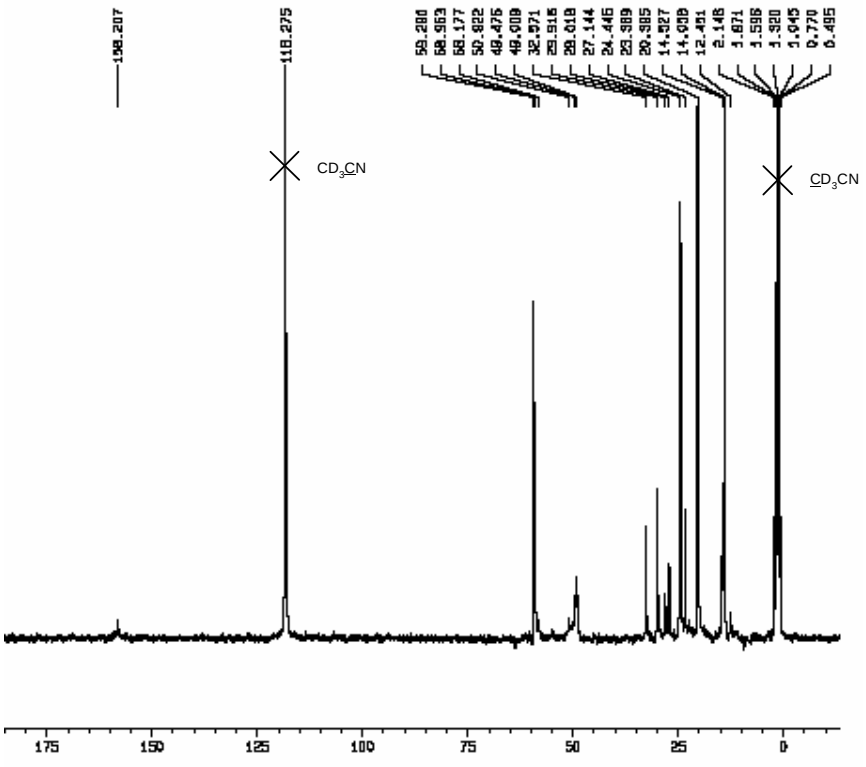

Figure 6.14. ^{13}C{^{1}H}-NMR spectrum of compound **3**.

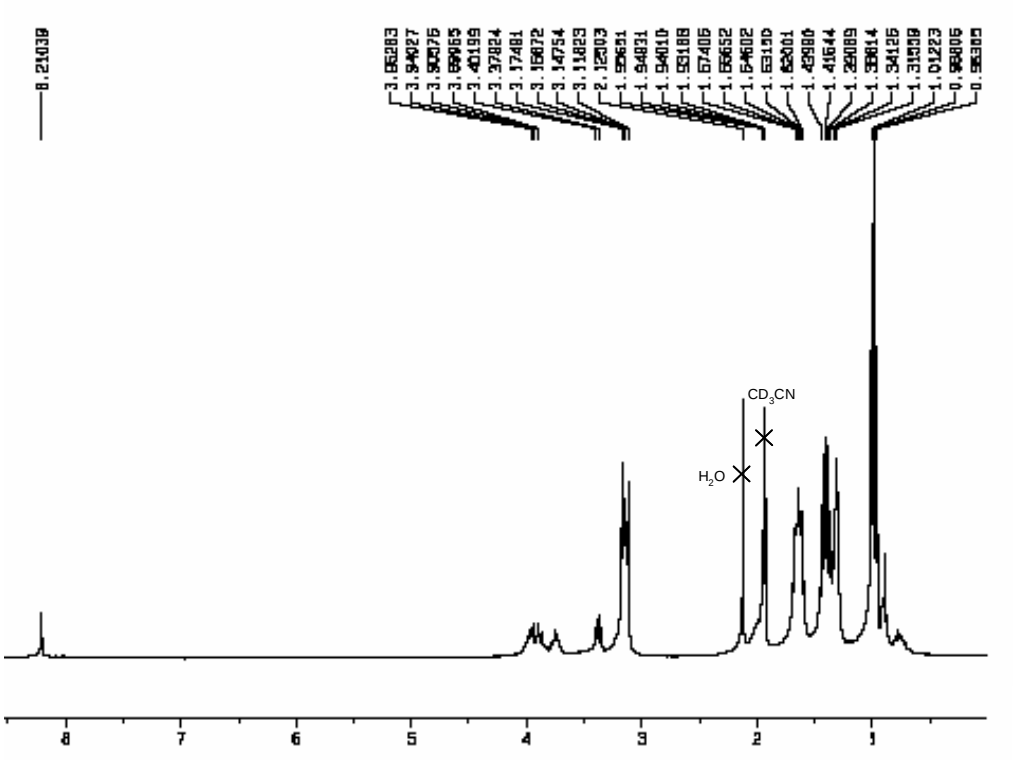

Figure 6.15. ^{1}H-NMR spectrum of compound **3**.

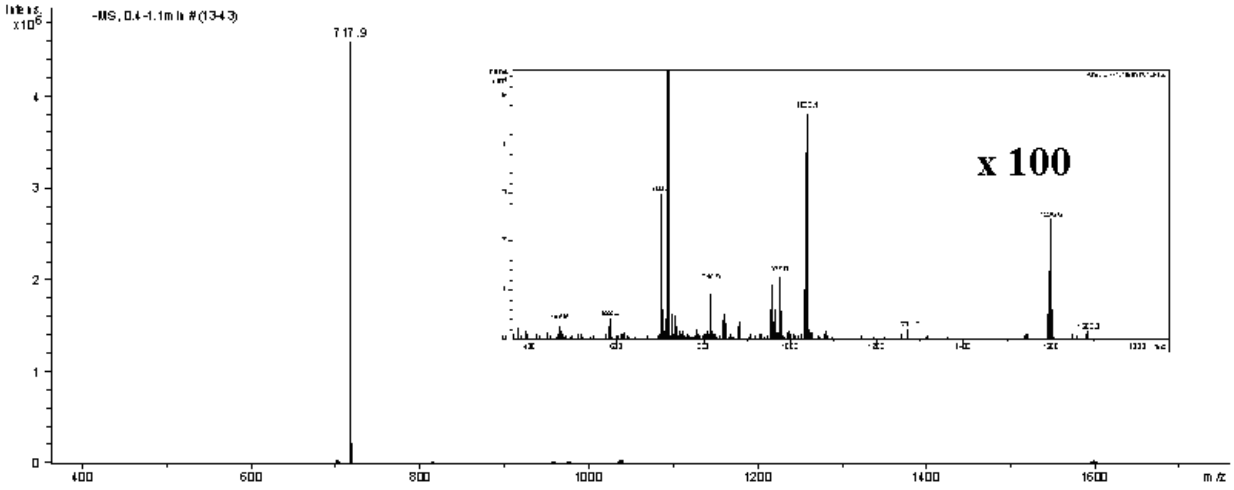

Figure 6.16. ESI-MS(-) spectrum of compound **3**.

6.6.4 Synthesis of 1-butyl-3-(3-triethoxysilylpropyl)-imidazolium bromide (4)

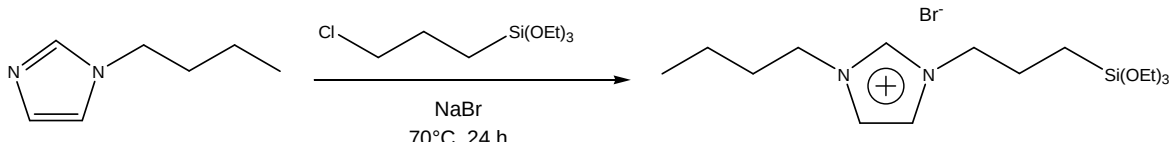

4

1-butylimidazole (0.7 mL, 5 mmol), (3-chloropropyl)-triethoxysilane (1.3 mL, 5.5 mmol, 1.1 eq) and sodium bromide (1.0 g, 15 mmol, 3 eq) were added to a well-dried Schlenk tube and allowed to react at 70°C under nitrogen for 24 h. The reaction mixture was washed twice with anhydrous Et_2O. The product was then redissolved in anhydrous CH_2Cl_2 and filtered through celite. Evaporation of the solvent gives the desired product as a yellow solid.

Yield: 1.64 g (80%).

^{29}Si-NMR (59.6 MHz, CD_2Cl_2, 25°C): δ −47.3 ppm. **^{13}C{^{1}H}-NMR** (62.5 MHz, CD_2Cl_2, 25°C): δ 136.5 (N<u>C</u>HN imidazolium), 122.5, 122.1 (C4 and C5, imidazolium ring), 58.1 (O<u>C</u>H$_2$), 51.2 ($CH_3(CH_2)_2$<u>C</u>H$_2$N), 49.1 (SiCH$_2$CH$_2$<u>C</u>H$_2$N), 31.9, 24.1, 19.1 (methylene groups), 17.9 (OCH$_2$<u>C</u>H$_3$), 13.0 (methyl), 6.7 (SiCH$_2$) ppm. **^{1}H-NMR** (360 MHz, CD_2Cl_2, 25°C) δ 10.34 (1H, s, NC<u>H</u>N), 7.62 (1H, s, C<u>H</u> imidazolium), 7.48 (1H, s, C<u>H</u> imidazolium), 4.38-4.24 (4H, m, Si(CH$_2$)$_2$C<u>H</u>$_2$N, NC<u>H</u>$_2$(CH$_2$)$_2$CH$_3$), 3.74 (6H, q, *J* = 7.20 Hz, CH$_3$C<u>H</u>$_2$O), 2.01-1.78 (4H, m, NCH$_2$C<u>H</u>$_2$CH$_2$CH$_3$, NCH$_2$C<u>H</u>$_2$CH$_2$Si), 1.31 (2H, sextet, *J* = 7.20 Hz, NCH$_2$CH$_2$C<u>H</u>$_2$CH$_3$), 1.13 (9H, t, *J* = 7.20 Hz, C<u>H</u>$_3$CH$_2$O), 0.89 (3H, t, *J* = 7.20 Hz, C<u>H</u>$_3$(CH$_2$)$_3$N), 0.60-0.48 (2H, m, SiC<u>H</u>$_2$) ppm. **Elemental Analysis** calcd (%) for **4**·(0.5 CH_2Cl_2), $C_{16.5}H_{34}ClBrN_2O_3Si$: C 43.85, H 7.58, N 6.20; found: C 43.85, H 8.06, N 6.03.

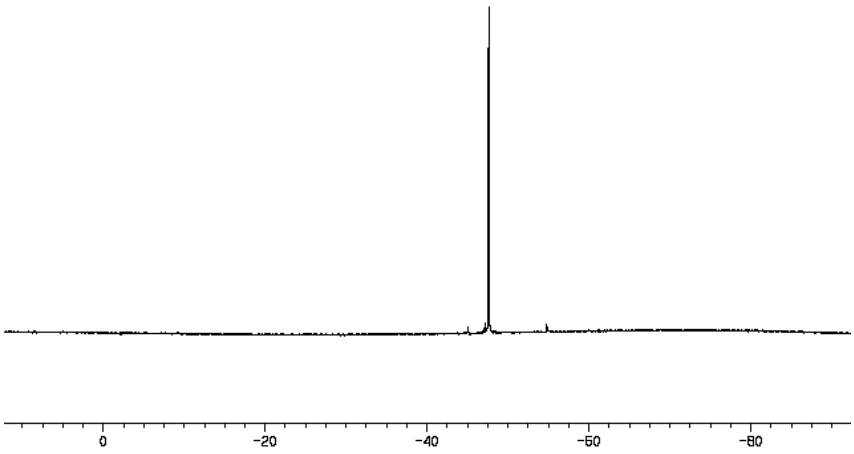

Figure 6.17. ^{29}Si-NMR spectrum of compound **4**.

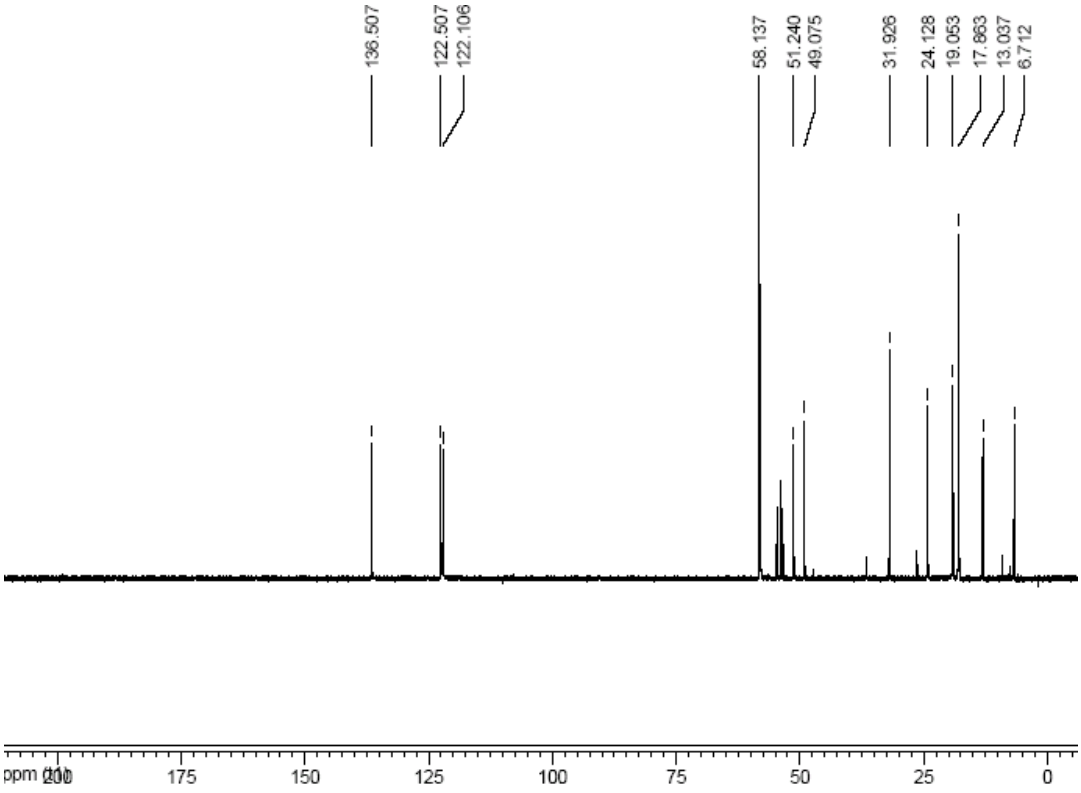

Figure 6.18. $^{13}C\{^{1}H\}$-NMR spectrum of compound **4**.

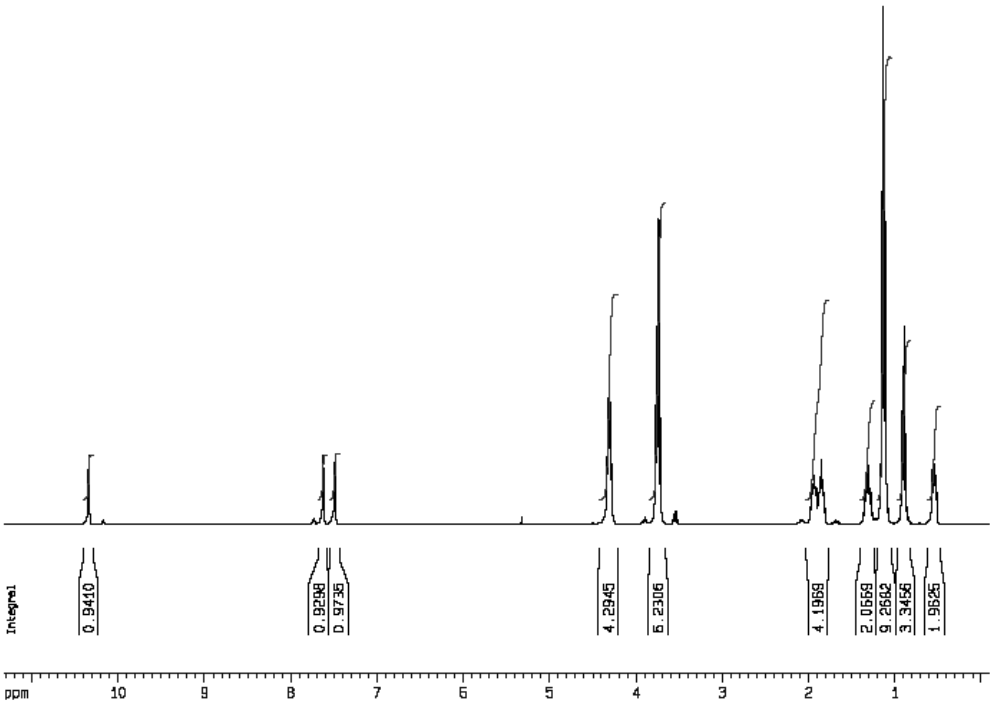

Figure 6.19. ^{1}H-NMR spectrum of compound **4**.

6.6.5 Synthesis of dichloro-*bis*-(1-butyl-3-(3-triethoxysilylpropyl)-imidazol-2-ylidene)-palladium(II) (5) [12]

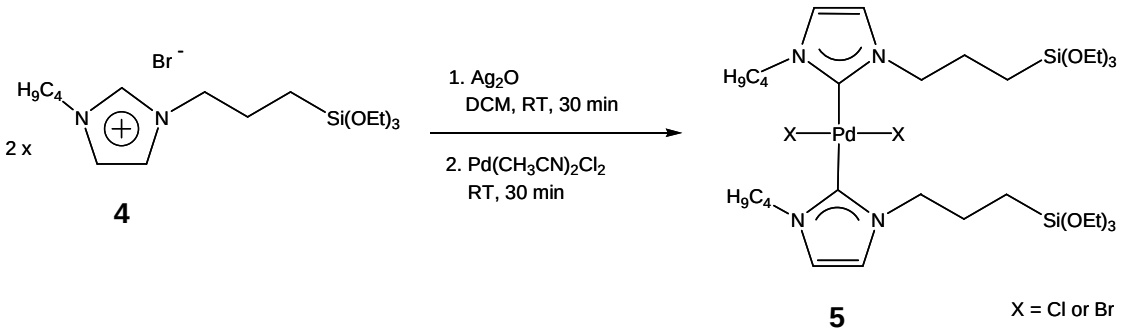

1-butyl-3-(3-triethoxysilylpropyl)-imidazolium bromide **4** (0.61 g, 1.5 mmol) was introduced in a well-dried Schlenk tube. Anhydrous CH_2Cl_2 (40 mL) and Ag_2O (0.209 g, 0.90 mmol) were then added. The reaction mixture, vigorously stirred, was allowed to react at room temperature, under nitrogen. After 30 min $Pd(CH_3CN)_2Cl_2$ [13] (0.197 g, 0.77 mmol) was added and the mixture was stirred for other 30 min, then filtered through celite. Evaporation of the solvent gives the desired product as a yellow solid.

Yield: 0.55 g (88%).

FT-IR (KBr, cm^{-1}) 3119, 2973, 2930, 2884, 1465, 1426, 1389, 1365, 1315, 1293, 1256, 1231, 1191, 1166, 1100, 1074, 1017, 982, 953, 879, 779, 745, 704. **$^{13}C\{^1H\}$-NMR** (62.5 MHz, CD_2Cl_2, 25°C): δ 170.6 (C-Pd), 121.1, 120.9 (C4 and C5, imidazol-2-ylidene), 58.9 (OCH_2), 51.1, 50.9 ($CH_3(CH_2)_2CH_2N$ and $SiCH_2CH_2CH_2N$), 33.7, 25.2, 20.7 (methylene groups), 18.7 (OCH_2CH_3), 14.2 (methyl), 8.2 ($SiCH_2$) ppm. **^{1}H-NMR** (360 MHz, CD_2Cl_2, 25°C) δ 6.92 (2H, s, CH imidazol-2-ylidene), 6.87 (2H, s, CH imidazol-2-ylidene), 4.47 (8H, t, $Si(CH_2)_2CH_2N$, $NCH_2(CH_2)_2CH_3$), 3.79 (12H, q, *J* = 7.20 Hz, CH_3CH_2O), 2.24-1.98 (8H, m, $NCH_2CH_2CH_2CH_3$, $SiCH_2CH_2CH_2N$), 1.51-1.37 (4H, m, $NCH_2CH_2CH_2CH_3$), 1.19 (18H, t, *J* = 7.20 Hz, CH_3CH_2O), 1.04-0.94 (6H, m, $N(CH_2)_3CH_3$), 0.73-0.63 (4H, m, $SiCH_2$) ppm. **ESI-MS(+)** (CH_3CN) *m/z* = 799.3, calcd. for $\{[C_{10}H_{17}N_2Si(OC_2H_5)_3]_2PdCl\}^+$ = 799.9; 843.3, calcd. for $\{[C_{10}H_{17}N_2Si(OC_2H_5)_3]_2PdBr\}^+$ = 844.4. **Elemental Analysis** calcd. (%) for $C_{32}H_{64}Cl_2N_4O_6PdSi_2$: C 46.06, H 7.73, N 6.71; calcd. (%) for $C_{32}H_{64}Br_2N_4O_6PdSi_2$: C 41.63, H 6.99, N 6.07; found: C 42.42, H 7.18, N 6.00, ascribed to the dibromo complex, with a small contamination of the dichloro analogue (as confirmed by ESI-MS analysis).

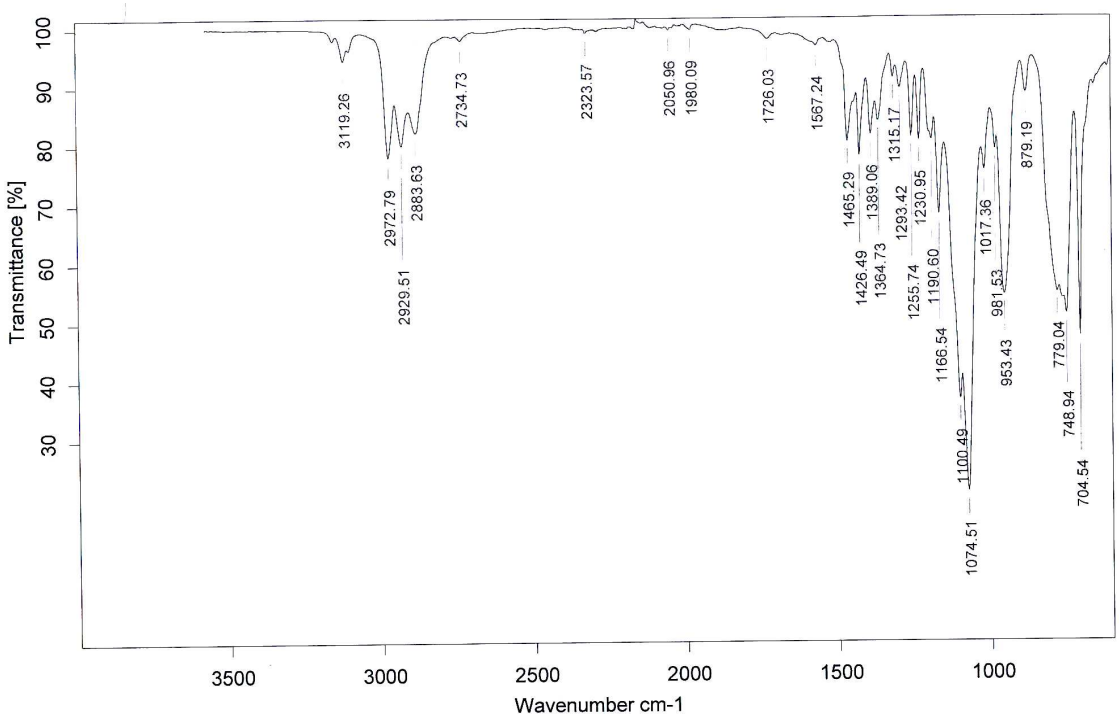

Figure 6.20. FT-IR spectrum of compound **5**.

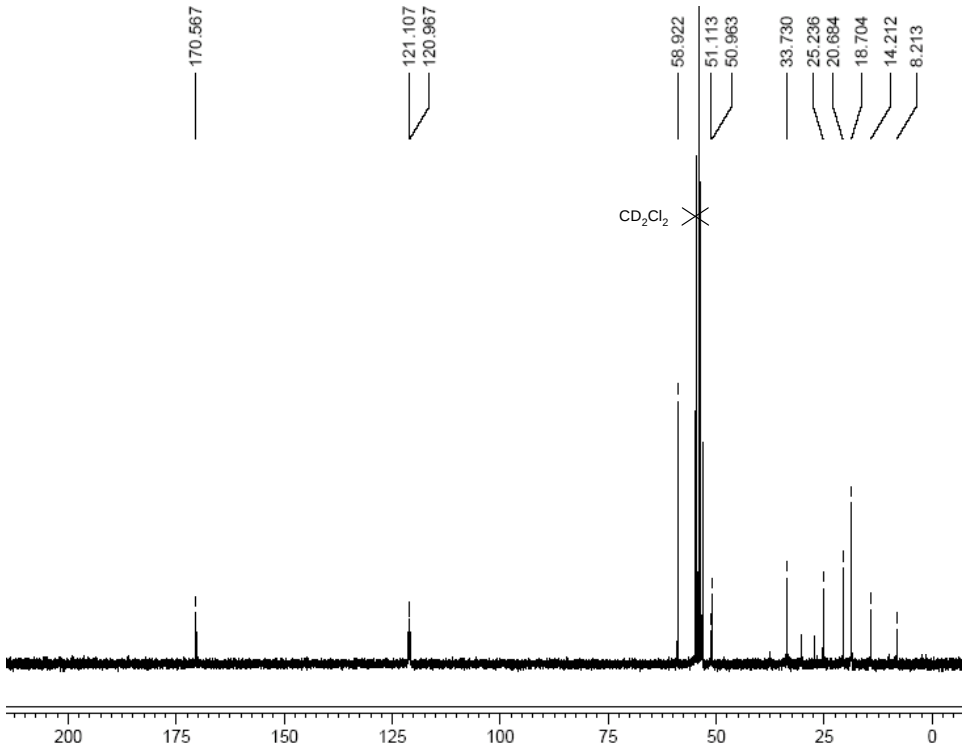

Figure 6.21. $^{13}C\{^{1}H\}$-NMR spectrum of compound **5**.

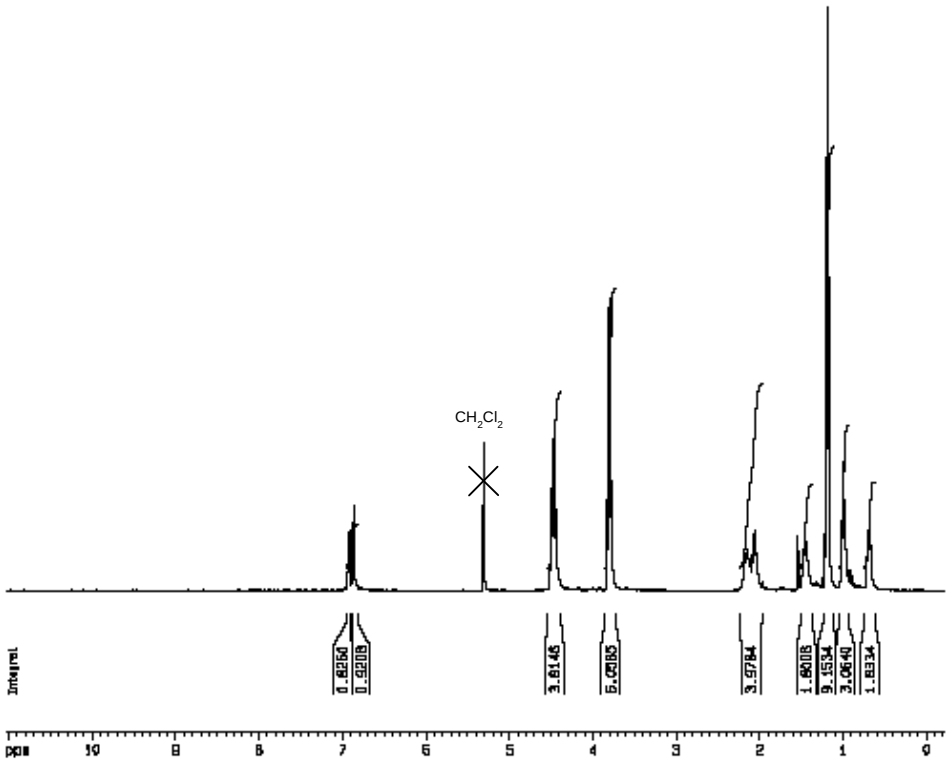

Figure 6.22. ^{1}H-NMR spectrum of compound **5**.

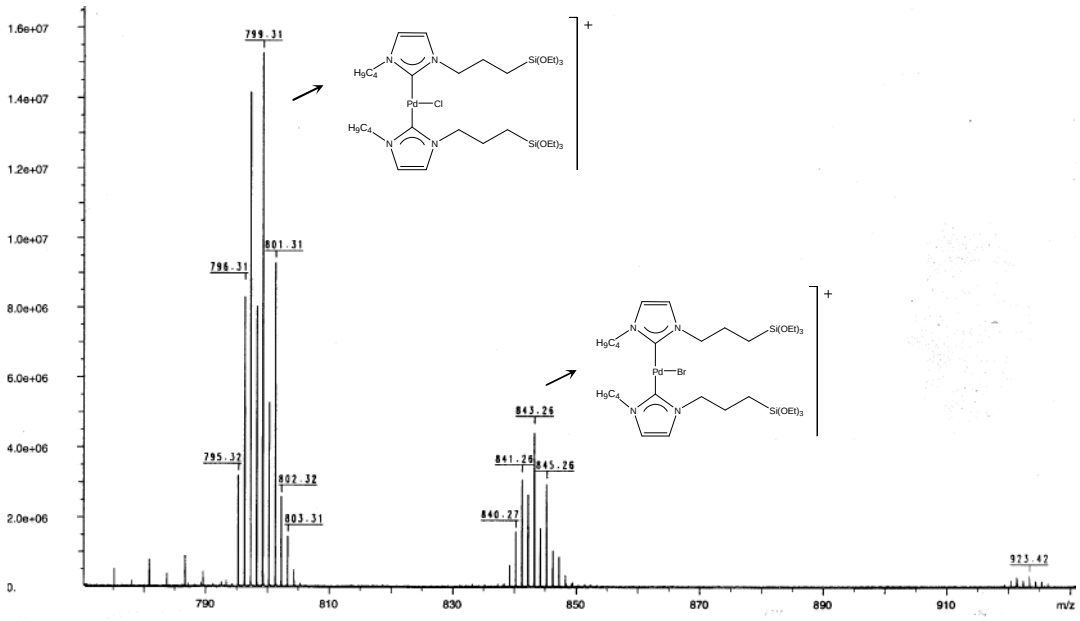

Figure 6.23. ESI-MS(+) spectrum of compound **5**.

6.6.6 Synthesis of $(n\text{-}Bu_4N)_{3.5}H_{0.5}[PdBr_2(C_{10}H_{17}N_2Si)_2O(\gamma\text{-}SiW_{10}O_{36})]$ (6) [11]

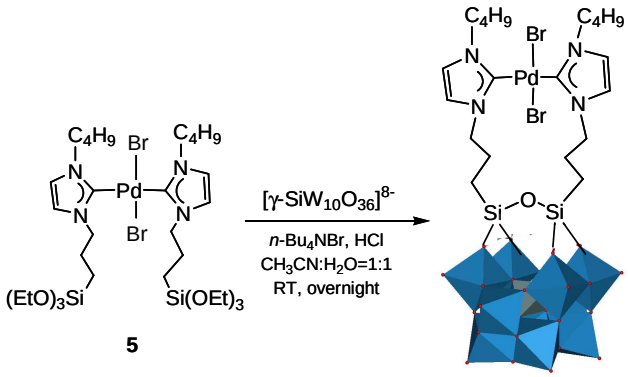

$K_8[\gamma\text{-}SiW_{10}O_{36}]$ (0.826 g, 0.3 mmol) was suspended in H_2O (1.4 mL). $(n\text{-}Bu_4N)Br$ (0.484 g, 1.5 mmol, 5 eq) and CH_3CN (9 mL) were added and the mixture was stirred at room temperature for 20 minutes. The compound **5** (0.25 g, 0.3 mmol), dissolved in 5 mL of anhydrous CH_3CN, and HCl 4 M (1.8 mmol, 6 eq) were successively added under vigorous stirring. The mixture was stirred overnight at room temperature. The product was obtained after filtration of the insoluble portion and evaporation of the organic solution. The crude compound was thoroughly washed with water.

Yield: 0.89 g (75 %).

FT-IR (KBr, cm^{-1}) 3165, 3128, 2961, 2934, 2873, 1635, 1483, 1466, 1425, 1380, 1152, 1097, 1055, 1043, 1003, 963, 946, 902, 886, 839, 820, 735, 602, 546, 509. **^{29}Si-NMR** (79.5 MHz, CD_3CN, 25°C) δ −62.8 (2 Si), -88.4 (1 Si) ppm. **^{183}W-NMR** (16.7 MHz, CD_3CN, 25°C) δ −107.4 (4 W), -135.8 (2 W), -142.1 (4 W) ppm. **^{13}C{^{1}H}-NMR** (62.5 MHz, CD_3CN, 25°C) δ 169.3 (C-Pd), 122.2, 121.8 (C4 and C5, imidazol-2-ylidene), 59.1 ($(CH_3CH_2CH_2CH_2)_4N^+$), 54.5, 51.1 ($CH_3(CH_2)_2CH_2N$ and $SiCH_2CH_2CH_2N$), 33.6, 25.8, 20.6 (methylene groups), 24.3 ($(CH_3CH_2CH_2CH_2)_4N^+$), 20.3 ($(CH_3CH_2CH_2CH_2)_4N^+$), 14.2 (methyl), 14.0 ($(CH_3CH_2CH_2CH_2)_4N^+$), 7.8 ($SiCH_2$) ppm. **^{1}H-NMR** (300 MHz, CD_3CN, 25°C) δ 7.05 (2H, s, CH imidazol-2-ylidene), 7.01 (2H, s, CH imidazol-2-ylidene), 4.71-4.19 (8H, m, $Si(CH_2)_2CH_2N$, $NCH_2(CH_2)_2CH_3$), 3.17 (32H, t, $(CH_3CH_2CH_2CH_2)_4N^+$), 2.60-2.21 (8H, m, $NCH_2CH_2CH_2CH_3$, $SiCH_2CH_2CH_2N$), 2.20-1.98 (4H, m, $NCH_2CH_2CH_2CH_3$), 1.89-1.77 (6H, m, $N(CH_2)_3CH_3$), 1.78-1.52 (32H, m, $(CH_3CH_2CH_2CH_2)_4N^+$), 1.40 (32H, q, $(CH_3CH_2CH_2CH_2)_4N^+$), 0.97 (48H, t, $(CH_3CH_2CH_2CH_2)_4N^+$), 0.71-0.44 (4H, m, $SiCH_2$) ppm. **ESI-MS(-)** (CH_3CN) *m/z* = 1007, calcd. for $\{[(C_{10}H_{17}N_2Si)_2O(\gamma\text{-}SiW_{10}O_{36})PdBr]\}^{3-}$ = 1009; 1470, calcd. for $\{[(C_{10}H_{17}N_2Si)_2O(\gamma\text{-}SiW_{10}O_{36})Pd]\}^{2-}$ = 1474. **Elemental Analysis** calcd. (%) for $C_{76}H_{160.5}Br_2N_{7.5}O_{37}PdSi_3W_{10}$: C 23.05, H 4.08, N 2.65; found: C 23.94, H 4.19, N 2.61.

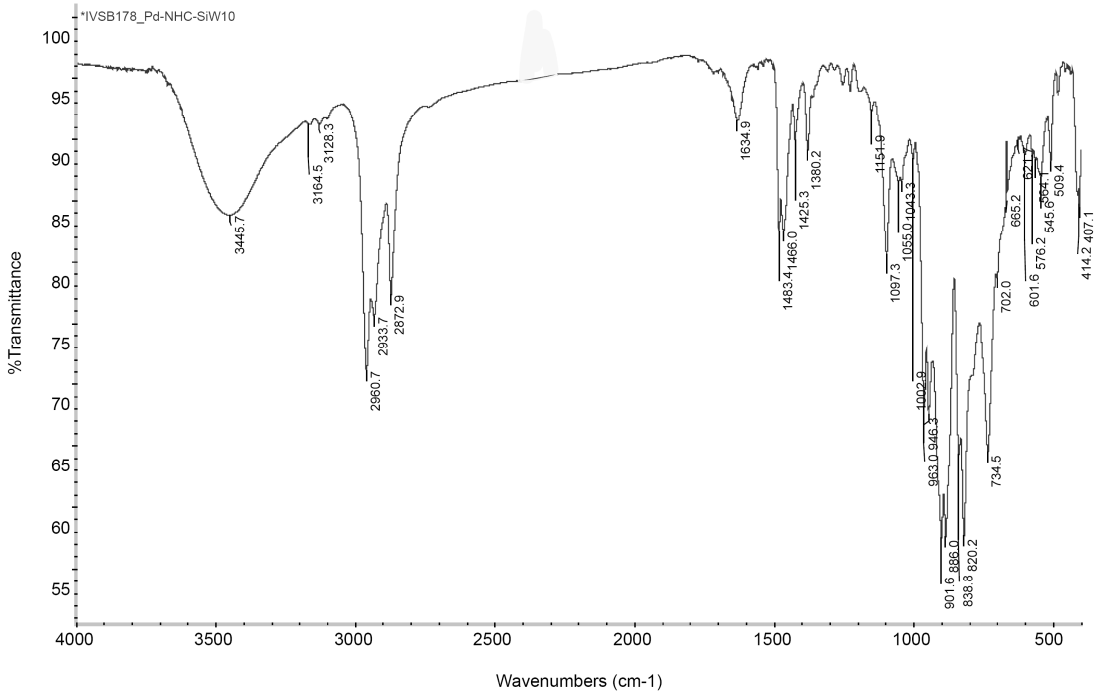

Figure 6.24. FT-IR spectrum of compound **6**.

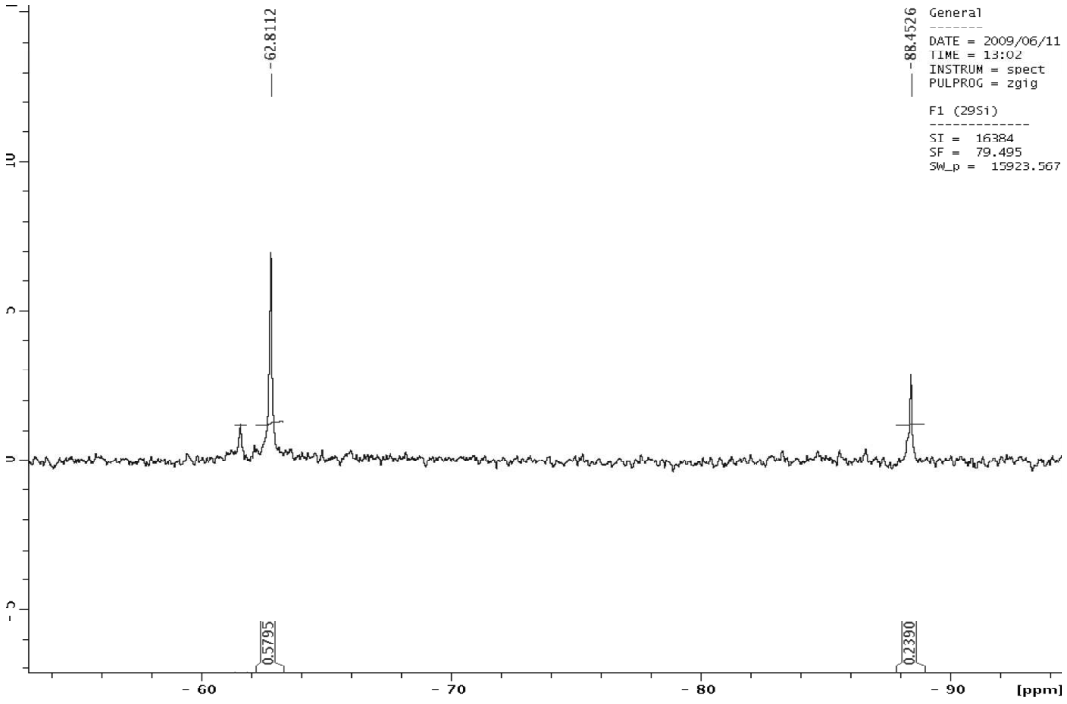

Figure 6.25. ^{29}Si-NMR spectrum of compound **6**.

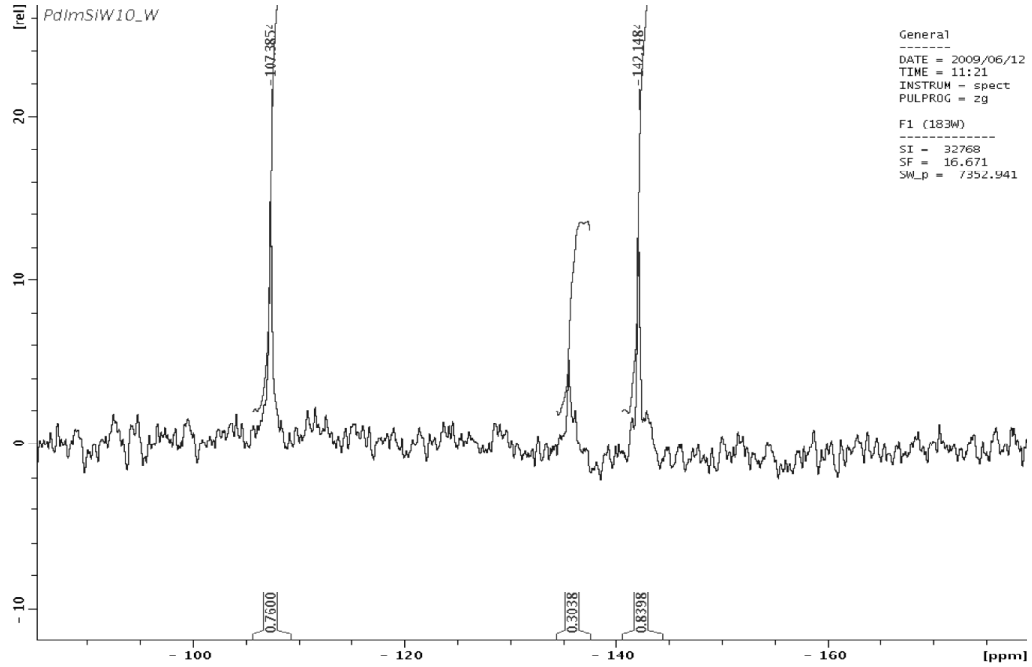

Figure 6.26. ^{183}W-NMR spectrum of compound **6**.

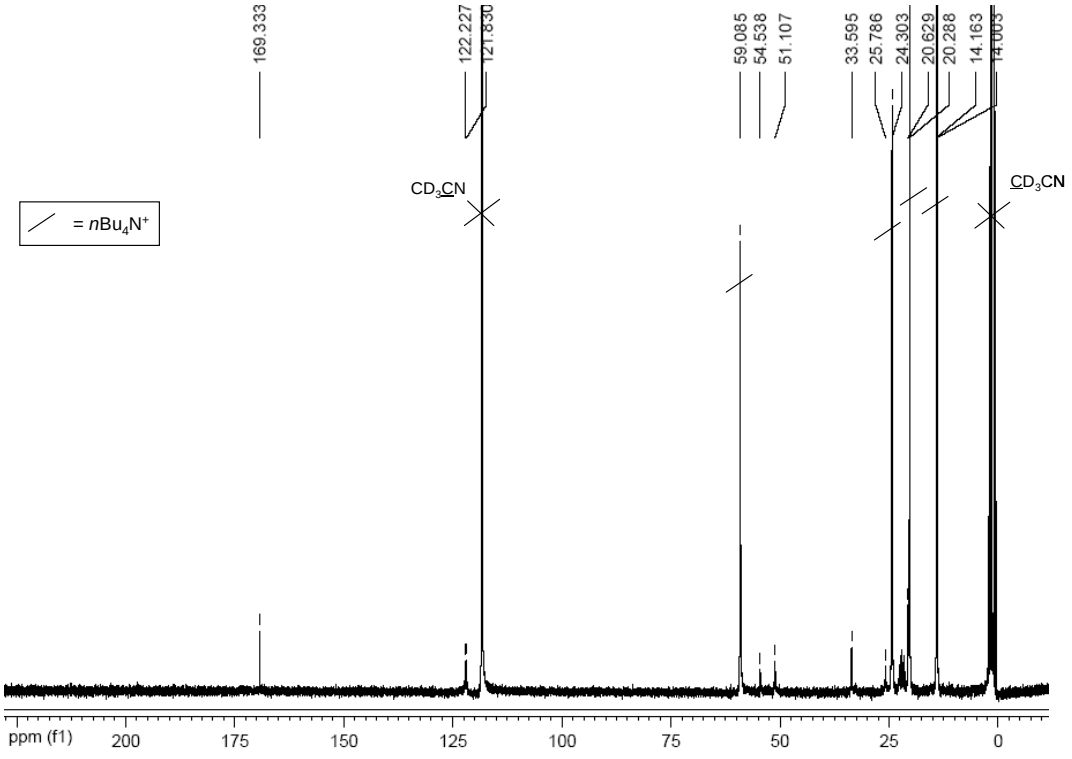

Figure 6.27. ^{13}C{^{1}H}-NMR spectrum of compound **6**.

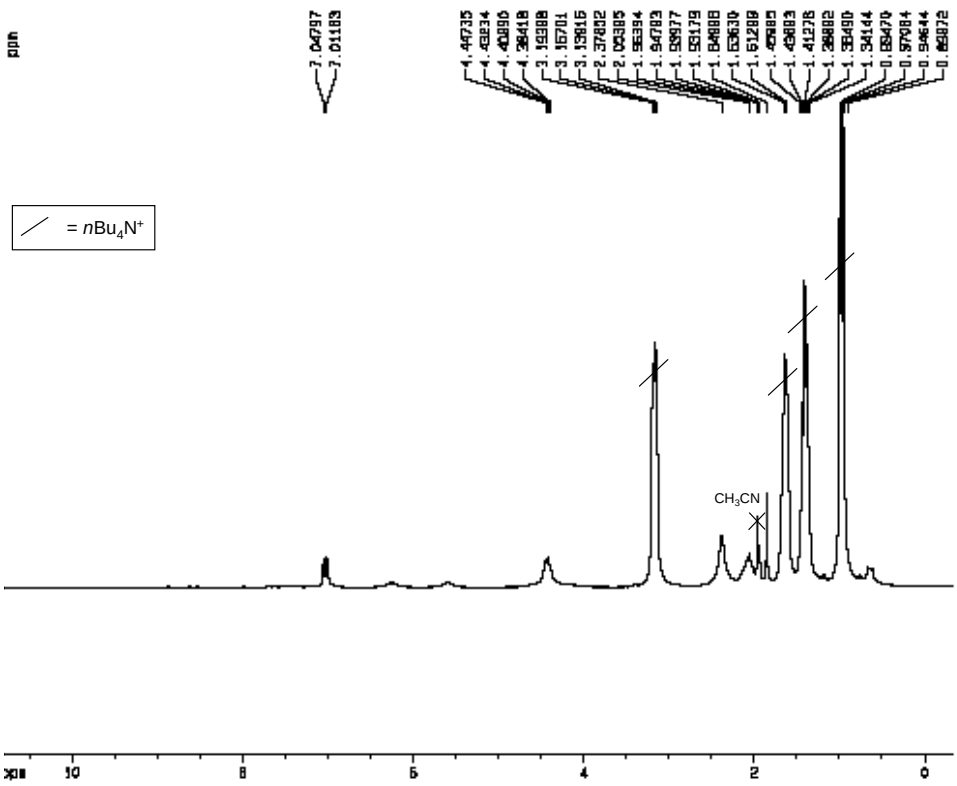

Figure 6.28. ^{1}H-NMR spectrum of compound **6**.

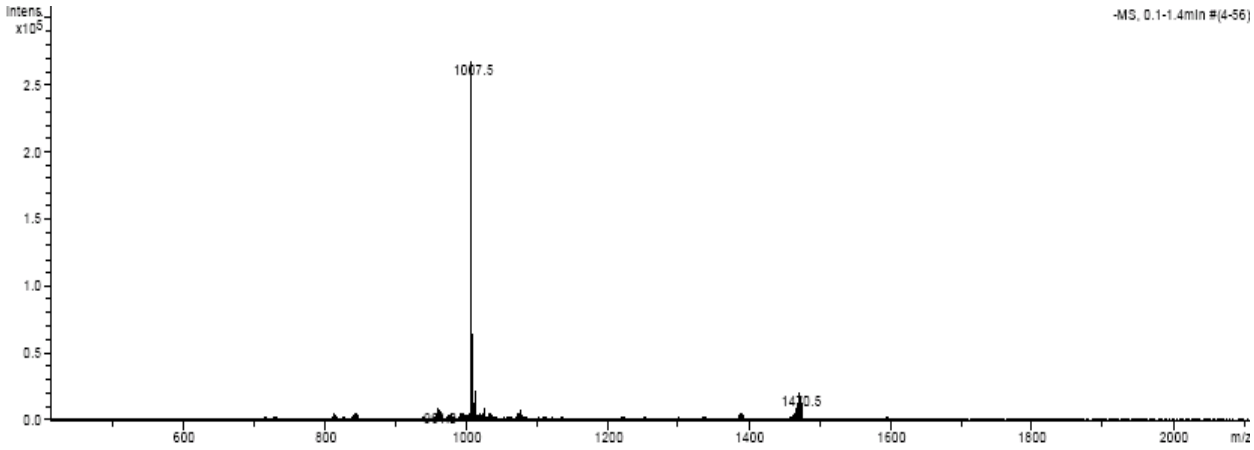

Figure 6.29. ESI-MS(-) spectrum of compound **6**.

6.6.7 General procedures for Suzuki-Miyaura cross-coupling reactions

6.6.7.1 Suzuki-Miyaura cross-coupling reaction of aryl halides with phenylboronic acid catalyzed by complex 6 under conventional heating [14]

The appropriate amount of a 0.025 M solution of catalyst **6** in DMF was placed in a closed vessel. $PhB(OH)_2$ (0.275 mmol, 1.1 eq.) in DMF (0.2 mL), Na_2CO_3 (0.5 mmol, 2 eq.) in H_2O (0.45 mL) and the aryl halide (0.25 mmol) were then added, followed by the addition of the appropriate amount of DFM, in order to match the volume of water. The reaction mixture was stirred in an oil bath (T = 80°C) for the appropriate amount of time, then cooled to room temperature. After the addition of water (2 mL ca.), the mixture was extracted with diethylether (3 x 3 mL ca.). The organic solutions were collected and dried over $MgSO_4$. The resulting solution was analyzed by gas-chromatography.

6.6.7.2 Microwave-assisted Suzuki-Miyaura cross-coupling reaction of aryl halides with phenylboronic acid catalyzed by complex 6 [14]

We followed the same procedure described in the previous paragraph. The reaction vessel was placed in the single-mode cavity of the instrument and irradiated with power at 10 watt under simultaneous stirring and cooling by a stream of compressed air (pressure = 20-40 psi). The registered T_{bulk} are in the range 75-85°C. At the end of the reaction, the mixture was cooled to room temperature, then, after the addition of water (2 mL ca.), extracted with diethylether (3 x 3 mL ca.). The organic portions were collected and dried over $MgSO_4$. The resulting solution was analyzed by gas-chromatography.

6.6.8 General procedures for MW-assisted dehalogenation of aryl chlorides

0.1 mL (0.0025 mmol, 1 mol%) of a 0.025 M stock solution of catalyst **6** in DMF was placed in a closed vessel. *n*-$Bu_4NOH \cdot 30\ H_2O$ (0.5 mmol, 2 eq., 0.4 mL), DMF (0.4 mL) and the aryl chloride (0.25 mmol) were then added. The reaction vessel was placed in the single-mode cavity of the instrument and irradiated with power at 10 watt under simultaneous stirring and cooling by a stream of compressed air (pressure = 20-40 psi). The registered T_{bulk} are in the range 80-95°C. At the end of the reaction, the mixture was cooled to room temperature and extracted with diethylether (3 x 3 mL ca.). The organic phase was collected, dried over $MgSO_4$ and analyzed by gas-chromatography.

6.6.9 Computational details for complex 6

Computational resources and assistance were provided by the Laboratorio Interdipartimentale di Chimica Computazionale (LICC) at the Department of Chemical Sciences of the University of Padova. DFT calculations have been carried out using the Amsterdam density functional (ADF) code,[15] scalar relativistic effects were taken into account by means of the two-component zero-order regular approximation (ZORA) method,[16] adopting the Becke 88 exchange plus the Perdew 86 correlation (BP) functional.[17] The basis functions for describing the valence electrons are triple-zeta quality doubly polarized (TZ2P), specially optimized for ZORA calculations. Due to the large size of the molecule under investigation, the internal or core electrons (C, N, O: 1s; Si: 1s to 2sp; Br: 1s to 3d; Pd: 1s to 4sp; W: 1s to 4spdf) were kept frozen. The solvent effect was modeled by means of the ADF implementation[18] of the COSMO method.[19] This method requires a prior definition of atomic radii, which were set at their following recommended values (in Å): H: 1.3500; C: 1.7000; N: 1.6083; O: 1.5167; Si: 1.9083; Br: 1.850; Pd: 1.9750; W: 1.9917. In addition to the dielectric permittivity $\sum$, the solvent is modeled also by an empirical parametrization of non-electrostatic solvation terms derived from the solvation of alkanes.[20] Since these parameters are currently available only for water, energies and gradients can be reliably calculated only for this solvent.[21] Therefore, all calculations assumed water as solvent.

Cartesian coordinates (in Å) of the DFT optimized structure for complex 6

Atom	X	Y	Z (Angstrom)
1.Si	0.102645	1.612465	3.487004
2.O	-1.243099	2.326873	2.803858
3.W	-1.597374	2.883956	0.951413
4.O	-2.678957	4.235665	1.254699
5.O	0.048936	-0.033817	3.406587
6.Si	0.003837	-1.678385	3.471850
7.O	1.330727	-2.396599	2.752628
8.W	1.640957	-2.919530	0.882454
9.O	2.731391	-4.276427	1.139888
10.O	-0.004219	-1.386512	0.647107
11.Si	0.010164	-0.010126	-0.215760
12.O	1.384076	-0.029895	-1.153231
13.W	1.866565	-1.751339	-2.647276
14.O	2.031825	-0.031368	-3.619555
15.W	1.931791	1.674382	-2.648204
16.O	0.012640	1.766590	-2.930248
17.W	-1.899533	1.755621	-2.592923
18.O	-2.087579	0.055071	-3.571296
19.W	-1.964276	-1.671007	-2.615931
20.O	-0.052504	-1.764806	-2.947827
21.W	-1.703038	-2.873835	0.899972
22.O	-2.829216	-4.196256	1.180629
23.O	2.951760	-1.456391	0.760304
24.W	3.691840	-0.071473	-0.350637
25.O	3.598377	-1.360936	-1.834175
26.O	1.610757	-2.892401	-1.082063
27.O	-0.045779	-3.917299	0.890837
28.O	-1.357286	-2.341980	2.759913
29.O	1.447085	2.272614	2.749591
30.W	1.748686	2.840478	0.893475
31.O	1.711929	2.812082	-1.058438
32.O	2.876333	4.160826	1.167341
33.O	0.043516	1.347084	0.672907
34.O	0.090773	3.877130	0.940666
35.O	3.020473	1.333764	0.763213
36.O	-2.913691	1.422783	0.842943
37.W	-3.674470	0.054504	-0.269699
38.O	-3.610734	1.357360	-1.737856
39.O	-1.608402	2.871023	-1.007499
40.O	-5.372357	0.086429	0.176516
41.O	-2.971427	-1.366279	0.812317
42.O	-1.382884	0.018579	-1.123652
43.O	-3.662023	-1.230484	-1.761531
44.O	-2.450713	2.915045	-3.787827
45.O	5.399557	-0.106995	0.056848
46.O	3.644405	1.226386	-1.827834
47.O	2.489721	2.812289	-3.860826
48.O	2.391504	-2.886492	-3.883777
49.O	-1.712831	-2.833832	-1.057608
50.O	-2.550485	-2.776900	-3.850948
51.C	0.010660	-2.238298	5.262610
52.H	0.989136	-1.968107	5.694744
53.H	-0.010959	-3.340815	5.243269
54.C	0.136718	2.193044	5.269251

55.H	-0.810871	1.901014	5.751841
56.H	0.101890	3.295291	5.203330
57.C	1.318746	1.772736	6.163343
58.H	2.279010	1.950121	5.656790
59.H	1.265461	0.698882	6.394173
60.C	-1.118227	-1.711569	6.168654
61.H	-2.102845	-1.963506	5.747597
62.H	-1.070137	-0.616286	6.246396
63.C	1.247497	2.571976	7.468227
64.H	1.462236	3.631200	7.270661
65.H	0.236842	2.515513	7.879219
66.C	-0.962290	-2.319086	7.565569
67.H	-1.065840	-3.411366	7.512078
68.H	0.036213	-2.107160	7.954515
69.N	-1.920317	-1.841849	8.573787
70.N	2.159395	2.143023	8.538697
71.C	1.855188	1.290366	9.569489
72.C	-3.201313	0.135091	11.296421
73.H	-2.264222	0.624911	11.572418
74.H	-3.836696	0.902426	10.834955
75.C	-3.894081	-0.438055	12.531828
76.H	-4.296623	0.433088	13.073977
77.H	-4.773911	-1.037328	12.248085
78.C	-2.988594	-1.232958	13.479965
79.H	-2.693944	-2.184682	13.011084
80.H	-2.056938	-0.666030	13.637058
81.C	-3.658195	-1.497198	14.833353
82.H	-4.591565	-2.066724	14.714350
83.H	-3.000641	-2.065380	15.504858
84.H	-3.911352	-0.550435	15.334319
85.N	-2.866428	-0.839174	10.240764
86.C	3.211970	0.436282	11.530721
87.H	2.247399	-0.019038	11.770947
88.H	3.892292	-0.378973	11.251734
89.C	3.768514	1.202948	12.730310
90.H	4.034813	0.443990	13.483429
91.H	4.715232	1.699827	12.463418
92.N	2.991106	1.261923	10.329761
93.C	2.794822	2.214415	13.343813
94.H	2.539359	2.979913	12.595510
95.H	1.852559	1.695885	13.584243
96.C	3.354219	2.882638	14.603502
97.H	4.290271	3.418904	14.388378
98.H	2.642137	3.606543	15.021846
99.H	3.571526	2.136797	15.381768
100.C	-1.689586	-0.898639	9.543916
101.Pd	0.079387	0.205302	9.709759
102.Br	1.385649	-1.982826	10.046795
103.Br	-1.225011	2.412734	9.853875
104.C	-3.805140	-1.709438	9.705409
105.C	-3.209426	-2.341370	8.663503
106.C	3.977267	2.067709	9.780428
107.C	3.453352	2.622450	8.658517
108.H	4.954727	2.183990	10.226905
109.H	3.880760	3.318483	7.949467
110.H	-4.803003	-1.810211	10.106819
111.H	-3.582439	-3.102410	7.991379

6.7 Aluminum-substituted polyoxometalates for H_2O_2-based oxidations

6.7.1 Synthesis of $[Al_4(H_2O)_{10}(\beta\text{-}AsW_9O_{33})_2]^{6-}$

$AlCl_3$ (0.29 g, 2.22 mmol) was dissolved in 30 mL of water, then mixed with $Na_9[\alpha\text{–}AsW_9O_{33}]\cdot 19.5H_2O$ (1.0 mmol). The pH value was adjusted to 3 with a 4 M aqueous solution of HCl. The colorless solution was stirred at 70°C for one hour. After cooling to room temperature the solution was filtered. Colorless crystals were obtained by evaporating the filtrate at room temperature for few days in the presence of a 1 M aqueous solution of RbCl (complex **I**).
Yield: 0.914 g (35%).
FT-IR < 1000 cm^{-1} (KBr, cm^{-1}): 968, 835, 727, 477. **^{183}W NMR** Complex **I** is not soluble enough to record the spectrum. **Crystallographic data** (H100 Al4 As2 O96.80 Rb1.64 W18): crystal block with dimensions 0.40 x 0.16 x 0.09 mm, M= 5356.83, triclinic system space group *P*1(2), with a=12.5177(3) Å, =12.6671(4) Å, c=15.7160(5) Å, α=86.13(0)° β=82.68(0)°, γ=83.44(0)°. V=2451.95(68) $Å^3$ and Z=1.

6.7.2 Synthesis of $[Al_4(H_2O)_{10}(\beta\text{-}SbW_9O_{33})_2]^{6-}$

$AlCl_3$ (0.29 g, 2.22 mmol) was dissolved in 30 mL of water, then mixed with $Na_9[\alpha\text{–}SbW_9O_{33}]\cdot 19.5H_2O$ (1.0 mmol). The pH value was adjusted to 3 with a 4 M aqueous solution of HCl. The colorless solution was stirred at 70°C for one hour. A white precipitate formed, thus, after cooling to room temperature, the solution was filtered. Colorless crystals were obtained by evaporating the filtrate at room temperature for few days in the presence of 1 M aqueous solution of NH_4Cl (complex **II**).
Yield: 0.427 g (17%).
FT-IR < 1000 cm^{-1} (KBr, cm^{-1}): 960, 816, 704, 455. **^{183}W NMR** Complex **II** is not soluble enough to record the spectrum. **Crystallographic data** (H60 Al4 O100 Sb2 W18): crystal plate with dimensions 0.14 x 0.11x 0.04 mm, M= 5321.20, triclinic system space group *P*1 (2), with *a* = 12.5011(5) Å, *b* = b=12.5288(5) Å, *c* = 15.9248(7) Å, α=74.0()° β=88.08(0)°, γ=77.98(0)°, V = 2344.16(173) $Å^3$ and *Z* = 1.

6.7.3 General procedure for H_2O_2-based oxidations catalyzed by $[Al_4(H_2O)_{10}(\beta\text{-}AsW_9O_{33})_2]^{6-}$

$[Al_4(H_2O)_{10}(\beta\text{-}AsW_9O_{33})_2]^{6-}$ (0.8 μmol) was dissolved in the solvent (0.6 mL if CH_3CN or 1.2 mL if H_2O). Substrate (0.5 mmol) and 35% H_2O_2 (0.1 mmol) were added and the reaction vessel was then placed in a thermostated oil bath at the indicated temperature.

Reactions were sampled diluting a portion (50-100 μl) of the mixture in CH_2Cl_2 containing dodecane as external standard and Ph_3P as quencher, then monitored by quantitative GLC analysis.

6.7.4 $[Al_4(H_2O)_{10}(\beta\text{-}AsW_9O_{33})_2]^{6-}$ titration with BINOL

Mother solutions of both the catalyst and of the *S*-(-)-1,1'-binaphthalen-2,2'-diol (BINOL) ligand in CH_3CN were prepared, as indicated in Table 6.3.

Table 6.3. Mother solutions of the catalyst (A) and BINOL (B).

Mother solution	Mass of the compound, mg	CH_3CN volume, mL	Concentration, M
A	6.3	10	$1.04 \cdot 10^{-4}$
B	2.4	10	$8.38 \cdot 10^{-4}$

Different amount of both these mother solutions were used to prepare other solutions with the following POM: BINOL ratios:

POM	1	1	1	1	1	1	1	1	0
BINOL	0	0.5	1	2	3	4	6	8	1

CH_3CN was then added to each solution (in order to match the volume to 3 mL) and UV-vis analyses of them were finally performed.

6.8 Hydrogen peroxide titration

6.8.1 $Na_2S_2O_3$ standardization by iodometric titration

$$IO_3^- + 6\ H^+ + 5\ I^- \rightarrow 3\ I_2 + 3\ H_2O$$

$$6\ S_2O_3^{2-} + 3\ I_2 \rightarrow 6\ I^- + 3\ S_4O_6^{2-}$$

Deionized water (10 mL) and glacial acetic acid (10 mL) were put in a flask. 10% aqueous solution of KI (10 mL) and 0.25 M KIO_3 standard solution (1 mL) were then added.

The flask was kept in the dark for at least 2 minutes, thus allowing I_2 to form (the solution turned to yellow-orange). This solution was then titrated with the thiosulfate solution (prepared at least one week before dissolving 3.40 g of $Na_2S_2O_3$ in 250 mL of water and stored in the dark), until the colour becomes very light. At this point starch indicator was added and the solution turned to dark brown. Titration with thiosulfate was continued until the solution became colour-less (end point). Iodometric titration was repeated three times. Average concentration of the thiosulfate solution resulted 0.0863 M.

6.8.2 H_2O_2 titration

$$H_2O_2 + 2\ H^+ + 2\ I^- \rightarrow I_2 + 2\ H_2O$$

$$2\ S_2O_3^{2-} + I_2 \rightarrow 2\ I^- + S_4O_6^{2-}$$

Both 35% and 70% aqueous solutions of H_2O_2 were titrated.

40 μL of H_2O_2 solution were put in a flask, containing water (10 mL), 10% aqueous solution of KI (10 mL), glacial acetic acid (10 mL) and few drops of a $(NH_4)_2MoO_4 \cdot 4H_2O$ solution (the latter acts as catalyst for I_2 formation).

The flask was kept in the dark for two minutes and then titrated with a standard thiosulfate solution (prepared as described above), until the colour of the solution becomes very light. At this point, starch indicator was added and the solution turned to dark brown. Titration with thiosulfate was continued until the solution became colour-less (end point). Titration was repeated three times for both 35% and 70% H_2O_2 solutions. Average concentrations are reported below.

35% H_2O_2: 11.35 M

70% H_2O_2: 24.93 M.

6.9 GLC-analyses: procedures and conditions

Capillary column EQUITY^{TM} –5 (see Paragraph 6.1):

Oxidations with H_2O_2:

Carrier gas linear velocity = He, 40 cm/s;

Initial column temperature = 55°C (or 40°C) x 3 min;

Progress rate = 15°C/min;

Final column temperature = 250°C;

Injection temperature = 200°C;

Detection temperature = 280°C.

Suzuki-Miyaura cross-couplings and Dehalogenations:

Carrier gas linear velocity = He, 40 cm/s;

Initial column temperature = 80°C x 5 min;

Progress rate = 10°C/min;

Final column temperature = 180°C;

Injection temperature = 200°C;

Detection temperature = 280°C.

Quantitative evaluation of reagents and products (analytes in general) has been calculated using the internal standard method, through the following formula:

$$C_{analyte} = (A_{analyte}/A_{standard})\cdot(C_{standard}/F_{analyte})$$

where C = concentration, A = area of the signal in the chromatogram, F = calculated response factor.

Analyte concentration in the reaction mixture is calculated multiplying $C_{analyte}$ by the Dilution Factor used in preparing the sample to analyze.

6.10 References and notes

[1] C. Rocchiccioli-Deltcheff, R. Thouvenot *J. Chem. Res.* **1977**, 46.

[2] A. Tezè, G. Hervè *J. Inorg. Nucl. Chem.* **1977**, *39*, 999.

[3] J. Canny, A. Tezè, R. Thouvenot, G. Hervè *Inorg. Chem.* **1986**, *25*, 2114.

[4] C. Tournè, A. Revel, G. Tournè, M. Vendrell *C. R. Acad. Sci. Paris, Ser. C* **1973**, *277*, 643.

[5] M. Bösing, I. Loose, H. Pohlmann, B. Krebs *Chem. Eur. J.* **1997**, *3*, 1232.

[6] mizuno

[7] C. R. Mayer, P. Herson, R. Thouvenot *Inorg. Chem.* **1999**, *38*, 6152.

[8] a) G. S. Owens, M. M. Abu-Omar *J. Mol. Catal. A: Chem.* **2002**, *187*, 215. b) P. Bonhôte, A. P. Dias, N. Papageorgiou, K. Kalyanasundaram, M. Grätzel *Inorg. Chem.* **1996**, *35*, 1168. c) K. R. Seddon, A. Stark, M. J. Torres *Pure Appl. Chem.* **2000**, *72*, 2275.

[9] a) P. A. Z. Suarez, J. E. L. Dullius, S. Einloft, R. F. De Souza, J. Dupont *Polyhedron* **1996**, *15*, 1217. b) V. Farmer, T. Welton *Green Chem.* **2002**, *4*, 97.

[10] K. Yamaguchi, C. Yoshida, S. Uchida, N. Mizuno *J. Am. Chem. Soc.* **2005**, *127*, 530.

[11] C. R. Mayer, I. Fournier, R. Thouvenot *Chem. Eur. J.* **2000**, *6*, 105.

[12] C. K. Lee, J. C. C. Chen, K. M. Lee, C. W. Liu, I. J. B. Lin *Chem. Mater.* **1999**, *11*, 1237.

[13] Prepared following literature procedures, in particular: I. Abrunhosa, L. Delain-Bioton, A.-C. Gaumont, M. Gulea, S. Masson *Tetrahedron* **2004**, *60*, 9263.

[14] H. Qiu, S. M. Sarkar, D.-H. Lee, M.-J. Jin *Green Chem.* **2008**, *10*, 37.

[15] G. te Velde, F.M. Bickelhaupt, E.J. Baerends, C. Fonseca Guerra, S.J.A. van Gisbergen, J.G. Snijders, T. Ziegler, *J. Comput. Chem.* **2001**, *22*, 931.

[16] a) S. K. Wolff, T. Ziegler, E. van Lenthe, E. J. Baerends *J. Chem. Phys.* **1999**, *110*, 7689. b) J. Autschbach, *Calculation of NMR and EPR Parameters*, Wiley-VCH: Weinheim, **2004**, *14*. c) E. van Lenthe, E. J. Baerends, J. G. Snijders, *J.Chem. Phys.* **1993**, *99*, 4597. d) E. van Lenthe, PhD. Thesis, Vrije Universiteit, Amsterdam, the Netherlands, **1996**.

[17] a) A. D. Becke *Phys. Rev. A* **1988**, *38*, 3098. b) J. P. Perdew *Phys. Rev. B* **1986**, *33*, 8822.

[18] C. C. Pye, T. Ziegler *Theor. Chem. Acc.* **1999**, *101*, 396.

[19] a) A. Klamt, G. Schüürmann *J. Chem. Soc., Perkin Trans. 2* **1993**, 799. b) A. Klamt, V. Jones *J. Chem. Phys.* **1996**, *105*, 9972. c) A. Klamt *J. Phys. Chem.* **1995**, *99*, 2224.

[20] T. N. Truong, E. V. Stefanovich *Chem. Phys. Lett.* **1995**, *240*, 253.

[21] It is worth noting that the thermodynamics of solvation of hydrocarbons is profoundly different according to whether the solvent is water or any other liquid. W. Blokzijl, J. B. F. N. Engberts *Angew. Chem. Int. Ed. Engl.* **1993**, *32*, 1545.

Acronyms and abbreviations

AcO	Acetate ion, $CH_3CO_2^-$
BINOL	*S*-(-)-1,1'-binaphthalen-2,2'-diol
bmim	1-butyl-3-methylimidazolium
DFT	Density Functional Theory
DMF	*N*, *N*-Dimethylformamide
DMSO	Dimethylsulfoxide
emim	1-ethyl-3-methylimidazolium
ESI-MS	Electrospray Ionization Mass Spectrometry
FcH	Ferrocene
FID	Flame Ionization Detector
FT-IR	Fourier Transform – Infrared Spectroscopy
GC-MS	Gas Chromatography coupled with Mass Spectrometry
GLC	Gas-liquid Chromatography
IL	Ionic Liquid
KHMDS	Potassium *bis*-(trimethylsilyl)amide
MW	Microwave radiation
***n*-Bu_4N**	Tetrabutylammonium
NHC	*N*-Heterocyclic carbene
NMR	Nuclear Magnetic Resonance
POM	Polyoxometalate
PTFE	Polytetrafluoroethylene
$scCO_2$	Supercritical carbon dioxide
SILPC	Supported Ionic Liquid Phase Catalysis
TEM	Transmission Electron Microscopy
TLC	Thin Layer Chromatography
TOF	Turnover Frequency
TON	Turnover Number
TMSP	Transition Metal Substituted Polyoxometalate
UHP	Urea Hydrogen Peroxide adduct
UV-vis	Ultraviolet-visible Spectroscopy
VOC	Volatile organic compound (or solvent)

Ringraziamenti

Il lavoro descritto in questa Tesi di dottorato non sarebbe stato possibile senza la collaborazione di professori, colleghi e amici dell'Università di Padova e di quella di Roma – Tor Vergata, nonchè del gruppo di ricerca del prof. Martin Albrecht presso lo University College di Dublino (e precedentemente presso l'Università di Friburgo).

Desidero innanzitutto ringraziare il mio supervisore, il prof. Gianfranco Scorrano, per aver sempre seguito pazientemente e con interesse lo sviluppo del mio lavoro sperimentale.

Grazie alla dott.ssa Marcella Bonchio per tutto quello che mi ha trasmesso in questi anni, sia dal punto di vista chimco che umano. Il suo entusiasmo e il suo continuo stimolarmi e spronarmi sono stati preziosi, soprattutto nei momenti di difficoltà.

Grazie al dr. Mauro Carraro per tutti i consigli e l'aiuto datimi nel corso di questi anni e per aver sempre seguito il mio lavoro con grande interesse.

Un ringraziamento particolare va al dr. Andrea Sartorel per la sua pazienza e il sostegno continuo in tutti gli ambiti, nonchè per il suo prezioso apporto nella parte di calcolo computazionale.

Un grazie di cuore a tutti i compagni di laboratorio e di dottorato per aver condiviso con me tanti aspetti della vita quotidiana di chimici e non solo. In particolare grazie a Martino, Gloria, Francesca F., Francesca D. S., Andrea M., Ester, Lucia, Massimo, Silvia, Marta, Gianni, Cristiano, Francesco R., Paola, Miriam, Milko, Luca, Renato, Marco, Francesco S., Iria, Elisa, Emiliano.

Grazie alle prof. Valeria Conte e Barbara Floris dell'Università di Roma – Tor Vergata e a tutto il loro gruppo di ricerca, in particolare al Dr. Pierluca Galloni e ai dottorandi (Giulia, Alessia, Valentina).

I would like to thank prof. Martin Albrecht (University College Dublin) for giving me the opportunity to work in his research group, as well as for his great enthusiasm and for all his useful advices. Special thanks go to Dr. Manuel Iglesias (University College Dublin) for being so patient and for all the help he gave me, and to all the people in both the labs (in Fribourg and Dublin), in particular to Oliver, Claudio, Laszlo, Angele, Aurelie, Marion, Seva, Wadih, Anneke, Elsbeth, Tatiana, Fiona, Puia.

Infine, grazie di cuore ai miei genitori, ai miei parenti e a tutti gli amici della Ducceschi per il loro sostegno quotidiano e per l'affetto che mi dimostrano sempre.

A tutti, grazie davvero.

Serena